The Hong Kong Polytechnic University

Department of Building Services Engineering

Barriers to application of fault detection and diagnosis (FDD) techniques to air-conditioning systems in buildings in Hong Kong

Lee Sze Hung

A thesis submitted in partial fulfillment of the requirements

for the degree of Doctor of Philosophy

January, 2010

Certificate of Originality

I hereby declare that this thesis is my own work and that, to the best of my knowledge and belief, it reproduces no materials previously published or written, nor material that has been accepted for the reward of any other degree or diploma, except where due acknowledgement has been made in the text.

_____(Signed)

Lee Sze Hung (Name of student)

Department of Building Services Engineering

The Hong Kong Polytechnic University

Hong Kong SAR, China

January, 2010

Dedication

To my encouraging mother and my brother for giving a dream to me

and making it come true

Abstract

Abstract of thesis entitled : Barriers to application of fault detection and diagnosis (FDD) techniques to air-conditioning systems in buildings in Hong Kong

Submitted by : Lee Sze Hung

for the degree of : Doctor of Philosophy

at the Hong Kong Polytechnic University in January, 2010

Automatic fault detection and diagnosis (FDD) is already a well-developed and widely used technology in hi-tech industries, such as the aviation and nuclear power industries. The application of this technology in buildings is lagging behind despite a large amount of effort has been made on developing FDD models for detecting system faults and sensor faults in air-conditioning systems. Through analyses of operating records collected from existing air-conditioning plants and attempts to develop models and FDD algorithms for chillers in those plants, the barriers that hinder widespread application of FDD to buildings have been identified in the present research study.

Whether a technology will penetrate the market hinges on the benefits of using the technology. The benefit of using FDD, however, is indirect; its use may not necessarily lead to energy savings but can help early detection of system and sensor faults and avoid energy being wasted due to malfunctioning of equipment or control systems. Among various building services systems, air-conditioning systems dominate the energy use in buildings and, therefore, are often the targets of FDD applications. In order to provide a

picture of the achievable benefits of applying FDD to air-conditioning systems, the energy costs of several air-side system and chiller component faults were estimated by computer simulation. This work formed the first part of the PhD study.

Since FDD relies on measured performance data to tell whether any faults have emerged, the availability of accurate and reliable performance measurements is a pre-requisite to successful application of FDD. For a study on whether typical chiller plants can fulfil this pre-requisite, operating records of an existing chiller plant were extracted from the building management system (BMS) that controls and monitors the performance of the plant. Attention was focused on measurements of the performance of chillers, the dominant energy consuming equipment in the plant. Many problems were encountered with the BMS records in that many missing data and corrupted data were found. The operation and maintenance (O&M) practice of the O&M staff on the way in which they handled system malfunctioning or component failures in the chiller plant was also studied, which unveiled several key barriers, such as faulty sensors.

In preparation for developing a FDD algorithm for chillers in the plant where twin-circuit chillers with two screw compressors per circuit were used, a mathematical model was developed for the chillers. The chiller model is semi-empirical model comprising a set of linked thermodynamic component models with coefficients that need to be evaluated based on measured chiller performance data. The chiller model includes a new evaporator model that can simulate heat transfer in the two separate compartments (one for each circuit) at the refrigerant side. Unfortunately, continuation with trial FDD implementation could not proceed further with that chiller plant due to problems with the chiller performance data measuring and recording functions of the BMS, which could not

be resolved within a short period of time. Consequently, another chiller plant had to be found for continuation of the study. Nevertheless, the chiller model developed has been verified to be capable of predicting chiller performance that compared well with measured data and has the potential to be used for detecting and identifying chiller faults. Similar modelling approach was also used in developing models for other chillers in the later part of the study.

The second chiller plant studied had been incorporated with a chilled water circuit design that allows efficient measurement of full- and part-load performance of chillers and thus was selected as the target chiller plant for further studies. The chillers used in this plant were simpler, water-cooled single-circuit screw chillers and a chiller model was developed and tested with the field data. FDD strategy was developed based upon measurements from available sensors and flow meters rather than requiring other sensors to be installed specifically for chiller FDD. The fault classifiers were determined based on the experimental results of the ASHRAE 1043-RP project. The characteristic parameters that can indicate whether a chiller is in healthy condition were identified. Monitoring the differences of the parameters evaluated from the measurements from the corresponding reference values will allow whether faulty conditions existed to be told. The strategy has been validated with field data and found to be effective for chiller FDD.

Lastly, the barriers to adoption of FDD for chillers in an existing plant were reviewed and discussed in the light of the experience gained in the studies on the two chiller plants, and several recommendations were made to tackle the problems. Such barriers include unavailability of refrigerant measurements, faulty sensors and missing data. The minimum range of system variables that should be consistently measured and

logged in a BMS was also proposed for chiller FDD. Recommendations have also been made on the required accuracy of sensors, the periods of inspection and calibration of sensors, and the provision of uninterruptible power supply for and sufficient data storage capacity in a BMS.

Publications Arising From the Thesis

Journal Papers

1. Lee SH and Yik FWH, 2009, A study on the energy penalty of various air side system faults in buildings, *Energy and Building*, Vol.42(1): 2-10
2. Lee SH, Yik FWH, Lai JHK and Lee WL, 2010, Modelling air cooled double circuit chillers, *Applied Thermal Engineering*, Vol.30: 1179-1187
3. Yik FWH, Lee SH, Lai JHK and Chan KT, 2010, Experience of using a chilled water circuit design to expedite in situ chiller performance measurement, *Building Services Engineering Research and Technology*, Vol.31(3):279-300

Conference Papers

1. Lee SH., A study on the energy penalty of various air side system failures in buildings, Proceedings of the First International Conference on Building Energy and Environment (COBEE), China, 13-16 July 2008.
2. Lee SH Yik FWH and Lai JHK, Overcoming the difficulties in Chiller Plant Performance Evaluation using BMS data: A case study, 3rd Asia Pacific Conference on Building Commissioning in Hong Kong, Hong Kong, pp 37-46, 7 Nov 2008.

Acknowledgements

It has been a great pleasure to me throughout my studies as a PhD student at the Department of Building Services Engineering of The Hong Kong Polytechnic University. This work would never have been possible without the support of my family, which allowed me to pursue a PhD degree. Sincere thanks are due to my chief supervisor, Professor Francis Wai Hung Yik, and co-supervisors, Dr. Wai Ling Lee and Dr. Joseph Hung Kit Lai, for their kindness and considerable mentoring given to me.

I would also like to thank Mr. C.F.Wong, Senior Facilities Officer of the Facilities Management Office of The Hong Kong Polytechnic University, for providing me with access to a great amount of field chiller plant data needed in my study. The kindness of Professor Shengwei Wang in sharing with me the chiller test data of the ASHRAE Research Project 1043-RP is gratefully acknowledged.

Lastly, I would like to thank all colleagues in the Department for letting me have a great place to finish my research.

Table of Contents

List of Figures

List of Tables

Nomenclature

An	Nozzle throat area of each compressor, m^2
AU	Overall heat transfer coefficient of evaporator or condenser, kW/^oC
c	Specific heat capacity, kJ/kg^oC
COP	Coefficient of performance of chiller
Eff	Pump efficiency
ε	Heat transfer effectiveness
δ	Relative error of the model prediction
h	Specific enthalpy, kJ/kg
K	Flow resistance of evaporator or condenser, Pa / $(l/s)^2$
m	Mass flow rate, kg/s
η	Efficiency
N	Number of operating condenser fans
PLR	Chiller part load ratio
P	Pressure, kPa
PI	Performance index
ΔP	Water pressure drop across evaporator or condenser, kPa
R	Residual value
δR	Uncertainty in the estimate of R

Q	Cooling output, kW
T	Temperature, ^{o}C
v	Specific volume, m^3/kg
x	Value of the variable
γ	Mean isentropic coefficient
V	Volumetric displacement, m^3/s
W	Electrical power, kW

Subscripts

A	Circuit A of chiller
a	Air
Aa	First section of evaporator at circuit A of chiller
Ab	Last section of evaporator at circuit A of chiller
AC	Compressor at circuit A of chiller
Af	Fan at circuit A of chiller
A,isen	Isentropic work of compressor at circuit A of chiller
A1	Superheated refrigerant leaving evaporator at circuit A of chiller
A1,s	Saturated refrigerant leaving evaporator at circuit A of chiller
A2	Refrigerant discharged by compressor at circuit A of chiller
A3	Refrigerant leaving condenser at circuit A of chiller
A4	Refrigerant entering evaporator at circuit A of chiller
B	Circuit B of chiller

BC	Compressor at circuit B of chiller
Bf	Fan at circuit B of chiller
B,isen	Isentropic work to compressor at circuit B of chiller
by	Bypass flow
B1	*S*uperheated refrigerant leaving evaporator at circuit B of chiller
B1,s	Saturated refrigerant leaving evaporator at circuit B of chiller
B2	Refrigerant discharged by compressor at circuit B of chiller
B3	Refrigerant leaving condenser at circuit B of chiller
B4	Refrigerant entering evaporator at circuit B of chiller
C	Compressor of chiller
cd	Condenser of chiller
cdA	Condenser at circuit A of chiller
cdB	Condenser at circuit B of chiller
cde	Condenser water entering chiller
cdl	Condenser water leaving chillers
ch	Chiller
CL	Cooling load
dis	Refrigerant leaving the compressor discharge
evp	Evaporator of chiller
evpA	Evaporator at circuit A of chiller
evpB	Evaporator at circuit B of chiller

evsh	Degree of superheat at the suction of compressor
isen	Isentropic compression
M	Measured data
MF	Measured data with fault
mr	Mass flow rate
nl	Nominal capacity of chiller
oa	Air leaving air-cooled condenser
out	Outdoor air
p	Predicted value
PI	Performance index
pump	Water pump
pump1	Diverted refrigerant of each compressor at circuit A of chiller
pump2	Diverted refrigerant of each compressor at circuit B of chiller
pv	Vapour refrigerant
r	Chilled water entering chiller
ref	Refrigerant
ri	Chilled water entering individual chiller *i*
s	Chilled water leaving chiller
sec	Chilled water measured in the secondary loop
si	Chilled water leaving in individual chiller *i*
sr	Secondary chilled water return from buildings

ss	Secondary chilled water supply to buildings
sub	Sub-cooled refrigerant leaving the condenser
suc	Refrigerant entering the compressor suction
s1	Chilled water entering circuit B's evaporator
s2	Chilled water leaving circuit B's evaporator
tot	Total
w	Water

1. INTRODUCTION

1.1 Motivation

Driven by concerns about depletion of fossil fuel reserve and global warming, the health and well-being of building occupants and the productivity of people in workplace, technological advancements continue to emerge to make buildings to perform better, especially in aspects of energy efficiency and indoor environmental quality. Old system designs and equipments have been replaced by new ones that are more energy efficient, and more extensive use of electronic devices, such as micro-processor based controllers, has allowed systems and equipment to perform much better than and beyond operating limits of those that they replaced. Furthermore, nearly all medium to large size commercial buildings built in the past 20 to 30 years are equipped with computer-based building management systems (BMS) to control and monitor the operation of all services systems and equipment in the buildings. These technologies can facilitate reliable and economical provision of safe, healthy and comfortable indoor environments in an environmentally friendly manner. Some of the available technologies have become widely adopted but among those that have not, some are technically feasible and should also be financially viable. For such technologies, the barriers to their widespread application should be identified and explained such that effective means can be devised to break the barriers.

Automatic fault detection and diagnosis (FDD) is a relatively new technology to the building industry. Application of FDD to a building involves implementing algorithms in the control and monitoring system within individual equipment or in a central BMS to detect the occurrence of any faulty conditions of equipment and measuring devices, and to evaluate and report such faults together with indications of the likely causes, to the building operators. FDD is a valuable supplement to a BMS, as it can help avoid the negative impacts of faulty sensors and equipment on the performance of the BMS and, in turn, the performance of the systems under its control. With a FDD system, operators' attention can be drawn to any system malfunctioning or performance degradation once such abnormalities are detected. Its use allows corrective actions to be taken promptly to minimise energy waste and equipment downtime, and provides the needed information for implementing conditioned-based operation and maintenance (O&M), which would help minimise O&M cost of buildings (Katipamula and Brambley, 2005a).

Among various services systems in a commercial building, the heating, ventilating air-conditioning and refrigeration (HVAC&R) system is the dominant energy consumer. In respect of operational control and maintenance work, the HVAC&R system is also the most demanding system. The system will perform adequately only if its equipment and sensors are all properly functioning. Poor performance or malfunctioning of even a small number of the components in the system can lead to poor indoor environmental conditions and large amount of energy being wasted. For example, condenser fouling may reduce the COP by 20 to 30% (Jia and Reddy, 2003) and faulty control sensor may increase the annual energy use of air handler by 50% (Kao and Piece, 1983). Therefore, a substantial portion of the control and monitoring functions of a BMS is devoted to the

HVAC&R system. However, a BMS is only capable of providing HVAC&R system control and monitoring but does not provide automatic FDD for the HVAC&R system, unless a FDD system is embedded into the BMS.

Without an automatic FDD system, detection and diagnosis of system faults have to be performed manually by plant operators, according to a regular maintenance schedule or when system breakdown or complaint arises (Rossi, 1999; Haves, 1999). Even if the plant operators are vigilantly scrutinising plant operation records from time to time, many faults are not immediately evident (e.g. water system leakage and equipment performance deterioration), and may remain unnoticeable until the faults become increasingly serious. When the presence of a fault is obvious, the accuracy of the diagnosis is dependent on the experience of the operators and the accuracy and relevance of the information at hand. However, system faults and sensor faults could exhibit similar symptoms and some system faults will become apparent only under specific conditions, which could confuse the operators. Recognising the limitations of manual fault diagnostic processes allows one to appreciate the advantages of implementing an automatic FDD system.

Although FDD has been identified to be a promising technology that can help detect system faults and, in conjunction with prompt rectification work, it can help enhance the reliability and stability of the system, until now, its use remains sparse after years of its introduction into the building industry. A clear understanding of the nature and causes of the hurdles that hinder widespread application of FDD in buildings will help remove the hurdles to the use of FDD. Therefore, this study was intended to identify

the gaps that hinder the use of FDD through pilot implementation of this technology in existing chiller plants.

1.2 Fault Detection and Diagnosis

The function of FDD is to detect any malfunctioning of the system and diagnose its primary causes, enabling rectification of the fault before serious damage to the system occurs. According to *Annex 25* of the International Energy Agency (IEA), FDD may consist of three processes: fault detection, fault diagnosis and fault evaluation. Fault detection is the process to detect the fault that occurred in a system. It usually relied on comparing the actual performance against a reference. Significant deviation from the reference indicates the occurrence of a fault. The fault diagnosis is the process to determine the kind, the location and the time of occurrence of the fault. This is more difficult to implement as it requires thorough understanding of how the faults can influence the operating conditions of the system, which is usually dependent on the severity level of the faults. This process becomes even more difficult if multiple or simultaneous faults occur. The final step, fault evaluation, is to assess the impact of a fault on the overall performance of the system so as to justify whether and when it is financially viable to rectify the fault. However, since it is difficult to quantify various fault impacts and the associated energy costs, the process of fault evaluation is usually neglected and the first two processes constitute most FDD applications.

1.3 FDD methods

FDD development began in the early 1970s (Simani et al, 2003) but little attention had been paid to the application of FDD to HVAC&R systems until the late 1980s and early 1990s (Katipamula and Brambley, 2005a). The recent review by Katipamula and Brambley (2005a; 2005b) provided a comprehensive account of the historical, the recent and the authors' prediction of the future developments of FDD, with emphasis on its applications to HVAC&R systems. Additionally, Katipamula and Brambley, (2005a) categorised various FDD methods into the following classes and discussed the strengths and weaknesses of each class of methods:

1. Quantitative Model-Based methods based on detailed or simplified physical models. Detailed models were considered to be less promising than the simplified ones, as they have the weaknesses that the models can be complex and computationally intensive, requiring large efforts to develop and many inputs for system description, some of which may not be readily available. Besides, the requirement for extensive user input is prone to poor judgement or errors.

2. Qualitative Model-Based methods which may be Rule-Based or Qualitative Physics-Based. The basis of the Rule-Based methods may be expert systems, first-principles or limits and alarms. Methods of this type are easier to develop and implement but are limited to specific systems and their successful application relies heavily on the expertise and knowledge of the developer.
3. Process History Based methods that use a Black-Box or Gray-Box approach. Among the Black-Box methods include those that use statistical methods, artificial neural networks (ANN) and other pattern recognition techniques. Unlike

the Black-Box approach which does not require an understanding of the physics of the system being modelled, development of Gray-Box methods requires thorough understanding of the systems whereas both require expertise in statistics.

1.4 HVAC FDD Application

A large number of research papers relevant to application of FDD to HVAC&R systems and equipment are available in the open literature. These FDD studies usually vary or differ only from the methods adopted for the detection of various equipment and system faults.

1.4.1 Chillers and Refrigeration Equipment

Grimmelius et al. (1995) adopted expert knowledge for detecting and diagnosing chiller faults in a 77-tons reciprocating chiller. Stylianou and Nikanpour (1996) adopted a combination of thermodynamic model developed by Gordon and Ng (1995), pattern recognition and expert knowledge techniques that was outlined by Grimmelius et al. (1995), to detect and diagnose selected faults in a reciprocating chiller. However, the model is not comprehensive enough to evaluate the sensitivity of the FDD technique (Katipamula and Brambley, 2005b).

Stylianou (1997) explored the work of Stylianou and Nikanpour (1996) by including a statistical pattern recognition algorithm (SPRA) to evaluate the residuals, so as to improve the accuracy in diagnosing faults. Because this approach relies heavily on availability of training data for both normal and faulty conditions, it is difficult to

implement in field application, and experimental work is usually required for testing of the method.

Rossi (1995) designed a rule-based FDD method for air conditioning equipment, which is capable of detecting the faults of condenser fouling, evaporator fouling, liquid line restriction, compressor valve leakage and refrigerant leakage. Rossi and Braun (1997) established a steady state model to predict temperatures in normal operating conditions to generate residuals for detecting and diagnosing five faults for packaged air conditioners. Breuker and Braun (1998b) evaluated the method proposed by Rossi and Braun (1997) for diagnosing the five faults, based on a 3TR (tons of refrigeration) rooftop air conditioner with both normal and faulty experimental results. Li and Braun (2003) made improvements on the previous rule-based FDD method by Rossi (1995) on rooftop air conditioners. One of them adopted a low order polynomial to fit the training data for the general regression neural network. Another improvement made was that the constant covariance matrixes for both normal and faulty operations were not assumed to improve the sensitivity and robustness of the model. Two new classifiers, namely the normalized distance fault detection classifier and the distance fault diagnosis classifier were used instead to improve the fault detection and diagnostic capability of the model.

Bailey (1998) developed an artificial neural network (ANN) to identify faults of a 70TR air-cooled screw chiller using experimental data. The shortcoming of this approach was that extensive data must be available for developing ANN models under both fault-free and faulty operating conditions.

Sreedharan and Haves (2001) tried to find out which chiller model was more suitable for the development of FDD by comparing three chiller models on their relative

modelling performance for a 90TR centrifugal chiller. However, no valid conclusions could be drawn as their accuracies in modelling the chiller were found to be similar.

Castro (2002) adopted a k-nearest neighbour classifier to detect faults and a rule based method to diagnose five different faults in a reciprocating chiller. Experimental data that include both fault-free and faulty data, with one fault occurring at a time at different levels of severity, were used for development and evaluation of the FDD method.

Cui and Wang (2005) proposed a semi-physical model in conjunction with a set of performance indices for detecting faults of centrifugal chillers, which were similar to those suggested by Mclntosh et al. (2000) and Jia and Reddy (2003). The method was validated with experimental data produced in the ASHRAE Research Project RP-1043.

Reddy (2007a) proposed a FDD method based on the fault diagnostic rules established from five characteristics features. Reddy (2007b) further identified four different chiller FDD methods and assessed them in terms of fault detection capability and on the overall FDD capability with the intention to find out the best one for use. Multiple linear regression black box models were found to be the most effective in detecting and diagnosing the occurrence of faults.

1.4.2 Air Handling Units

Many FDD studies had been conducted to develop FDD methods for air handling units (AHU), which are the major equipment at the air-side of an air conditioning system. Several studies related to applying FDD methods to AHUs had been conducted, which focused mainly on the faults of sensors, controllers and air-conditioning components

associated with the AHUs, and these studies differed from each other mainly in the FDD methods adopted. Glass et al. (1995) adopted a qualitative model based method to detect faults in an AHU. Faults were detected based on the deviations between the measured qualitative outputs with the model prediction. The model was tested with experimental work. However, the sensitivity and the ability of the method in dealing with fault alarms were not tackled.

Yoshida et al. (1996) used autoregressive exogenous (ARX) model and the extended Kalman filter to detect abrupt fault of AHU. The ARX model was unable to diagnose faults to an acceptable accuracy but the Kalman filter seemed to be better in providing fault diagnostics.

Haves at al. (1996) utilized radial bias function updated by a recursive gradient-based estimator to detect the faults of coil fouling and valve leakage of the cooling coil of an AHU. The FDD scheme was tested with the data simulated using a simulation tool called HVACSIM+ (Clark, 1985).

Three consecutive studies on the establishment of FDD method on VAV systems were conducted by Lee et *al.* (1996a, 1996b, 1997). Lee et al. (1996a) developed two methods to detect eight different faults in a laboratory AHU. The first method involved the use a residual between measured and expected values estimated at nominal conditions for detecting the presence of a fault. In the second method, variables estimated using autoregressive moving average with exogenous input (ARMX) and autoregressive exogenous (ARX) model were compared with normal parameters to detect the presence of a fault.

In another study, Lee et al. (1996b) trained an artificial neural network (ANN) to detect the same type of faults previously studied (Lee et al., 1996a). The ANN was trained using both fault-free and faulty data. The study showed that the ANN model could successfully detect faults from the experimental data, but the accuracy of this scheme in real application was uncertain since the faults generated inside laboratory were severe and noise-free.

Lee et al. (1997) extended their work to include two ANN models. The first ANN model was used to identify the fault, while the second was used to identify the cause of the fault. The authors stated that this two stage approach was simpler than the single stage ANN model method, by replacing a single ANN model that encompassed all considered faults with multiple ANN models that were less complex, with each of them dealing with a subset of residuals and symptoms associated with a complete diagnosis of all faults.

Peitsman and Soethout (1997) established different ARX models to predict the performance of an AHU and compared the results with the measured values to detect faults. Most faults were correctly detected and diagnosed. The authors indicated that some multiple faults were distinguishable by ranking of diagnosis according to their improbability, but the details on how to implement the scheme were not provided.

Katipamula et al. (1999) adopted a rule based decision tree method to diagnose the faults of outdoor air ventilation and economizer. House et al. (2001) also established expert rule sets to detect faults of AHUs including stuck cooling coil valve, cooling coil fouling and leaky heating coil valve.

Carling (2002) evaluated the performance of three fault detection methods for AHU: 1) qualitative model based method (Glass et al., 1995), 2) rule-based approach

(House et al., 2001), and 3) simplified steady state model-based method. Both normal and faulty data were collected from a real AHU for analysis. The qualitative method was easy to implement, but it could only detect a few faults. The rule-based method could detect more faults but the method required more analysis and customization during start-up. The third method took considerable time of specifying the threshold and calibrating the model and it also required extra sensors for implementation. This method also generated more number of false alarms in the case of varying water flow rate and airflow since the model was erroneous in predicting the fluctuation of the flow rates.

1.5 Commercial FDD products

Most FDD research studies only focused on developing FDD methods for detecting failures in air conditioning systems (Katipamula and Brambley, 2005b). These studies are usually analytical or empirical studies conducted inside laboratories and the methods still stay in research stage. Only few studies involved application of FDD to the services systems in existing buildings. More recent efforts are devoted to the development of commercially available tools and trial implementations in real buildings. At present, there are a number of available FDD tools including (Friedman and Piette, 2001a; 2001b; 2001c; Casto and Nejad, 2005):

1. ENFORMA (Architectural Energy Commission);
2. UCB Tools (Centre for Environmental Design Research (CEDR) at UC Berkeley);
3. Universal Translator (UT) (Pacific Energy Centre and Pacific Gas and Electric Co.);
4. Whole Building Diagnostics (WBD) (Pacific Northwest National Laboratory, Honeywell and University of Colorado);

5. PACRAT (Facility Dynamics Engineering);
6. EEM Suite (Silicon Energy);
7. IMDS (Supersymmetry, LBNL, En-Wise, C. Stockman and A. Sebald); and
8. CITE-AHU (NIST Building and Fire Research Laboratory and CSTB, France).

These commercially available FDD tools are for use in real buildings, but some are manual tools that require the users to identify the problems by themselves. The above-listed tools that fall in this category are ENFORMA, UCB tools and EEM Suites (Friedman and Piette, 2001b). The others are automatic tools which can indicate the causes of the faults. UT is a semi-diagnostic tool that can provide automatic diagnostics for economizers with the use of logic trees (Rule-based method) but manual diagnostics are required for equipment run-time and cycling (Friedman and Piette, 2001c). WBD is divided into two modules: a whole building energy (WBE) module and an outdoor air economizer (OA/E) module (Katipamula et al, 1999; Pratt et al, 2002). The WBE module tracks the energy use of buildings and compares it with the estimated energy consumption from a neural network model for fault detection only. The OA/E module is for fault diagnosis of economizers using logic trees. PACRAT is an automated tool for air handlers, chillers, hydronic systems, whole building energy use and zone distribution, which is based on logic trees. IMDS adopts the DOE-2 chiller model to correlate the power and the temperatures for detecting chiller faults. The final one, CITE-AHU, adopts the Air-Handling Unit Performance Assessment Rule (APAR) for testing and analysis of air handling units.

None of the abovementioned tools are based on black-box models. Most of them, including PACRAT, WBD, UT and CITE-AHU employ rule-based methods to detect and

diagnose faults while IMDS is based on a physical chiller model. Compared to the black-box models, which only correlate mathematically the system inputs and outputs without using any physical relations, rule-based models, including those first-principles based models, comprise cause-effect relations which should be more comprehensible to operation and maintenance personnel. In addition, black-box models require huge amount of data for their training before they can perform FDD, which increases the difficulty in implementation, although simulation or emulation may accelerate the training period. These add costs to the implementation, which hindered market penetration of black-box models.

Several demonstration studies on the use of the abovementioned FDD tools had been conducted. Piette et al (1998; 1999) demonstrated the application of IMDS in a building in San Francisco. Demonstration of the use of WBD had also been conducted to diagnose operational problems of air handlers in Denver Airport (Pratt et al, 2002). These researches indicated that although many previous undetected HVAC&R system faults were identified using these FDD tools, many difficulties were encountered, for example, in establishing the linkage between WBD and the existing BMS control, problems were encountered with data collection during installation, and WBD failed to identify the problems due to temperature sensor errors during trial implementation.

These technical difficulties they encountered are regarded as one type of the typical barriers to adoption of FDD in real buildings. Since wider application of FDD technology can be hindered by such hurdles, the major objective of the present study was to find out the key barriers to implementation of FDD in existing buildings.

1.6 The Scope and Approach

The main objectives of this research study were to identify the barriers to adoption of FDD through pilot application of the technology to an existing building, and to formulate measures for overcoming the identified barriers. Since the benefit of adopting FDD is uncertain and the cost of investment can be high, building owners would hesitate to adopt this technology in their buildings, unless they are informed of the energy cost saving that could be achieved through investing into the technology. The cost for the energy that would be wasted due to presence of a fault, which could be avoided through early detection and rectification of the fault with the use of FDD, would become a benefit of applying FDD. The first (preliminary) stage of the study, therefore, included computer simulation studies for providing ballpark figures for the energy penalties of various faults in an air-conditioning system, which accounts for a very substantial portion of the total energy use in typical commercial buildings.

Since chillers dominate the energy use in commercial buildings, and chiller faults are usually more difficult to detect manually, the second (main) stage of the study was intended to be a trial implementation of FDD to an existing chiller plant. The planned works included development of a model-based FDD strategy as well as the required fault classifiers to be used in conjunction with the model and the operating records of the chiller plant that could be extracted from the BMS serving the plant, for off-line FDD analysis. The original research plan included monitoring of the plant conditions paying specific attention to the emergence of any chiller faults, as well as consistent evaluation of the plant operating records, especially before and after a fault had been identified and rectified, which would allow sufficient data to be captured for development of the fault

classifiers and verification of the effectiveness of the FDD strategy. Where possible, simulated faults would be introduced to the plant for experimental measurements, but this would be limited to a few faults that would not cause serious interruption to the normal operation of the plant and would not cause any damage to the equipment. Furthermore, any problems encountered in the implementation process would be recorded and analyzed so as to unveil the typical problems that one would face when attempting to implement FDD in an existing chiller plant, and to propose means for resolving the problems.

Many problems with the BMS data were encountered, which prevented trial FDD implementation to be continued with that chiller plant. The major problem was with the available chiller performance data caused by the unsatisfactory measuring and recording functions of the BMS, which could not be resolved within a short period of time. Consequently, another chiller plant had to be found for continuation of the study.

The second chiller plant was selected for further studies because its chillers have recently be replaced by brand new chillers and it had adopted a new chilled water circuit design that allows efficient measurement and recording of full- and part load performance of chillers. The objective of the study, therefore, included verification of the effectiveness of the new chilled water circuit in facilitating expeditious *in-situ* chiller performance tests.

Through analysis of the BMS records of the operating data for chillers in the second plant, the range of measurements available was found to be insufficient to support development of a FDD strategy for detecting all the important chiller faults, and this would indeed be a major hurdle to successful FDD application. The FDD strategy was, therefore, developed based upon the available measurements only, which restricted the range of faults that it can detect. The performance indices that can indicate whether a

chiller is in healthy condition were identified, and the fault classifiers were determined, based on the experimental results of the ASHRAE Research Project 1043-RP. The effectiveness of the FDD strategy was finally verified based on the normal operating data obtained from the second plant as well as experimental data with the plant with two faults introduced. The major barriers that were encountered in the study were then reviewed, and suggestions were proposed to tackle the barriers.

1.7 Organization of materials presented in the thesis

The following eight chapters in this thesis were organized following the sequence of work carried out in the present study. Chapter 2 presents the results of a series of simulation studies for prediction of the energy waste that would be incurred by various typical air-side system faults and chiller faults, which could be avoided through using a FDD system.

Analysis of the chiller operating data of the first chiller plant and the problems identified from the analysis are summarized in Chapter 3. These problems or unfavourable conditions had to be removed before FDD could be applied to the plant. Some migration methods were developed, which helped overcome some of the problems and allowed an approximate evaluation of the chiller plant performance to be made, which are also described in that chapter.

Chapter 4 presents the findings of an analysis on the maintenance records of the chiller plant, which was intended to identify frequently occurring faults in the plant and the way in which the operation and maintenance personnel handled those faults. The typical problems with daily operation and maintenance of the chiller plant were identified,

which include, for example, the way in which fault alarms were handled and the repair works were recorded. These are important because even if faults are detected through the use of a FDD system, the chiller plant would still be unable to function properly if the faults are not properly tackled and recorded for subsequent analysis. The maintenance records would also be essential to plant performance evaluation and preventive maintenance planning.

A thermodynamic model, which was intended for FDD application to chillers in the first plant, was developed and details of the model, including empirical verification of its predictions, are presented in Chapter 5. The chillers in the plant are twin-circuit chillers with two screw compressors per circuit but no chiller model that can simulate the performance of chillers of these characteristics was available. Therefore, a new chiller model was developed from scratch, and the model includes an evaporator model that comprises two separate refrigerant compartments through which the chilled water tubes would pass from one compartment to the other and back. Despite this, continuation with trial FDD implementation could not proceed further with the first chiller plant due to the problems with the chiller performance data measuring and recording functions of the BMS. Consequently, another chiller plant had to be found for continuation of the study.

Chapter 6 begins with a brief introduction to a new chilled water circuit for chiller performance measurement, which was proposed by Yik (2008) and has been incorporated into the second chiller plant. Described in this chapter includes the preliminary analysis of the plant performance data retrieved from the BMS for verifying the measurement accuracies of the instruments available and for analyzing the operating conditions of the chiller plant, as well as the experimental work done to verify the effectiveness of the

chilled water circuit design and to measure chiller performance for comparison with the manufacturers' data.

Chapter 7 introduces the thermodynamic chiller model for the water-cooled screw chiller in the second chiller plant, which was used in the FDD study. This is followed by descriptions of the establishment of fault classifiers for detecting chiller faults, which was based on the ASHRAE 1043-PR laboratory chiller test data; and the use of measured and simulated chiller performance data to demonstrate the ability of the FDD method in chiller fault detection.

Chapter 8 discusses the barriers to applying FDD as found in the present study. Since the major problems encountered include unavailability of required measurements, faulty sensors and missing data, the minimum set of measurements that would allow all the significant chiller faults to be detected has been identified and recommendations in standards and guidelines on instrument provisions for chiller plants have been reviewed in this chapter, together with various other barriers to successful implementation of FDD to chiller plants.

The final chapter (Chapter 9) concludes this thesis with a summary of the key findings reported in all preceding chapters, followed by a few recommendations for further works that would help remove the barriers to FDD application in buildings in Hong Kong.

2. ENERGY PENALTY OF AIR SIDE SYSTEM FAULTS AND CHILLER FAULTS

2.1 Overview

Automatic fault detection and diagnosis (FDD) can help upkeep building energy efficiency by facilitating early detection of occurrence of system faults, especially those in air-conditioning systems. This enables rectification works to be done before much energy is wasted due to such faults. However, building owners may be unwilling to invest in FDD unless they are convinced of the benefit, which is the cost of wasted energy that can be avoided. For obtaining some ballpark figures on the benefit of adopting a FDD system, estimations have been made by detailed computer simulation of the energy cost impacts of a range of common faults in variable air volume (VAV) systems and water chillers of a central air-conditioning system. Five VAV system faults, namely room air temperature sensor offset, stuck VAV box damper, supply air temperature sensor offset, stuck outdoor air damper and stuck/leaking cooling coil valve, and four chillers faults, namely condenser fouling, refrigerant leakage, reduced condenser water flow and reducted evaporator water flow, were studied. The simulation findings show that the stuck open VAV box damper would be the most severe type of air-side system fault whilst reduced condenser water flow was the most severe type of chiller faults in terms of energy penalties. The simulation studies performed are described in detail in this chapter.

2.2 The simulation tool

The detailed building energy simulation software EnergyPlus was used in this study. Funded by the US Government, a team that comprised the US Army Construction Engineering Research Laboratories (CERL), University of Illinois (UI), Lawrence Berkeley National Laboratory (LBNL), Oklahoma State University (OSU), GARD Analytics and Department of Energy (DOE) developed EnergyPlus in 1996 (Crawley, 2001). EnergyPlus embraces the advantages of two already widely used simulation programs, DOE-2 and BLAST, as well as some features of another widely used program TRNSYS.

A review of existing simulation programs, which included APACHE, BLAST, DOE-2, EnergyPlus, HAP v4.0, TRACE 700, VisualDOE, AirModel, ASEAM, System Analyzer, HBLC, HVACSIM+, SPARK, TRNSYS, ENFORMA and Visualize-IT Energy Information and Analysis Tool (California Energy Commission, 2002), indicated that EnergyPlus and AirModel are the most suitable simulation programs for FDD studies. When equipped with EnergyPlus, the user can: i) simulate both building thermal load and systems; ii) change the weather file for comparison of actual data with simulated data; iii) modify the input modules to simulate real faults; and iv) select the specific parameters for analysis. Therefore, EnergyPlus was selected as the tool for simulation of the impacts of air-side and water-side system faults in the present study.

2.3 The model building

Based on findings of a survey of 64 commercial buildings in Hong Kong, Chan and Chow (1998) summarized the representative characteristics of this type of buildings

in Hong Kong. A 40-storey office building model that possesses such typical characteristics has been established (Lee et. al, 2003) and is adopted in this study to represent a typical commercial office buildings in Hong Kong to provide a basis for the simulation study for predicting the energy impacts of air conditioning system faults. Table 2.1 summarizes the characteristics of the office building and the air conditioning system in the building. As shown in the floor plans in Figure 2.1, each floor in the building was divided into four exterior zones and four interior zones, all of which were air-conditioned, and one core zone without air-conditioning, for the cooling load and air conditioning energy use simulations.

Table 2.1 Characteristics of the typical office building

General	
Floor dimension (LxW) (m)	36 x 36
Floor to floor height (m)	3.2
Orientation	N/E/S/W
Window to wall ratio	0.5
Design criteria	
Summer indoor temperature (^{o}C)	25.5
Relative humidity (%)	54
Ventilation rate (L/s/person)	10
Occupancy density (m^2/person)	9
Equipment load density (W/ m^2)	25
Lighting load density (W/ m^2)	25
Infiltration (ach)	0.1
Air conditioning system	
Air side system	VAV with reheat
Chilled water distribution system	Single-loop pumping system with differential pressure bypass control
Type of chiller	Air cooled reciprocating chiller
Number of chillers	7
Rated cooling capacity for each chiller (kW)	1125.4
Rated power for each chiller (kW)	400
COP at full load at 35^{o}C outdoor air temperature	2.81

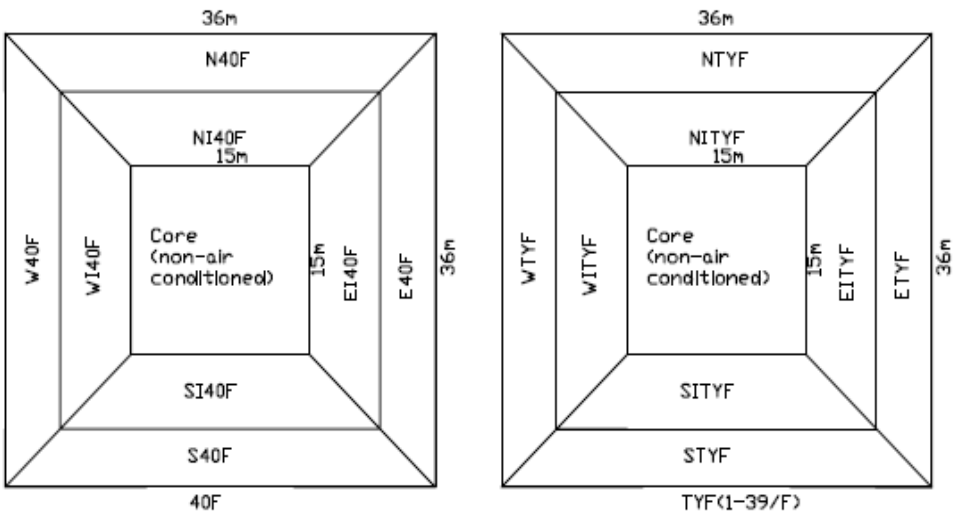

Figure 2.1 The typical floor plan for the 40-storey office building

Each floor in the building was served by a VAV air-conditioning system consisting of an air-handling unit (AHU) with a variable speed supply fan and a cooling coil; supply and return air ducts and outdoor, return and exhaust air dampers; and VAV boxes in individual zones. Each VAV box serving an exterior zone was installed with an electric heater to provide winter space heating. Figure 2.2 shows the control schematic diagram of the system.

At the VAV AHU, a fixed amount of outdoor air (OA) would mix with the return air (RA) from the air-conditioned spaces and the mixed air would be cooled by the cooling coil to the supply air temperature set point. The supply air from the AHU would be distributed via the ducting system to the VAV boxes, which would regulate the flow rate of supply air to the zones according to the space air temperatures in the respective zones. The total supply air flow rate would be controlled by regulating the supply air fan speed such that the static pressure in the supply duct would be maintained at the set point

level. The cooling output of the AHU would be controlled by the supply air temperature controller, through regulating the flow rate of chilled water though the cooling coil.

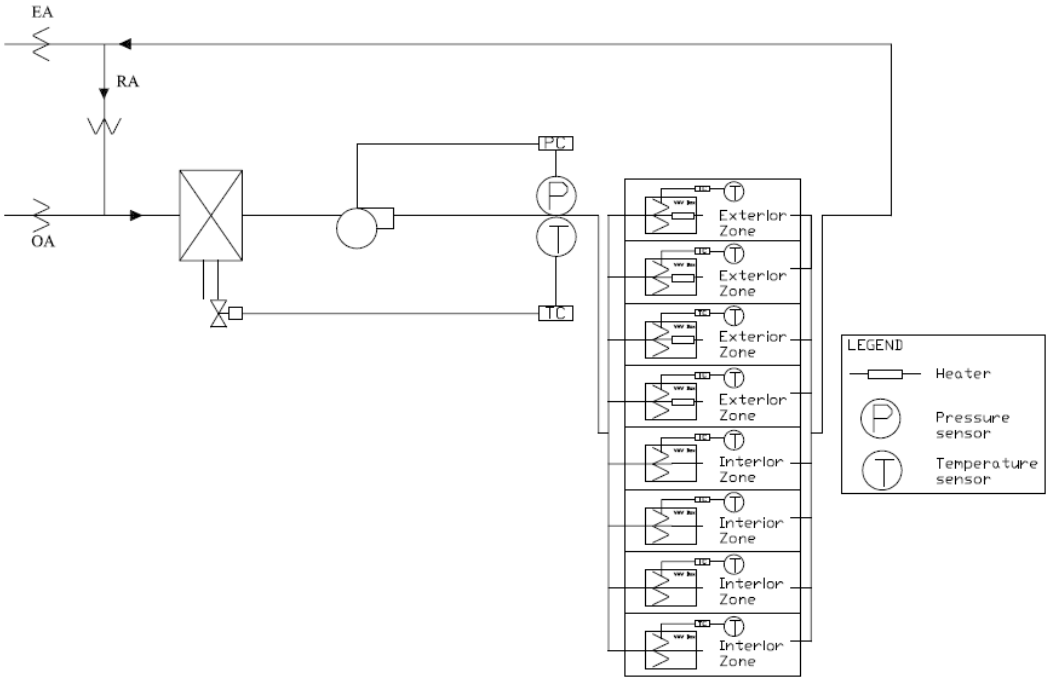

Figure 2.2 The VAV system control schematic diagram

The water-side system, as shown in Figure 2.3, comprised seven air cooled reciprocating chillers, each with a rated cooling capacity of 1125kW, and a rated power demand of 400kW. Each chiller would operate together with a matching chilled water pump with a rated power demand of 32kW. The differential pressure bypass control valve in the chilled water distribution system would allow surplus chilled water to bypass the air-side systems while it is moderated to maintain a constant differential pressure across the main chilled water supply and return pipes such that the chilled water flow rates through the operating chillers would stay at constant levels to ensure proper chiller operation.

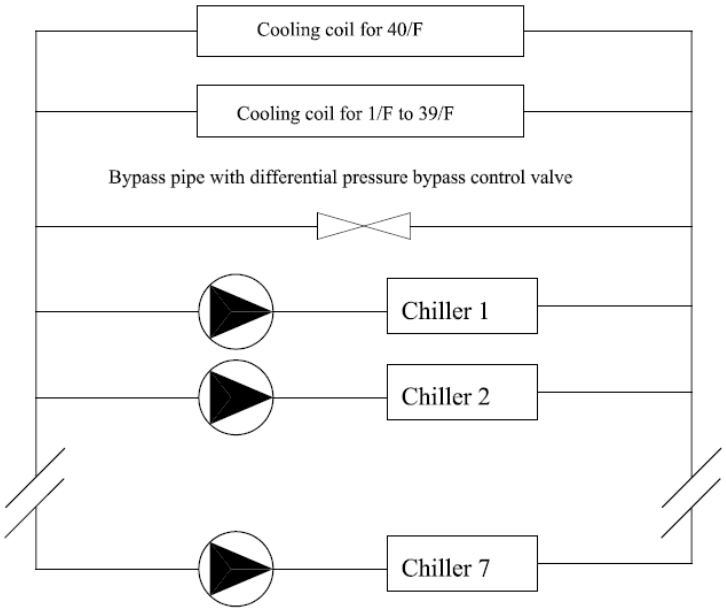

Figure 2.3 The water side system schematic

2.4 VAV air conditioning system faults

VAV air-conditioning systems are widely adopted in commercial buildings because their fan power demand will drop with the supply air flow demand under part-load operations. However, any system, control and sensor faults may reduce the energy benefit and lead to occupant discomfort. Typical faults found in VAV systems are due to improper design, application and operation of the systems, such as improper return and outdoor air damper settings, improper diffuser selection, improper exhaust systems and improper system control (Linder and Dorgan, 1997).

Through surveys of designers, installers and maintenance crew, Yoshida (1996) and Yoshida et al. (1996) found that the symptoms of typical VAV system faults include poor air quality, water leakage, poor room air temperature control, excessive or insufficient supply flow rate, excessive air filter pressure drop, abnormal noise or vibration, etc.

Insufficient air flow rates were found to be the most common problem based on inspections of about 10,000 ventilations systems in Sweden (Mansson, 1998). A site survey of VAV terminals in a large commercial building in Hong Kong (Qin and Wang, 2005) identified 12 types of faults, namely temperature sensor error, DDC error, diffuser damper closed as requested by tenants, design flow too large, VAV boxes dismantled by tenant, damper actuator failure, part of diffuser being wrapped by adhesive tape, temperature set-point too low, abnormal space temperature requested by tenants, temperature sensor located too close to VAV diffuser outlet, too many people in a room and VAV box not accessible.

The root causes of the faults found in the survey studies reviewed above can be classified into three categories: i) mechanical failures (damper failure, diffuser wrapped, malfunctioning of cooling coil valve); ii) sensor/controller failures (improper system control, temperature/flow sensor failure, PI controller failure); and iii) design failures (VAV terminal under/over capacity, improper diffuser selection, sensor improperly located, improper design flow rate and temperature design set-point).

Since the design failures cannot be detected by a FDD system, only the mechanical failures and the sensor/controller failure were considered in this study. The typical VAV system faults are related to stuck dampers, malfunction of cooling coil valves and sensor/controller faults. Therefore, the study focused on the energy and performance impacts of five VAV system faults, namely room air temperature sensor offset, stuck VAV box damper, supply air temperature sensor offset, stuck outdoor air damper and stuck/leaking cooling coil valve. The simulation approaches used to study these faults are summarized in Table 2.2.

Table 2.2 Description for the simulated faults

Faults	Fault type	Simulation approach
Room air temperature sensor offset	Negative sensor offset	Change room air temperature set-point from 25.5°C to 21.5°C
	Positive sensor offset	Change room air temperature set-point from 25.5°C to 29.5°C
Stuck VAV box damper	Stuck open	Set minimum air flow fraction to 1 for all VAV boxes
Supply air temperature sensor offset	Negative sensor offset	Change supply air temperature set-point from14°C to 10°C in summer, and from 16°C to 12°C in winter
	Positive sensor offset	Change supply air temperature set-point from14°C to 18°C in summer, and from 16°C to 20°C in winter
Stuck outdoor air damper (manual fault)	Stuck closed	Change the outdoor air flow to zero
	Stuck open	Use 25% more outdoor air for cooling
Stuck/leaking cooling coil valve	Stuck open	Set the chilled water flow to its maximum value
	10% cooling coil valve leakage	Change the minimum water flow to 10% of the maximum water flow rate
	25% cooling coil valve leakage	Change the minimum water flow to 25% of the maximum water flow rate
	40% cooling coil valve leakage	Change the minimum water flow to 40% of the maximum water flow rate

Among the five types of faults studied, some are easy but some are more difficult to detect. The room temperature sensor offset cannot be detected directly from the faulty sensor's own output signal (Qin and Wang, 2005); its detection requires comparison of the flow rates through different VAV boxes serving the same zone or the frequencies that the VAV box damper under the control of the faulty sensor stays at the maximum or minimum opening positions. For stuck VAV box damper, as its occurrence can cause the room air temperature to drift away from the set-point value, it can be readily identified by monitoring the deviations of the room air temperature from the temperature set-point (House et al., 1999). For detection of supply air temperature sensor offset, the measured supply air temperature can be compared with its expected value. The latter can be determined from the supply air flow, the temperature and relative humidity of the mixed air and the chilled water temperature by using an empirical model derived from fault-free operation data (Lee et al, 1997). A residual that is higher or lower than the threshold will confirm the presence of supply air temperature sensor drift. Stuck outdoor air damper,

which is not a control system fault, can be easily identified by comparing the outdoor air flow with the preset value.

Stuck or leaking cooling coil valve will cause a change in the supply air temperature when the cooling load or outdoor air temperature varies, which, in turn, will cause the cooling coil valve control signal to change continuously due to the integral control action of the PID controller. Therefore, a stuck cooling coil valve can be identified by checking the supply air temperature and cooling coil valve control signal (Lee et al., 1996a). Leaking cooling coil valve may lead to overcooling whenever there is a low load demand. This fault can be identified by checking the temperature change of air entering and leaving the cooling coil, the supply air flow, and the cooling coil valve control signal. If this fault exists, when the cooling coil valve controller is attempting to fully close the valve, the valve will still allow chilled water to pass through the cooling coil to cool down the supply air, resulting in a drop in the temperature of the air passing through the cooling coil, which can indicate the occurrence of the fault.

However, as Dexter et al. (1996) and Haves et al. (1996) pointed out, the temperature of the air leaving a cooling coil is seldom directly measured but is estimated from the supply air temperature measurement by assuming a constant temperature rise across the supply air fan. Because measurement of the mixed air temperature is unreliable, they further recommended the outdoor air temperature be used for FDD.

2.4.1 Room air temperature sensor offset

In a VAV system, the position of the VAV box damper, and thus the flow rate of supply air through the VAV box, would be regulated according to the deviation of the room air temperature signal fed back by the sensor from the set point value. In the

simulation, room temperature sensor offsets were introduced by changing the room air temperature set point from 25.5°C to 21.5°C (negative sensor offset) and 29.5°C (positive sensor offset).

With positive temperature sensor offset, the sensor reading would be lower than the actual value. Hence, the room air temperature would actually be controlled to meet 29.5°C even though the sensor would report that the temperature would be 25.5°C (assuming 4°C offset). Figure 2.4 shows a comparison of room air temperature in an exterior zone with and without positive temperature sensor offset for a week in July. Over the whole week, the room air temperature was maintained close to the respective ('false' and 'true') set-points during the air-conditioned period. There are periods during which the room air temperature was slightly higher than 25.5°C for the case without positive sensor offset, which would occur whenever the cooling capacity of the air-handling unit (AHU) was insufficient to cater for the zone sensible cooling load. Such high room load situations could occur at the beginning of the air-conditioned period in a day following a long non-air-conditioned period, or when the weather condition exceeded the outdoor criteria used in sizing the AHU. During the non-air-conditioned periods, the room air temperature was 'floating', depending on the heat balance in the room.

Positive room temperature sensor offset will lead to reduced energy use, but at the sacrifice of human comfort, which could lead to tenant complaints. Table 2.3 shows the annual cooling energy use with the fault occurring on every floor and with the fault occurring on just one single floor. For the latter case, the reduction in the annual total cooling energy use would be 0.48%.

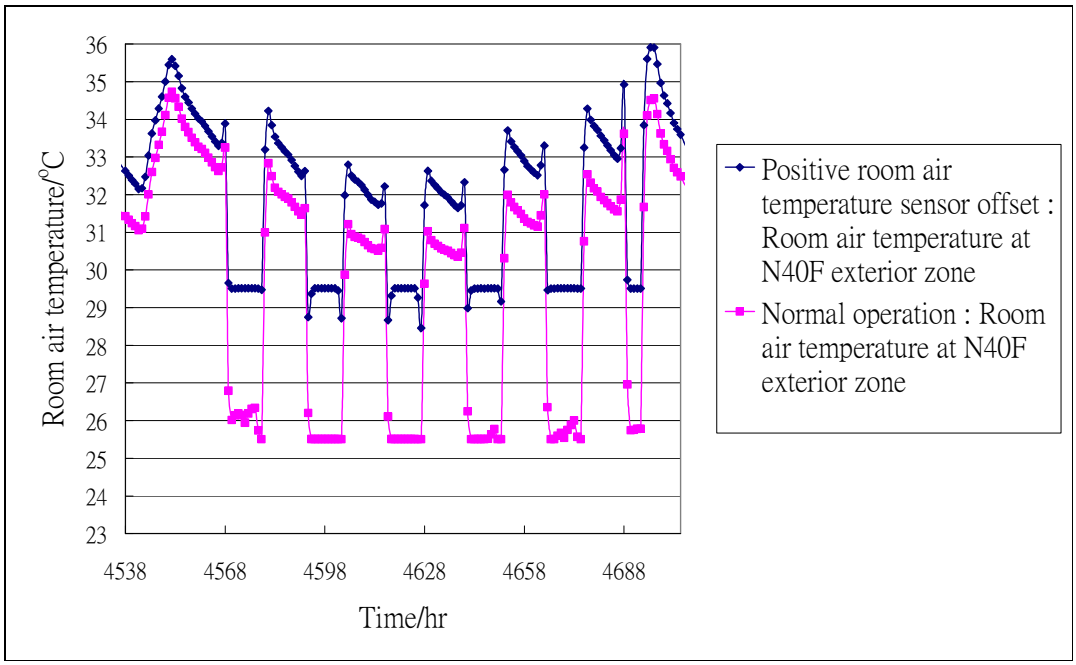

Figure 2.4 Room air temperature in an exterior zone with and without positive room air temperature sensor offset for a week in July

Table 2.3 Predicted energy consumption with and without positive room air temperature sensor offset

	Normal	With positive sensor offset	% increase (fault occurring on all floors)	% increase (fault occurring on one single floor only)
Chiller energy (MJ)	13488951	10553599	-21.76	-0.54
Fan (MJ)	3019854	2188158	-27.54	-0.69
Pump (MJ)	1499996	1229643	-18.02	-0.45
Heating (MJ)	144626	663366	358.68	8.97
Total (MJ)	18153426	14634766	-19.38	-0.48
Peak Demand (KVA)	21492268	18997137	-11.61	-0.29

Conversely, a negative room air temperature sensor offset will lead to increased fan, pump and chiller energy consumption. The actual room air temperature would drop to 21.5°C instead of 25.5°C (assuming a 4°C offset). Figure 2.5 shows a comparison of

room air temperature in an exterior zone with and without a negative temperature sensor offset for a week in July. The figure shows that although the negative offset would in effect lower the set-point, the room air temperature could not be brought to this lowered set-point due to the limited cooling capacity of the VAV AHU, even though the fan was operating at full speed in attempt to meet the required temperature set-point, as shown in Figure 2.6. However, the lowered set-point temperature would be achieved on other days while the cooling load stayed within the capacity of the VAV AHU.

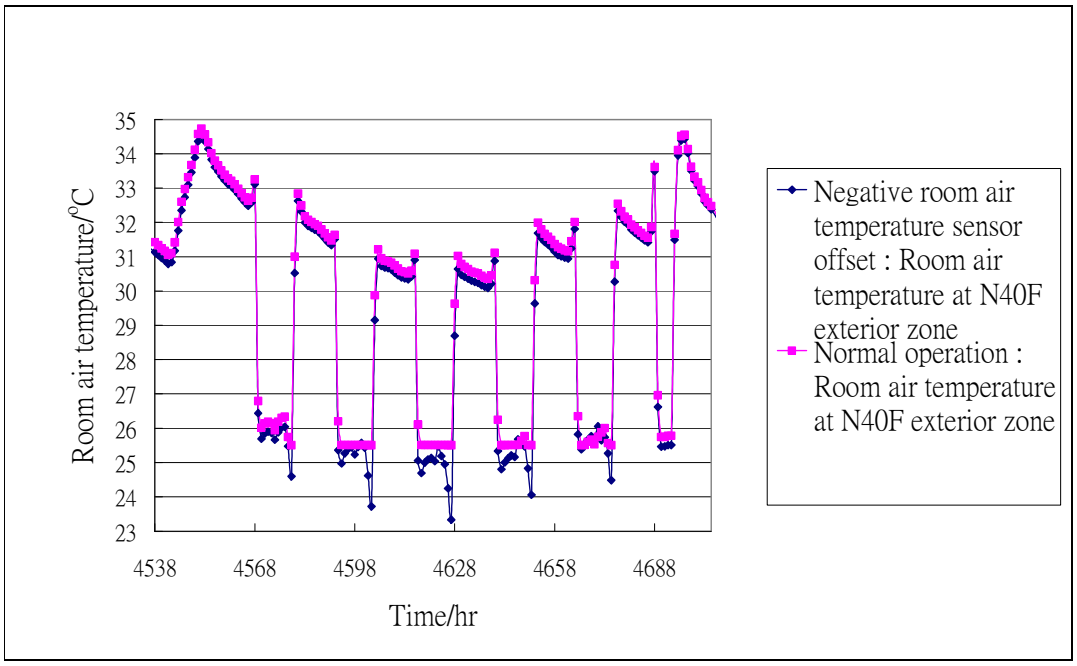

Figure 2.5 Room air temperature in an exterior zone with and without negative room air temperature sensor offset for a week in July

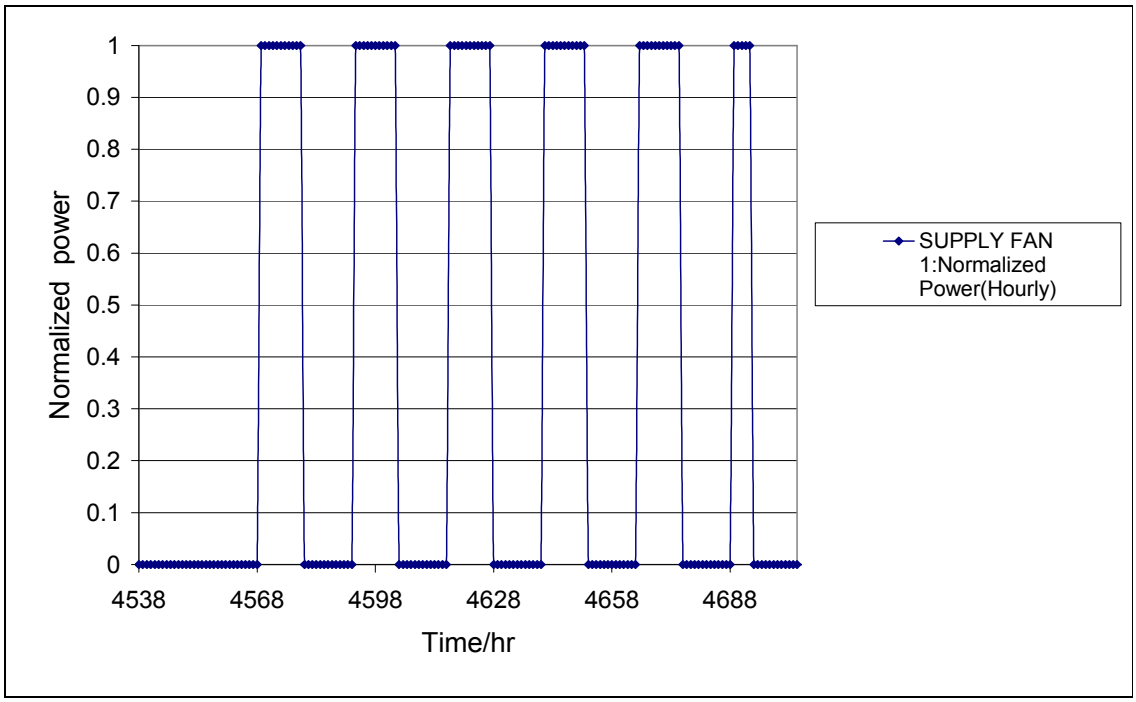

Figure 2.6 Normalized fan power of supply fan 1 with negative room air temperature sensor offset for a week in July

Negative sensor offset is a more serious fault because it would not only increase the energy use; it would also adversely affect human comfort. As building occupants may adapt to the cooler temperature by wearing more clothes, this fault may not be brought to the attention of the plant operators but, with a FDD system, building operators would be aware of the fault once it becomes significant. Table 2.4 shows the energy wastage for this type of fault. If the fault occurred only on one floor, the energy waste would be about 0.53% of the annual total cooling energy use and the electricity peak demand of the building would increase by around 0.04%.

Table 2.4 Predicted energy consumption with and without negative room air temperature sensor offset

	Normal	With negative sensor offset	% increase (fault occurring on all floors)	% increase (fault occurring on one single floor only)
Chiller energy (MJ)	13488951	15626244	15.84	0.40
Fan (MJ)	3019854	4625665	53.18	1.33
Pump (MJ)	1499996	1691300	12.75	0.32
Heating (MJ)	144626	50560	-65.04	-1.63
Total (MJ)	18153426	21993770	21.15	0.53
Peak Demand (KVA)	21492268	21816154	1.51	0.04

2.4.2 Stuck VAV box damper

The results for the case with stuck closed damper are omitted because, if this fault occurred, complaints from building occupants would alert the building operators to this fault. As shown in Table 2.2, the stuck open VAV box damper was simulated by setting the minimum air flow fraction to 100% for all VAV boxes, causing the damper to stay fully open throughout the simulation. The energy impact of the fault would be very serious. Figures 2.7 and 2.8 show the normalized air flow rate of VAV system 1 (serving the topmost floor) and VAV system 2 (serving the 39 typical floors), with and without the fault for a week in January. As expected, the air flow rate stayed at its peak value due to presence of this fault, which was much higher than the required flow rate under normal condition. Additionally, this overcooled the zone, causing the heater to further reheat the cooled air to meet the set-point. Figure 2.9 compares the heating energy use with and without the fault for a week in January, showing the much increased heating energy use compared to the normal case.

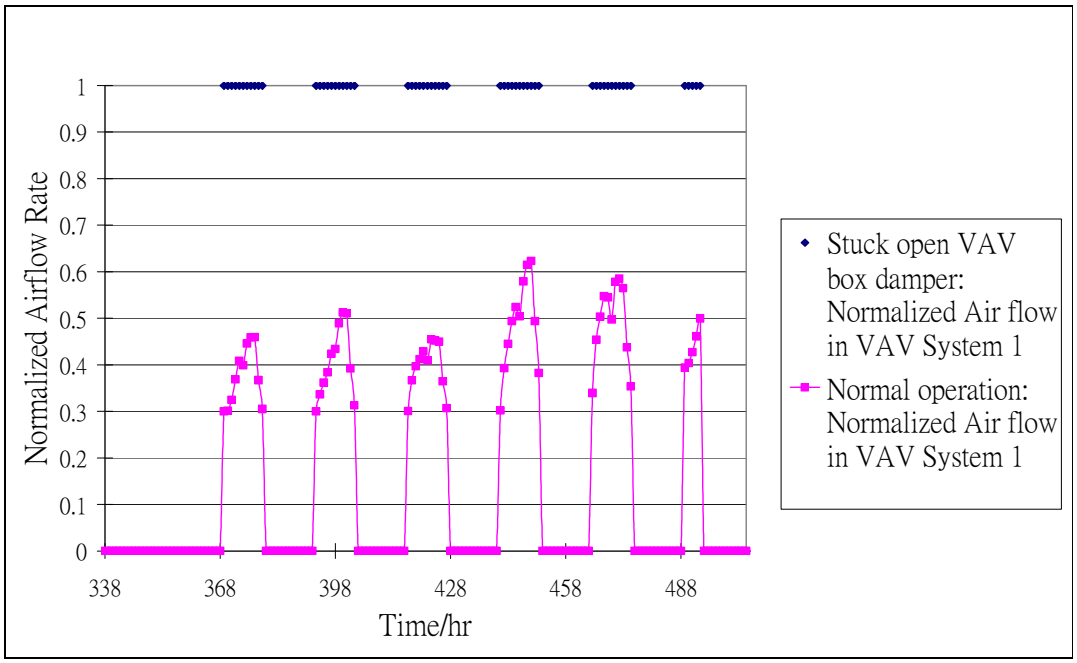

Figure 2.7 Normalized air flow rate for VAV system 1 with and without stuck open VAV damper fault for a week in January

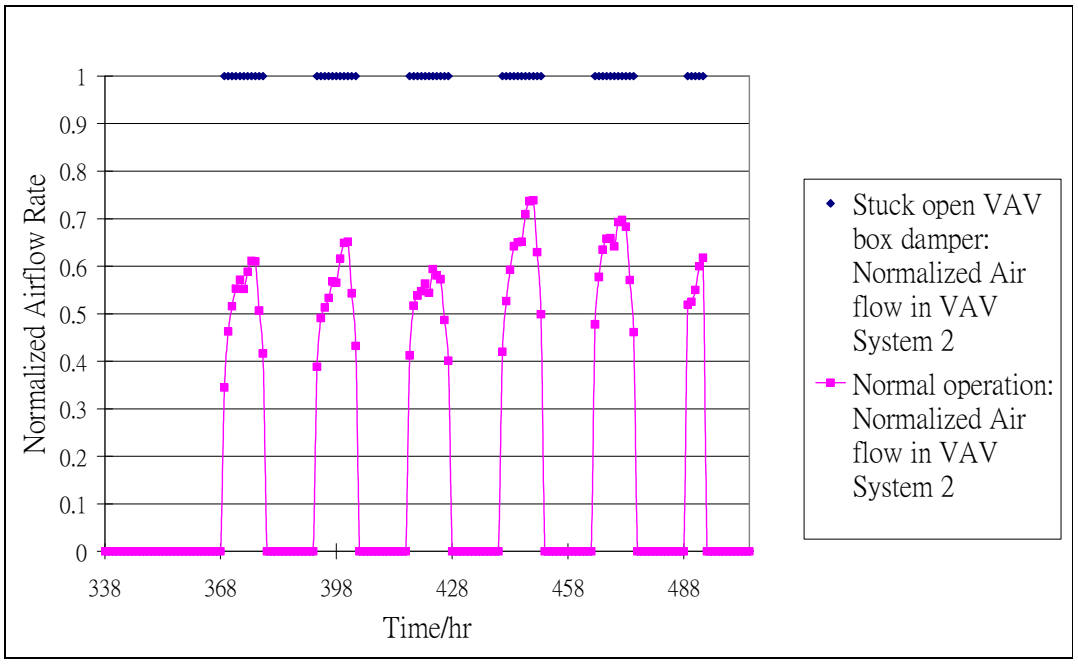

Figure 2.8 Normalized air flow rate for VAV system 2 with and without stuck open VAV damper fault for a week in January

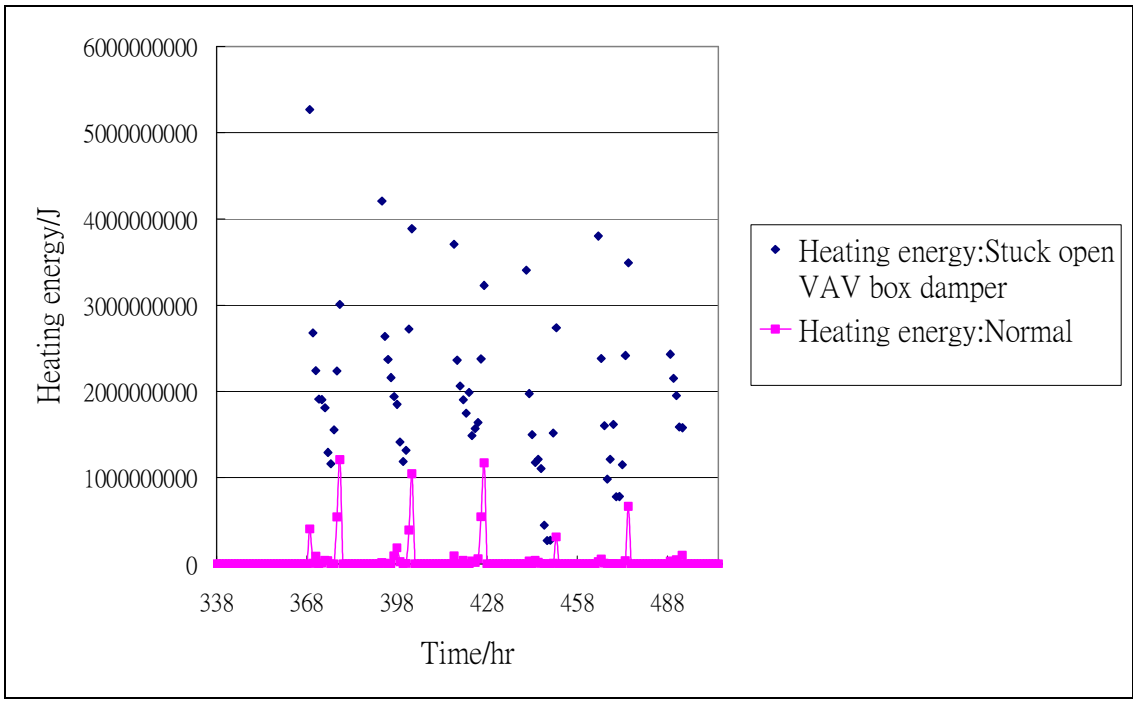

Figure 2.9 Heating energy use with and without stuck open VAV damper fault for a week in January

Table 2.5 Predicted energy consumption with and without stuck open VAV box damper

	Normal	VAV box damper stuck open	% increase (fault occurring on all floors)	% increase (fault occurring on one single floor only)
Chiller energy (MJ)	13488951	15957162	18.30	0.46
Fan (MJ)	3019854	4695330	55.48	1.39
Pump (MJ)	1499996	1723131	14.88	0.37
Heating (MJ)	144626	2415981	1570.51	39.26
Total (MJ)	18153426	24791604	36.57	0.91
Peak Demand (KVA)	21492268	21763165	1.26	0.03

The increase in energy use of the chillers and pumps was also large, as they are required to cool down the full flow of air to its supply temperature set-point. Table 2.5 shows the predicted annual total HVAC energy consumption of the building. If this fault

occurred only on one floor, the increase in energy use in the building would be around 0.91%. The impact on the peak demand, however, was minimal, as the VAV boxes would stay close to fully open without the damper fault during periods when the building load peaked.

2.4.3 Supply air temperature sensor offset

For this fault, two types of offsets, namely positive sensor offset and negative sensor offset were simulated. A positive temperature sensor offset will give rise to a lower sensor reading than the actual value. For instance, if the actual supply air temperature is 18^{o}C, the sensor will only feedback a temperature of 14^{o}C (assuming 4 ^{o}C offset). Under the cooling mode, the fault will lead to a warmer supply air temperature, so the VAV box dampers will have to open wider to allow more air to be supplied to cool the zones unless and until the dampers are already fully open. This will lead to an increase in fan energy use but may lead to a reduction in energy use of the chilled water plant. When heating is required in the exterior zones, the reheat energy use will also be reduced.

Conversely, a negative temperature sensor offset will produce a higher sensor reading than the actual value. This fault will lead to a cooler supply air temperature and thus the degree of opening of VAV box dampers will reduce so as to maintain room air temperature control unless and until the dampers have reached the minimum opening position. Consequently, the fan energy use will be reduced but the chilled water plant energy use will become higher. The reheat energy use for the exterior zone in winter will also be increased.

In the study, the positive sensor offset was simulated by increasing the supply air temperature set point from initially 14°C to 18°C in summer and from initially 16°C to 20°C in winter over a one-year simulation. For the negative offset simulation, the supply air temperature set point was changed from 14°C to 10°C in summer and from 16°C to 12°C in winter.

Figure 2.10 and Figure 2.11 show respectively a comparison of the supply air temperature with and without positive temperature sensor offset for a week in January and July. These figures show that the supply air temperature can be maintained at the set-point level with and without the offset during the air-conditioned periods. Figure 2.12 shows a comparison of the damper position for a VAV box in one of the exterior zones when there was a positive sensor offset at the supply air temperature sensor for a week in July. It can be seen that the damper tended to open wider to let more air to flow into the zone to maintain the required temperature set-point. However, the room temperature set-point could not be met even through the damper was already fully opened, as shown in Figure 2.13.

Table 2.6 shows the predicted total energy consumption of the building HVAC system if this fault occurred. The results show that the total energy consumption would be reduced, but occupant comfort will be sacrificed due to the higher supply air temperature. If the fault occurred on one floor only, the energy impact would be about 0.28% less than in the normal case. Again, this fault is easily identifiable by building operators as the high room temperature would attract complaints from building occupants.

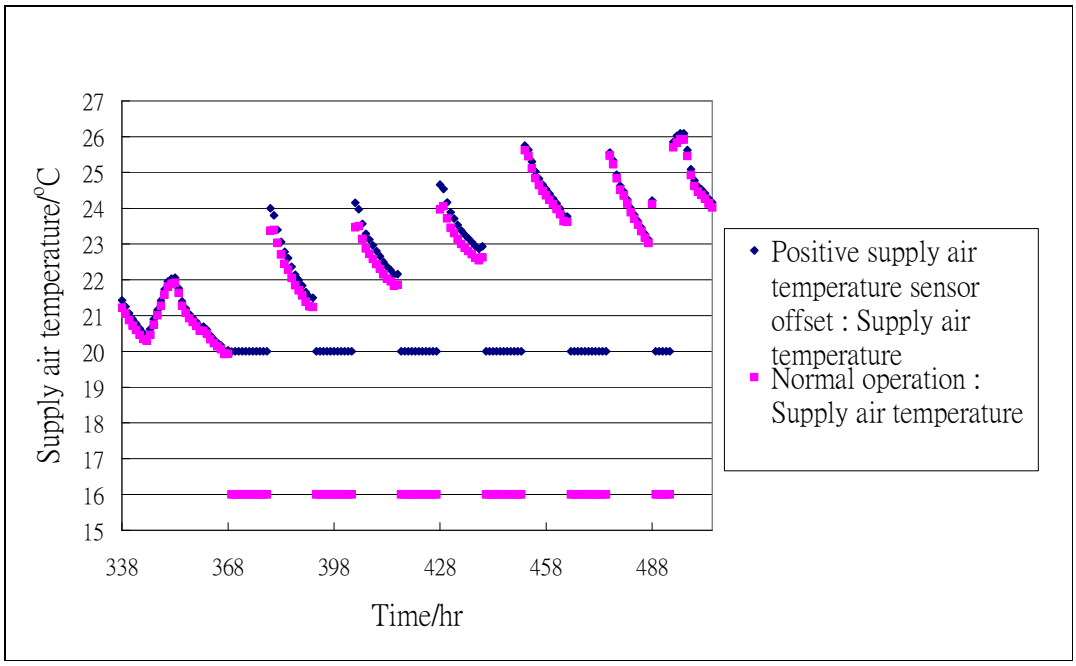

Figure 2.10 Supply air temperature with and without positive supply air temperature sensor offset for a week in January

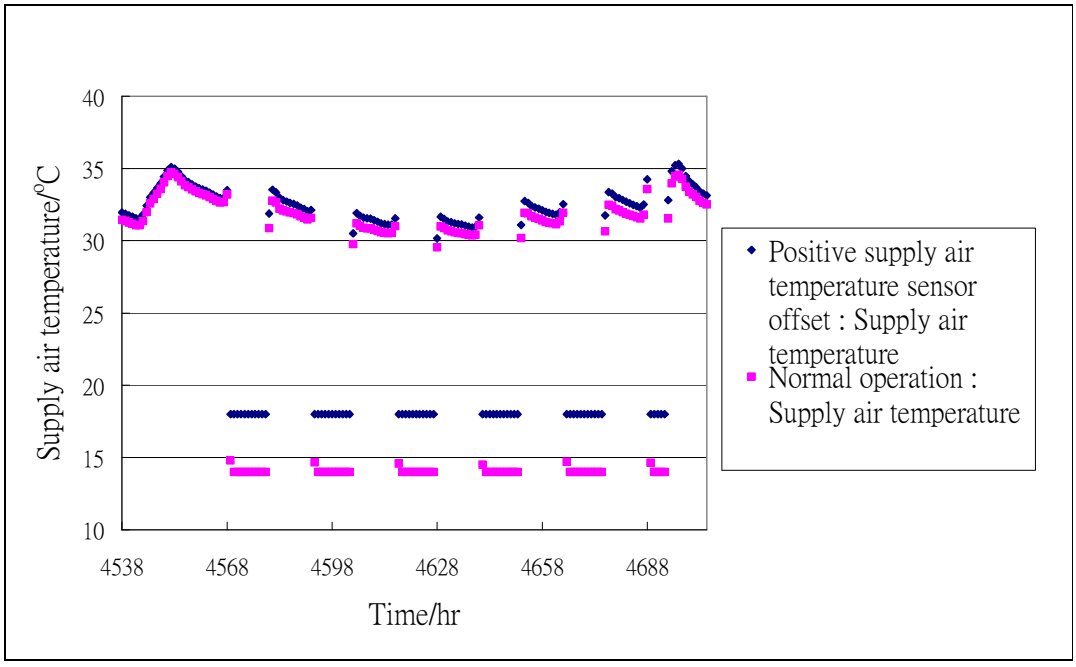

Figure 2.11 Supply air temperature with and without positive supply air temperature sensor offset for a week in July

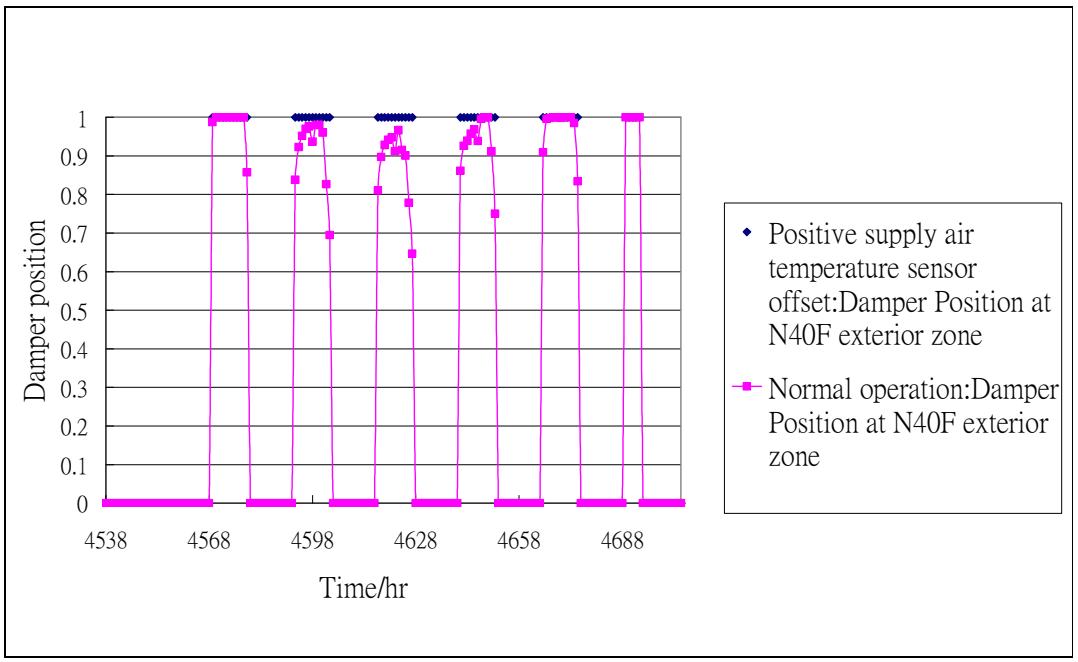

Figure 2.12 Damper position for a VAV box in an exterior zone with and without positive supply air temperature sensor offset for a week in July

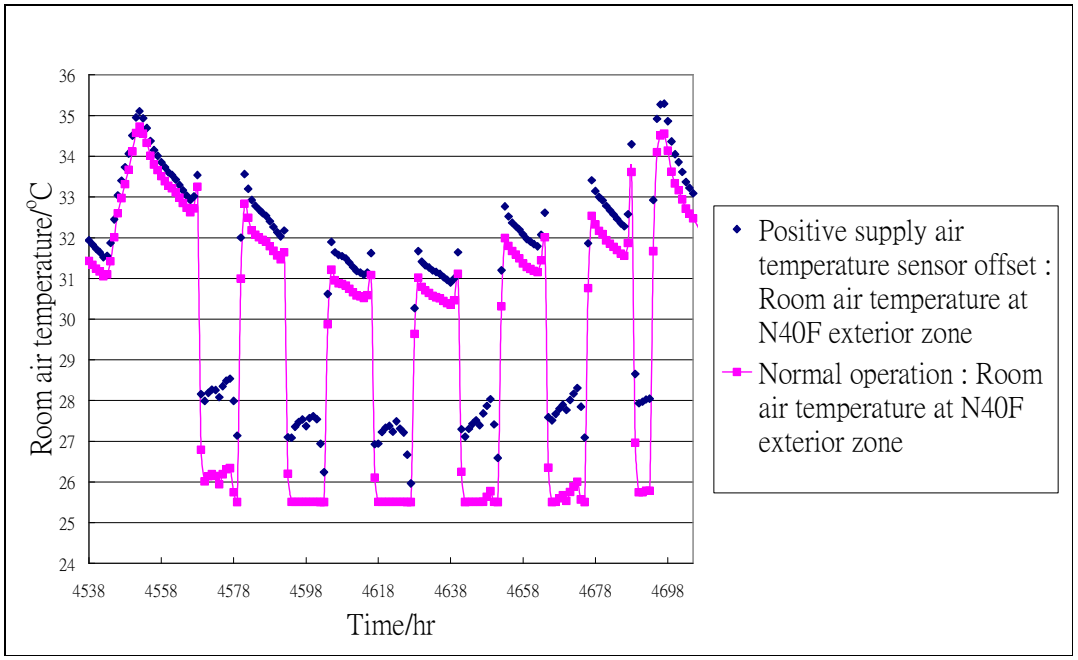

Figure 2.13 Room air temperature in an exterior zone with and without positive supply air temperature sensor offset for a week in July

Table 2.6 Predicted air-conditioning energy consumption with and without positive supply air temperature sensor offset

	Normal	With positive sensor offset	% increase (fault occurring on all floors)	% increase (fault occurring on one single floor only)
Chiller energy (MJ)	13488951	10958211	-18.76	-0.47
Fan (MJ)	3019854	3809955	26.16	0.65
Pump (MJ)	1499996	1307797	-12.81	-0.32
Heating (MJ)	144626	50593	-65.02	-1.63
Total (MJ)	18153426	16126555	-11.17	-0.28
Peak Demand (KVA)	21492268	19161276	-10.85	-0.27

Figure 2.14 and Figure 2.15 show respectively a comparison of supply air temperature with and without negative temperature sensor offset for a week in January and July. Note that the supply air temperature could not be cooled down to 10°C when there was a negative supply air temperature sensor offset on the summer days (Figure 2.15), because the cooling capacity of the air handling unit was insufficient to cater for the increase in cooling demand, which helped curb the energy waste. However, if the system was oversized, which is rather common, more energy would be wasted due to the existence of this fault.

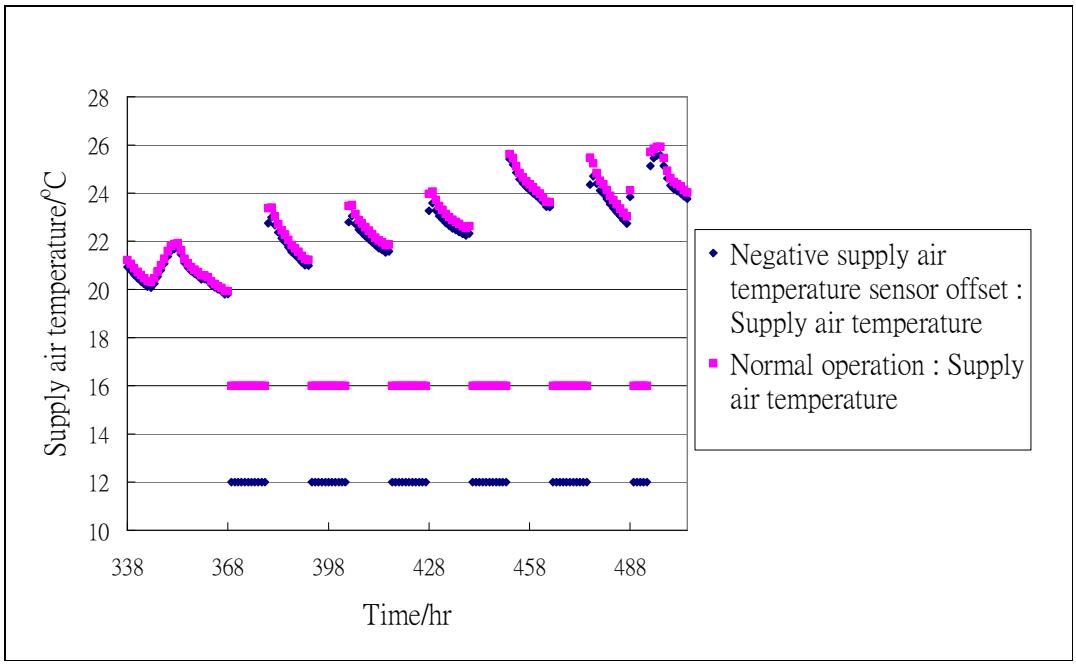

Figure 2.14 Supply air temperature with and without negative supply air temperature sensor offset for a week in January

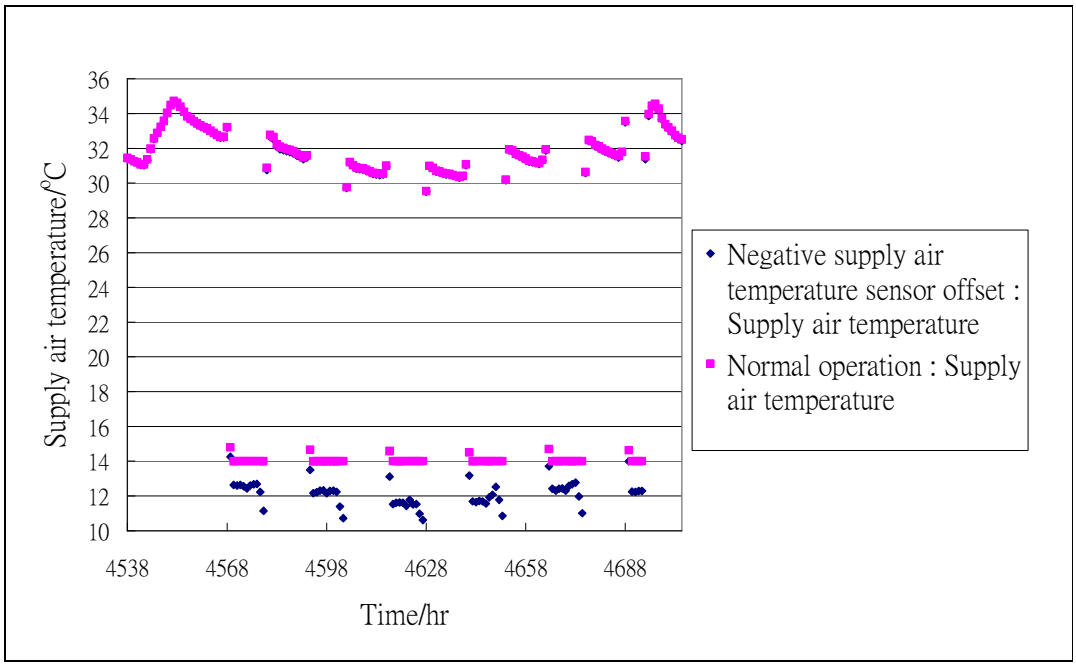

Figure 2.15 Supply air temperature with and without negative supply air temperature sensor offset for a week in July

Figure 2.16 compares the damper position of a VAV box serving the exterior zone in July when there was negative sensor offset by 4°C. As the supply air temperature was lowered, so would be the air flow rate needed to meet the cooling demand of individual zones. The VAV box damper would be positioned to a smaller degree of opening under the dictate of the indoor temperature sensor to reduce supply air flow to the required rate. The room air temperature could be maintained for both cases with and without the fault. This fault would lower the fan energy consumption, but the chilled water plant energy use and the reheat energy use would both be increased (Table 2.7). If the fault only occurred on one floor of the building, the average energy impact would be around 0.29% of the whole building energy use for air-conditioning. The peak demand impact per floor would be around 0.03% increase of the total peak demand of the whole building.

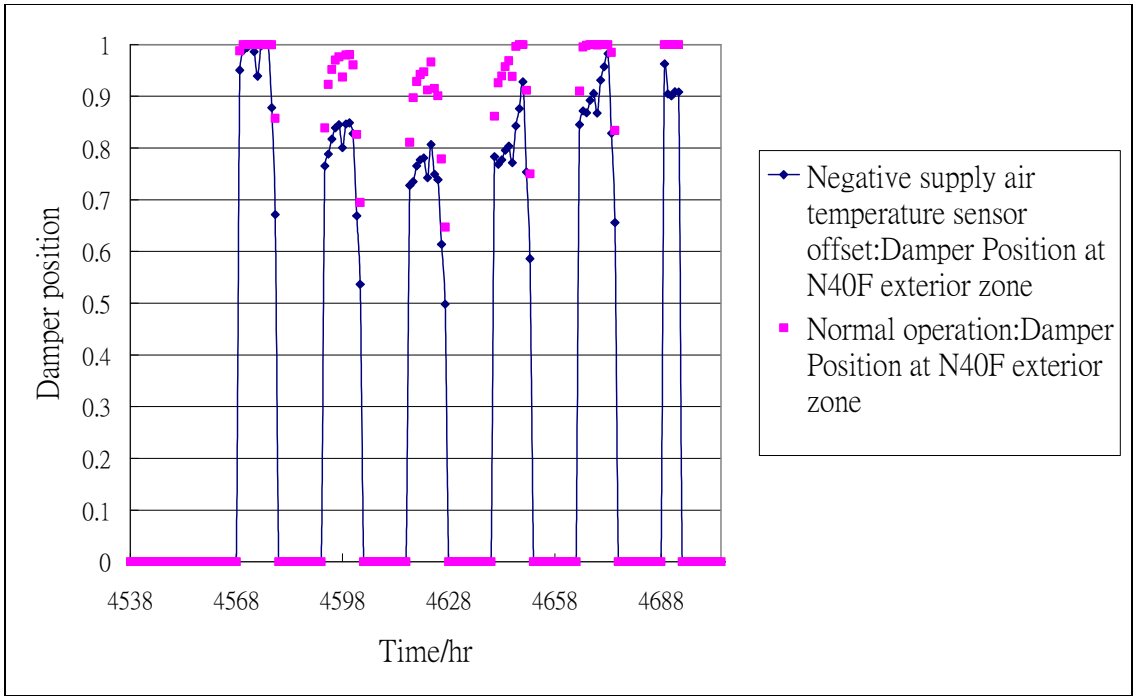

Figure 2.16 Damper position for a VAV box in an exterior zone with and without negative supply air temperature sensor offset in July

Table 2.7 Predicted air-conditioning energy consumption with and without negative supply air temperature sensor offset

	Normal	With negative sensor offset	% increase (fault occurring on all floors)	% increase (fault occurring on one single floor only)
Chiller energy (MJ)	13488951	15682739	16.26	0.41
Fan (MJ)	3019854	2614900	-13.41	-0.34
Pump (MJ)	1499996	1621774	8.12	0.20
Heating (MJ)	144626	315934	118.45	2.96
Total (MJ)	18153426	20235347	11.47	0.29
Peak Demand (KVA)	21492268	21726408	1.09	0.03

2.4.4 Stuck outdoor air damper

This fault is not a control system fault as the outdoor air damper is manually set. For this fault, two types of fault conditions were simulated, namely stuck closed outdoor air damper and stuck open outdoor air damper. For the stuck closed outdoor air damper fault, it was simulated by changing the outdoor air flow to zero. This fault would only deteriorate the indoor air quality as pollutants would be returned back and accumulated in the zone. The occupants could detect the higher odour level if the pollutant can be sensed but the problem would become more serious if it was not detectable. Therefore, this fault should be an important target for a FDD system to detect, although energy may be saved. Table 2.8 shows a comparison of the energy use between the normal and the faulty conditions. If the fault occurred only on one floor, the amount of energy that could be saved would be about 0.29% of the total energy use.

For the case with stuck open outdoor air damper, its effect would be an increase in outdoor intake into the air-conditioning system and thus an increase in the cooling energy use. In the simulation study, the assumption was made that the outdoor air flow rate

would be increased by 25%. Table 2.9 summarizes the increase in total energy use for this fault. If the fault occurred only on a single floor, the energy waste would be 0.08% of the total energy use. The corresponding increase in the peak demand would be around 0.02%. The ability to detect this fault is important to FDD as its consequences are not easily identifiable by building operators.

Table 2.8 Predicted energy consumption with and without stuck closed outdoor air damper

	Normal	Outdoor air damper stuck closed	% increase (fault occurring on all floors)	% increase (fault occurring on one single floor only)
Chiller energy (MJ)	13488951	11521466	-14.59	-0.36
Fan (MJ)	3019854	3019002	-0.03	0.00
Pump (MJ)	1499996	1332129	-11.19	-0.28
Heating (MJ)	144626	144135	-0.34	-0.01
Total (MJ)	18153426	16016733	-11.77	-0.29
Peak Demand (KVA)	21492268	18976930	-11.70	-0.29

Table 2.9 Predicted energy consumption with and without stuck open outdoor air damper

	Normal	Outdoor air damper stuck open	% increase (fault occurring on all floors)	% increase (fault occurring on one single floor only)
Chiller energy (MJ)	13488951	13986094	3.69	0.09
Fan (MJ)	3019854	3020251	0.01	0.00
Pump (MJ)	1499996	1547224	3.15	0.08
Heating (MJ)	144626	144913	0.20	0.00
Total (MJ)	18153426	18698482	3.00	0.08
Peak Demand (KVA)	21492268	21669587	0.83	0.02

2.4.5 Stuck/leaking cooling coil valve

For this fault, four conditions were studied, namely stuck open cooling coil valve, 10% cooling coil valve leakage, 25% cooling coil valve leakage and 40% cooling coil valve leakage. The case with stuck closed cooling coil valve was not studied as operators would be called upon to rectify this fault once it occurred. The stuck open cooling valve fault was simulated by setting the chilled water flow to its maximum value. Figure 2.17 and Figure 2.18 show the normalized chilled water flow rate at cooling coil 1 (representing the coil serving the topmost floor) and cooling coil 2 (representing all the coils serving the 39 typical floors) with and without the fault for a week in January. This fault led to energy penalty due to the extra cooling required, and additionally the extra heating required for offsetting the over-cooling (Figure 2.19). For this reason, the heating energy use was more than 3 times that in the normal case, as shown in Table 2.10. Extra energy was also wasted at the water side HVACR system.

As shown in Figure 2.20, reheat of the supply air was needed in both cases, with and without the fault, on the selected day in January during which the VAV box dampers were closed to the minimum damper position (0.3) to reduce the energy use for reheat. Therefore, the impact of the fault on fan energy use was minimal on that day. However, the room air temperature cannot be maintained. When the room air temperature is cooled down to below the heating set-point of 22^{o}C, the heater would be activated and consume energy until the room air temperature set-point could be put under control. Therefore, with a stuck open cooling coil valve, the extra cooling so caused would entail also a higher heating rate to bring the room air temperature up to the heating set-point. For the other air conditioned periods, the room air temperature was floating between the heating

and cooling set-points, as shown in Figure 2.21. If the fault occurred only on one floor, the energy waste would be about 0.39% of the total energy use. The peak demand impact per floor would be around 0.03%. In reality, this fault could often be found as building operators might fully open the cooling coil valve when there were problems with the control over the control valve (e.g. hunting).

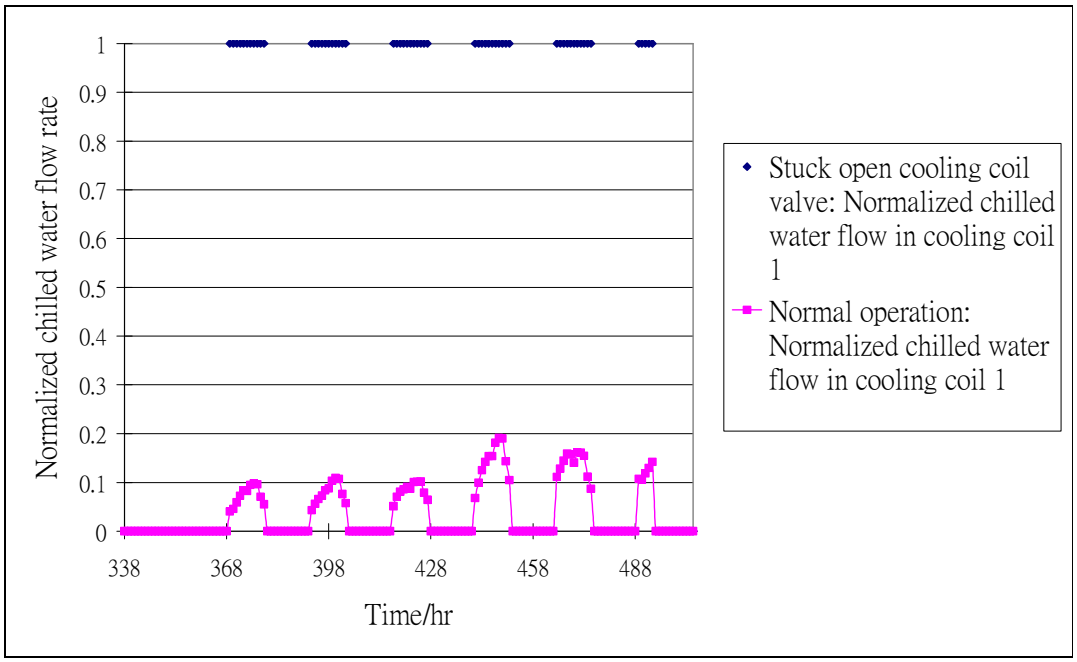

Figure 2.17 Normalized chilled water flow of cooling coil 1 with and without stuck open cooling coil valve for a week in January

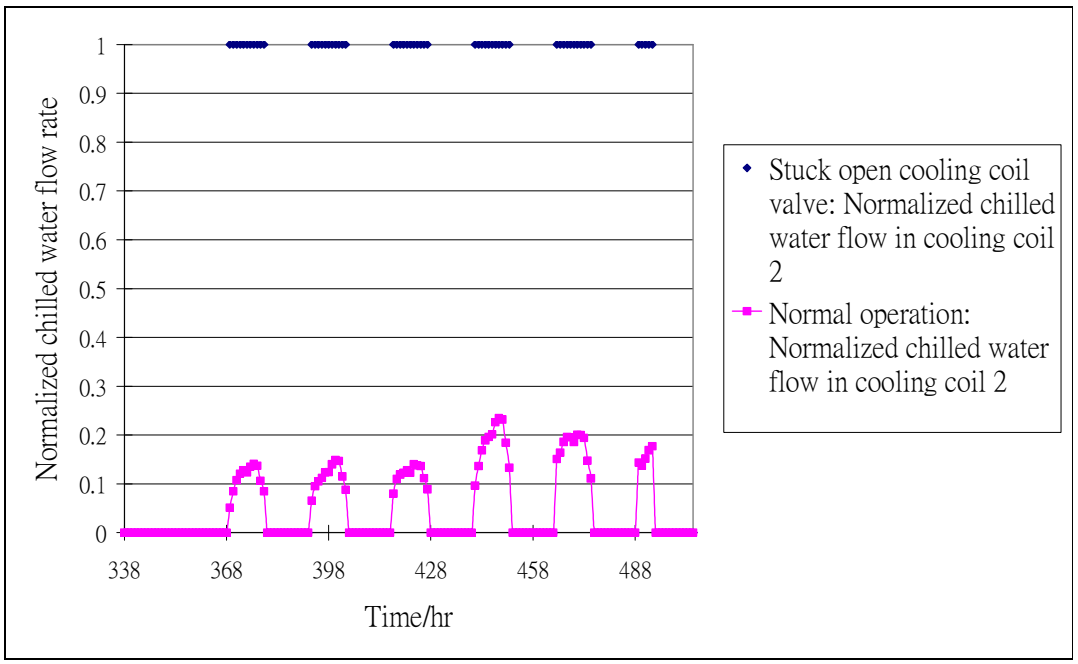

Figure 2.18 Normalized chilled water flow of cooling coil 2 with and without stuck open cooling coil valve for a week in January

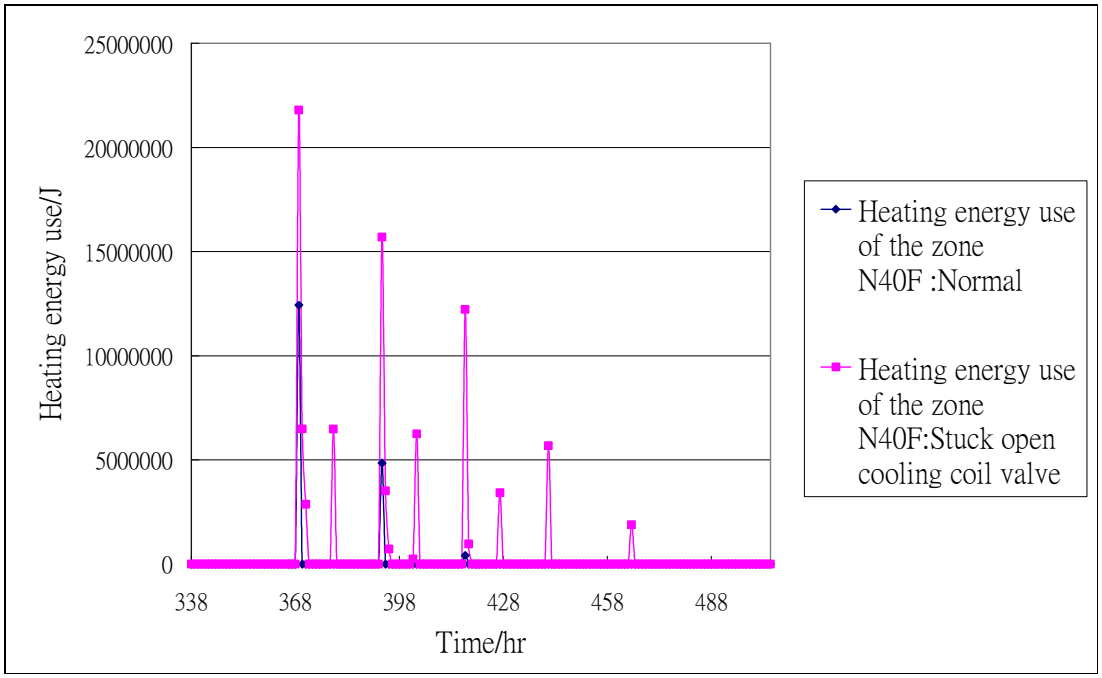

Figure 2.19 Heating energy use in an exterior zone with and without stuck open cooling coil valve for a week in January

Table 2.10 Predicted energy consumption with and without stuck open cooling coil valve

	Normal	Cooling coil valve stuck open	% increase (fault occurring on all floors	% increase (fault occurring on one single floor only)
Chiller energy (MJ)	13488951	16303616	20.87	0.52
Fan (MJ)	3019854	2560585	-15.21	-0.38
Pump (MJ)	1499996	1643996	9.60	0.24
Heating (MJ)	144626	505571	249.57	6.24
Total (MJ)	18153426	21013767	15.76	0.39
Peak Demand (KVA)	21492268	21726398	1.09	0.03

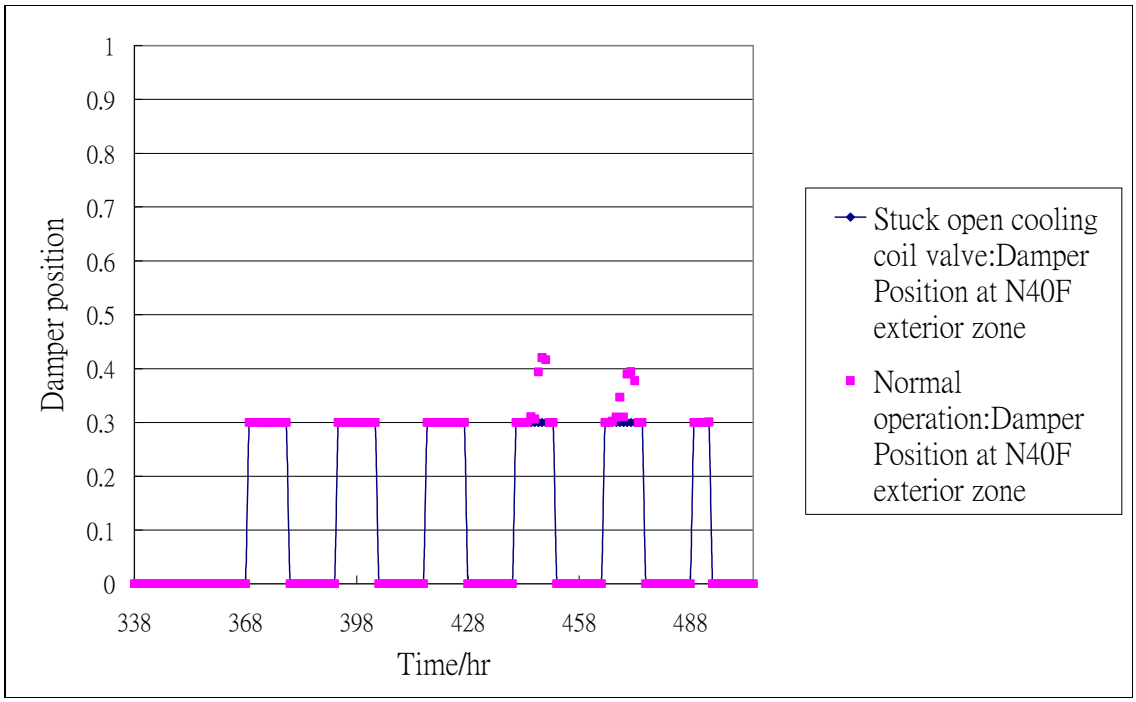

Figure 2.20 Damper position for a VAV box in an exterior zone with and without stuck open cooling coil valve for a week in January

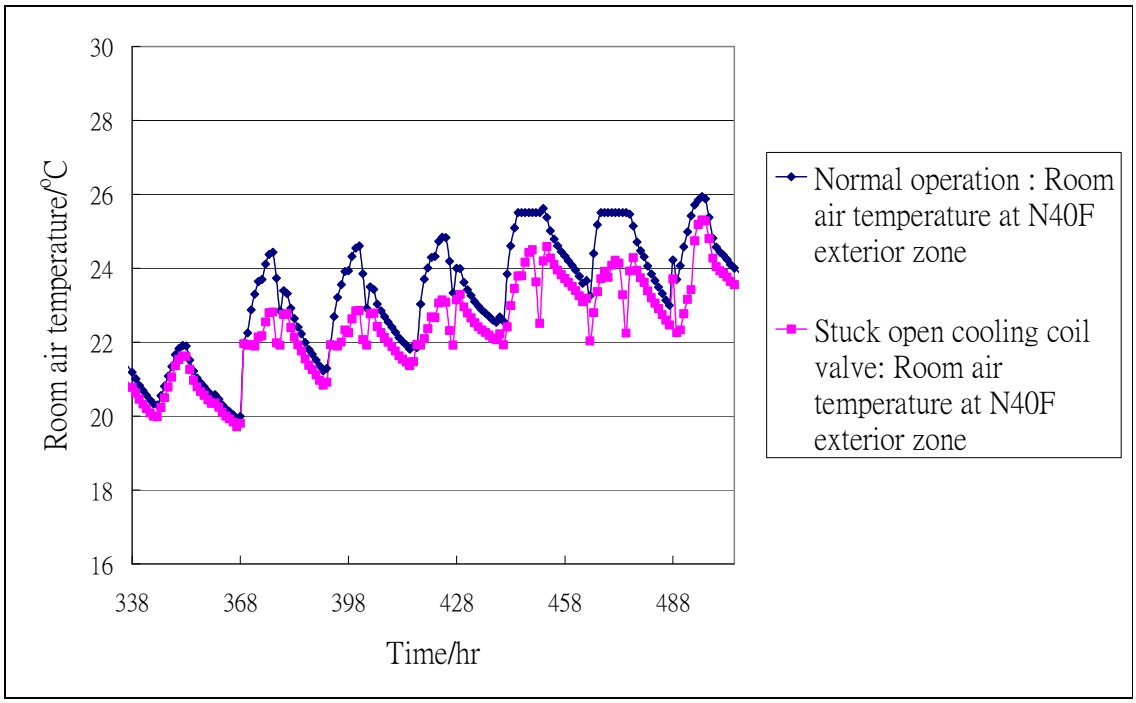

Figure 2.21 Room air temperature in an exterior zone with and without stuck open cooling coil valve for a week in January

The cases with 10%, 25% and 40% leaking cooling coil valve were simulated by changing the minimum water flow respectively to 10%, 25% and 40% of the maximum water flow rate under the normal state. The impacts were similar to, but less serious than, stuck open cooling coil valve, producing energy waste on unnecessary cooling and extra heating to offset the cooling. Table 2.11 shows the energy impact of these faults. It can be seen that the higher was the cooling coil valve leakage, the more energy would be wasted. With such faults, the VAV damper would close and the variable speed fan would reduce in speed to meet the cooling load. The chillers and pumps, however, would consume more energy for coping with the increases in cooling and re-heating incurred by the fault. As shown in Table 2.11, if the faults occurred only on one single floor, the energy waste would be 0.02%, 0.08% and 0.14% for 10%, 25% and 40% cooling coil valve leakage

respectively. Besides, there would not be significant changes in the peak electricity demand, because the chilled water flow would be high anyway when the cooling demand peaked. Since this type of fault is common, it should be seriously considered in devising a FDD system for HVAC&R systems in buildings.

Table 2.11 Predicted energy consumption with and without 10%, 25%, and 40% leaking cooling coil valve

		% increase (fault occurring on all floors)			% increase (fault occurring on one single floor only)		
	Normal	10% leakage	25% leakage	40% leakage	10% leakage	25% leakage	40% leakage
Chiller energy (MJ)	13488951	0.50	3.07	5.96	0.01	0.08	0.15
Fan (MJ)	3019854	-0.15	-2.16	-4.34	0	-0.05	-0.11
Pump (MJ)	1499996	0.60	2.30	3.76	0.02	0.06	0.09
Heating (MJ)	144626	40.29	117.80	179.87	1.01	2.94	4.50
Total (MJ)	18153426	0.72	3.05	5.45	0.02	0.08	0.14
Peak Demand (KVA)	21492268	0	0	0	0	0	0

2.5 Chiller faults

Among all mechanical and electrical equipments in a modern building, chillers are most often the dominant energy consumers. For office buildings in Hong Kong, chillers typically account for 35-40% of their annual energy use (Chan and Yu, 2002). However, various chiller faults may occur due to inadvertent changes in operation conditions, improper installation and operation, inadequate maintenance, wear and tear and aging of components, etc., which may result in interruption in air-conditioning provision, unsatisfactory indoor environment, waste of energy, shortened equipment life and

unscheduled equipment downtime. If the chiller faults can be detected and rectified promptly, energy waste can be minimized, reliability of air-conditioning provision can be raised, maintenance and repair costs can be lowered and useful life of chillers can be extended, which are the major benefits of applying FDD to HVAC systems.

Similar to the air-side system faults discussed above, simulation predictions had been carried out to provide ballpark figures of the energy impacts of various chiller faults. However, the chiller model in the simulation program are not detailed enough to directly model the effects of the chiller faults; the effects of chiller faults can only be reflected in the simulation predictions by artificially changing the relevant input parameters, e.g. by scaling up the normal chiller power demand by a certain percent to mimic the effect of condenser fouling. This work, therefore, commenced with a literature search for ascertaining the effects of common chiller faults, through which to obtain the needed input conditions for use in modelling the consequential effects of presence of chiller faults. The findings of the literature review are summarized below and the simulation results are presented in the following section.

Stouppe and Lau (1989) reported on the causes of 15,716 failures that led to insurance claims in HVAC equipment over a period from 1980 to 1987. For hermetic air-conditioning units, 76% of the failures were attributed to electrical components, 19% to mechanical components, and 5% to items in the refrigeration circuit. For the electrical failures, 87% were due to failures in the motor windings. The causes for motor failures included deterioration of insulation, unbalanced or single phase operations, short circuiting and refrigerant contamination. The mechanical failures usually occurred in the compressor valve, bearings or connecting rods due to general fatigue in the valves and

valve springs, liquid slugging and loss of lubrication. However, the authors did not report on rectification costs for the stated faults.

Stylianou (1996) listed the typical faults occurring in vapor compression and absorption refrigeration equipment. For vapor compression equipment, the three most important faults, in respect of their frequency of occurrence and the adverse effects on equipment efficiency and mechanical integrity, were: i) lack of refrigerant; ii) presence of air in the refrigerating circuit; and iii) presence of refrigerant in the lubricating oil. Lack of refrigerant would result from leakage through shaft seal of the compressor, the tube plates in the condenser and the service valves of the compressor; and other leakage paths, such as small holes in the refrigerant tubing and loose fitting or poor connections caused by corrosion, vibration or poor workmanship. Lack of refrigerant would lead to reduced energy efficiency and negative environmental impacts.

Presence of air in the refrigerating circuit was found to be one of the typical chiller faults, but this fault may only occur in chillers operating at sub-atmospheric pressures, e.g. chillers using refrigerant R11 and R123. Therefore, purge valves are provided at the condensers of such chillers for removal of air collected in the condenser as uncondensed gas (Arora, 1981). At present, few chillers still utilize low pressure refrigerants, and thus this fault is becoming less critical.

Liquid refrigerant in oil can be caused by liquid refrigerant floodback when the system is on and refrigerant migration when it is off. The compressor may be damaged since the refrigerant will tend to remove the lubricating oil, leading to components exposed to wear and causing premature failure of the compressor.

In an analysis of service records for a HVAC service company specialized in equipment for large commercial chain stores, Breuker and Braun (1998a) found that among the faults in rooftop air-conditioners that had led to inadequate thermal comfort, about 60% were electrical and control failures, while mechanical problems only accounted for about 40%. Although compressor failures did not occur as frequently as the other faults (only accounted for 5% of total service call), the repair cost was the highest. Breuker and Braun (1998a) also analyzed the causes of compressor failures. Although most failures in hermetic compressors were perceived to be due to motor failure, they found that these were usually the results of mechanical problems that overloaded the motor. The primary cause of mechanical failures in positive displacement compressors was contaminated liquid refrigerant in the compressors, which could be due to evaporator fouling, condenser fouling, refrigerant overcharge, and a faulty thermal expansion valve. High compressor temperature and electrical supply problems may also lead to early compressor faults.

Comstock and Braun (1999) conducted an extensive survey with the major American chiller manufactures to determine the most likely and costly faults associated with centrifugal and screw chillers. Their survey findings showed that for centrifugal chillers, the most common type of faults was control box or starter failure. Although such faults may cause system downtime, they are easy to detect and fix. Refrigerant leakage was found to be a frequently occurring fault that would incur significant repair costs. The fault was relatively simple to rectify, but its environmental impact may warrant means for their early detection. In respect of repair cost, motor burnout was the most expensive to repair, accounting for more than 25% of the total repair cost. Compressor and electrical problems jointly accounted for 64% of the total repair cost.

For screw chillers, which were becoming more popular in commercial buildings, survey findings showed that water-cooled screw chillers were similar to centrifugal chillers in respect of the range of faults that might occur, but screw chillers seemed to have fewer failures in the compressors and more problems in the piping system (Comstock and Braun, 1999). One special issue found was that the frequency of occurrence and the associated repair cost of refrigerant leakage in water-cooled screw chillers were relatively high. As to air-cooled screw chillers, their survey unveiled that the repair cost for rectifying the fault of motor burnout was halved compared to other chiller types despite having about the same frequency of occurrence.

Among the large number of types of chiller faults identified by Comstock and Braun (1999), most of them can be detected easily even without a FDD system. For example, the occurrence of motor burnout, control box starter failure or condenser fan loss is obvious. Application of FDD should focus on those that may degrade the performance of chillers but are difficult to detect manually. Therefore, the faults that Comstock and Braun (1999) chose for experimental study included: i) reduced condenser water flow; ii) reduced evaporator water flow; iii) refrigerant leakage; iv) refrigerant overcharge; v) excess oil; vi) condenser fouling; vii) non-condensable in the refrigerant; and viii) defective expansion valve.

Cui (2005) also opined that those failures that can be easily detected with simple sensors should not be selected as target faults for surveillance by a FDD system. Reduced condenser water flow and reduced evaporator water flow belong to these failures since they can be readily detected by using precise flow meters for their direct measurement. The faults associated with lubrication (e.g. faulty oil cooler and faulty oil pump) were

also regarded as unimportant to FDD studies, as they can be identified by measuring oil temperature and oil pressure.

According to the literature reviewed above, the typical kinds of chiller faults include compressor failure, reduction of water flow rate, refrigerant leakage, fouling, and faults associated with lubrication. Compressor failure is obvious and can be easily diagnosed manually, which do not require the use of FDD (Comstock and Braun, 1999). Therefore, this fault was not considered in the simulation study.

Oil failures were also not considered because they can be easily detected with the use of oil temperature and pressure sensors. However, flow rate reductions were considered even though these faults can be detected with the use of precise flow meters, because such flow meters are not normally installed in individual chillers given that the chilled and condenser water flow rates are typically held constant. Therefore, the following four chiller faults were selected for the simulation study, namely condenser fouling, refrigerant leakage, reduction of condenser water flow and reduction of evaporator water flow rate.

2.6 Energy simulation

Simulation prediction of the energy impacts of chiller faults was carried out based on the same office building used in the abovementioned study on air-side system faults. However, instead of air-cooled chillers, the chiller plant in the building was assumed to be composed of five water-cooled centrifugal chillers, each with a rated cooling output of 2000kW and a coefficient of performance (COP) of 5. Therefore, the chiller energy consumption of the building will become lower but the pumping energy consumption will

increase due to the presence of extra pumps and extra energy will be used for the cooling towers. Again, the chilled water distribution system was assumed to be a single-loop system with differential pressure bypass control.

As explained above, four typical chiller faults were simulated, namely condenser fouling, refrigerant leakage, reduction of condenser water flow and reduction of evaporator water flow rate.). The methods used to simulate the energy impacts associated with these faults, as summarized in Table 2.12, were based on the experimental results of the ASHRAE research project 1043-RP (Comstock and Braun, 1999). The flow rate reduction faults were simulated by adjusting the pump power in response to higher pump head, again according to the experimental results of the ASHRAE project.

For each simulated fault, the assumption was made first that the fault occurred in all the five chillers. The energy penalty due to the fault thus found was then divided by five to yield the result for the case where the fault occurred in only one chiller. Implicitly, this is based on the assumption that each chiller in the plant had the same probability of being called upon to operate throughout the year.

2.6.1 Condenser fouling

The energy penalty due to condenser fouling was simulated by changing the data on the power and COP of the chillers that were input into the simulation program. The impacts on the chiller power and COP corresponding to the four level of severity of the fault, as shown in Table 2.12, were based the findings of Comstock and Braun (1999). They characterized the fault into four severity levels by reducing 12%, 20%, 30% and 45% condenser tubes so as to reduce the heat transfer coefficient of the condenser.

Table 2.12 The studied faults and the simulation approach

Faults	Severity	Fault simulation approach
Condenser fouling	12% reduction in condenser tube	Increase the chiller power by 0.6% and reduce the COP by 0.8%
	20% reduction in condenser tube	Increase the chiller power by 0.7% and reduce the COP by 0.9%
	30% reduction in condenser tube	Increase the chiller power by 1.9% and reduce the COP by 1.9%
	45% reduction in condenser tube	Increase the chiller power by 3.9% and reduce the COP by 4.1%
Refrigerant leakage	10% refrigerant leakage	Increase the chiller power by 0.6% and reduce the COP by 0.4%
	20% refrigerant leakage	Increase the chiller power by 0.4% and reduce the COP by 0.2%
	30% refrigerant leakage	Reduce the chiller power by 0.9% and increase the COP by 1.2%
	40% refrigerant leakage	Reduce the chiller power by 0.5% and increase the COP by 0.8%
Reduced condenser water flow	10% reduction in flow	Reduce the rated flow rate of condenser pump by 10% and reduce the condenser water pump power by 5%; increase the chiller power by 0.8% and reduce the COP by 0.8%
	20% reduction in flow	Reduce the rated flow rate of condenser pump by 20% and reduce the condenser water pump power by 7.5%; increase the chiller power by 2.7% and reduce the COP by 2.5%
	30% reduction in flow	Reduce the rated flow rate of condenser pump by 30% and reduce the condenser water pump power by 12.5%; increase the chiller power by 3.9% and reduce the COP by 3.2 %
	40% reduction in flow	Reduce the rated flow rate of condenser pump by 40% and reduce the condenser water pump power by 17.5%; increase the chiller power by 7% and reduce the COP by 6.1%
Reduced evaporator water flow	10% reduction in flow	Reduce the rated flow rate of primary water pump by 10% and reduce the primary water pump power by 5.7%; chiller power is unchanged and reduce the COP by 0.2%
	20% reduction in flow	Reduce the rated flow rate of primary water pump by 20% and reduce the primary water pump power by 8.6%; increase the chiller power by 0.4% and reduce the COP by 0.5%
	30% reduction in flow	Reduce the rated flow rate of primary water pump by 30% and reduce the primary water pump power by 14.3%; increase the chiller power by 0.4% and reduce the COP by 1.5%
	40% reduction in flow	Reduce the rated flow rate of primary water pump by 40% and reduce the primary water pump power by 20%; increase the chiller power by 0.5% and reduce the COP by 2.4%

Table 2.13 summarizes the predicted energy impact when the fault occurred. It can be seen that the higher the percentage of fouling, the more energy would be wasted. This fault would cause an increase in energy use of the chillers. Since all chillers are fed

with the same condenser water, the chance to have only one chiller to be fouled is not realistic. The energy waste that this fault would incur, assuming it occurred in all the five chillers, would be 0.88%, 1.05%, 2.27% and 5.05% for 10%, 20%, 30% and 40% condenser fouling respectively.

Table 2.13 Predicted energy consumption with and without condenser fouling

		% increase (fault occurring on all chillers)			
	Normal	10% fouling	20% fouling	30% fouling	40% fouling
Chiller energy (MJ)	8357300	1.50	1.95	3.85	8.55
Fan (MJ)	3018760	0	0	0	0
Pump (MJ)	1880700	0	0	0	0
Heating (MJ)	144650	0	0	0	0
Heat rejection energy use of cooling towers (MJ)	803020	0	0	0	0
Total (MJ)	14154730	0.88	1.15	2.27	5.05
Peak Demand (KVA)	19437727	0.40	0.45	0.74	1.79

2.6.2 Refrigerant leakage

Since the chiller model in EnergyPlus cannot model the effect of changes in refrigerant charge level, it was impossible to estimate the energy impacts of refrigerant leakage through simulation. Instead, reference was made to Comstock and Braun's study (1999) for determining the changes needed to the input data on the chiller performance to reflect the effect of refrigerant leakage. Comstock and Braun studied the effect of refrigerant leakage by removing refrigerant from the chiller by an amount of 10%, 20%, 30% and 40% in turn. Table 2.14 shows the energy impact of this fault. It was interesting that a little energy saving can be achieved in 30% and 40% of refrigerant leak. Comstock and Braun's study (1999) explained that the studied chiller may have a significant safety

factor of refrigerant charge and the expansion valve of the chiller was still able to compensate for the refrigerant loss (see page 73 in Comstock and Braun, 1999). If the fault occurred only in one chiller, the energy would be wasted by 0.04% and 0.03% for 10% and 20% refrigerant leak while energy would be saved by 0.09% and 0.05% for 30% and 40% refrigerant leak.

Table 2.14 Predicted energy consumption with and without refrigerant leakage

		% increase (fault occurring on all chillers)				% increase (fault occurring on one single chiller only)			
	Normal	10% leak	20% leak	30% leak	40% leak	10% leak	20% leak	30% leak	40% leak
Chiller energy (MJ)	8357300	1	0.60	-2.20	-1.40	0.20	0.12	-0.44	-0.28
Fan (MJ)	3018760	0	0	0	0	0	0	0	0
Pump (MJ)	1880700	0	0	0	0	0	0	0	0
Heating (MJ)	144650	0	0	0	0	0	0	0	0
Heat rejection energy use of cooling towers (MJ)	803020	0	0	0	0	0	0	0	0
Total (MJ)	14154730	0.59	0.35	-1.29	-0.82	0.12	0.07	-0.26	-0.16
Peak Demand (KVA)	19437727	0.20	0.15	-0.43	-0.27	0.04	0.03	-0.09	-0.05

2.6.3 Reduced condenser water flow

The energy penalty of this type of fault was simulated by changing the input data on the chiller performance based on the findings of Comstock and Braun (1999) and by reducing both the rated water flow rate through condenser water pump and the water pump power to reflect the effect of a higher pump head, as shown in Table 2.12. Table 2.15 shows the energy impact of this type of fault. It can be seen that this fault may significantly increase the energy use of the chillers, but the pumping power can be reduced. Since most energy use was wasted in the chiller, the total energy impact was very significant. If the fault occurred only in one chiller, the energy use would increase by

0.08%, 0.52%, 0.84% and 1.32% for 10%, 20%, 30% and 40% condenser water flow rate reduction, respectively.

Table 2.15 Predicted energy consumption with and without reduced condenser water flow

		% increase (fault occurring on all chillers)				% increase (fault occurring on one single chiller only)			
	Normal	10% reduced	20% reduced	30% reduced	40% reduced	10% reduced	20% reduced	30% reduced	40% reduced
Chiller energy (MJ)	8357300	1.63	5.78	9.29	14.13	0.33	1.16	1.86	2.83
Fan (MJ)	3018760	0	0	0	0	0	0	0	0
Pump (MJ)	1880700	-4.3	-6.23	-9.68	-13.1	-0.86	-1.25	-1.94	-2.62
Heating (MJ)	144650	0	0	0	0	0	0	0	0
Heat rejection energy use of cooling towers (MJ)	803020	0	0	0	0	0	0	0	0
Total (MJ)	14154730	0.39	2.58	4.18	6.58	0.08	0.52	0.84	1.32
Peak Demand (KVA)	19437727	0.01	0.74	1.2	1.98	0.002	0.15	0.24	0.4

2.6.4 Reduced evaporator water flow

Similar to the simulation of reduced condenser water flow rate, this fault was simulated by changing the input data of chiller with reference to Comstock and Braun (1999)'s finding, as well as regulating the water flow rate in the primary water pump and the pump power to reflect the effect of a higher pump head, as shown in Table 2.12. Table 2.16 shows the predicted total energy consumption of building HVAC&R system. It can be seen that the energy impact of this fault is less serious than the fault of reduced condenser water flow rate since the increase in the amount of chiller energy use was comparatively low. Some pumping energy saving can be achieved, but the total energy use increased. If the fault occurred only in one chiller, the energy use would increase by

–0.06%, –0.01%, 0.12% and 0.2% for 10%, 20%, 30% and 40% evaporator water flow rate reduction.

Table 2.16 Predicted energy consumption with and without reduced evaporator water flow

		% increase (fault occurring on all chillers)				% increase (fault occurring on one single chiller only)			
	Normal	10% reduced	20% reduced	30% reduced	40% reduced	10% reduced	20% reduced	30% reduced	40% reduced
Chiller energy (MJ)	8357300	0.24	1.13	2.83	4.35	0.05	0.23	0.57	0.87
Fan (MJ)	3018760	0	0	0	0	0	0	0	0
Pump (MJ)	1880700	-3.45	-5.37	-8.06	-11.9	-0.69	-1.07	-1.61	-2.38
Heating (MJ)	144650	0	0	0	0	0	0	0	0
Heat rejection energy use of cooling towers (MJ)	803020	0	0	0	0	0	0	0	0
Total (MJ)	14154730	-0.32	-0.05	0.6	0.98	-0.06	-0.01	0.12	0.2
Peak Demand (KVA)	19437727	-0.14	-0.09	0.04	0.12	-0.03	-0.02	0.01	0.02

2.7 Discussion

The energy impacts of five types of air-side system faults and four chiller faults were studied using simulation based on a typical office building model. As found from the fault simulations, stuck open VAV box damper was the most severe fault in respect of the amount of incurred energy wastage, which was about 36% of the total cooling energy use in the building if the fault occurred on every floor of the building. The occurrence of negative room air temperature sensor offset would also cause significant energy wastage, but the impact would be variable, depending on the severity of the sensor drift. Stuck open cooling coil valve and negative supply air temperature sensor offset could also incur waste of energy; each amounted to more than 10% of the total cooling energy use in the building had the fault occurred on every floor of the building. The stuck open outdoor air

damper, leaking cooling coil valve and all studied chiller faults were less serious; their energy impacts would be within 7% of the total building cooling energy use. Other air side system faults could lead to reductions in the total building cooling energy use, but they would adversely impact the indoor thermal environment, and thus should be identified promptly.

For the chiller faults, the reduced condenser water flow was the most severe faults in terms of energy use, which contributed more than 6% of the total cooling energy use in the building if 40% of reduced water flow occurred in all chillers. Condenser fouling also incurred a significant amount of energy use in building, amounted to 5% of the total building cooling energy use if 40% of surface area of condensers of all chillers were fouled. This fault was very important not only in terms of the amount of energy waste; its frequency of occurrence is also high in water-cooled centrifugal chillers (Comstock and Braun, 1999). Although the refrigerant leakage and the reduced evaporator water flow rate were less serious in energy wastage, these two faults were also important for FDD since these faults were in high rank in term of frequency of occurrence, especially in screw chillers according to the survey conducted by Comstock and Braun (1999). The refrigerant leakage was also very expensive to repair (Comstock and Braun, 1999).

The impact of air-handling unit faults may be over-estimated as some faults can be easily identified from complaints of building occupants. These include positive room air temperature sensor offset, positive supply air temperature sensor offset, VAV box damper stuck closed and cooling coil valve stuck closed, which could lead to unbearably high room air temperatures. Therefore, detection of such faults would not require the use of a FDD system. Some types of faults are more difficult to ascertain as the building

occupants may not even notice the fault symptoms. Outdoor air damper stuck closed and outdoor air damper stuck open belong to this type of faults. Some faults, such as negative room air temperature sensor offset, negative supply air temperature sensor offset, VAV box damper stuck open, cooling coil valve stuck open and cooling coil valve leakage may lower the room air temperature, but building occupants may adapt to it and thus would not file complaints. Some may even think that the air conditioning system is good as it can provide more than enough cooling to the conditioned zone. Therefore, these faults are also important to FDD.

For chiller faults, they are usually difficult to detect even for the experienced O&M personnel since many system faults could become apparent only under specific conditions, e.g. condenser fouling may only be evident under high load conditions. These faults are usually identified through thorough investigation by the chiller maintenance personnel according to regular maintenance schedule or requests from the O&M personnel due to system breakdown or any compliant arises. Recognising the limitations of manual diagnosis allows us to appreciate the advantages of chiller FDD.

The benefits of FDD, i.e. the energy cost saving that using FDD can bring is the deterministic factor that influences building owner's decision on whether or not to adopt FDD in their buildings. Energy simulation in this study may provide evidence of the benefits that adopting the FDD technology can bring. Apart from energy savings, FDD can also help the building operators identify potential faults by continuously monitoring the system operation, which would significantly reduce the time for the building operators to identify the fault themselves. FDD will not become a common provision in buildings unless and until the building owners realize the benefits of applying FDD.

3. PERFORMANCE EVALUATION OF CHILLER PLANT BASED ON BMS DATA

3.1 Overview

The energy impacts of various air-side system and chiller faults have been estimated, as presented in the preceding chapter. The present study focused subsequently on the application of FDD to chillers because:

1. Chillers consume a dominant portion of the air-conditioning energy use in buildings in Hong Kong. Faults in chillers or control components may result in waste of energy, insufficient or interrupted space cooling provision and shortened equipment life (Wang and Cui, 2005). Therefore, ensuring chillers will always operate efficiently is a key operation and maintenance (O&M) objective.

2. Chiller faults are generally more difficult to detect manually by plant operators and are costly to rectify. For these reasons, there is a greater need for FDD.

3. The required resources input would be much smaller than applying FDD to the large quantity of air-side systems in a building. Therefore, the chiller plant should be the first target when a building owner makes the first attempt to adopt FDD.

Nowadays, most buildings that are equipped with central air-conditioning systems are also equipped with building management systems (BMS) to facilitate monitoring and

control of the air-conditioning plants. For evaluation of the coefficient of performance (COP) of chillers, which is the most widely used indicator of energy performance of chillers, the system variables to be monitored and trend-logged by the BMS should include the entering and leaving chilled water temperatures and flow rate and the electric power demand of each chiller (Anderson and Dieckert, 1990; Yik and Burnett, 1995). More recently, an analytical or empirical chiller model (e.g. the Gordon and Ng chiller model (Gordon and Ng., 1995)) may be used in conjunction with the measured performance data to detect chiller faults (Sreedharan, 2001). The output of such model may be a performance index or predicted normal performance. A fault could have arisen if the index lies outside the normal range, or the measured performance is deviating significantly from the predicted normal performance. More elaborated fault detection and diagnosis (FDD) systems can identify the type of fault arisen and real-time FDD is possible.

Effective performance monitoring and control of any engineering systems require the presence of sufficient, suitable, accurate and reliable sensors for measuring operating conditions of the systems, which applies to chiller plants. The measured data should also be properly recorded such that plant performance evaluation can be done retrospectively and periodically for detecting if any abnormality or deterioration in system performance has taken place. However, measuring sensors may also become faulty, and when this happens, there will be missing or inaccurate data. This will render performance evaluation or FDD impossible or their results meaningless or misleading. Therefore, special attention should be paid to detecting if there are sensor faults, but this can be a difficult task as symptoms of sensor and system faults could be indistinguishable while multiple faults of both types may occur simultaneously. Ensuring sensors are routinely maintained and

calibrated is essential to proper functioning of any control and BMS systems (BSRIA, 2003) as well as the engineering systems that they control and monitor.

Therefore, this study paid particular attention to identification of the kinds of problems that O&M personnel may encounter in making an attempt to improve chiller plant energy efficiency. Since the range and quality of plant performance records that can be made available are crucial to evaluation of chiller plant performance, and the results of such evaluation are needed to underpin chiller FDD and formulation of appropriate O&M strategies, findings on the kinds of problems that were encountered in analyzing chiller plant operating data retrieved from the BMS records in a building, which included missing data, faulty sensors and insufficient sensor provisions, are highlighted in this chapter.

3.2 Characteristics of chiller plant studied

The operating records of an existing chiller plant over the period from Dec. 2004 to Dec. 2005 were analyzed in the study. Figure 3.1 shows a simplified schematic of the chilled water plant. The chiller plant consists of five identical air-cooled screw chillers, each with a cooling capacity of 300 tons of refrigeration (TR, 1TR = 3.517kW), rated under the operating conditions of entering condenser air temperature at 35˚C, entering/leaving chilled water temperatures at 12˚C/7˚C and chilled water flow rate at 50*l*/s. The rated electric power demand of each chiller was 406kW. The rated COP is, therefore, around 2.6.

As shown in Figure 3.1, the chilled water distribution system of the plant is a two-loop pumping system. Each of the five chillers operates in conjunction with a dedicated

constant speed primary-loop chilled water pump, while three identical variable-speed chilled water pumps are provided in the secondary-loop for distributing chilled water to air-side equipments. The rated flow rate and pumping pressure of the primary-loop pumps are respectively 50*l*/s and 200kPa, and those of the secondary-loop pumps are 125*l*/s and 430kPa. However, the rated power and efficiency of these pumps are unknown as their O&M manuals were unavailable.

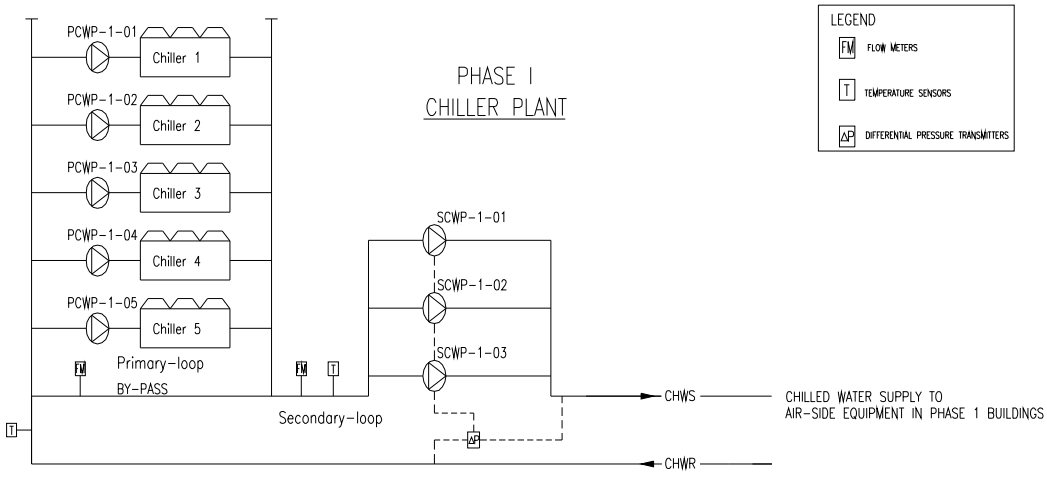

Figure 3.1 Schematic of the chilled water system

3.3 System operation and control

3.3.1 Chiller sequencing control

According to verbal descriptions given by the plant operators, the chiller plant is continuously run with chillers operated in either the day mode or the night mode for all

days in the year irrespective of whether it is a weekday, Saturday, Sunday or public holiday.

In the day mode, the sequencing control strategies used to start and stop chillers and chilled water pumps are based on the cooling demand and the return chilled water temperature. The cooling demand is determined from measurements of the supply and return chilled water temperatures at the main pipes and the total flow rate in the secondary-loop. In this mode, at least one chiller together with its associated primary chilled water pump will be run but one more group of chiller and primary pump will be started if:

1. the cooling demand overshoots the total cooling capacity of the operating chiller(s) and such condition has lasted continuously for 40 minutes; or

2. the secondary chilled water return temperature is higher than the preset level ($15^{o}C$) and such condition has lasted for 40 minutes irrespective of the cooling demand.

On the contrary, one chiller and one primary pump will be stopped if one of following condition occurs:

1. the total cooling capacity of the operating chiller(s) is greater than the cooling demand by 110% of the rated capacity of one running chiller and such condition has lasted continuously for 20 minutes; or

2. the secondary chilled water return temperature is lower than the preset level ($11^{o}C$) and such condition has lasted for 20 minutes irrespective of the cooling demand.

In the night mode, only one chiller is operated and its compressors will be automatically cycled to start or stop according to the chilled water supply temperature by the internal control system of the chiller.

The rationale behind the four criteria for starting and stopping chillers in the day mode had not been clarified; the O&M personnel only claimed that it was only their conventional practice. However, as a reference variable for chiller sequencing control, the cooling demand is preferred to the return chilled water temperature, as the latter can only reflect indirectly changes in the cooling load, which is less accurate compared to using cooling demand directly. Although setting a time delay for the switching action is needed, which will help avoid rapid cycling on and off of chillers and thus maintain stability of system operation, the time delay settings adopted are too long, which will lead to under- or over-cooling in the building. Therefore, it is recommended to reduce the time delay of chiller sequencing.

3.3.2 Pump start-stop control

When a chiller unit needs to be started, its associated primary chilled water pump will be started ahead of the chiller by a lead-time of 1 minute. The sequence will be reversed when the chiller is to be stopped, i.e. when a chiller is stopped, its associated primarily chilled water pump will not be stopped until a 1 minute time-lag has lapsed.

The number of secondary-loop chilled water pumps that will be run is dependent on the number of operating chillers. Only one secondary pump will be operated if there are two or less chillers running. When more than two chillers need to be run, two secondary pumps will be operated. Their running speed is moderated according to the

measured differential pressure across the main supply and return chilled water pipes in the secondary loop of the plant. Maintaining a nearly constant differential pressure across the main supply and return pipes in the secondary-loop would help ensure the differential pressure across any downstream branch will always be equal to or greater than the design pressure difference across each branch. However, as far as minimization of pumping energy use is concerned, this is not the optimal location for measuring differential pressure for use as the feedback signal for secondary-loop pump speed control, unless the nearest branch from the plant is the critical branch (Yik, 1995).

3.4 BMS monitoring sensor

A variety of sensors were installed to enable the BMS to monitor operation of the chiller plant, which include discrete sensors installed at various locations in the chilled water piping system (see Figure 3.1) and those factory-installed sensors inside the chillers. Flow meters are available for measuring the total chilled water supply flow rate in the secondary-loop and the flow rate through the de-coupler bypass pipe but no flow meters are available for measuring the chilled water flow rate through individual chillers. The measurements of the sensors are recorded and stored in the BMS system, at sampling intervals of 15 minutes.

As no technical information about the installed sensors was available, the accuracy of similar sensors available in the market was sourced from manufacturers' technical data, as summarized in Table 3.1. Reference was made to these data in analyses that required knowledge about accuracy of sensors.

Table 3.1 Assumed measurement accuracies of sensors in chiller plant

Type	Measured system variables	Accuracy
Thermistors	Secondary main chilled water supply and return temperatures and inside chillers for measuring temperatures of chilled water entering and leaving individual chillers	±0.3˚C
Electromagnetic Flow meters	Chilled water supply in and bypassing the secondary-loop	±3% of full scale
Differential pressure transmitter	Pressure difference between secondary-loop main supply and return chilled water pipes	±2% of full scale
Kilowatt meters	Power demands of chillers and pumps	±1% of full scale

3.5 Available plant operating data

The chiller plant operation records analyzed in the study were retrieved from the BMS. The raw data available cover the range of system variables as summarized in Table 3.2.

Table 3.2 System variables available from BMS data

System variable
Chilled water supply and return temperatures at each chiller
Main secondary-loop supply and return chilled water temperatures
Bypass chilled water flow rate
Secondary-loop chilled water flow rate
Current demand of each compressor (4 in total) in each chiller
Current demand of each primary-loop chilled water pump (5 in total)
Current demand of each secondary-loop chilled water pump (3 in total)
Electricity supply frequency for each secondary-loop chilled water pump
Differential pressure across the main supply and return pipes in the secondary-loop
Condensing temperature (2 in total) in each chiller
Evaporating temperature (2 in total) in each chiller
Outdoor air temperature (not used since it is inaccurate)
Outdoor air temperature from another chiller plant

In the study, the records of the outdoor air temperature, the chilled water supply and return temperatures and flow rate in the secondary loop, temperature of chilled water

entering and leaving each chiller and the electric current of the major equipment were analyzed. However, the outdoor air temperature data was considered unreliable as data with negative values were observed but such outdoor temperatures never occurred throughout the time span of the data. Therefore, the outdoor temperature records from the BMS of a nearby building of the same owner were obtained for use in the study.

3.6 Lacking adequate amount of sensors

Lacking adequate amount of sensors was the first problem encountered in the study. As there were no flow meters available in the primary chilled water loop, the chilled water flow rate through each chiller could only be estimated based on the assumption that the flow rates through all the running chillers were identical, which was verified to be a good approximation based on a statistical analysis that will be discussed in a later section.

Lacking differential pressure transmitters for the measurement of pumping pressure also restricted the estimate of the pump efficiency, and therefore, whether the pumps were operating efficiently could not be told.

3.7 Compilation of data and identification of missing data

When retrieved from the BMS, the chiller plant operating data were saved into 117 separate files. Each of them comprises periodic measurements of one system variable together with the date and time of each measurement.

To ease analysis, a FORTRAN program was written to compile the data that scatter among the large number of files into a time series of synchronized records in one

single file. Initial inspection of the data unveiled that there were many missing data in the set of data. Therefore, the program was enhanced such that it can also report periods with continuous valid data (data are missing between each consecutive pair of these periods). A list of the availability of valid data has been compiled. A summary of the findings of an analysis on the available data is shown in Table 3.3, which shows the duration with missing data for individual parameters. It can be seen that there were frequent occurrence of missing data. The total duration with missing data amounted to 249 days, during which the longest continuous period with missing data spanned about 121 days.

Table 3.3 Summary on periods with missing data for important parameters

	Total duration of data missing	Longest continuous period of missing data		
		Duration	From	To
Any among the parameters below*	249 days	121 days	15/12/2004 0:00	15/4/2005 1:30
Secondary Ch. W. flow rate	145 days	56 days	26/8/2005 12:15	22/10/2005 9:30
Bypass Ch. W. flow rate	129 days	56 days	26/8/2005 12:15	22/10/2005 9:30
Secondary Ch. W. supply temperature	130 days	56 days	26/8/2005 12:15	22/10/2005 9:30
Secondary Ch. W. return temperature	129 days	56 days	26/8/2005 12:15	22/10/2005 9:30
Chiller 1 return temperature	131 days	56 days	26/8/2005 12:15	22/10/2005 9:30
Chiller 2 return temperature	133 days	56 days	26/8/2005 12:15	22/10/2005 9:30
Chiller 4 return temperature	136 days	56 days	26/8/2005 12:15	22/10/2005 9:30
Chiller 5 return temperature	129 days	56 days	26/8/2005 12:15	22/10/2005 9:30
Chiller 1 current	183 days	121 days	15/12/2004 0:00	15/4/2005 1:15
Chiller 2 current	184 days	121 days	15/12/2004 0:00	15/4/2005 1:15
Chiller 4 current	184 days	121 days	15/12/2004 0:00	15/4/2005 1:15
Chiller 5 current	223 days	121 days	15/12/2004 0:00	15/4/2005 1:15
Primary pump 1 current	104 days	38 days	07/3/2005 11:30	15/4/2005 1:15
Primary pump 2 current	105 days	38 days	07/3/2005 11:30	15/4/2005 1:15
Primary pump 4 current	106 days	38 days	07/3/2005 11:30	15/4/2005 1:15
Primary pump 5 current	107 days	38 days	07/3/2005 11:30	15/4/2005 1:15

* Excluding individual chilled water supply temperature;
Note that Chiller 3 was excluded from the analysis as it did not operate during the period covered by the data obtained.

3.8 Pre-processing data by moving average

Considering that the heat and mass transfer dynamics of the plant and equipment are much faster than the dynamic changes in cooling load and outdoor air condition, the chillers may be assumed to be operating in a quasi-steady state. Nevertheless, the plant

operating records may reflect snap-shots of transient states of the system variables, which will happen when equipments are switched on and off to cope with load variations. Since our proposed chiller performance analysis is based on steady state operation of chillers, it was considered necessary to remove the transient variations in the data series before analyzing chiller performance. Therefore, moving average values of the time series were computed based on a fixed moving time window of a width of 60 minutes. After this data pre-processing procedure, the data can better reflect the quasi-steady state performance of the system.

Figure 3.2 shows a comparison between the original data and the moving average data. As shown in the figure, the peaks and troughs are compressed and the dynamic changes are smoothened by this process, which better reflects the steady operation of chillers. As there was a considerable amount of missing data in the data set, a missing data at a particular time instance could be compensated in the moving average calculation by averaging only the available data in the time window. This was the other purpose served by applying moving average to pre-treat the data.

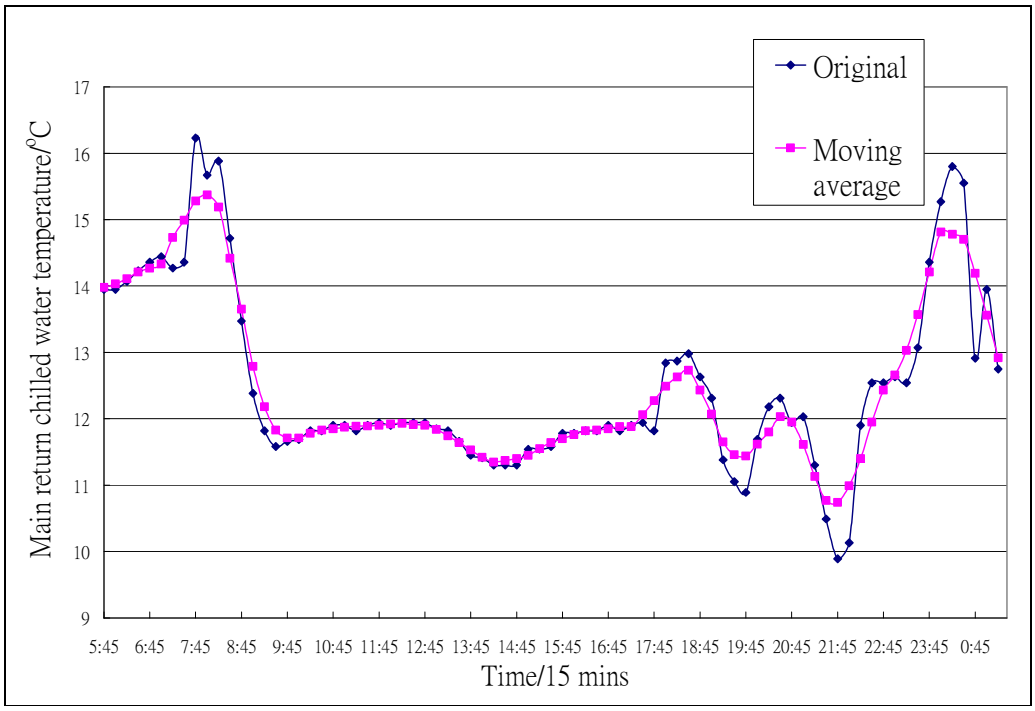

Figure 3.2 Comparison between original data and moving average data of secondary chilled water return temperature [From 5:45, 20/5 to 1:15, 21/5]

3.9 Verification of the accuracy of the measured data

Automatic control and performance monitoring of chiller plants require properly functioning measuring instruments. Sensors, however, may suffer from various faults, including drift, bias, drop in sensitivity and even malfunctioning. Presence of such faults may lead to improper control actions, poor system performance, energy penalty and increased operation and maintenance costs. Therefore, the first step taken in this study was to verify the accuracy of the available BMS plant operation records.

Firstly, in-situ measurement was conducted to verify the accuracy of plant measurements. Simple statistical analysis was then performed to identify if there were systematic errors in the plant performance measurements. A sensor was considered to be

faulty when there is a large deviation between the measurement and the reference. The accuracy of the sensor was further checked by energy balance calculation. The energy balance was calculated by analyzing the difference between the cooling load that is transported to the air-side equipment through the secondary loop and the cooling output of the chillers. A significant difference of this residual value from zero indicates abnormality in the measured data. After detecting and validating the sensor faults, the coefficient of performance of chillers can be estimated with an acceptable accuracy.

In this study, Chiller 3 was excluded because, as the operation record shows, it had not been operated throughout the year. Nonetheless, the recorded temperature data at the chilled water outlet of Chiller 3 were inspected, which unveiled that the measured temperature was often higher than 12^{o}C when other chillers were running. It seems that there was no chilled water leaking through Chiller 3 while it was shut down.

3.9.1 Verification of accuracy of measured data by simple in-situ measurement

Site inspection unveiled that no auxiliary thermometers or thermal wells were available in the piping system for verification of the measurement accuracy of the water temperature sensors. Simple *in-situ* measurements, which involved bleeding-off chilled water from the pipe and measurement of the water temperature using a mercury-in-glass thermometer, had been conducted at locations close to where water temperature sensors were installed. The verification measurements unveiled that the main chilled water supply and return temperature sensors in the secondary-loop and the chilled water return temperature sensors inside individual chillers were ‘reasonably’ accurate (given the crude

method of measurement used and noting that deviations were within ±0.8°C). However, the chilled water supply temperature sensors in individual chillers were outputting readings that are 1.8°C lower than the corresponding water temperatures measured *in-situ* whilst the *in-situ* measurements matched reasonably well with the main chilled water supply temperature when there was surplus flow through the bypass pipe. The built-in supply temperature sensors in the chillers, therefore, were suspected to be faulty.

Electrical measurement was also performed using a power analyzer (model: Fluke 41b) to verify the accuracy of the electric current meter readings for each compressor of each chiller. The measurements showed that the meters were functioning properly and their readings were reasonably accurate.

3.9.2 Chilled water flow rate through individual chillers

Flow meters were provided in the chiller plant for measurement of the secondary-loop chilled water flow rate and the bypass flow rate. However, there were no sensors available for measurement of the chilled water flow rates through individual chillers, which is understandable, as provision of flow meters for this purpose is commonly considered to be unnecessary because the chilled water flow rate through a chiller should stay at constant level. Verification of flow rate could have been done by using a portable ultrasonic flow meter but pipes with sufficient straight-runs were unavailable in the plant which precluded the use of this method. Nonetheless, an analysis was conducted to check if each chiller could be fed steadily with the same chilled water flow rate.

In this analysis, the total primary-loop chilled water flow rate was taken as the sum of the secondary-loop chilled water flow rate (m_{sec}) and the bypass flow rate (m_{by}).

The chilled water flow rate through an individual running chiller (m_i) was determined by dividing the total primary-loop chilled water flow rate (m_{sec} + m_{by}) by the number of operating chillers (N), as shown in equation (3.1).

$$m_i = \frac{m_{\text{sec}} + m_{by}}{N} \tag{3.1}$$

Because many chiller power data were missing, the number of operating chillers was inferred from the chiller compressor power data in conjunction with the associated primarily-loop pump power data. If both data in a time record were above zero, the concerned chiller was regarded as running at that time. The chilled water flow rate in each chiller was then estimated using equation (3.1).

Figure 3.3 shows the frequency distribution of the chilled water flow rate in each chiller and Table 3.4 summarizes the statistics of the chilled water flow rate for each chiller. These results indicate that the chillers were fed with chilled water at flow rates that were close to their rated flow rate, because:

i) about 70% of the data fall into the range of ±1*l*/s from the rated chilled flow rate (50*l*/s);

ii) their mean values were very close to the rated chilled water flow rate;

iii) the standard deviations were all very small (<±3% of mean).

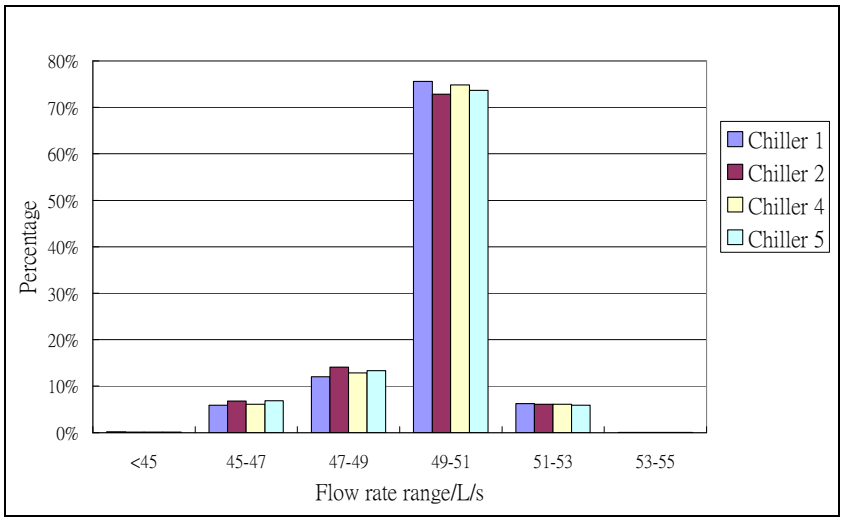

Figure 3.3 Frequency distribution of chilled water flow rate through Chillers 1, 2, 4 and 5

Table 3.4 Statistical analysis on the chilled water flow in each chiller

Chilled water flow rate	Chiller 1	Chiller 2	Chiller 4	Chiller 5
Mean	49.7*l*/s	49.6*l*/s	49.6*l*/s	49.6*l*/s
Standard deviation	1.41*l*/s	1.43*l*/s	1.41*l*/s	1.43*l*/s

3.9.3 Chilled water supply and return temperatures at individual chillers

Simple statistical analyses were performed to identify if there were systematic errors in the measurements of individual temperature sensors, by comparing their measurements with those of a reference sensor, which is believed to be accurate. Unfortunately, no direct temperature measurements for the chilled water returning to chillers were available for use as the reference. Nonetheless, as both the secondary-loop main supply and return chilled water temperature sensors had been verified to be reasonably accurate through on-site measurements (see description in the preceding

section), the return chilled water temperature at each chiller (T_r), which would be the temperature resulting from mixing of the main return chilled water in the secondary-loop with the bypass chilled water, can be estimated based on the supply and bypass flow rates (m_{sec} & m_{by}) and the main supply and return temperatures (T_{ss} & T_{sr}) in the secondary-loop, as shown in the following equation.

$$T_r = \frac{m_{by} T_{ss} + m_{\text{sec}} T_{sr}}{m_{by} + m_{\text{sec}}} \tag{3.2}$$

The return chilled water temperature calculated using equation (3.2) should lie between the main supply and return chilled water temperatures in the secondary-loop whenever there is surplus flow through the bypass pipe (i.e. when m_{by} is positive). When deficit flow occurs in the bypass pipe, the return chilled water temperature at each chiller would then be equal to the main return chilled water temperature in the secondary-loop. The return water temperature determined from this method was taken as the reference for verifying whether the return chilled water temperature sensors in each chiller had been faulty.

A statistical analysis on the deviations of the readings of individual sensors from the reference readings was conducted to indicate whether there was sensor bias and if so how significant. This was studied through computing their mean bias error (algebraic sum of the deviations) and root mean squared deviation from the reference readings. The results, summarized in Table 3.5, show that the readings from the supply temperature sensor in Chillers 1 and 4 had significant positive mean bias errors, which contradicts with the *in-situ* measurement results mentioned above. However, the mean bias errors of

the return temperature sensor readings were much smaller (less than ±1°C), and thus the sensors may be taken as reasonably reliable.

Table 3.5 Statistical analysis on the deviations of individual chilled water temperature sensor readings from the reference readings

	Chiller 1		Chiller 2		Chiller 4		Chiller 5	
Individual sensor	Supply	Return	Supply	Return	Supply	Return	Supply	Return
Main bias error (°C)	2.97	-0.21	-3.15	0.27	2.99	0.41	-1.07	-0.31
Root mean square error (°C)	3.49	0.66	3.22	0.3	3.52	0.43	1.32	0.42

Figures 3.4, 3.5, 3.6 and 3.7 show the relations between the chilled water supply temperatures measured by the sensors in the chillers and the reference supply water temperature for Chillers 1, 2, 4 and 5 respectively. Figure 3.4 and 3.6 suggest that both positive temperature sensor errors (data scattered above the straight line with equation y=x) and negative temperature sensor errors (data scattered below the straight line with equation y=x) may occur even through the mean bias errors for Chillers 1 and 4 were positive.

Furthermore, Figures 3.4, 3.5, 3.6 and 3.7 show also that the main supply chilled water temperature could rise to above 14°C, which can hardly be considered normal. Therefore, further analysis on the main supply water temperature was conducted, which will be discussed in the later section.

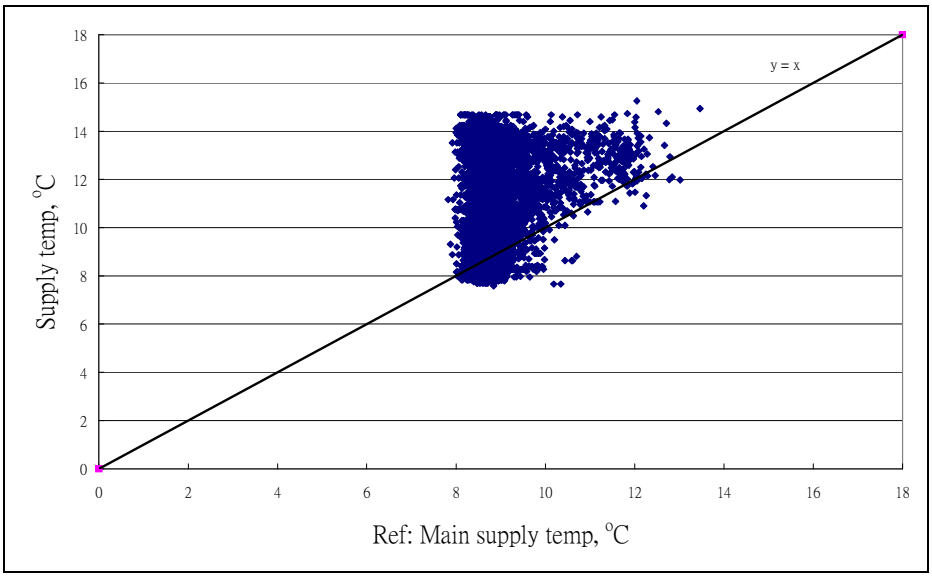

Figure 3.4 Correlation between chilled water supply temperature of Chiller 1 and the reference temperature

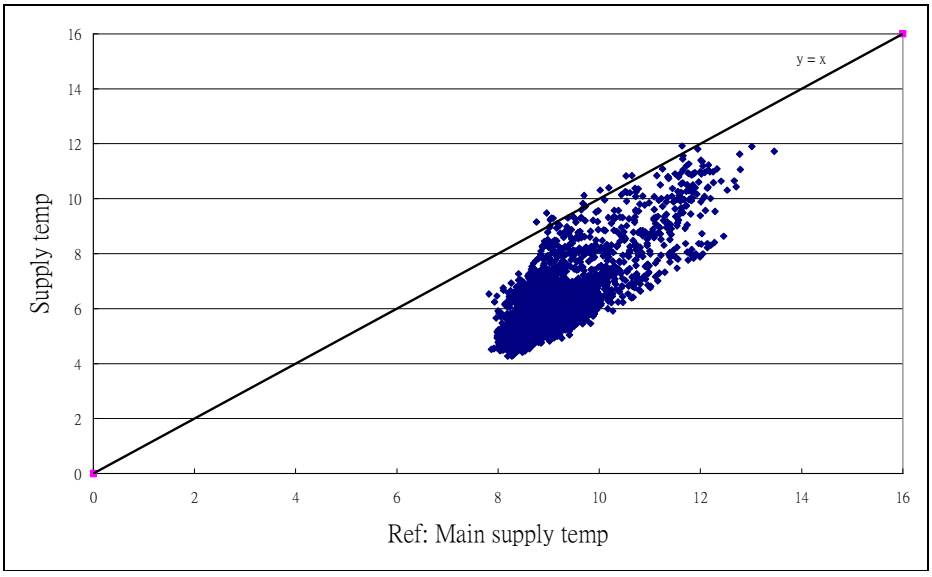

Figure 3.5 Correlation between chilled water supply temperature of Chiller 2 and the reference temperature

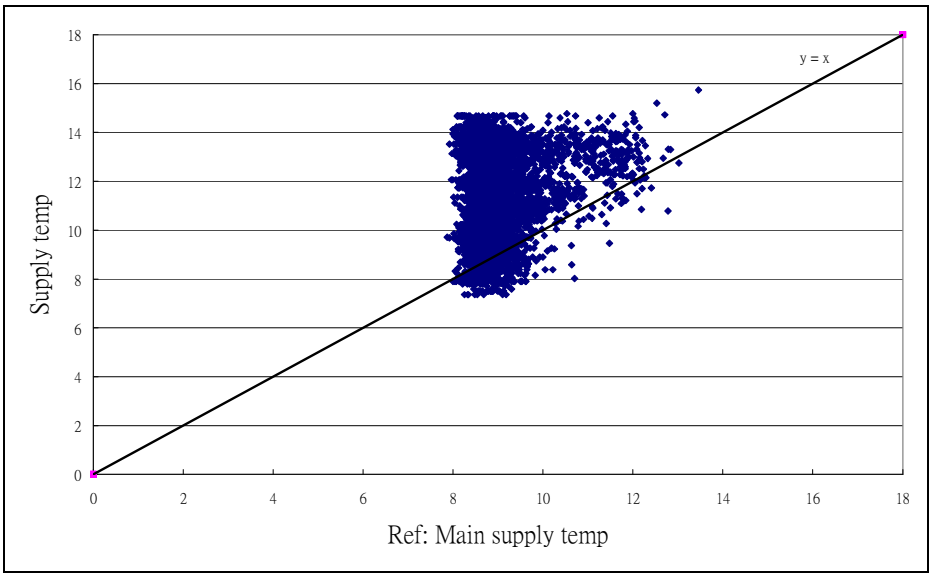

Figure 3.6 Correlation between chilled water supply temperature of Chiller 4 and the reference temperature

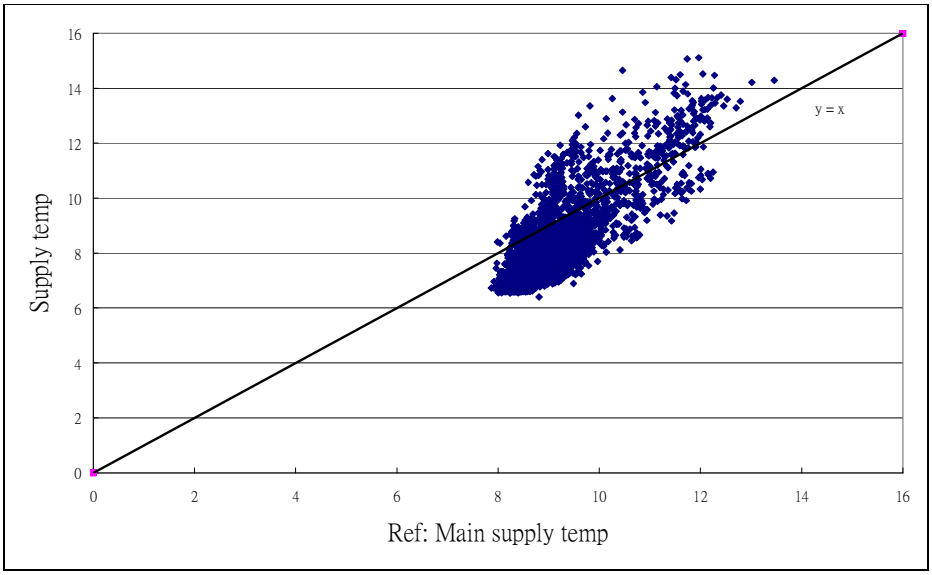

Figure 3.7 Correlation between chilled water supply temperature of Chiller 5 and the reference temperature

As shown in Figures 3.4 and 3.6, the supply chilled water temperatures measured by the sensors in Chillers 1 and 4 had no statistically significant correlation with the measurements of the reference sensor. Many chilled water supply temperatures measured by the chillers' own sensors were higher than the secondary-loop chilled water supply temperature by several degrees, which gave rise to the positive mean bias errors for these chillers as mentioned above (Table 3.5). These may only be possible during periods when a chiller has just been started or stopped while the chilled water pump was running. However, about 65% and 66% of the temperatures measured by the sensors in Chillers 1 and 4 respectively were greater than the reference supply chilled water temperature by more than two degrees under surplus flow condition, which would not be realistic unless a chiller is turned on and off frequently. Besides, it was observed from the data records that such situation could last for several hours, which rules out the possibility that it was due to transient effects. Therefore, the temperature data measured by the supply temperature sensors in Chillers 1 and 4 were regarded as erroneous and were not used in further analysis.

Figures 3.5 and 3.7 illustrate that there are significant correlations between the reference readings and the readings measured by the supply water temperature sensors in Chillers 2 and 5, but there could be serious bias with the sensors. This is also verified by the negative mean bias errors for these sensors, as shown in Table 3.5.

These results indicate a need for a calibration check on the supply temperature sensors in Chillers 1 and 4 to see if replacement is needed while the supply chilled water temperature sensors in Chillers 2 and 4 should be re-calibrated.

As to the return chilled water temperature at each chiller, Figures 3.8, 3.9, 3.10 and 3.11 show respectively the relations of the chilled water return temperatures measured by the sensors in Chillers 1, 2, 4 and 5 with the expected return chilled water temperature, which is the mixed temperature of the return and bypass chilled water.

It can be seen that the majority of the measurements scattered around the straight line that represents perfect correlation for all the chillers studied, which are consistent with the result shown in Table 3.5. Hence, the return water temperature sensors in the chillers may be regarded as normal over the majority of time during the period covered in this study. Nonetheless, many instances of large deviations can also be observed, especially for the return chilled water temperature sensor in Chiller 1. A further study into these outlining conditions, based on energy balance between the primary and the secondary loop, has been done (described in a later section).

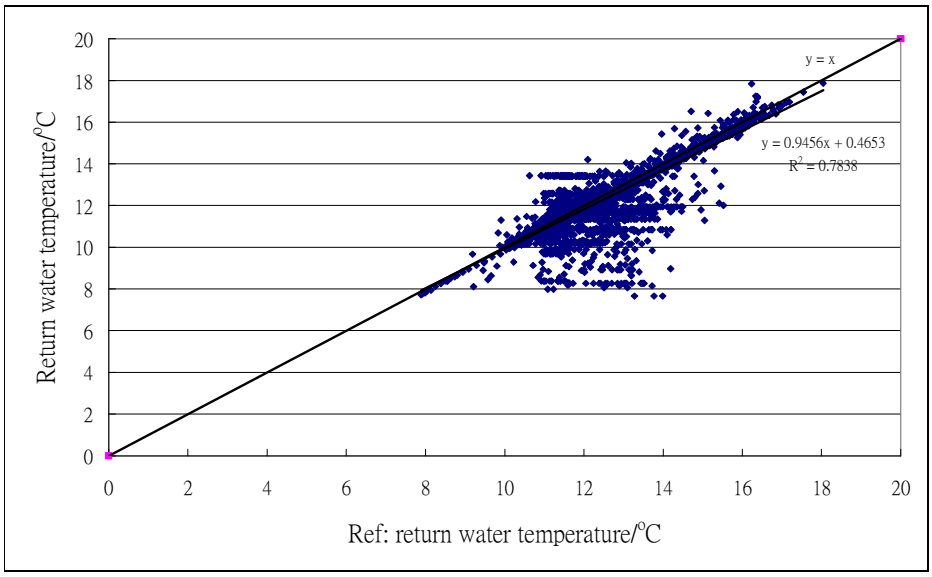

Figure 3.8 Correlation between chilled water return temperature of Chiller 1 and the reference temperature

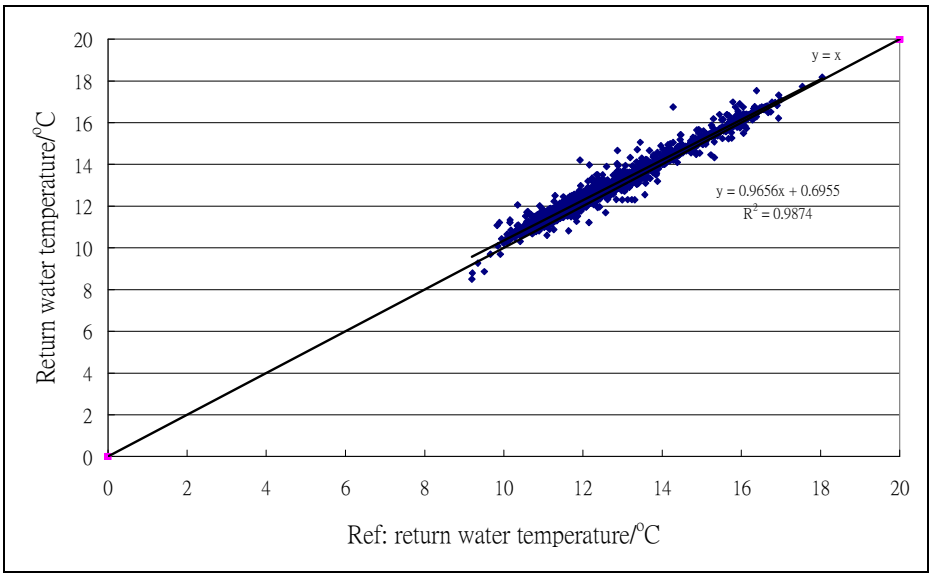

Figure 3.9 Correlation between chilled water return temperature of Chiller 2 and the reference temperature

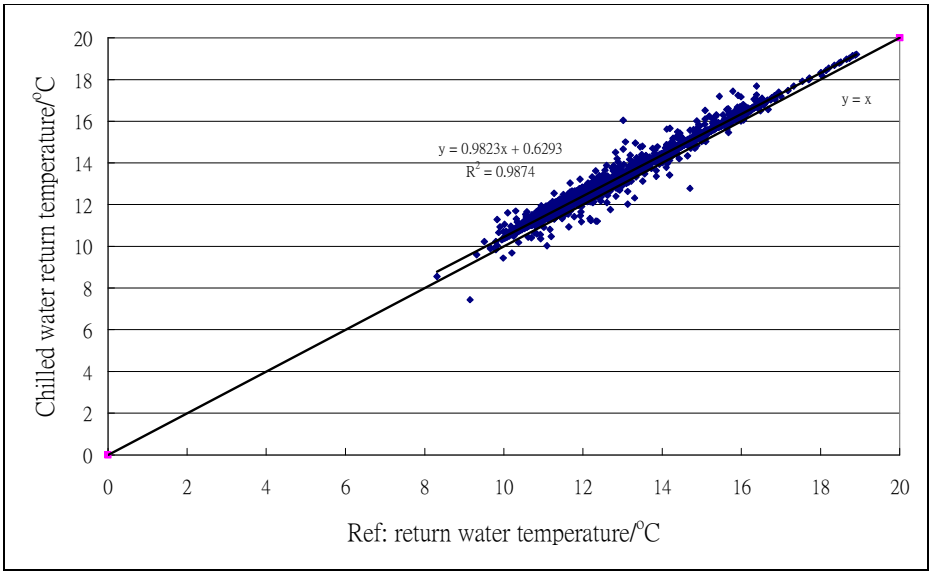

Figure 3.10 Correlation between chilled water return temperature of Chiller 4 and the reference temperature

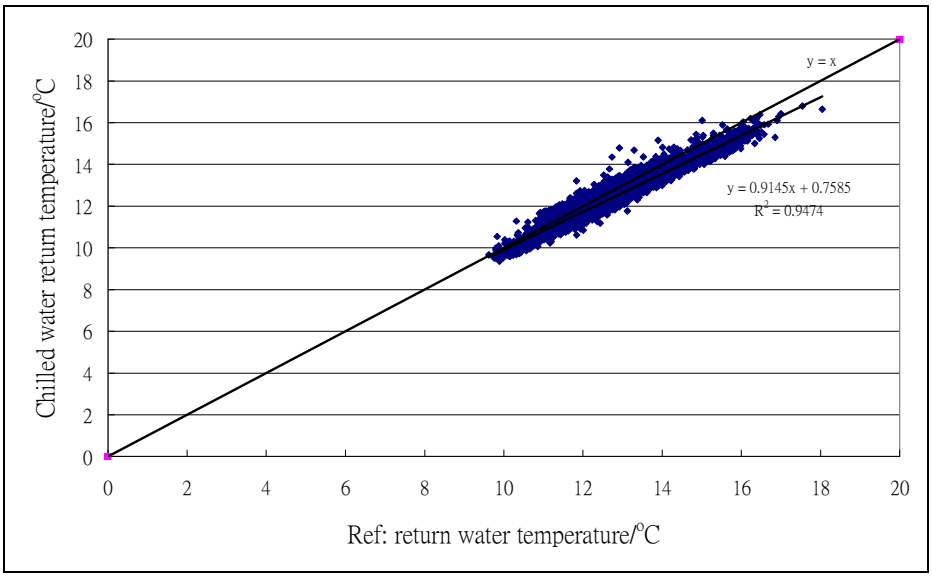

Figure 3.11 Correlation between chilled water return temperature of Chiller 5 and the reference temperature

3.10 Sensor fault detection by energy balance calculation

After verifying the accuracy of individual temperature sensors through basic statistical analysis, the sensor readings were counter-checked by carrying out energy balance estimation on the chiller plant (assuming steady state operation). In theory, the cooling load that is transported to the chiller plant by the chilled water flow from the secondary-loop should equal the total rate of cooling output of the operating chillers in the primary-loop. Therefore, the difference between the two, referred to as the residual cooling load (R_{CL}), as depicted by equation (3.3), should be zero. A significant difference of this residual value from zero indicates abnormality in the measured data.

$$R_{CL} = \left[\sum m_i \cdot c_w \cdot (T_{ri} - T_{si})\right] - m_{\text{sec}} \cdot c_w \cdot (T_{sr} - T_{ss}) \tag{3.3}$$

Where

m_i = chilled water flow rate through the i^{th} running chiller

m_{sec} = total chilled water flow rate in the secondary-loop

T_{ri} & T_{si} = the return and supply chilled water temperatures at the i^{th} running chiller

T_{sr} & T_{ss} = the main return and supply chilled water temperatures at the secondary-loop

c_w = specific heat of water

Such relationship can provide a reliable means for assessing the accuracy of measurements since any system faults do not destroy the relationship governed by the energy conservation. Thus, inspection of the residual cooling load can help identify if there were serious sensor faults and thus verify if the measured data can be used reliably for chiller plant performance evaluation. If the measurement was found to be inaccurate, the data should not be used for further analysis. However, the energy balance method, in its own right, cannot be used to identify whether individual sensors were faulty. This can be done only if reference sensors that can be used for a direct comparison and are known to be accurate are available. In the present case, the secondary main supply and return chilled water temperature sensors were taken as the reference sensors since they were verified to be reasonably accurate through on-site measurements, as discussed in Section 3.9.1.

As pointed out in the preceding discussions, the chilled water supply temperature sensors in the chillers were unable to provide reliable readings. Hence, the supply chilled water temperature (T_{si}) of individual chillers was assumed to be equal to the main supply

temperature in the secondary-loop (T_{ss}), and the latter was used to replace T_{si} in the analysis. The major purpose of the energy balance analysis, therefore, was to verify if, after making this substitution of measurements, the measurements could provide a reasonably accurate basis for chiller performance evaluation. The data pertaining to a chiller were included in the analysis when both the compressor power of the chiller and the power of the associated chilled water pump were significantly greater than zero, which indicate that the chiller was running.

Since the residual cooling load may depart from zero due to inevitable inaccuracies in the measurements used for its evaluation, the uncertainties in the residual cooling load given rise by uncertainties in the measurements were computed to provide the needed reference for determining if the non-zero residual cooling load were natural or due to erroneous measurements. The uncertainties (δR) in an estimation (R) made from measurements (V_i) that are themselves subject to uncertainties (δV_i) can be quantified using the Kline and McClintock's method, as shown in equation (3.4) (Yik and Chiu, 1998).

$$R = f(V_1, V_2, ...V_n)$$

$$\delta R = \sqrt{\sum_{i=1}^{n} \left(\frac{\partial R}{\partial V_i} \cdot \delta V_i \right)^2} \qquad (3.4)$$

Where

R = an estimate made from variables V_1 to V_n

δR = uncertainty in the estimate R

δV_1 to δV_n = uncertainties in the variables V_1 to V_n

The uncertainty limits for the estimates of residual cooling load (R_{CL}, equation (3.3)), determined using equation (3.4), can provide a reference for judging if the residual values are within the expected range given rise by the expected uncertainties in the variables used for their estimation. In the calculation, the measurement inaccuracies of the temperature sensors and flow meters (Table 3.1) were taken as the uncertainties in the temperature and flow measurements (δT_{ri}, δT_{si}, δT_{sr} & δT_{ss} and δm_{sec}).

Recall that the chilled water flow rates through individual chillers are unknown but the estimated values (see previous descriptions) were all close to the rated value. According to Chebyshev's rule, at least 75% of measured data should fall within 2 standard deviations from the mean (Hogg, 1993). Hence, the uncertainty in the chilled water flow rate of each chiller (δm_i) was taken as twice the standard deviation found in the previous estimates (Table 3.4), which are about 2.8*l*/s. With reference to equations (3.3) and (3.4),

$$\delta R_{CL}{}^2 = \sum\left[\left(c_w \cdot (T_{ri} - T_{si}) \cdot \delta m_i\right)^2 + \left(m_i \cdot c_w \cdot \delta T_{ri}\right)^2 + \left(m_i \cdot c_w \cdot \delta T_{si}\right)^2\right] + \left(c_w \cdot (T_{sr} - T_{ss}) \cdot \delta m_{\text{sec}}\right)^2 + \left(m_{\text{sec}} \cdot c_w \cdot \delta T_{sr}\right)^2 + \left(m_{\text{sec}} \cdot c_w \cdot \delta T_{ss}\right)^2$$

$$\delta R_{CL} = \sqrt{\sum\left[\left(c_w \cdot (T_{ri} - T_{ss})\delta m_i\right)^2 + \left(m_i \cdot c_w \cdot \delta T_{ri}\right)^2 + \left(m_i \cdot c_w \cdot \delta T_{ss}\right)^2\right] + \left(c_w \cdot (T_{sr} - T_{ss}) \cdot \delta m_{\text{sec}}\right)^2 + \left(m_{\text{sec}} \cdot c_w \cdot \delta T_{sr}\right)^2 + \left(m_{\text{sec}} \cdot c_w \cdot \delta T_{ss}\right)^2} \qquad (3.5)$$

As an illustration, the uncertainty values of the measurements that were used in the calculation and the uncertainty in the residual cooling load calculated using equation (3.5) for one of the operation conditions are shown in Table 3.6. Under this condition, all

chillers were operating to cope with the building load and, as the result shows, the residual cooling load is within the uncertainty due to individual measurements.

Table 3.6 Calculation of uncertainty of residual cooling load

Measurement	m_1	m_2	m_4	m_5	m_{sec}	T_{r1}	T_{r2}	T_{r4}	T_{r5}	T_{sr}	T_{ss}
Measurement data	50	50	50	50	198	15.37	15.32	15.65	14.94	15.28	11.4
Uncertainties of measurement	2.82	2.86	2.82	2.86	6.3	0.3	0.3	0.3	0.3	0.3	0.3
Residual cooling load	66.2										
Uncertainty of Residual cooling load	418										

The residual cooling loads calculated from the plant records are shown in Figure 3.12. In this analysis, the data between the months December 2004 and March 2005 were ignored since it had abnormally high supply chilled water temperatures. This problem will be further discussed in the next section.

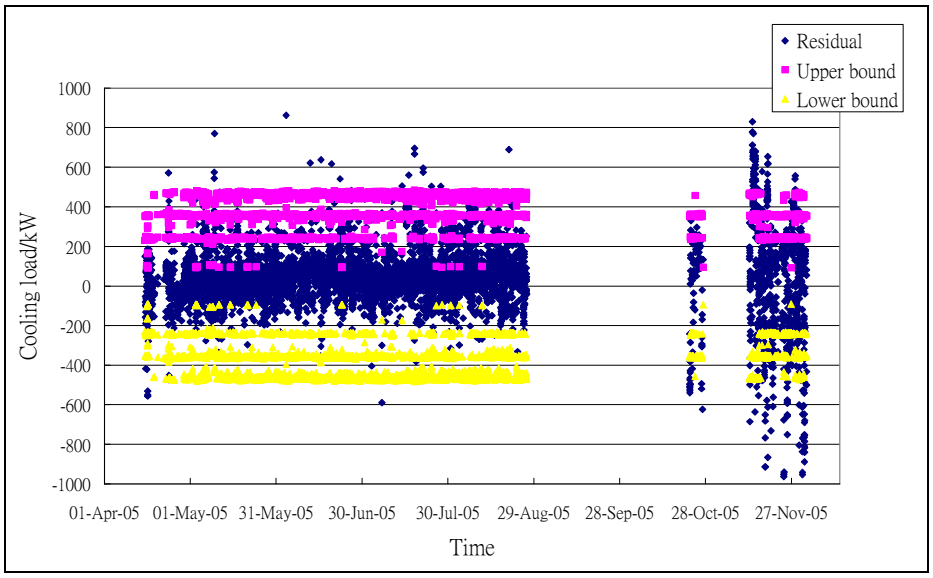

Figure 3.12 Residual cooling load – the difference between the total cooling output of chillers in the primary-loop and the load transported to the plant by chilled water flow in the secondary-loop based on moving average data

It can be seen from Figure 3.12 that the vast majority of the residuals falls within the uncertainty limits. Residual cooling loads of such magnitudes could arise simply because of the uncertainties in the variables that were used in their estimation. Therefore, the hypothesis that such residual cooling loads were due to uncertainties in the measured variables or estimates made from other measured variables cannot be rejected. Nevertheless, there are 1,645 outliers which represent cases where faulty conditions might have existed. It follows that identification of faults should concentrate on those outliers.

Further tests on the data in those records which belong to the outliers were conducted for identification of faults. For an analysis of the abnormal operating conditions which were highly likely to be caused by faulty sensor readings, only those

data where the return chilled water temperature of a chiller is higher than or lower than the calculated return water temperature by 2˚C or more when the chiller was operating were extracted for a closer examination. The frequency of occurrence of such serious deviation of sensor reading from the reference value was counted and the results are summarized in Table 3.7.

Table 3.7 Frequency of occurrence of sensor reading deviating from reference value by ±2˚C

	Chiller 1	Chiller 2	Chiller 4
Chilled water return temp. higher than the reference value by 2˚C	17	2	1
Chilled water return temp. lower than the reference value by 2˚C	153	0	0

It was found that among the 1,645 data that stayed outside the uncertainty ranges which could be explained by the uncertainties in measurement of the sensors under normal conditions, 89% of the built-in return chilled water temperature sensor readings are within the ±2˚C range. There are totally 17, 2 and 1 data records which had an abnormally high chilled water return temperature for Chillers 1, 2 and 4 respectively. It was found that the abnormal data include 1 from Chiller 1, 2 from Chiller 2 and 1 from Chiller 4, which were due to the influence of transient operation of chillers.

For the potentially faulty data records with high chilled water return temperature at Chiller 1, it was found that continuous positive sensor drift (higher than 2^{o}C above the calculated return water temperature) occurred during the period from 18:15 to 20:15 on 13/11/2005. However, for the others cases of abnormally high chilled water return temperature, they occurred intermittently and their reasons were unknown.

For those cases of abnormally low chilled water return temperature for Chiller 1, it was found that this condition occurred in seven continuous periods as listed below, which are believed to be due to a negative sensor drift (lower than the calculated return water temperature by 2^{o}C or more). For the other cases, the fault occurred intermittently for which no reasons can be determined.

12:45-17:30	on	22/10/2005,	
13:45-16:00	on	17/11/2005,	
20:45-22:00	on	17/11/2005,	
20:15-21:45	on	19/11/2005,	
13:15-19:15	on	25/11/2005,	
15:00-17:30	on	26/11/2005,	and
13:00-17:30	on	1/12/2005	

The occurrence of several periods of continuous positive and negative sensor drift was noticed for Chiller 1, which seemed unreasonable. Noting that most of the abnormalities occurred after 12:30 on October 2005, a graph showing the temperature residual between the chilled water return temperature and the estimated return temperature was plotted, as shown in Figure 3.13, for a visual inspection. This shows that the temperature residual deviated largely from zero and therefore, temperature sensor drift was confirmed after 12:30 on 22/10/2005. Further analysis of the sensor drift was conducted by studying the relations of return temperature residual with the return chilled water temperature of Chiller 1 after 12:30, 22/10/2005, as shown in Figure 3.14. This suggests that the sensor drift was not constant but was dependent on the return chilled water temperature, which also explains why both positive and negative sensor drifts co-existed in the temperature sensor.

As some abnormal data in the plant operation records were found to be due to the influences of transient operation of chillers, instead of using moving average data at 15min intervals, hourly average values of the recorded data were computed to minimize

such influences. After this, the analysis was repeated using the hourly average data. Figure 3.15 shows the residual cooling load computed based on hourly average temperature and water flow data. Again, the data pertaining the first four months were not used in the analysis.

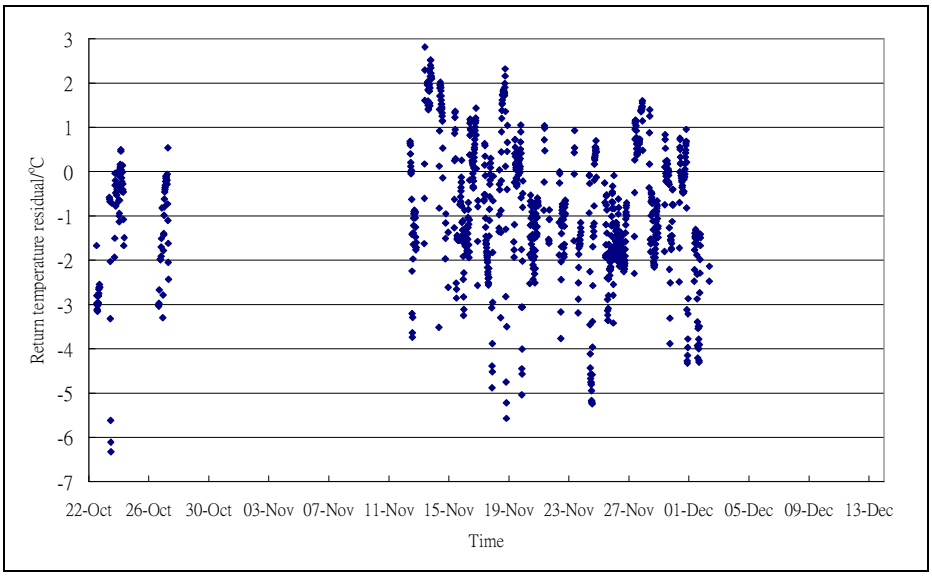

Figure 3.13 The difference between the chilled water return temperature and the calculated chilled water return temperature based on moving average data after 12:30 on 22/10/2005

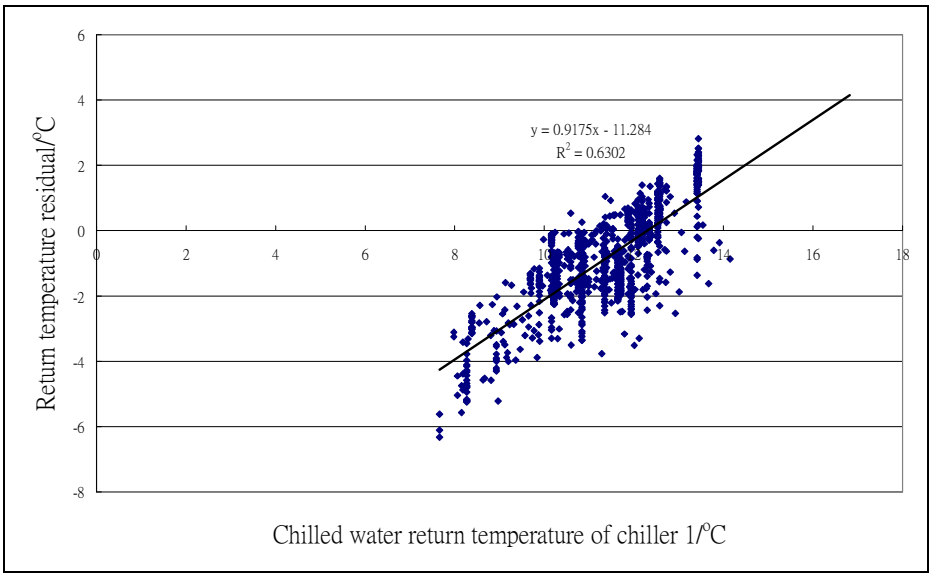

Figure 3.14 The relationship between the return temperature residual (sensor drift) and the chilled water return temperature based on moving average data after 12:30 on 22/10/2005

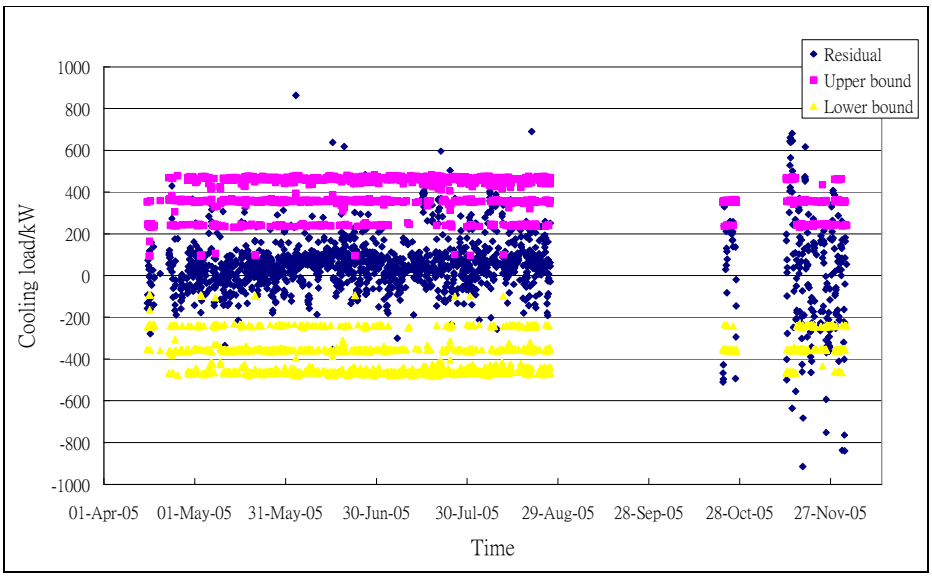

Figure 3.15 Residual cooling load – the difference between the total cooling output of chillers in the primary-loop and the load transported to the plant by chilled water flow in the secondary-loop based on hourly average data

There are 377 records that lie outside the boundaries of uncertainty explainable by uncertainties in measurement by normal sensors. Compared to the earlier results, no influence of transient operation on operation records was observed. It was found that among the 377 records, 89% of the return chilled water temperature readings fall within the ±2˚C range, which is regarded as normal. Table 3.8 shows the total hours of occurrence of return chilled water temperature readings exceeding this range. These abnormal data were only due to the influence of sensor faults as the abnormal data due to transient operation of chillers are removed.

Table 3.8 Frequency of occurrence of hourly average sensor reading deviating from reference value by ±2˚C

	Chiller 1
Chilled water return temp. higher than the reference value by 2˚C	3
Chilled water return temp. lower than the reference value by 2˚C	37

As suggested by the previous discussion that the return chilled water temperature reading of Chiller 1 was highly abnormal after October 2005, the temperature residual between the measured chilled water return temperature and the estimated return chilled water temperature of Chiller 1 after 13:00 on 22/10/2005 was calculated and presented in Figure 3.16, which confirmed the previous conclusion that the chilled water return temperature sensor of Chiller 1 was likely to be faulty after 22/10/2005.

Furthermore, the relations between the temperature residual and the return chilled water temperature of Chiller 1 after 13:00 on 22/10/2005 was as shown in Figure 3.17. The temperature sensor drift was estimated and found to be approximately equal to the drift estimated before, as shown by the equation in Figure 3.14.

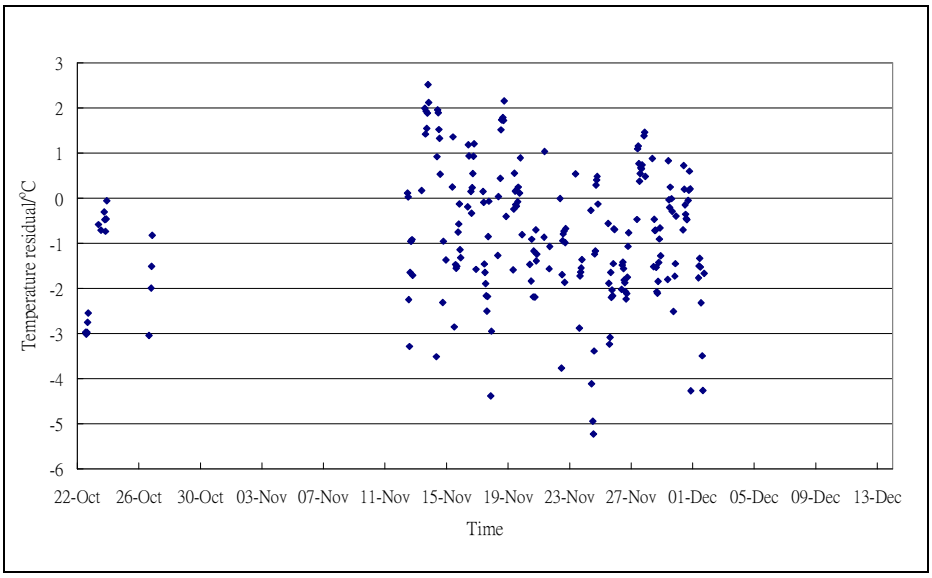

Figure 3.16 The difference between the chilled water return temperature and the calculated chilled water return temperature based on hourly average data after 13:00 on 22/10/2005

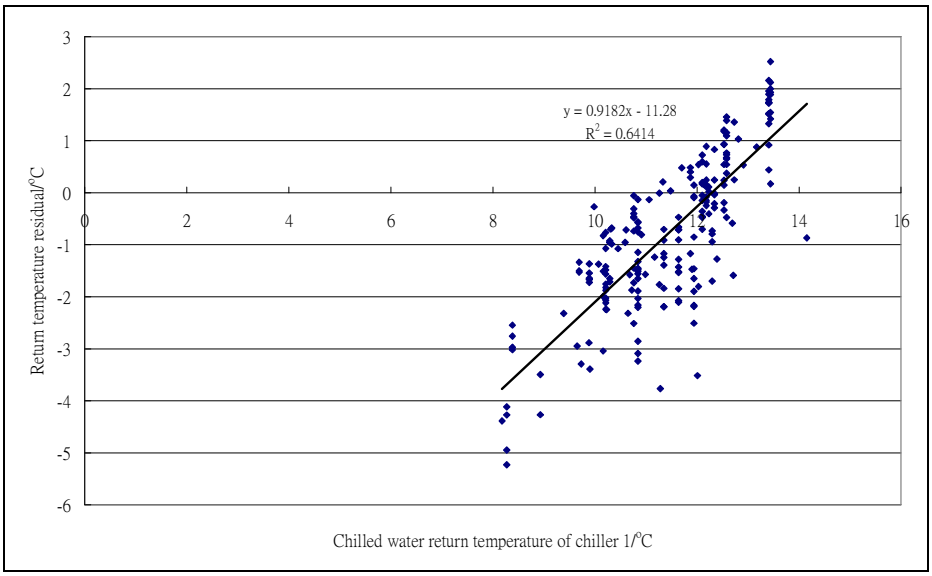

Figure 3.17 The relationship between the return temperature residual (sensor drift) and the chilled water return temperature based on hourly average data after 13:00 on 22/10/2005

From the energy balance calculation and comparison with the reference value, the return chilled water temperature sensor in Chiller 1 was found to be faulty after 22/10/2005, which is consistent with the previous results that some return chilled water temperature data for Chiller 1 are deviating largely from the reference return chilled water temperature, as shown in Figure 3.8.

Rather than hourly average, initial attempt was made to use moving average to remove the transient data, hoping that identification of faults with use of the moving average data could identify occurrence of faults more precisely. However, the moving average was found to be incapable of removing the transient condition completely. Finally, the hourly average was adopted, which can better reflect the steady state operation of chillers. After validating the accuracy of measurement, the data that can be used for further performance evaluation were extracted from the set of raw data.

3.11 Abnormally high secondary-loop chilled water supply temperature

Notwithstanding that the main chilled water supply temperatures measured by the sensor installed at the main supply pipe in the secondary-loop were verified to be reasonably accurate, it can be seen from Figures 3.4 to 3.7 that the main supply temperature could rise to above 14˚C when the chilled water plant was running under surplus flow condition, which is abnormal. With chilled water supply at a temperature much higher than the design level (7˚C), the cooling capacity of air-handling equipment, especially the latent capacity, would be seriously reduced, resulting in high indoor temperature and humidity. Such abnormally high supply temperatures could occur only if

some chillers had chilled water flowing through their evaporators but their compressors were stopped or certain control strategy, such as supply temperature set-point reset, was adopted.

Figure 3.18 shows the frequency distribution of the secondary-loop chilled water supply temperature under surplus flow conditions. About 75% of the data were found staying within the range from 8-10˚C with the majority (50% of all data) in the range of 8-9˚C, while a significant amount of data were greater than 10˚C, which is abnormal. Therefore, graphs showing the trends of monthly and daily average values of the supply temperatures were plotted for a visual inspection, as shown in Figures 3.19 and 3.20 respectively.

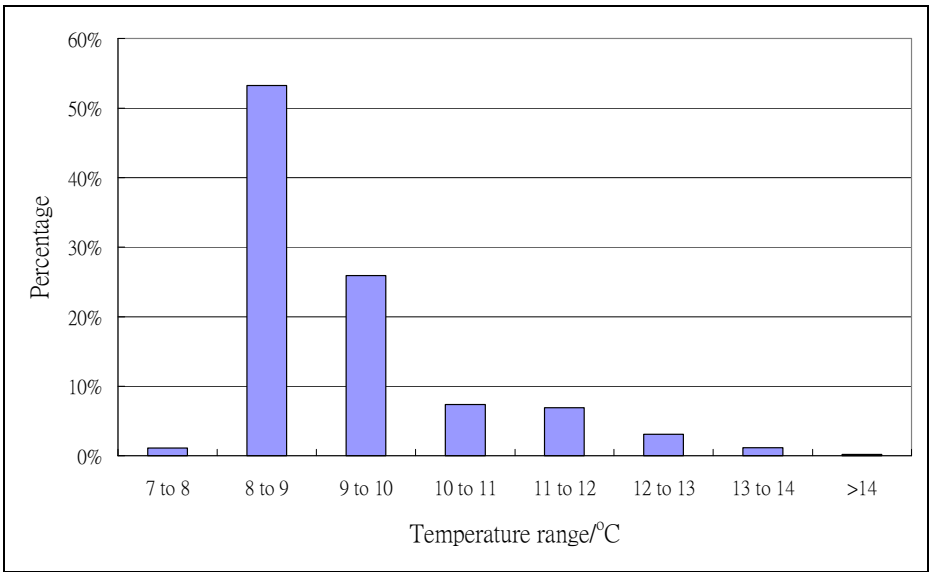

Figure 3.18 Frequency distribution of secondary chilled water supply temperature under surplus flow condition.

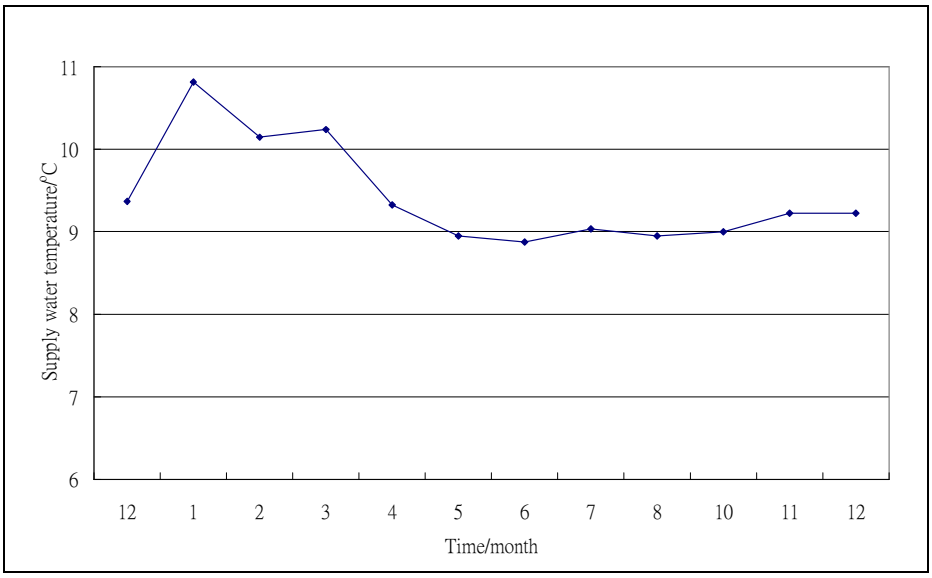

Figure 3.19 Trends of monthly average chilled water supply temperature

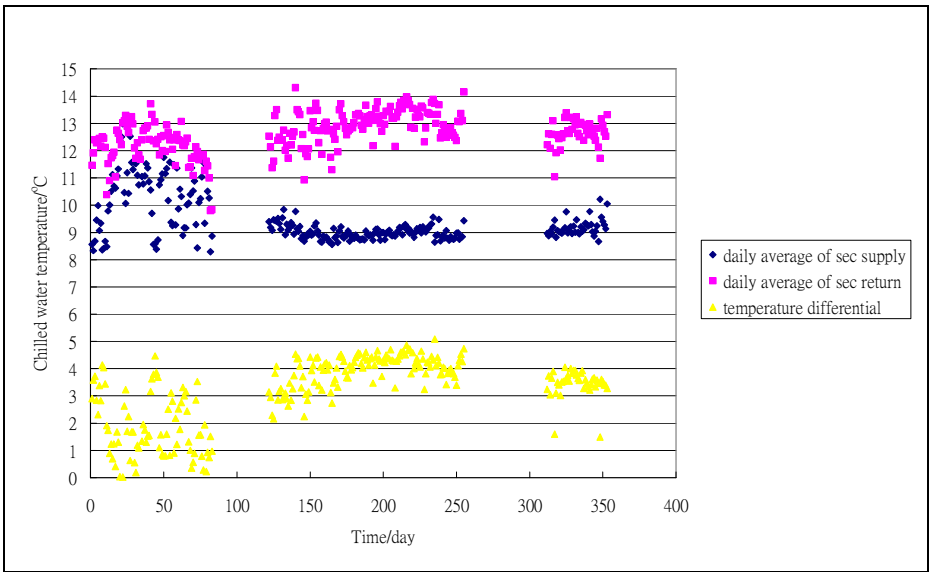

Figure 3.20 Trends of daily average chilled water supply and return temperature and temperature differential

Figure 3.19 unveiled that there were seasonal changes in the supply temperature, with supply temperature staying at higher levels during January and March in 2005.

Figure 3.20 also indicates that the temperature was unreasonably high especially in the first 90 days, which is within the months between December 2004 and March 2005. This figure also highlights that the temperature differential between the secondary-loop chilled water supply and return temperatures was fluctuating and relatively low during those days.

Figure 3.21 shows the trends of the secondary-loop chilled water flow rates in the year. It was seen that the secondary chilled water flow rate in the first 90 days were relatively low compared to those in the middle part of the data. The relationship between the total cooling demand and the secondary-loop chilled water flow rate in the first 90 days and in the remaining days are shown in Figure 3.22, and denoted by different symbols. It shows that a minimum chilled water flow rate of about 50*l*/s would be maintained even if the cooling load dropped to zero, which would be possible if some air-handling equipment are equipped with three-way control valves or some control valves are leaky or jammed such that they could not be fully closed, resulting in chilled water flowing through cooling coils without picking up much heat. Verbal response of the O&M staff confirmed that there were no three-way valves installed. Water leakage, therefore, may be the major reason for this observation.

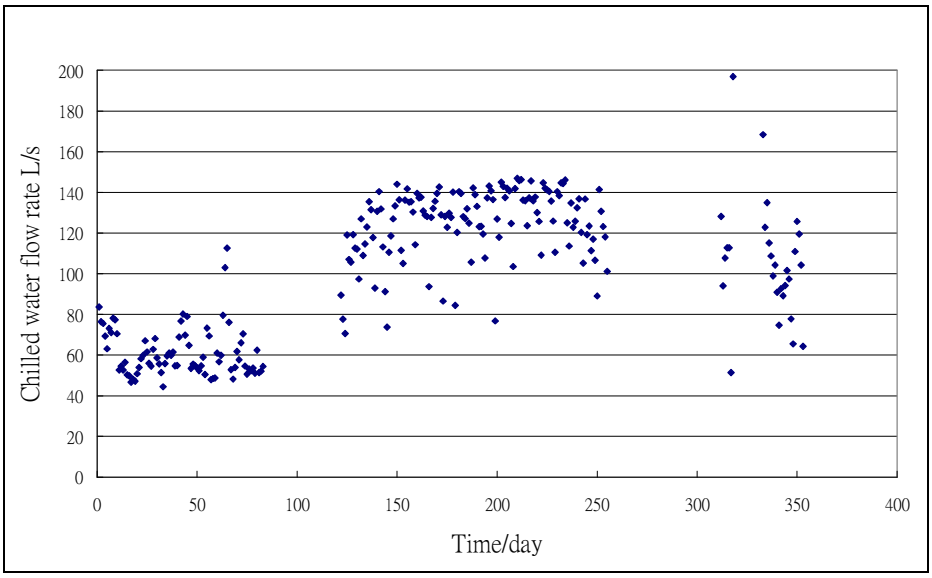

Figure 3.21 Trends of daily average secondary chilled water flow rate

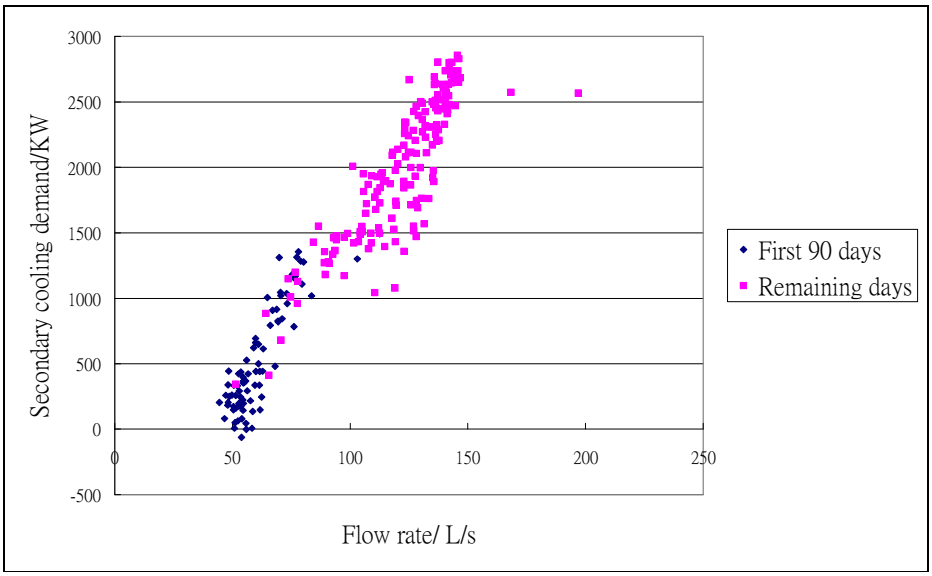

Figure 3.22 Comparison between the secondary cooling load and the secondary chilled water flow rate in the first 90days and the remaining days

3.12 COP of THE CHILLERS

The coefficient of performance of chillers was calculated based on the estimated cooling load (Q) and power demand (W_{ch}). In the light of the analysis results on the measurement accuracy of the sensors, the cooling loads on the chillers were calculated from the rated water mass flow rate, the entering chilled water temperatures measured by the sensors in the chillers and the leaving chilled water temperatures, which were measurements of the sensor at the main supply pipe in the secondary-loop. With the removal of outliers identified in Table 3.8 and Figure 3.15, the chiller cooling load can be estimated with abnormal data excluded.

The electric current of each compressor in each chiller was separately measured. Because of missing data, only those data where all electric current records of all compressors in each chiller were available was used in the calculation. The accuracy of the electric meters was verified through site measurements using a power analyzer and found to be reasonably reliable. The power factor was also measured and found to be varying between 0.83 and 0.89. Based on the electric current records and by assuming that the voltage and the power factor stayed steadily at 380V and 0.85, the electric power was estimated using equation (3.6)

$$W_{ch} = \sqrt{3} \cdot V \cdot I \cdot \cos\phi \tag{3.6}$$

The coefficient of performance (COP) of chillers was then computed based on the estimated cooling load and electricity consumption, as shown in equation (3.7). The COP statistics of Chiller 1, 2, 4 and 5 are shown in Table 3.9.

$$COP = Q / W_{ch} \tag{3.7}$$

Table 3.9 Statistics of COP and proportion of runtime of the chillers

	COP <2	2 ≤COP ≤3	COP >3
Chiller 1	9%	89%	2%
Chiller 2	0%	78%	22%
Chiller 4	0%	53%	47%
Chiller 5	39%	57%	4%

It can be seen that the COP values were different among the chillers. Chillers 2 and 4 were apparently more energy efficient as their COPs were all the time above 2, while the other two chillers exhibited significant proportions of runtime during which their COPs were below 2. Given the significant difference in COP, Chillers 1 and 5 may be faulty or have deteriorated in performance since the same type of chillers should exhibit similar chiller performance in normal operating condition. Chillers 2 and 4 should therefore be preferentially operated to minimize the chiller energy use before any retrofit work or replacement is done on the other chillers.

3.13 Efficiencies of pumps

The efficiency of the primary chilled water pumps can be calculated using equation (3.8). However, there were no pumping pressure sensors and flow meters for measurement of chilled water pump performance. In the absence of the required measurement data, the rated flow rate of the primary chilled water pumps was assumed to be equal to the primary chilled water flow rate for all operating conditions, while the pumping pressure for the primary chilled water pumps was assumed to be equal to the pumping pressure at the rated chilled water flow. The efficiency of the primary chilled water pumps can finally be estimated, which was approximately 0.75.

For the variable speed secondary-loop chilled water pumps, no pressure sensors or flow meters were available and thus their pumping efficiencies cannot be estimated.

However, it was observed that the power supply frequency of pump 1 was sometimes different from the power supply frequency of pump 2 and pump 3 when they were in operation at the same time. For identical variable speed pumps connected in parallel, operating the pumps at different speeds may lead to inefficient operation and even problems.

$$Eff = \frac{P_{pump} * V_{pump}}{W_{pump}} \tag{3.8}$$

3.14 System operation check

For avoiding the influence of missing data, only data records where the secondary-loop chilled water supply and return temperatures and flow rate, the chilled water return temperatures, the compressor power and the pumping power of individual chillers and pumps were all available and proved to be accurate, were adopted for the analysis of system operation of chillers.

Statistics of the number of chillers operated at different cooling load ranges have been compiled from the plant records, and the results are summarized in Figure 3.23. It can be observed from this set of results that there was the tendency to operate more chillers than required to cope with the cooling load when the cooling load exceeded the rated cooling capacity of one chiller. For example, when the cooling load was in the range of 300 to 600TR, only two chiller would need to be operated but for more than 55% of the time where the cooling load was within this range, three chillers were run. However, when the cooling demand is under the rated capacity of one chiller, for more than 90% of time, only one chiller was operated.

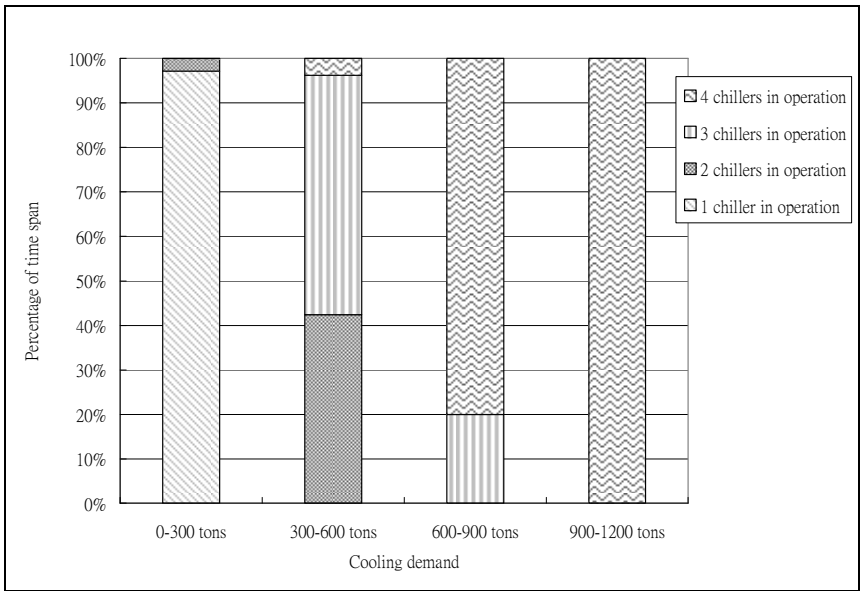

Figure 3.23 Number of chillers operating a range of cooling capacity

There are valid reasons for operating chillers in the way as observed above, which include:

i) It may be more energy efficient to run more chillers than the minimum number required to cope with the load such that chillers may be kept running in their most efficient operating region (for the chiller plant under concern, this is unlikely to be the case when the cooling load stayed below 600TR); or

ii) Chiller output capacity has deteriorated such that each cannot output its rated output anymore.

Other than these reasons, the sequencing control strategy should be reviewed with a view to enhance the energy efficiency of the plant.

Figure 3.24 shows the statistics of cooling load on individual chillers, which unveil that Chillers 1, 2 and 5 were most often loaded within 60-80% of their rated

capacity. Chiller 5, however, was loaded in this range only for 46% of its total operating time. It can be seen that the chillers are usually run in less than 80% of load. This may not be energy efficient as the efficiency of screw chiller usually peaks when it is running at full load.

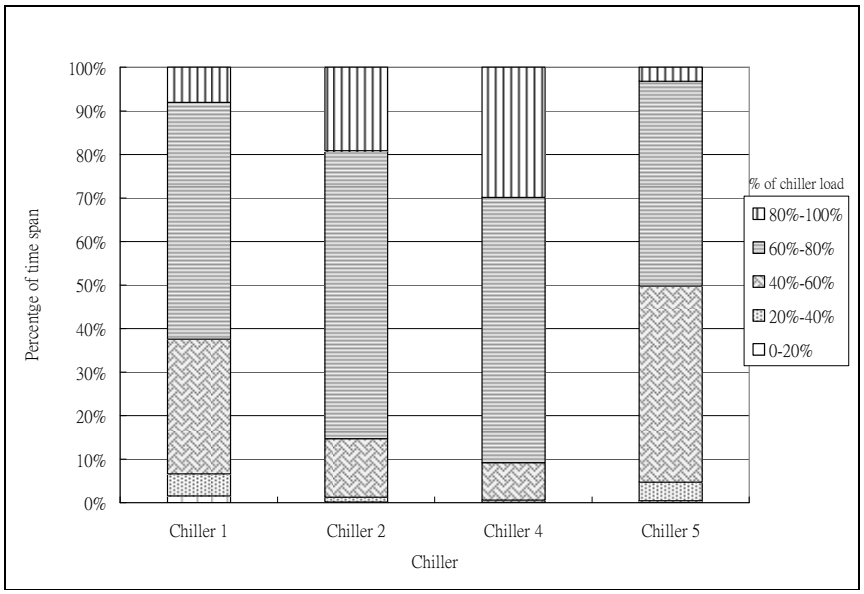

Figure 3.24 Statistics of load on individual chillers

From the raw data records, it was also discovered that sometimes, the chiller capacity was sufficient to provide cooling while the chilled water return temperature was higher than 15^{o}C. It seems that using the chilled water return temperature to sequence the chiller operation may not be a satisfactory sequencing control strategy, and the control should be based solely on the cooling demand.

3.15 Discussion

A preliminary study has been conducted to analyze the performance of an existing chiller plant. Several deficiencies in the operation records of the chiller plant were noted.

Huge amount of missing data is one of the major problems. According to the BMS operators, the data loss was due to the lack of an uninterruptible power supply (UPS) to backup the electricity supply for the BMS. Consideration, therefore, should be given to equipping the BMS with a UPS to minimize loss of control functions and operation data records. The way in which operating data are logged, stored and organized should be reviewed in order to facilitate periodic review of plant performance and sensor faults.

Adequate and properly functioning measuring instruments are crucial to chiller performance monitoring and optimal control of chiller plants. Lacking adequate amount of sensors was the first problem encountered in this study. There were no flow meters available in the primary chilled water loop such that the chilled water flow rate through chillers could only be estimated with the assumption that the flow rates through all running chillers were identical. Use of balancing valves that allow flow rate to be determined from the pressure drop across the valve and the number of turns set at the valves should be considered. Lacking differential pressure transmitters for pump pressure measurement also restricted the estimate of the pump efficiency.

The current study also unveiled that some temperature sensors were faulty, including the chilled water supply temperature sensors of Chillers 1, 2, 4 and 5 and the chilled water return temperature of Chiller 1. The chilled water supply temperature sensors of Chillers 1 and 4 should be replaced, while the chilled water supply temperature sensors of Chillers 2 and 5 and the chilled water return temperature sensor of Chiller 1 should be re-calibrated. Besides re-calibration or replacement, the accuracy of measurement of the sensors should be upgraded to meet requirements in ASHRAE Standard 114 when each is due for replacement.

After estimation of the COP of the chillers, Chillers 2 and 4 were found to be more energy efficient and should be preferably operated so as to minimize the energy use before any retrofit work or replacement is made on the other chillers. The current chiller sequencing control strategy should also be reviewed since there was tendency to operate more chillers than required to cope with the cooling demand such that the chillers are usually partially loaded to less than 80% of full load condition. This is not energy efficient for screw chillers, which peaks in COP at full load condition.

4. PROBLEMS WITH CHILLER PLANT MAINTENANCE RECORDS

4.1 Overview

As presented in Chapter 3, an analysis of the operation records of an existing chiller plant was carried out. The chiller plant studied is, in fact, one of the chiller plants serving a large building complex, and is referred to here as the Phase 1 chiller plant. The analysis unveiled many problems with the chiller plant performance data extracted from the building management system (BMS), especially in missing data and accuracy of the data. For obtaining an understanding of the reasons that had given rise to the problems, the operation and maintenance (O&M) records of the chiller plant were collected from the O&M staff there for an analysis.

Analysis of the O&M records unveiled that faulty sensors were common and the frequent occurrence of fault alarms were most often handled by resetting the alarms time after time. Records of the maintenance works carried out were found to be unclear and incomplete, which made it impossible to keep track with the problems. Such problems should be resolved before FDD can be applied to an existing building. In the following parts of this chapter, details of the analysis on the O&M practices and the associated problems are reported.

4.2 Work relation between the in-house O&M staff and the BMS and chiller MCs

The maintenance records collected include records of services rendered by the BMS maintenance contractor (MC), fault alarm records (including alarm records entered into and stored in a computer file and handwritten fault alarm records in a logbook kept in the plant room), and the maintenance work records kept by the O&M staff from 2002 to 2006. The maintenance work records contain information on chiller repair and maintenance works and the associated costs. The data were analyzed to unveil the dominant faults in the chiller plants, the extent of work undertaken by the BMS MC and the in-house maintenance staff, and the maintenance cost of the chiller plant.

The BMS MC was originally the contractor who supplied and installed the BMS for the building, and has subsequently been employed as the MC for the BMS system. However, the building management did not employ also the original chiller installation contractor to act as their chiller MC. Instead, the chiller maintenance work was done mainly by in-house staff, except some specific works that were beyond the capacity of the in-house staff to handle, such as identification and diagnosis chiller faults, major chiller repair works, etc., which were outsourced from the chiller supplier.

According to the verbal responses of the in-house O&M staff to our enquiries, all BMS maintenance works were undertaken by the BMS MC. When a BMS system fault was noticed, the BMS MC would be called upon to perform a check. Apart from contingent repair work, the BMS MC would make regular site visits to perform scheduled maintenance tasks, such as calibration of sensors, control panel maintenance, preventive

maintenance of network control units (NCU) and direct digital control (DDC) units, functionality checks of hardware devices, etc.

On the contrary, when a chiller fault alarm was encountered, the in-house O&M staff would undertake an initial check and reset the system. If the problem was so severe that the system could not be reset and brought back to normal working order, the in-house O&M staff would request their management to issue a job sheet to their maintenance team to provide the required rectification work. If it is beyond the capability of the in-house maintenance staff to diagnose and rectify any chiller faults, services of the chiller MC would be call for. The in-house maintenance practice seemed to be rather complicated and involved many parties, which could lead to loss of information and delay in the maintenance work.

4.3 Information collected

The information collected includes:

1. Service Orders issued to the BMS MC from December 2004 to December 2005, which include brief descriptions on the maintenance tasks performed by the BMS MC in the period for the BMS serving the entire complex (including other chiller plants serving other building blocks).

2. A computer printout of fault alarm records for the chiller plant under concern from 2000 to 2006 (hereinafter referred to as Alarm Records A), which is a list of chiller fault alarms and the corresponding action taken by the plant operators.

3. Handwritten fault alarm records for the chiller plant from 2002 to 2006 (hereinafter referred to as Alarm Records B), which report the types of fault alarms and the date that those alarms were encountered, and the date of completion of the rectification works. No indication, however, was given on whether the work was undertaken by the in-house O&M staff or the chiller MC.

4. Maintenance work records kept from 2002 to 2006, including chiller repair and maintenance works carried out by the in-house O&M staff or the chiller MC, and the associated costs.

The collected information was studied and the findings are discussed in the following sections of this chapter.

4.4 Records of services by BMS MC

The Service Orders issued to the BMS MC covered a total of 103 pieces of work done in the entire complex within the period from December 2004 to December 2005. The kinds of work involved include: preventive maintenance and replacement of BMS and control components, such as network control units (NCU) and direct digital control (DDC) units, fan coil thermostats and valve actuators; sensor calibration and replacement, including air and water temperature sensors and air humidify sensors; power analyzer installation and replacement; BMS program additions and modifications; and testing and commissioning of chiller plant.

The Service Orders show that preventive maintenance of NCU and DDC was undertaken by the BMS MC once every three months. The tasks for maintaining NCU and DDC are as shown in Table 4.1.

Table 4.1 Preventive maintenance tasks of network control unit and direct digital control preformed by O&M personnel

Network Control Unit	Direct Digital Control
1. Clean exterior surfaces	1. Clean exterior surfaces
2. Clean interior surfaces	2. Check field/communication wires connection
3. Power supply examination	3. System Isolation
4. Self-diagnostic exercise	4. Power supply examination
5. Check communication cable connection	5. DDC program examination
6. Check field wire connection	6. Change of state reporting
7. Check system isolation	7. Check the operation voltage
8. Check backup battery operation	8. Verify alarm condition operation of DDC
9. General operation examination	
10. Function module calibration	
11. Data upload operation	

Table 4.2 summarizes the fault descriptions and the services done by the BMS MC, which were extracted from the Service Orders. Preventive maintenance of DDC or NCU was not covered by the Service Orders. It was observed that abnormal sensors were often rectified by sensor replacement; likewise DDC and other components. Replacement of the temperature and humidify sensors in the Phase 1 chiller plant studied in Chapter 3 appeared three times within 9 months, with sensor replacement made each time at the same location. Verbal response from the in-house O&M staff indicated that they were not satisfied with the quality and the type of the sensors that the BMS MC had replaced. The in-house O&M staff requested for outdoor type sensors in lieu of indoor type sensors and the problems had not been resolved yet.

There were 8 records of sensor calibrations but those works were for specific sensors, of which 4 were carried out after abnormal conditions had been found. However, there were no records that indicate periodic calibration had been done for all sensors in individual plants. It is possible that periodic calibration of sensors was part of the basic work covered by the maintenance contract with the BMS MC, or was outsourced from

another service provider and thus no Service Order had to be issued for this work. This, however, is inconsistent with the presence of preventive maintenance work for other system components, such as NCU and DDC.

Table 4.2 The fault details and services done

Components	Fault details	Services done
Sensors	Defective fan coil thermostat at HJ wing	Sensor replacement
	Abnormal PAU temperature sensor	
	Abnormal chilled water supply temperature sensor of chiller 1 in phase JCA	
	Abnormal temperature and humidity sensor in phase 1 and phase 2	
	Abnormal AHU humidity sensor	
	Abnormal temperature and humidity sensors in phase 1	
	Abnormal PAU temperature and humidity sensor	
	Abnormal temperature and humidity sensors in phase 1	
		Sensor calibration in phase 4A
		Sensor calibration of chilled water return temperature sensor of chiller 1 and main chilled water supply temperature sensor in phase 5
		Sensor calibration of chilled water supply temperature sensor of chiller 2 in phase 5
		Sensor calibration in library
	Abnormal PAU temperature sensor in library	Sensor calibration
	Abnormal supply temperature sensor in library	
	Abnormal mean chilled water return temperature sensor in phase 5	
	Abnormal supply and return pressure sensor in phase 4A	
Current integrators	Abnormal current integrator of chillers in phase 2A	Replacement
	BMS data cannot be assessed, integrator malfunction in phase 1	Power reset
Control	AHU cannot be controlled	Replacement of DDC controller
	Abnormal BMS reading in phase JCA	Reload NCU
	Bypass valve is out of control in phase 4A	Replacement of DX9100 control module
	DDC offline in phase 4A	Restart MCB board and check DDC panel
	Abnormal AHU supply and return temperature	Replacement of DDC controller
	Abnormal chiller on/off in the phase JCA	Testing and commissioning of chiller plant
Cooling coil valve	Defective cooling coil valve	No response given

Excluded the preventive maintenance of NCU and DDC

For the Phase 1 chiller plant, other than preventive maintenance of NCU and DDC, maintenance works that had been carried out within the period covered by the Service Orders at hand included replacement of one abnormal humidity sensor and two abnormal

humidity/temperature sensors and resetting abnormal current integrators. The few maintenance work done is inconsistent with the many sensor problems identified in the previous chapter on operating records of this plant.

4.5 Chiller Fault Alarm Records A and B

The chiller fault alarm records, including Alarm Records A for 2000-2006 and the handwritten Alarm Records B for 2002-2006, were studied. Alarm Records A included separate alarm records for individual chillers (Chillers 1 to 5) in the Phase 1 chiller plant, providing information on the time and date of occurrence of individual alarms, their respective alarm codes categorized under two groups (for circuit A & circuit B in each chiller) and remarks on the actions taken.

Inspection of the information in Alarm Records A unveiled that the usual practice of the plant operators was to check the chiller concerned and rectify the problem once a fault alarm was detected. Very often, they would deal with the alarm by resetting the chiller. When repeated resetting failed to remove the alarm, or they were unable to reset the system or remove certain alarms through resetting the system, a 'complaint note' might be issued to urge the maintenance team to rectify the fault. If the maintenance team could not rectify the fault themselves, the chiller MC would be called upon to take the appropriate corrective actions to rectify the fault.

Alarm Records B included: the date; description about the alarm and, for a few, also the actions taken; the date that rectification work was completed; and, in some records, a further remark. The kinds of fault alarms recorded in Alarm Records B were

mostly warning signals, indicating abnormality of chillers. Whether the rectification works involved work done by the chiller MC or the in-house team was unknown.

Before presenting the alarm statistics, a general description about the refrigeration circuit and control of the chillers in the Phase 1 plant, the possible causes and consequences of those fault alarms that had reportedly occurred are discussed in the following section. Reference has been made to relevant information about the chiller alarms and trouble shooting methods described in the chiller manufacturer's documents.

4.6 General description of the chillers and their control systems

As described in the previous chapter, all the five chillers in the Phase 1 plant are air-cooled screw chillers of the same make and model. Each chiller has two independent refrigerant circuits, each of which consists of two compressors. The cooling capacity of the chiller model is 300 tons of refrigeration (TR, 1TR=3.517kW), rated under the entering condenser air temperature of 35^{o}C, entering/leaving chilled water temperatures of 12^{o}C/7^{o}C and chilled water flow rate of 50l/s. This means that each refrigerant circuit can provide 150TR under the rated condition.

Operational and safety control of the chiller is performed by the factory-installed automatic control system. Cooling output is regulated by cycling on and off of the compressors for achieving the target chilled water supply temperature. Capacity control is provided by pilot-operated solenoid valve, capable of changing the capacity to 25%, 50%, 75% and 100% of full load. The control system will also continuously monitor the signals from various built-in safety devices and will issue alarm signals when abnormal conditions are detected. The control system comprises a number of control boards. There

is a basic board, which holds the program that controls chiller operation, a compressor control board (CPM), a board that controls the electronic expansion valve, various fan stages, loaders, oil pumps or additional motor cooling valves, and another board that reads sensor readings, including oil pressure, condensing temperature or reclaim temperature, or to control the number of operating fans. These control boards are also subject to control fault alarms.

The chiller control system can issue a variety of alarm signals to aid operators in troubleshooting. Occurrence of the fault alarms may cause the compressors, the refrigerant circuit or the entire unit to shutdown. The manufactures' document provides some fault alarm descriptions to help operators identify which part of the chiller has failed or become abnormal and make corresponding maintenance or repair decisions. After the cause of the fault is corrected, the fault alarm can be reset, either manually or automatically, depending on the type of fault.

4.7 Statistics of chiller fault alarms

With reference to the chiller fault alarm records, the frequency of occurrence of fault alarms with Chillers 1 to 5 in the Phase 1 chiller plant was counted. The fault alarm statistics for each of these chillers are summarized in Table 4.3.

Note that the number of times that a specific alarm occurred does not necessarily mean that the corresponding fault had occurred for the same number of times in the chiller concerned because the same fault alarm would arise repeatedly if the chiller was allowed to continue to operate after the alarm had been reset, before the fault had actually been rectified.

Table 4.3 Fault alarms of Chillers

Faults[1]	Chiller 1				Chiller 2				Chiller 3				Chiller 4				Chiller 5			
	Circuit A		Circuit B		Circuit A		Circuit B		Circuit A		Circuit B		Circuit A		Circuit B		Circuit A		Circuit B	
	AC1[2]	AC2[2]	BC3[2]	BC4[2]	AC1	AC2	BC3	BC4	AC1	AC2	BC3	BC4	AC1	AC2	BC3	BC4	AC1	AC2	BC3	BC4
MOPD	0	4	0	1	1	0	1	1	1	3	52	32	7	30	0	8	2	0	1	1
LDS	2		1		8		10		0		1		2		2		91		7	
LOPC	1	5	2	4	0	0	3	0	2	8	23	0	2	21	2	1	0	0	2	1
OLCL	3		8		1		8		37		14		0		0		0		0	
ICPSOP	0	0	12	12	0	0	0	0	0	1	0	2	2	0	1	1	0	0	7	18
NMC	0	3	1	0	7	0	1	0	2	0	0	0	2	2	18	0	8	3	2	0
LSST	12		1		3		5		7		1		1		3		13		2	
CDOP	0	14	1	1	0	0	0	1	0	0	0	0	0	0	0	13	0	0	1	0
MSCTF	3	0	1	0	0	0	1	0	0	1	1	3	0	0	4	14	1	1	0	0
HPST	0	0	0	0	0	0	0	0	0	0	0	0	2	26	0	2	0	0	0	0
ETF	0	0	0	0	0	0	0	0	0	0	1	10	0	0	1	9	0	0	0	0
EWFCF	2				0				7				0				11			
OSF	0	0	0	0	0	0	1	0	0	1	3	2	0	0	1	1	0	2	0	0
SPTF	1		0		0		1		4		0		0		4		0		0	
LC-cpm	0	0	1	0	0	0	0	0	0	0	0	0	0	0	0	2	2	0	0	0
OPTF	0	0	0	0	0	0	0	0	0	1	0	0	1	0	0	1	0	0	1	0
LC-4XDO	0	0	0	0	0	0	0	0	0	1	0	0	0	0	2	0	1	0	0	0
LC-4XA1	0				0				0				4				0			
CU	0	1	0	0	0	0	1	0	0	0	1	0	0	0	0	0	0	0	1	0
EFP	2				0				1				0				0			
CPR	0	0	0	0	0	0	0	0	0	0	0	0	0	0	2	0	0	0	1	0
LC-fan	0		1		0		0		0		1		0		0		0		0	
LC-SM	0				0				1				0				0			
CF	0	0	0	0	0	0	0	0	0	0	0	0	0	1	0	0	0	0	0	0
Total	100				54				225				195				180			

Notes on descriptions of faults [1] and chiller codes [2] are shown in the next page.

[1] Descriptions of faults:

MOPD = Maximum oil pressure difference;
LDS = Low discharge superheat;
LOPC = Low oil pressure compressor;
OLCL = Oil level circuit low;
ICPSOP = Insufficient compressor pre-start oil pressure;
NMC = No motor current;
LSST = Low saturated suction temperature;
CDOP = Current drop in one phase;
MSCTF = Motor sensor compressor thermistor failure;
HPST = High pressure stat tripped;
ETF = Economizer transducer failure;
EWFCF = Evaporator water flow control failure;
OSF = Oil solenoid failure;
SPTF = Suction pressure transducer failure;
LC-cpm = Loss of communication with the cpm board;
OPTF = Oil pressure transducer failure;
LC-4XDO = Loss of communication with the 4XDO board;
LC-4XA1 = Loss of communication with the 4XA1-2-AO board;
CU = Current unbalance>18%;
EFP = Evaporator frost protection;
CPR = Current phase reversal;
LC-fan = Loss of communication with fan board;
LC-SM = Loss of communication with system manager;
CF = Contactor failure

[2] Compressor codes:

AC1 = compressor 1 at circuit A of chiller ;
AC2 = compressor 2 at circuit A of chiller;
BC3 = compressor 3 at circuit B of chiller;
BC4 = compressor 4 at circuit B of chiller

As shown in Table 4.3, for Chiller 1, 15 types of fault alarms, which amounted to a total of 100 fault alarms, were recorded from 2000 to 2006. The most frequently occurring alarms were insufficient compressor pre-start oil pressure at circuit B (ICPSOP) and current drop in one phase of compressor 2 at circuit A (CDOP).

For Chiller 2, there were a total of 54 fault alarms in 11 types in these years. Low discharge superheat at both circuit A and B (LDS) and low oil level in circuit B (OLCL) accounted for the largest number of fault alarms with Chiller 2.

For Chiller 3, a total of 225 fault alarms in 18 types were recorded. This chiller suffered from the largest number of fault alarms among all chillers in the same plant. Maximum oil pressure difference at circuit B (MOPD) and low oil level in circuit A and B (OLCL) were the major types of fault alarms. Low oil pressure of compressor 3 at circuit B (LOPC) was also frequently encountered.

For Chiller 4, the fault alarms amounted to 195 with 18 alarm types. The dominant fault alarms are maximum oil pressure difference (MOPD), high pressure stat tripped (HPST), low oil pressure of compressor 2 at circuit A (LOPC) and no motor current of compressor 3 at circuit B (NMC).

For Chiller 5, the number of fault alarms recorded totalled 180 in 15 types, among which low discharge superheat at circuit A (LDS) dominated, followed by insufficient pre-start oil pressure of compressor 4 at circuit B (ICPSOP) and low saturated suction temperature at circuit A (LSST).

Figure 4.1 provides a summary of the fault alarms encountered and reported in the Alarm Records.

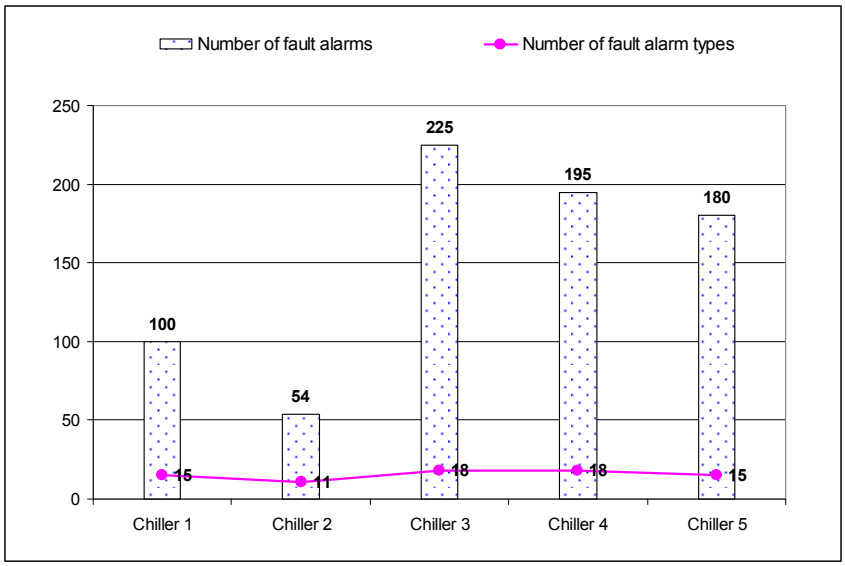

Figure 4.1 Summary of the fault alarms for Chillers in Phase 1 plant

Among all chillers in the plant, maximum oil pressure difference was the most frequent fault alarm, as shown in Figure 4.2. Low discharge superheat and low oil pressure in compressors accounted for 17% and 10% of the total number of fault alarms respectively. These three faults amounted to almost 50% of the total fault alarms. Although the number of fault alarms is not equal to the number of faults that occurred, such large number of fault alarms should be given due attention and effort should be made to minimize the occurrence of these alarms.

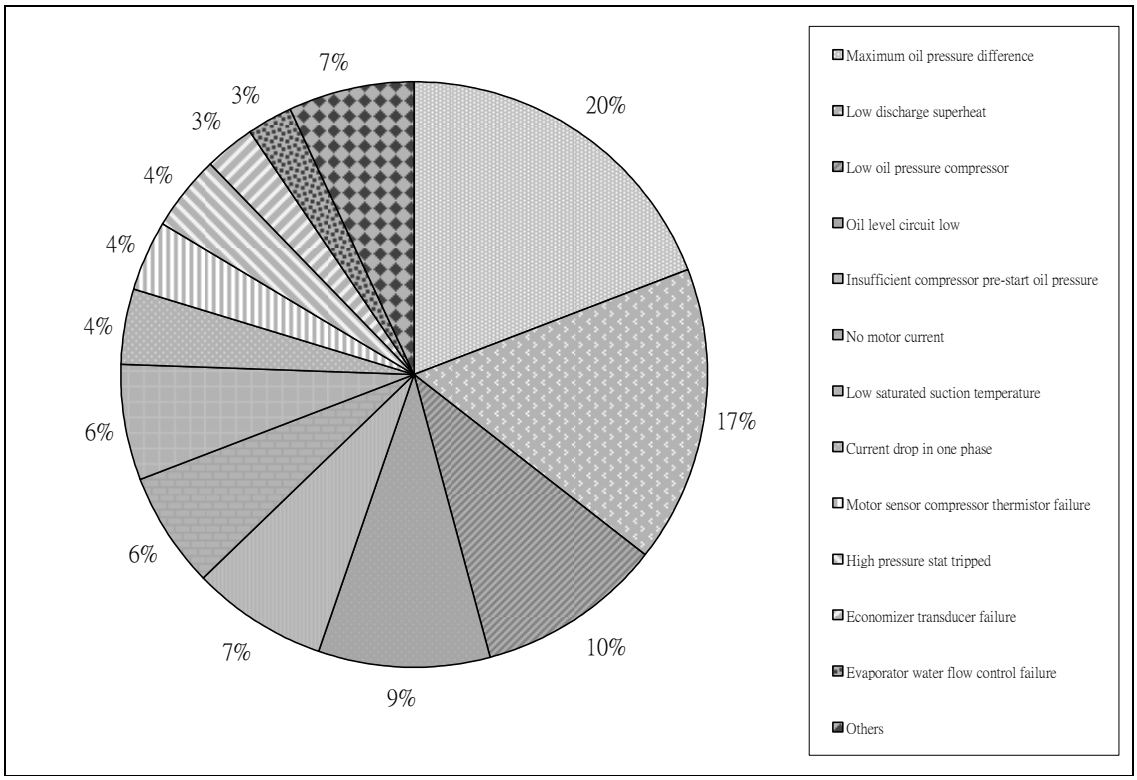

Figure 4.2 The frequency of the total fault alarms of all chillers in phase 1 chiller plant

4.8 Further observation from the chiller alarm records

4.8.1 Falling number of alarms

The fault alarms of the chillers for the years 2000-2006 were counted based on fault alarm Records A, as shown in Table 4.4. It was observed that the number of fault alarms was comparatively low in the beginning of the year 2000. This may be because the chillers were relatively new and, therefore, fewer alarms had arisen. The table shows also that the number of fault alarms was decreasing and few alarms were recorded after year 2004. For Chiller 1, there were zero and three alarms only in 2005 and 2006 respectively. For Chiller 2, no alarms were recorded in 2004 and 2006 and there was only one in 2005. For Chiller 3, no fault alarms were recorded after 2003. For Chiller 4, only three and two

fault alarms were recorded in 2005 and 2006 respectively. For Chiller 5, the fault alarms were comparatively higher in the year 2005, amounted to 11 fault alarms, but there were only two and three faults alarms in 2004 and 2006 respectively.

Table 4.4 Number of Fault alarms of Chillers in the years 2000-2006

Years	Chiller 1	Chiller 2	Chiller 3	Chiller 4	Chiller 5
2000	10	3	12	11	17
2001	8	22	88	41	38
2002	27	21	40	55	75
2003	32	7	85	57	34
2004	20	0	0	26	2
2005	0	1	0	3	11
2006	3	0	0	2	3

There are two possible reasons for the abovementioned reduction in number of fault alarm records: i) there were actually less or no fault alarms with the chillers in recent years; or ii) fault alarms occurred but were not recorded.

The in-house O&M staff claimed that there were actually less fault alarms for Chillers 2 and 3 because the chillers had been overhauled due to oil pump failure for Chiller 2 and refrigerant leakage for Chiller 3. Therefore, there was a sharp decline of the fault alarms for Chillers 2 and 3 after the year 2004.

However, the in-house O&M staff could not explain why the fault alarms decrease so much for Chillers 1, 4 and 5 after 2004, even though there was comparatively more alarms for Chiller 5 in the year 2005. The two reasons mentioned above remain possible. The latter reason should be more likely unless effective preventive maintenance strategy was adopted and properly carried out for chillers in recent years. Even if the latter reason was true, it does not necessarily mean that chiller alarms were not given due attention; alarms could still be properly dealt with but just unrecorded. Finally, no valid conclusions

can be drawn since the information given by the in-house O&M staff was not detailed and comprehensive.

4.8.2 Missing records

Records in Alarm Records A and B were inconsistent. In some cases, when Alarm Records B shows that maintenance was being conducted within a period, there was no corresponding record in Alarm Records A reporting that a 'complaint note' had been issued to the maintenance team or chiller MC for remedial work. In some other cases, when Alarm Records A shows that a 'complaint note' had been issued, no corresponding records could be found in Alarm Records B on the work done and when the work was completed. Based on these findings, it is reasonable to believe that some alarm records could have been omitted either in Alarm Records A or in Alarm Records B or both.

4.8.3 Logged chiller operation data for verification of the fault alarms

Since a study on the plant operation data trend-logged by the BMS had been conducted, an attempt has been made to see if the plant operation records could provide further insights into the causes of the fault alarms. However, the plant operation data were often missing at those times when fault alarms were detected. Where plant operation data are available, a chiller could be found not operating when an alarm was recorded.

For instance, for the fault alarms with Chiller 4, three alarms were recorded in 2005. Plant operation data were missing when the first alarm was detected at 8:45 on 16/3/2005; plant operation data are available only after 15/4/2005. For the other two alarms detected at 8:00 on 6/5/2005 and 4:30 on 9/5/2005, although plant operating data

at these times are available, the data indicate that the chiller was not operated. In addition, the internal sensor readings, including, condensing temperature, discharge pressure, suction temperature, suction pressure, and oil pressure corresponding to the time of occurrence of the three alarms were missing.

There were eleven fault alarms with Chiller 5 in the year 2005. However, plant operating records are available only at the time of occurrence of one fault alarm, detected at 5:15 on 7/5/2005. However, same as before, the chiller was found not operating when the alarm was detected. Again, internal sensor readings at the time this alarm was detected are unavailable.

The in-house O&M staff provided two possible explanations on the problem of missing data: 1) a complete stoppage of the chiller unit after detecting a fault alarm; and 2) a traffic jam when retrieving synchronized data. For the second reason, the problem has been tackled through improvement of the BMS system by the BMS MC upon request of the in-house O&M staff.

4.9 Maintenance work records

Maintenance work records showing the maintenance work done and the associated costs for the chiller plants in Phase 1 in the years 2004-2006 were obtained from the in-house O&M staff, and a summary is shown in Table 4.5. The direct labour cost was HK$262,100 per year. The total repair cost for the Phase 1 chiller plant over the years from 2004 to 2006 was HK$1,452,989. Therefore, the average annual repair cost was HK$484,300, and the annual total cost was HK$746,400.

Table 4.5 Maintenance costs including replacement of broken parts, annual maintenance, spare parts and improvement works

Year	Title / Scope of Work	Sum
2004	Synthetic oil 5L	$1,400.00
	Spare parts	$5,255.00
	Spare parts	$13,775.00
	Spare parts	$3,294.00
	Spare parts	$550.00
	Spare parts	$23,500.00
	Replacement of oil level sensor in chillers	$6,500.00
	Cleaning & inspection of cooler tube with eddy current test of chillers	$24,000.00
	Replacement of Lubrication Oil, Oil filters and Contactors Parts for the chillers	$45,000.00
	Replacement of Lubrication Oil of Chiller and replacement of oil level sensor	$3,900.00
2005	**Repair & Maintenance Works on the chillers**	$370,000.00
	Replacement of oil level sensor for chiller	$2,750.00
	Replacement of high discharge pressure switches for chiller	$4,400.00
	Supply parts for Carrier chillers and condenser fan motor	$23,100.00
	Supply lubricating oil	$22,000.00
	Replacement of evaporator, oil and filters of Chiller 3	$368,000.00
	Replacement of flow switch	$1,750.00
	Supply parts for chillers	$11,180.00
	Replacement of flow switch	$1,750.00
	Condenser fan motor cable socket	$1,860.00
	Supply parts for chillers	$112,500.00
	Supply parts for chillers	$33,040.00
	Purchase oil level sensor for future replacement	$8,600.00
	Replacement of Soft Starter of chillers	$46,500.00
	Supply parts for chillers	$17,211.00
	Replacement of temperature controller	
	Purchase step controller for future replacement	
	Purchase low water temperature switch for future replacement	
	Overhaul compressor of chiller	$90,000.00
2006	**Replacement of evaporator of Chiller 3**	$12,000.00
	Railing on chiller top	$46,000.00
	Canopy for chillers	$69,000.00
	Chiller panel	$600.00
	Repair the condenser of Chiller 1	$15,800.00
	Supply master display board for chiller	$10,250.00
	Supply parts for Carrier chillers	$11,180.00
	Supply and fix parts for Carrier chillers	$11,000.00
	Replacement of evaporator of Chiller 3	$14,000.00
	Material	$4,984.00
	Material	$4,870.00
	Bobbin gasket	$3,500.00
	Bobbin gasket	$3,500.00
	Purchase filter & o ring, filter, transducer, sensor for future replacement	$4,490.00
	Total year 04-06	$1,452,989.00

As shown in Table 4.5, a considerable amount of maintenance work had been performed for the chiller plant over the some 30 months covered by the records. It is reasonable to expect that many of these maintenance works were performed for

addressing previous fault alarms, which could take place soon after an alarm had been detected or when certain alarms had appeared many times. Some of the records are pertaining to supply of failed components and execution of the associated repair work. Some others were for purchases of spare parts for future replacement.

Unfortunately, it was not possible to relate the maintenance works to the alarm records because: the descriptions for some work items are not clear enough to show specifically for which equipment the work was performed; or no alarm records are available at those times close to the date that the works were performed. For example, the last alarm record available from Alarm Records A and B for Chiller 3 was on 30 December 2003, but the replacement of evaporator of this chiller took place in 2005 and further work was done in 2006.

The plant operation data also indicate that Chiller 3 was not operated in 2005. Yet, as indicated in Table 4.5, there was a large amount of work done on this chiller in 2005. This chiller was eventually overhauled in 2006. It is unknown if Chiller 3 has become fully operational since then.

4.10 Summary of problems found in the maintenance records

Records of maintenance works for the BMS and the chillers in the Phase 1 chiller plant have been studied, and observations made from the available records have been reported. This study revealed that sensor faults were frequently encountered, including sensors of the BMS for monitoring operation of the air-conditioning system and built-in sensors in chillers for ensuring safe operation of the chillers. Abnormal performance of sensors was rectified most often by replacement. Ad hoc sensor calibrations were

observed but whether regular calibration of all sensors was conducted was not shown in the Services Orders issued to the BMS MC.

The way in which O&M personnel addressed fault alarms was mainly to reset the alarm and repeated resetting of the same alarm could frequently be found, indicating that chillers could be running continually with the same fault before the fault was rectified. Chiller alarms occurred frequently for all the five chillers but fewer and fewer alarm records have been maintained more recently. There are two reasons to explain the reduction in the number of fault alarms: i) there were actually few or no alarms for chillers or ii) fault alarm were not properly recorded. Few alarms only occurred when an effective preventive maintenance of chillers were adopted. If not, this may imply that the chiller fault alarms were not regularly recorded and maintained.

Maintenance works done by the in-house O&M staff or chiller MC were not clearly recorded, rendering it not possible to keep track with the problems, such as specific alarms for which the works were done.

Considering that the faults and alarms record were not properly recorded to enable regular review of plant performance and preventive maintenance plan, the records should include information about in which equipment the faults or alarm took place, diagnosed causes of the faults or alarms, the action taken for dealing with the identified faults and the associated cost. These records should be reviewed regularly in conjunction with the plant operating records to underpin plant performance evaluation, appraisal of performance of maintenance contractors and maintenance management decisions.

4.11 Impacts on the present study

The study on the maintenance records of the Phase 1 chiller plant indicated many O&M problems, such as faulty sensors and frequently occurring alarms, and maintenance tasks not properly performed and recorded. Inspection of equipment and BMS system were not carried out regularly to ascertain that the equipments and sensors were properly functioning. This implied that a proper O&M programme had not been established.

In lack of a proper O&M programme for ensuring that proper plant operation would be carried out and reliable records of performance data would be maintained, even with the help of an automatic FDD system for detecting faults, reliable and energy efficient operation of the plant would remain unachievable since the faults detected by the FDD system must be properly handled and recorded by the O&M personnel. In addition, unreliable BMS data, including missing data records, and faulty data, would also hinder successful application of FDD to an existing plant. Therefore, an effective O&M programme should be established and implemented for ensuring BMS data are reliable for FDD implementation and the faults detected by the FDD system should be properly handled by the O&M personnel. Further discussions on measures for tackling the barriers will be given in Chapter 8.

5. PERFORMANCE MODELLING OF AIR COOLED TWIN-CIRCUIT SCREW CHILLERS

5.1 Overview

In preparation for a trial FDD implementation for the Phase 1 chiller plant, a mathematical model was developed for the chillers in this plant, which would be an essential part of the FDD algorithm to be developed for the chillers. The chillers in the plant are twin-circuit chillers with two screw compressors per circuit, but no model for this type of chillers has hitherto been developed. Notwithstanding that trial implementation of FDD to the plant was not possible (see discussions in Chapters 3 & 4), since the model development work formed a major part of this study and a new evaporator modelling method has been devised and incorporated into the model, the chiller model is presented in this chapter. The model was developed based on a sub-set of chiller performance records extracted from the raw BMS records, with unreliable and incomplete data removed (see Chapter 3).

Various empirical, physical and dynamic modelling techniques have been employed to model the performance of chillers (Browne and Bansal, 2001). Empirical models are either 'black-box' or 'grey-box' models developed based on curve-fit or thermodynamic models established from empirical data. Such models (e.g. Leverenz and Bakker, 1983; Peitsman and Bakker, 1996) are relatively straightforward to establish but their application is limited to the specific chillers from which the empirical data were

obtained. Physical models [e.g. Browne and Bansal, 1998] developed based on fundamental governing principles, such as mass and energy conservation, are more detailed and more widely applicable, but they are also more difficult to establish and use, as they usually involve a wide range of characteristic parameters of the modelled chiller which could be difficult to quantify. Dynamic modelling [e.g. Jia, 2002] is similar to physical modelling, but takes into account the rate of change of the system variables with time. The choice of which modelling approach to take is dependent on the intended application of the model. When a model is needed solely for analyzing the performance or for detecting and diagnosing faults of one or a number of identical existing chiller(s), the 'grey-box' approach will suffice. The chiller model presented in this chapter is intended to serve these purposes.

Although a large variety of chiller models have been developed, few are for air-cooled screw chillers and among them, none can model in detail chillers that comprise multiple, separate refrigerant circuits, despite that chillers of this type are already widely used for their good part-load performance. Chan & Yu developed an air-cooled screw chiller model with four refrigeration circuits [Yu and Chan, 2006; Chan and Yu, 2006] by assuming that the evaporators in the four refrigeration circuits would operate in parallel, as depicted in Figure 5.1. This implies that the same amount of heat transfer surface in the entire evaporator would remain available for cooling the chilled water even if only one circuit was in operation [Yu and Chan, 2006]. In reality, however, the evaporator is compartmentalized with each compartment belonging to one refrigerant circuit.

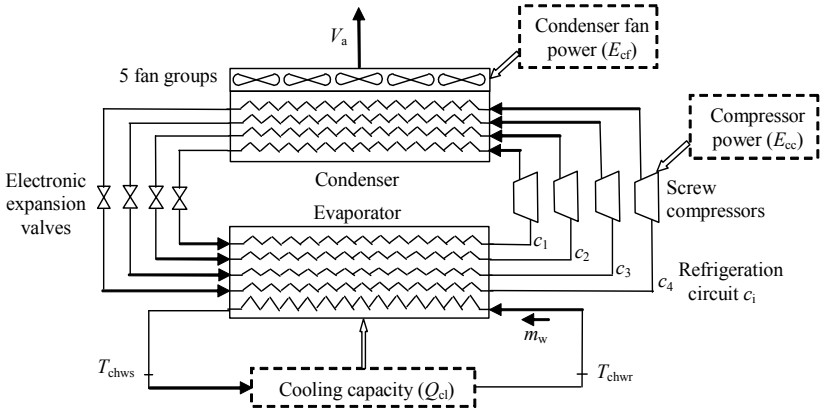

Figure 5.1 Systematic diagram of the chiller with four refrigeration circuits

Presented in this chapter is a steady-state thermodynamic model for an air-cooled chiller with two separate refrigerant circuits, denoted as circuits A and B, and two screw compressors per circuit, as shown in Figure 5.2. The evaporator shell comprises two separate compartments, each belonging to one refrigerant circuit. The tubes inside the evaporator are in a two-pass arrangement allowing chilled water to flow within the tubes from one shell compartment to the other and back. In order to properly model the heat transfer from the chilled water inside the tubes to the refrigerants in the two separate shell compartments, an evaporator model that comprises three sections, as shown in Figure 5.3, was developed. In this model, the first and the third sections jointly represent the shell compartment in circuit A and the second section represents the shell compartment in circuit B.

As shown in Figure 5.3, although the evaporating temperatures in the evaporators in the two circuits may differ from each other, the evaporating temperature in the evaporator of each circuit was assumed to be isothermal, which is a reasonable assumption, given that the refrigerant in each evaporator would be undergoing phase

change at the corresponding saturation temperatures as well as vigorous mixing (Wylen et al., 1994).

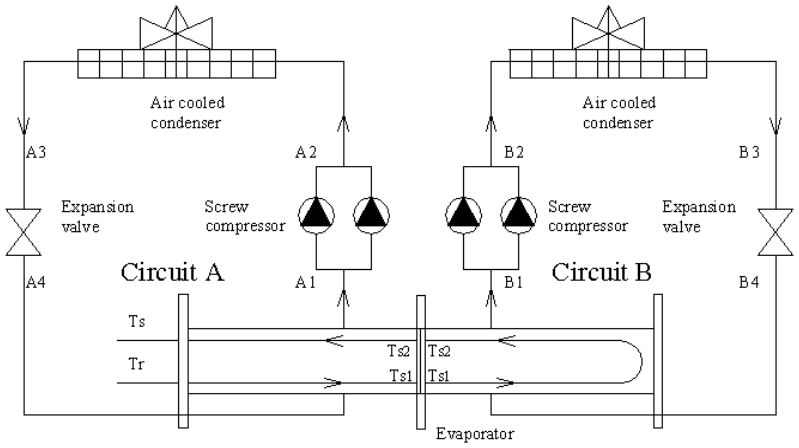

Figure 5.2 Schematic diagram for an air-cooled twin-circuit screw chiller

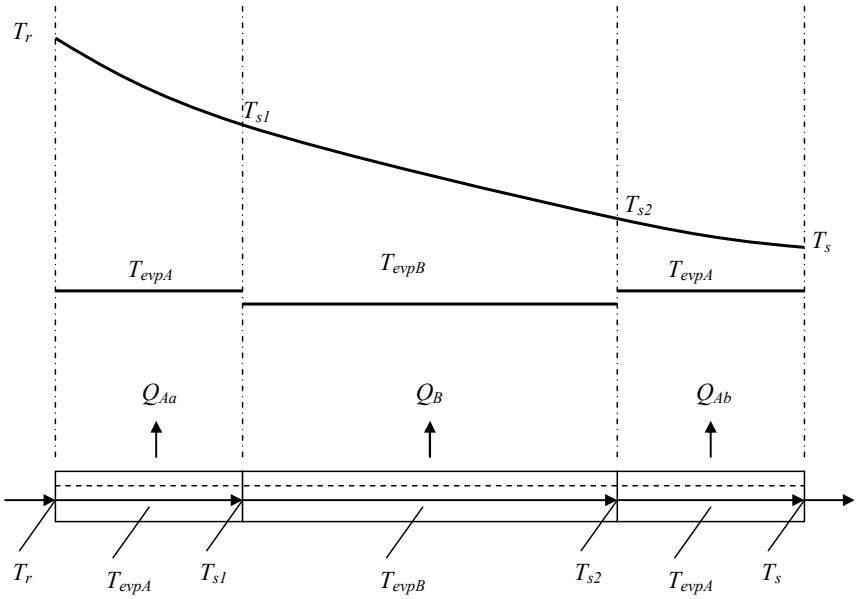

Figure 5.3 The three-heat-exchanger model for the evaporator

The characteristics of the chiller being modelled and the modelling assumptions made are described in Section 5.2. The methods used to model the performance of individual chiller components are described in Section 5.3. Section 5.4 is on evaluation of

the coefficients in the component models, which was based on performance data records of an existing chiller. Since the chiller plant from which operating data were obtained comprises five sets of identical chillers and the chiller model was intended for application to all chillers in the plant, a comparison of the model predictions with measured operating data of another chiller in the same plant was carried out. The comparison results are presented in Section 5.5. Section 5.6 concludes this chapter.

5.2 Characteristics of the modelled chiller

Collection of measured chiller performance data for the chiller model development work and for verification of the model predictions have been described in Chapter 3. The key characteristics of the chillers are summarized in Table 5.1. All the five chillers are identical, air-cooled twin-circuit screw chillers, each with a cooling capacity of 300 tons of refrigeration (TR, 1TR = 3.517kW). For each refrigerant circuit, there are two identical screw compressors, one electronic expansion valve, and four heat rejection fans, and these components are identical between the two circuits. The refrigerant used is R134a.

Table 5.1 Performance characteristics of the modelled chiller

Chiller characteristics	Value
Rated cooling capacity	1055kW
Rated chilled water entering / leaving temperatures	12˚C/7˚C
Rated chilled water flow rate	50*l*/s
Rated condenser air entering temperature	35˚C
Rated condenser air flow rate	42.77*l*/s
No. of condenser fans	8
Total condenser fan power	8kW
No. of compressors	4
Total rated compressor power	398kW

Since any one of the two circuits (circuits A & B, Figure 5.2), or both, in a chiller may be operated at any one time, and each circuit may have its cooling output adjusted independently from each other through varying the refrigerant flow rates in the two circuits, knowledge about the automatic control strategy being used to distribute the load between the two circuits and to sequence the operation of the compressors in each circuit is crucial to the development of a model for the chiller. However, this information was not given in the chiller manufacturer's catalogue while the local chiller supplier could not provide the information. Fortunately, the total power demands of the compressors in the two refrigerant circuits were separately measured and recorded by the building management system (BMS), which allowed the control strategy to be identified by observing the changes in the power demands.

Inspection of the available chiller power demand records unveiled that the operating sequence of the two refrigerant circuits in a chiller was as shown in Figure 5.4, which was based on the observations described below:

1. When the cooling load on the chiller was small but rising, only one circuit would be operated until the circuit was loaded to slightly exceeding half of the total cooling capacity of the chiller at which time the other circuit would be called upon to operate.

2. When the two circuits were operating simultaneously, the compressor power demands of the two circuits were approximately equal.

3. When both circuits operated together and the load dropped to about 40% of the total cooling capacity of the chiller, the circuit that came into operation earlier would be shut down.

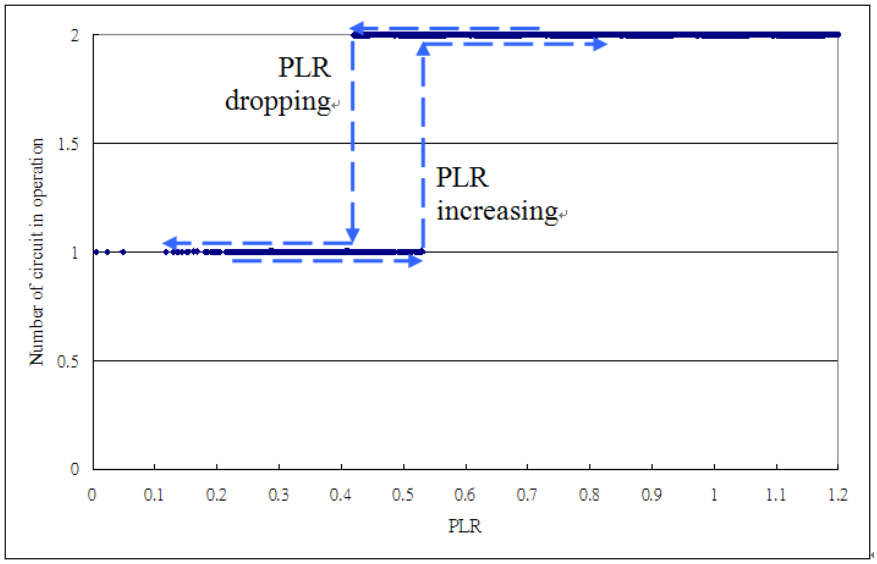

Figure 5.4 Number of refrigeration circuits in operation under rising and reducing cooling load on the chiller

Based on these observations, the sequencing control strategy assumed in the model is that circuit A will be started first when the part-load ratio of the chiller (*PLR*), which is the ratio of the actual cooling load on a chiller to the rated cooling capacity of the chiller, is lower than 0.52. Both circuits will be run whenever the *PLR* exceeds 0.52. Circuit A will be stopped when the *PLR* drops to 0.42. When the load rises again, both circuits will be run when the *PLR* rises beyond 0.52. This time, when the *PLR* falls to 0.42, circuit B will be stopped. The cycle will be repeated until the chiller is shut-down. The method for determining the number of compressors to be run in each circuit is described in the next section together with descriptions on the compressor model.

Furthermore, since the two circuits comprise identical components and the total power demands of compressors in the two circuits, when both are in operation, were found to be approximately equal, it is considered reasonable to assume that the two

circuits have equal rated cooling capacity and would each output half of the total cooling output when both circuits are in operation.

Typically, the condenser fans of an air-cooled chiller would be cycled on and off with reference to a high and a low condensing temperature settings under the control of a built-in head pressure control algorithm. When the condensing temperature of the refrigerant in the condenser exceeds the high setting, more condenser fans would be switched on one by one until the condensing temperature drops below the high setting or all fans are running. The number of running condenser fans will remain unchanged as long as the condensing temperature stays within the dead-band between the high and the low settings. When the condensing temperature drops below the low setting, the running condenser fans will be switched off one by one until the condensing temperature rises above the low setting or all fans are stopped. The high and low temperature settings for the chiller being modelled, however, were initially unknown but observation of the operating records of the chiller (Figure 5.5) unveiled that the high and low condensing temperature settings were 55°C and 42°C respectively.

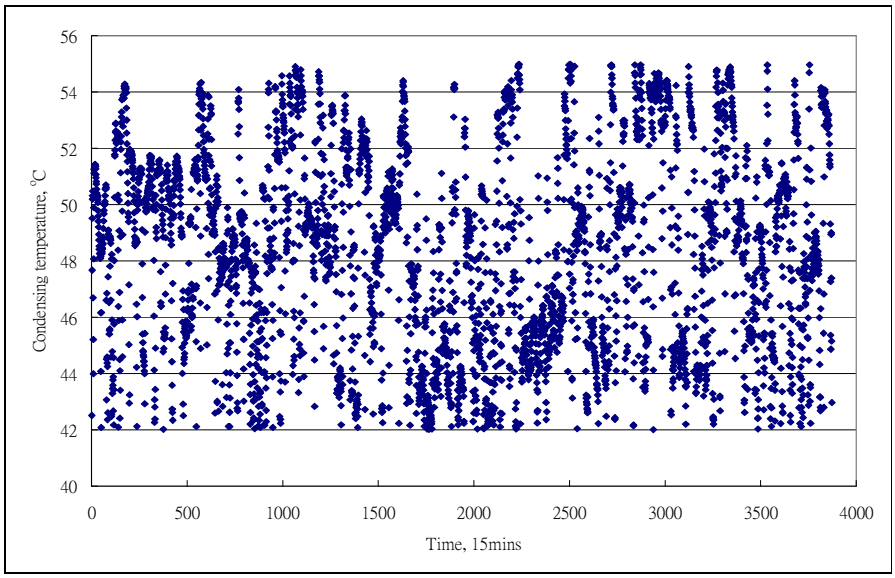

Figure 5.5 Condensing temperature records

Besides the abovementioned assumptions, the following assumptions were made in the development of the chiller model:

1. The standard vapour compression cycle applies to both circuits;

2. The expansion valve will keep the state of the refrigerant entering the compressor at a degree of superheat of 3°C at all times (Chan and Yu, 2004);

3. The refrigerant pressure drops across the condenser and the evaporator are negligible;

4. The refrigerant enthalpy will remain unchanged as it passes through the expansion device;

5. The refrigerant leaving the condenser is at a saturated liquid state without sub-cooling; and

6. Heat exchange between the refrigeration system and its surroundings is negligible.

The last assumption implies that the heat rejection rate at the condenser will always be equal to the sum of the cooling output rate at the evaporator and the power input to the compressors.

5.3 Model development

Given that the chiller has two refrigeration circuits, circuits A and B, the chiller may operate in any one of the following three modes:

1. Only circuit A operates

2. Only circuit B operates

3. Both circuits operate

Since the same model can be used to simulate either circuit in the chiller while only one of the two circuits is in operation, a model for a single circuit (based on circuit A) and a model for both circuits in operation were developed, as described below.

5.3.1 Evaporator of Circuit A

When only circuit A operates, the cooling output of the evaporator can be related to the properties of the chilled water and the refrigerant, as shown in equations (5.1) to (5.3).

$$Q_A = m_w \cdot c_w \cdot (T_r - T_s) \tag{5.1}$$

$$Q_A = m_{refA} \cdot (h_{A1} - h_{A3}) \tag{5.2}$$

$$Q_A = \varepsilon_{evpA} \cdot m_w \cdot c_w \cdot (T_r - T_{evpA}) \tag{5.3}$$

Where ε_{evpA}, the evaporator effectiveness, in equation (5.3) is given by:

$$\varepsilon_{evpA} = 1 - \exp(-\frac{AU_{evpA}}{m_w \cdot c_w}) \tag{5.4}$$

The term AU_{evpA} in equation (5.4), the overall heat transfer coefficient of the evaporator, can be expressed as a function of the chilled water flow rate and the cooling output rate as shown in equation (5.5) (Wang et al., 2000). The coefficients a_1, a_2 and a_3 in the model have to be evaluated based on operating data of the specific chiller to be modelled (see Section 5.4).

$$AU_{evpA} = \frac{1}{a_1 \cdot m_w^{-0.8} + a_2 \cdot Q_A^{-0.745} + a_3} \tag{5.5}$$

Equations (5.1) & (5.3) can be combined to yield the following equation for evaluation of the evaporating temperature of the refrigerant.

$$T_{evpA} = T_s + \frac{Q_A}{m_w \cdot c_w}(1 - \frac{1}{\varepsilon_{evpA}}) \tag{5.6}$$

Having evaluated T_{evpA}, the corresponding refrigerant evaporating pressure can be determined using the Clausius-Clapeyron equation below (Bourdouxhe et al., 1997).

$$P_{evpA} = \exp(b + \frac{c}{T_{evpA} + 273.15}) \tag{5.7}$$

The values of the coefficients in the above equation are: b = 15.489 and c = –2681.99.

5.3.2 Compressors in circuit A

The actual power input to the staged compressors in circuit A is given by Bourdouxhe et al. (1997):

$$W_{AC} = m_{refA} \cdot \frac{w_{A,isen}}{\eta_{isen} \cdot \eta_{cc}} \tag{5.8}$$

Where, from equation (5.2), m_{refA}, the refrigerant mass flow rate, is given by:

$$m_{refA} = \frac{Q_A}{h_{A1} - h_{A3}} \tag{5.9}$$

The isentropic compressor work per unit mass of refrigerant is given by Chan and Yu (2006):

$$w_{A,isen} = \frac{\gamma}{\gamma - 1} \cdot P_{evpA} \cdot v_{A1} \cdot \left[\left(\frac{P_{cdA}}{P_{evpA}} \right)^{\frac{\gamma-1}{\gamma}} - 1 \right] \tag{5.10}$$

The constant coefficient γ for the refrigerant R134a is 1.072 (Bourdouxhe et al., 1997). The specific volume of the superheated refrigerant at the compressor suction (v_{A1}) in equation (10) can be evaluated from the saturated specific volume of the refrigerant in the evaporator, $v_{A1,s}$, the refrigerant degree of superheat at the compressor suction, T_{evsh}, and the evaporating pressure of the refrigerant in the evaporator, P_{evpA}, using equation (5.11) (Jia, 2002).

$$\frac{1}{v_{A1}} = \frac{1}{v_{A1,s}} - (-0.0007 + 0.00002 \cdot P_{evpA}) \cdot T_{evsh} \tag{5.11}$$

The following regression model for screw compressor developed by Solati (2002) was used in the chiller model for evaluating the isentropic efficiency (η_{isen}):

$$\eta_{isen} = 0.01 \cdot (b_1 \cdot T_{cdA}{}^2 + b_2 \cdot T_{cdA} + b_3 \cdot T_{evpA}{}^2 + b_4 \cdot T_{evpA} + b_5 \cdot T_{cdA}{}^2 \cdot T_{evpA} + b_6 \cdot T_{cdA} \cdot T_{evpA} + b_7 \cdot Q_{nl} + b_8) \quad (5.12)$$

Where

$b_1 = -0.0316958$; $b_2 = 2.90112$; $b_3 = -0.0296849$; $b_4 = -1.45279$;

$b_5 = 0.000321176$; $b_6 = 0.00683086$; $b_7 = 0.00170575$; $b_8 = -16.5018$

The combined motor and transmission efficiency (η_{cc}) for a single compressor and two compressors working in parallel can be determined using equations (5.13) & (5.14) but the coefficients c_1 to c_3 and d_1 to d_3 had to be estimated by regression using operating data of the chiller (see Section 5.4):

$$\eta_{cc} = c_1 + c_2 \cdot PLR + c_3 \cdot PLR^2, \text{ for a single compressor in operation} \quad (5.13)$$

$$\eta_{cc} = d_1 + d_2 \cdot PLR + d_3 \cdot PLR^2, \text{ for two compressors in operation} \quad (5.14)$$

The refrigerant flow rate (m_{refA}) through a single compressor can also be determined using equation (5.15) for the full load condition and equation (5.16) for the part load condition (Bourdouxhe et al., 1997). Equation (5.16) differs from equation (5.15) only in the additional term V_{pumpA}, which is the refrigerant flow rate that is re-circulated to suction when the sliding valve is opened under part-load operation (Bourdouxhe et al., 1997).

$$m_{refA} = \frac{1}{v_{A1}} \cdot \left[V_C - An \cdot \sqrt{P_{evpA} \cdot v_{A1}} \cdot \left(\frac{P_{cdA}}{P_{evpA}}\right)^{\frac{\gamma+1}{2\cdot\gamma}} \cdot \sqrt{\gamma \left(\frac{2}{\gamma+1}\right)^{\frac{\gamma+1}{\gamma-1}}} \right] \quad (5.15)$$

$$m_{refA} = \frac{1}{v_{A1}} \cdot \left[V_C - V_{pumpA} - An \cdot \sqrt{P_{evpA} \cdot v_{A1}} \cdot \left(\frac{P_{cdA}}{P_{evpA}}\right)^{\frac{\gamma+1}{2\cdot\gamma}} \cdot \sqrt{\gamma \left(\frac{2}{\gamma+1}\right)^{\frac{\gamma+1}{\gamma-1}}} \right] \quad (5.16)$$

If the refrigerant flow rate determined using equation (5.9) exceeds the refrigerant flow rate through one compressor while it is running at full load as determined using equation (5.15), both compressors in the circuit would need to be run to cope with the load. However, if the reverse is true, V_{pumpA} will have to be greater than zero in order that the refrigerant flow rates estimated from equations (5.9) & (5.16) will agree with each other, which means that only one compressor needs to be run under that condition. This is the method used in the model to determine how many compressor(s) in a circuit would be run. The values of the volumetric displacement (V_C) and the nozzle area (An) of each compressor, which are needed in determining refrigerant flow rate using equation (5.15) or (5.16), had to be estimated based on the manufacturer's performance data for the full-load condition (see Section 5.4).

The specific enthalpy of the superheated refrigerant at the discharge and suction sides of the compressor (h_{A2} & h_{A1}) can be found using equations (5.17) & (5.18).

$$h_{A2} = h_{A1} + \frac{w_{A,isen}}{\eta_{isen} \cdot \eta_{cc}} \quad (5.17)$$

$$h_{A1} = h_{A1,s} + c_{pv} \cdot T_{evsh} \quad (5.18)$$

5.3.3 Condenser in circuit A

The heat rejection rate in the condenser in circuit A can be described by the following equations:

$$Q_{cdA} = Q_A + W_{AC} \tag{5.19}$$

$$Q_{cdA} = m_a \cdot c_a \cdot (T_{ao} - T_{out}) \tag{5.20}$$

$$Q_{cdA} = m_{refA} \cdot (h_{A2} - h_{A3}) \tag{5.21}$$

$$Q_{cdA} = \varepsilon_{cdA} \cdot m_a \cdot c_a \cdot (T_{cdA} - T_{out}) \tag{5.22}$$

Where

$$\varepsilon_{cdA} = 1 - \exp(-\frac{AU_{cdA}}{m_a \cdot c_a}) \tag{5.23}$$

$$AU_{cdA} = e_1 \cdot Q_{cdA}^{\ e_2} m_a^{\ e_3} \tag{5.24}$$

Equation (5.19) is based on the assumption that the refrigeration system is isolated from the surroundings. Equations (5.20) & (5.21) relate the heat rejection rate to the states and flow rates of the condenser air and refrigerant while equation (5.22) relates the heat rejection rate to the condensing temperature of the refrigerant (T_{cdA}) and the outdoor air temperature (T_{out}), using the effectiveness method. The heat transfer effectiveness (ε_{cdA}) is as defined in equation (5.23), where the overall heat transfer coefficient of the condenser (AU_{cdA}) can be evaluated using equation (5.24). The coefficients e_1 to e_3 in this equation, however, have to be estimated by regression based on available chiller performance data

(see Section 5.4). The condensing temperature and the condensing pressure can finally be estimated using equations (5.25) & (5.26) respectively.

$$T_{cdA} = T_{out} + \frac{Q_{cdA}}{\varepsilon_{cdA} \cdot m_a \cdot c_a} \tag{5.25}$$

$$P_{cdA} = \exp(b + \frac{c}{T_{cdA} + 273.15}) \tag{5.26}$$

The same values of the coefficients b & c in equation (5.7) are applicable to the respective coefficients in equation (5.26).

The condenser air mass flow rate (m_a) in the above condenser model would vary depending on the number of condenser fan(s) being run under the head pressure control of the chiller. As discussed in Section 5.2, cycling on and off of condenser fans is determined by comparing the refrigerant condensing temperature with the high and low temperature settings. In each new time-step, the number of condenser fan(s) that should be run, N_A, will first be assumed to be equal to that in the previous time step (when the chiller has just been started, this number will be set at 1), but whether this number of condenser fan(s) would be sufficient to keep the condensing temperature within the dead-band between the high and low settings will be checked. If the condensing temperature is found to be over 55°C or below 42°C, the number of fan(s) to be run will be adjusted up or down by one at a time, and the condensing temperature of the refrigerant will be checked again each time until the condensing temperature is kept within the dead-band or all or no fans are running.

Having determined the number of fan(s) to be run, m_a can be determined, as follows:

$$m_a = \frac{N_A}{N_{tot}} \cdot m_{a,tot} \tag{5.27}$$

5.3.4 Expansion valve in circuit A

The modelled chiller is equipped with an electronic expansion valve. Inside the expansion valve, a piston is driven by an electronically controlled linear stepper motor to move up and down to vary the cross sectional area of the refrigerant flow path such that the refrigerant is kept in a superheated vapour state at the suction side of the compressor. A series of calibrated orifices are installed into the wall of the refrigerant inlet port. When the refrigerant passes through the orifices, the refrigerant expands and becomes a mixture of liquid and gas. Despite the complex components involved, in the chiller model, the expansion device is modelled simply by assuming that the throttling process is adiabatic, thus the entering and leaving enthalpies of the refrigerant are equal, as depicted by equation (5.28).

$$h_{A3} = h_{A4} \tag{5.28}$$

5.3.5 COP of circuit A

The *COP* of circuit A of the chiller, when only circuit A is in operation (same applies when only circuit B is in operation), as defined in equation (5.29), takes into account the cooling output (Q_A), the total compressor power (W_{AC}) and the condenser fan power (W_{Af}).

$$COP_A = \frac{Q_A}{W_{AC} + W_{Af}} \tag{5.29}$$

5.3.6 Chiller model when both circuits A&B are in operation

As shown in Figure 5.3, the evaporator of a twin-circuit chiller is modelled by three heat exchangers in series. The two heat exchangers at both ends represent the evaporator in circuit A, and the middle one represents the evaporator in circuit B. The water tubes in the two heat exchangers at the two ends are submerged in the same bath of evaporating refrigerant at the shell side of the part of the evaporator in circuit A, and thus the evaporating temperature and pressure of the refrigerant in these two heat exchangers are identical. The cooling output of circuit A, Q_A, is the sum of cooling output of the first and the last heat exchangers, i.e.:

$$Q_A = Q_{Aa} + Q_{Ab} \tag{5.30}$$

It follows that:

$$Q_{Aa} = m_w \cdot c_w \cdot (T_r - T_{s1}) \tag{5.31}$$

$$Q_B = m_w \cdot c_w \cdot (T_{s1} - T_{s2}) \tag{5.32}$$

$$Q_{Ab} = m_w \cdot c_w \cdot (T_{s2} - T_s) \tag{5.33}$$

By assuming that Q_B equals half of the total cooling output of the chiller, the value of $(T_{s1} - T_{s2})$ is known:

$$(T_{s1} - T_{s2}) = \frac{Q_B}{m_w c_w} \tag{5.34}$$

The heat transfers from the chilled water to the evaporating refrigerant in the evaporators are governed by the effectiveness equations shown below:

$$Q_{Aa} = \varepsilon_{Aa} \cdot m_w \cdot c_w \cdot (T_r - T_{evpA}) \tag{5.35}$$

$$Q_{Ab} = \varepsilon_{Ab} \cdot m_w \cdot c_w \cdot (T_{s2} - T_{evpA}) \tag{5.36}$$

$$Q_B = \varepsilon_{evpB} \cdot m_w \cdot c_w \cdot (T_{s1} - T_{evpB}) \tag{5.37}$$

The effectiveness of the three heat exchangers and the overall heat transfer coefficient for the part of the evaporator in circuit B are as shown in equations (5.38) to (5.41) below.

$$\varepsilon_{Aa} = 1 - \exp(-\frac{AU_{Aa}}{m_w \cdot c_w}) \tag{5.38}$$

$$\varepsilon_{Ab} = 1 - \exp(-\frac{AU_{Ab}}{m_w \cdot c_w}) \tag{5.39}$$

$$\varepsilon_{evpB} = 1 - \exp(-\frac{AU_{evpB}}{m_w \cdot c_w}) \tag{5.40}$$

$$AU_{evpB} = \frac{1}{a_1 \cdot m_w^{-0.8} + a_2 \cdot Q_B^{-0.745} + a_3} \tag{5.41}$$

In the model, the assumption is made that the overall heat transfer coefficients AU_{Aa} and AU_{Ab} are approximately equal, as depicted by equation (5.42), and that equation (5.5) for the overall heat transfer coefficient of the part of the evaporator in circuit A (AU_{evpA}) remains valid.

$$AU_{Aa} \cong AU_{Ab} \cong 0.5 \cdot AU_{evpA} \tag{5.42}$$

Based on the above equations, the following iterative steps are used to estimate T_{evpB}.

1. Assume a value for T_{evpA}.

2. Using equation (5.35) and the assumed value of T_{evpA}, evaluate Q_{Aa}.

3. Using this value of Q_{Aa} and equation (5.31), evaluate T_{s1}.

4. Based on the assumption that $Q_A = Q_B = 0.5\ Q_{evp}$ and using this value of T_{s1} and equation (5.32), evaluate T_{s2} and then $Q_{Ab} = Q_A - Q_{Aa}$.

5. Using equation (5.36), T_{evpA} can be determined and checked with the value assumed in step 1. If the difference between them is large, the process will be repeated from step 1, taking the T_{evpA} value just estimated as the assumed value.

6. When a converged solution is found, T_{evpB} can be determined using equation (5.37).

For the other components, including the compressors, condensers and expansion valves, the same set of models developed for circuit A can be used for modelling the corresponding components in the two circuits when both are in operation.

5.3.7 The whole chiller model

A chiller simulation program has been developed by assembling the component models presented above. The inputs to the program include the chilled water supply (T_s) and return (T_r) temperatures and the outdoor air temperature (T_{out}) under the actual operating conditions. For each set of inputs corresponding to a particular operating

condition, the model will first determine the cooling load on the chiller (Q_{evp}), based on the known (constant) chilled water flow rate (m_w) and the input chilled water supply and return temperatures (T_s & T_r), and then the part load ratio (*PLR*). With reference to the *PLR*, whether only one circuit or both circuits will have to be run can be decided. When only one circuit needs to be run, the abovementioned alternate sequencing algorithm will be used to decide whether circuit A or circuit B will be operated. The iterative procedure for determining the evaporating temperatures in circuit A and circuit B will be implemented only if both circuits need to be run.

Because determination of the refrigerant mass flow rate, the compressor power and the heat rejection rate requires knowledge about the condensing temperature in the circuit (T_{cdA} &/or T_{cdB}) but the condensing temperature, in turn, can only be determined when the heat rejection rate is known, an iterative loop is implemented in the model to solve for the condensing temperature and the heat rejection rate simultaneously. Within this loop, there is another iterative loop for determining the number of condenser fans that need to be run. These nested iterative loops are implemented for each operating circuit. The convergence criteria used in computing the evaporating and condensing temperatures are both 0.01°C.

When a converged solution has been obtained, the compressor and condenser fan power demands, the evaporating and condensing temperatures of each circuit, and the total chiller power demand and *COP* will be output. The program will then proceed to the next set of input until all cases have been processed.

5.4 Coefficient evaluation

As noted in the above descriptions on the chiller model, there are a series of model coefficients that need to be evaluated based on known performance data for the chiller being modelled. For this purpose, the operating data of an existing chiller 2 for a period of 4 months (from February to May) were retrieved from the building management system. The set of data covered an outdoor temperature range from 12 to 30.8°C and a *PLR* range from 0.024 to 1.18.

The unknown coefficients in equations (5.5) & (5.41) for the overall heat transfer coefficients of the evaporators AU_{evpA} & AU_{evpB} were evaluated using the available chiller operation data that were pertaining to the condition where only a single circuit was operating. First, equation (5.5) was re-organized into:

$$\frac{1}{AU_{evpA}} = a_1 \cdot m_w^{-0.8} + a_2 \cdot Q_A^{-0.745} + a_3 \tag{5.43}$$

For each operating condition, the value of AU_{evpA} was determined beforehand using equation (5.44) and the corresponding data available in the records. Based on equation (5.43), multiple linear regression method was then used to evaluate the coefficients a_1 to a_3. The values so evaluated for these coefficients were 0.1748, 0.0549 and 0 respectively (R^2 = 0.98), and they apply to the evaporator models of both circuits.

$$AU_{evp} = m_w \cdot c_w \cdot \ln\left(\frac{T_r - T_{evp}}{T_s - T_{evp}}\right) \tag{5.44}$$

The overall heat transfer coefficients of the condensers (AU_{cdA}, AU_{cdB}) are described by equation (5.24), which was re-organized into:

$$\ln(AU_{cdA}) = \ln(e_1) + e_2 \cdot \ln(Q_{cdA}) + e_3 \cdot \ln(m_a) \tag{5.45}$$

For each operation record, the condenser air flow rate (m_a) was determined from the rated flow rate of each fan and the number of operating fans. The latter was estimated from the ratio of the power consumed by the operating fans to the total rated fan power of the chiller. By adding the compressor power and the cooling output of the chiller, the heat rejection rate (Q_{cdA}) was determined, which also allowed the leaving condenser air temperature (T_{ao}) to be found by using equation (5.20) and, in turn, the value of AU_{cdA} to be found using equation (5.46). On the basis of equation (5.45) and the set of pre-calculated values for $\ln(AU_{cdA})$, $\ln(Q_{cdA})$ and $\ln(m_a)$, the coefficients $\ln(e_1)$, e_2 & e_3 were evaluated using multiple linear regression method. The values of e_1 to e_3 so evaluated were 1, 0.6429 and 0.015 respectively (R^2 = 0.9).

$$AU_{cd} = m_a \cdot c_a \cdot \ln\left(\frac{T_{cd} - T_{out}}{T_{cd} - T_{ao}}\right) \tag{5.46}$$

For the combined motor and transmission efficiency, it was also estimated using the chiller performance data for the condition where only one single circuit was in operation. By re-arranging equation (5.8):

$$\eta_{cc} = m_{refA} \cdot \frac{w_{A,isen}}{\eta_{isen} \cdot W_{AC}} \quad ; \text{ when circuit A is in operation} \tag{5.47}$$

$$\eta_{cc} = m_{refB} \cdot \frac{w_{B,isen}}{\eta_{isen} \cdot W_{BC}} \quad ; \text{ when circuit B is in operation}$$

The refrigerant flow rate (m_{refA} or m_{refB}), the isentropic power ($w_{A,isen}$ or $w_{B,isen}$) and the isentropic efficiency (η_{isen}) in equation (5.47) can be determined using equations (5.9)

to (5.12) in conjunction with the available chiller performance data, which allowed a set of values for the combined motor and transmission efficiency (η_{cc}) corresponding to various operating conditions embraced by the available chiller performance data to be calculated. The unknown coefficients c_1 to c_3 in equation (5.13) for η_{cc} were then evaluated through multiple linear regression and the values found are -0.39, 1.4875 and 0.3043 respectively (R^2 = 0.98). Through a similar method, the values evaluated for the coefficients d_1 to d_3 in equation (5.14) for η_{cc} for two compressors working in parallel were -0.3422, 1.5444 and -0.1707 respectively (R^2 = 0.96).

As to the volumetric displacement (V_C) and the nozzle area (An) of each compressor in equations (5.15) & (5.16), they were estimated based on the rated operating condition of the chiller as stated in the chiller manufacturer's catalogue. The volumetric displacement of each compressor was estimated using equation (5.48) (Bourdouxhe et al., 1997) in which the power (W_{AC}) is the rated power of one compressor of the chiller.

$$V_C = \frac{W_{AC} \cdot (\gamma - 1)}{\gamma \cdot P_{evpA} \cdot \left[\left(\frac{P_{cdA}}{P_{evpA}} \right)^{\frac{\gamma-1}{\gamma}} - 1 \right]} \tag{5.48}$$

The nozzle throat area (An) of the compressor was calculated by re-arranging equation (5.15) into equation (5.49), with the refrigerant flow rate (m_{refA}) estimated using equation (5.9).

$$An = \frac{V_C - m_{refA} \cdot v_{A1}}{\sqrt{P_{evpA} \cdot v_{A1}} \cdot \left(\frac{P_{cdA}}{P_{evpA}}\right)^{\frac{\gamma+1}{2 \cdot \gamma}} \cdot \sqrt{\gamma \left(\frac{2}{\gamma+1} \right)^{\frac{\gamma+1}{\gamma-1}}}} \tag{5.49}$$

The results obtained were as follows:

Volumetric displacement of each compressor (V_C) =0.5638m^3/s

Nozzle area of each compressor (An) = 0.00092m^2

5.5 Comparison of model predictions with chiller operating records

Besides the set of data used in evaluation of the model coefficients, another set of measured operating performance data for another chiller (Chiller 4) of the same make and model in the same plant for a period of 3 months (from August to October) was collected for a comparison with the predictions of the chiller model. These data cover a wide range of part load ratio (PLR: 0.05-1.2) and outdoor air temperature (T_{out}: 22-37^{o}C). In addition to verification of the model prediction accuracy, this comparison was intended to verify at the same time whether it is valid to assume that:

1. The chiller model established based on the performance data of one chiller unit can be used to model the performance of another chiller unit of the same make and model in the same chiller plant. If so, the chiller model will facilitate development of optimized control and FDD strategies for all identical chillers in the plant.

2. The chiller model established based on operating data that covered a period from February to May can be applied to model chiller performance in another period in the year (August to October), such that the same model can be used for year-round chiller performance analysis.

It was considered reasonable to also make the second assumption above because, according to ASHRAE Handbook (2008), the refrigerant side heat transfer coefficient usually increases with an increase in the cooler load but flooded coolers have a relatively small change in heat transfer coefficient as a result of a change in load. In any case, the data used in the model development already covered nearly the full cooling output range of the chiller, and thus also the operating range of the chilled water temperatures, whereas the chilled water flow rate through the chiller was staying at a nearly constant level.

At the condenser side, the heat transfer coefficient of a condenser will vary mainly with the volumetric flow rate of air and the refrigerant flow rate (Kempiak and Crawford, 1992). Changes in the outdoor air temperature can affect the values of the air properties but the impact on the heat transfer coefficient of a condenser is small (Stoecker and Jones, 1982). In the model for the overall heat transfer coefficient of the condenser (equation (5.24)), the effect of air flow rate through the condenser has been taken into account. The effect of refrigerant flow rate has also been accounted for, through the use of heat rejection rate (Q_{cdA}) as a predictor variable.

The validity of the second assumption above was further verified by using the operating records of the second chiller to evaluate, once again, the model coefficients. The values of the coefficients a_1 to a_3 and e_1 to e_3 in equations (5.43) & (5.45) obtained this time were, for a_1 to a_3 in equation (5.43), 0.178, 0.044 and 0 respectively (R^2 = 0.93), while those of the coefficients e_1 to e_3 in equation (5.45) were 1, 0.639 and 0.019 respectively (R^2 = 0.89). These coefficient values are very close to the corresponding values of the coefficients reported in Section 5.4, which are further evidence to support that the assumption can be made without introducing significant prediction errors.

The model predictions have been compared with the recorded chiller operating data on the basis of the relative error of the model prediction (δ) as depicted by equation (5.50), where x_P is the predicted value of a variable under a specific operation condition of the chiller and x_M is the measured value of the variable under the same operating condition. Additionally, the mean bias error (*MBE*) and the standard deviation (*SD*) of the predictions from the measured values were evaluated using equations (5.51) and (5.52) for each predicted variable, where N_P denotes the number of data available for comparison with the predicted variable. The results, as summarized in Table 5.2, include the operating conditions where a circuit was the only circuit being run and when the circuit was operating concurrently with the other circuit. Figures 5.6 to 5.8 show the comparisons of the model predictions with the recorded chiller operating data.

$$\delta = \frac{x_P - x_M}{x_M} \tag{5.50}$$

$$MBE = \frac{1}{N_P}\sum_{i=1}^{N_P}(x_{P,i} - x_M) \tag{5.51}$$

$$SD = \sqrt{\frac{1}{N_P}\sum_{i=1}^{N_P}(x_{P,i} - x_M)^2} \tag{5.52}$$

Table 5.2 Accuracy of model predictions

Parameter	No. of data (N_P)	% of predictions within ±10% of measured value	Mean Bias Error (*MBE*)	Standard Deviation (*SD*)
COP	5674	96%	0.10	0.18
T_{evpA} (°C)	4990	84%	-0.13 °C	0.29 °C
T_{evpB} (°C)	4878	85%	0.01 °C	0.28 °C
$T_{cdA,}$ (°C)	4990	90%	0.22 °C	2.43°C
$T_{cdB,}$ (°C)	4878	90%	-0.38 °C	2.89 °C

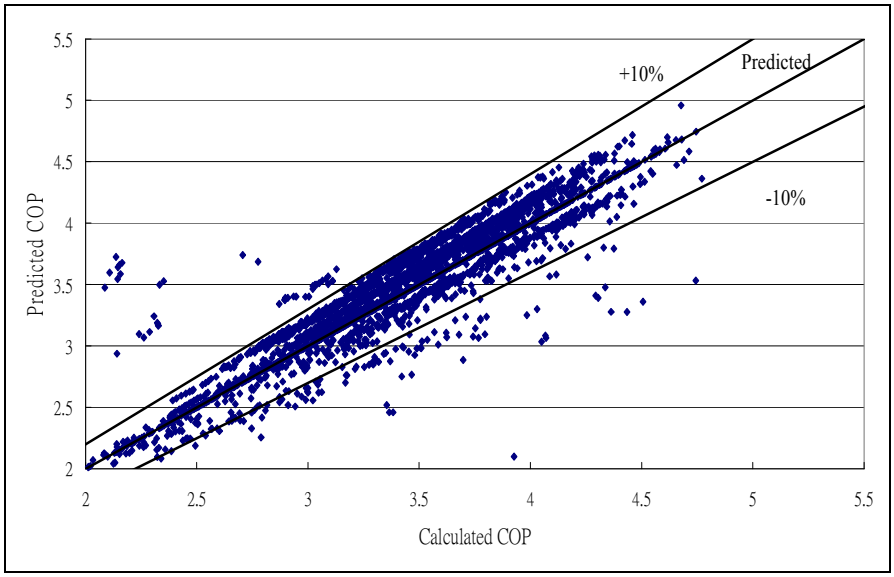

Figure 5.6 Comparison of COP predicted by the model and calculated from plant operating data

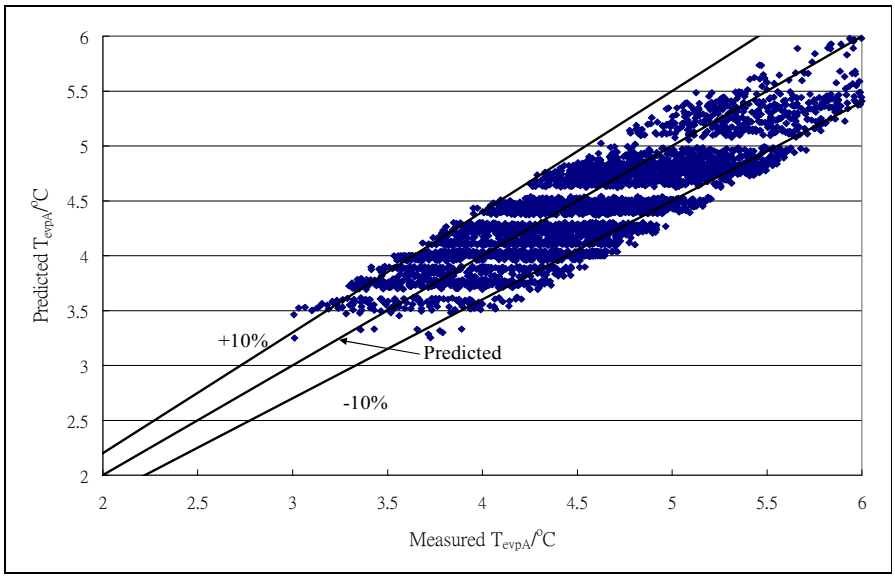

(a)

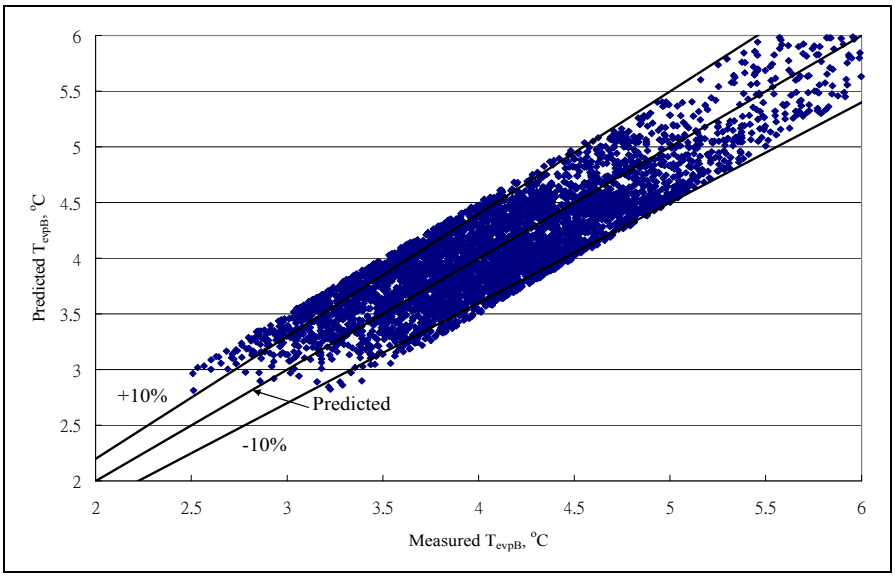

(b)

Figure 5.7 Comparison between predicted and measured evaporating temperature in: (a) circuit A; (b) circuit B

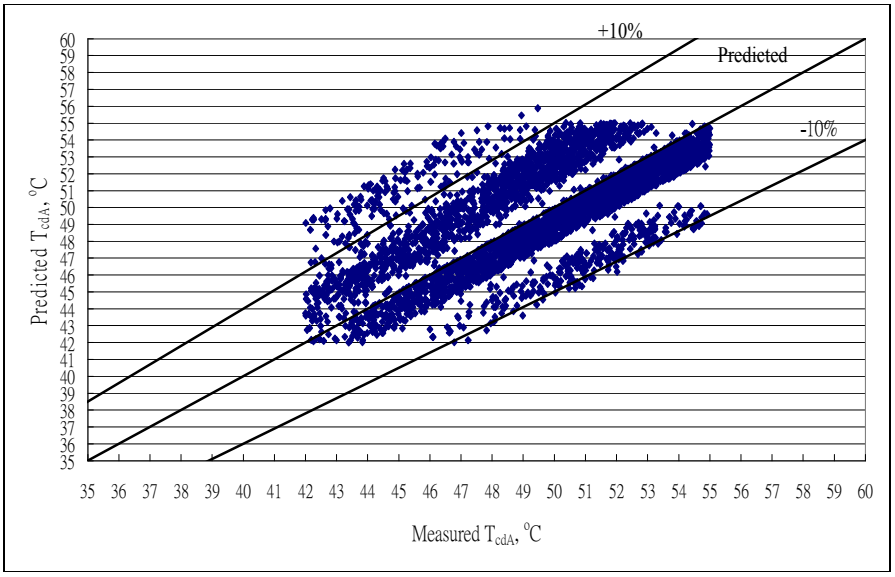

(a)

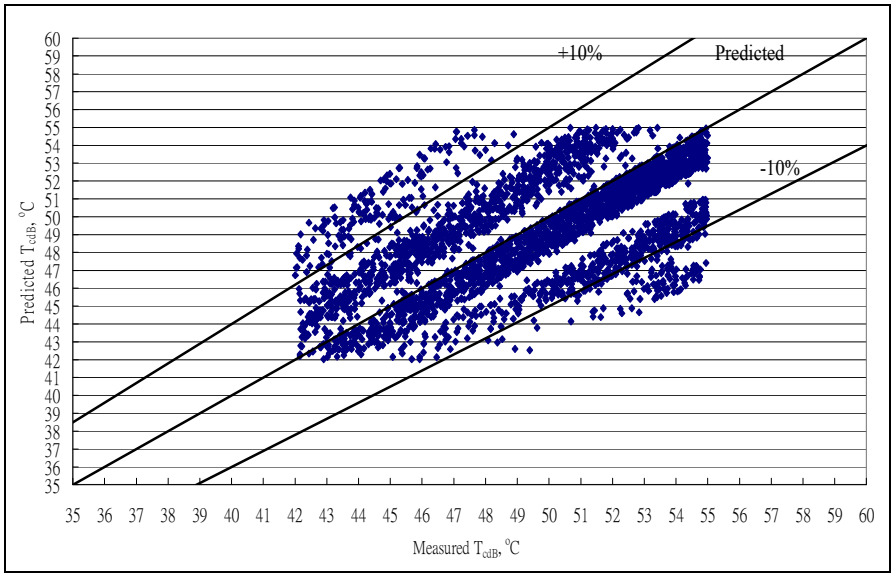

(b)

Figure 5.8 Comparison between predicted and measured condensing temperature in: (a) circuit A; (b) circuit B

As Table 5.2 and Figure 5.6 shows, the predicted *COP* of the chiller agrees well with the *COP* calculated from the chiller load and power demand data, with about 96% of the predicted values deviating from the respective calculated values by within ±10%. The

mean bias error and the standard deviation of the predicted *COP* values were respectively 0.1 and 0.18 only. The predicted evaporating temperatures in circuits A & B of the chiller (T_{evpA} & T_{evpB}, in ^{o}C) also compare well with the measured data, with about 84% and 85% of the predictions falling within ±10% of the respective measured values, and the mean bias errors and the standard deviations are small (<0.3^{o}C), as shown in Figure 5.7 and Table 5.2.

Although about 90% of the predicted condensing temperatures in circuits A and B are within ±10% of the respective measured values (Table 5.2), they were found scattering about the measured values in several cluster bands, as shown in Figure 5.8, which explains for the relatively large standard deviation values (up to 3^{o}C). Nonetheless, this is an expected outcome because the accuracy of the predicted condensing temperature is dependent on how accurately the number of condenser fans being run was predicted and any departure from the actual number would cause significant deviations between the predicted and the measured condensing temperature. With the wide dead-band used in determining whether or not to switch on or off condenser fans, having one more or one less fan running may not cause the condensing temperature to go above or below the high or low settings but the corresponding condensing temperatures could depart significantly from each other.

Comparison of the predicted number of circuit(s) being run with the measured records (indicated by the power demand of individual circuits) unveiled that the prediction deviated from the actual situation only in less than 5% of the cases. When the control algorithm in the chiller model was disabled and replaced by the actual number of

circuits in operation as ascertained from the measured records, the difference in the predicted energy use was found to be about 1% only.

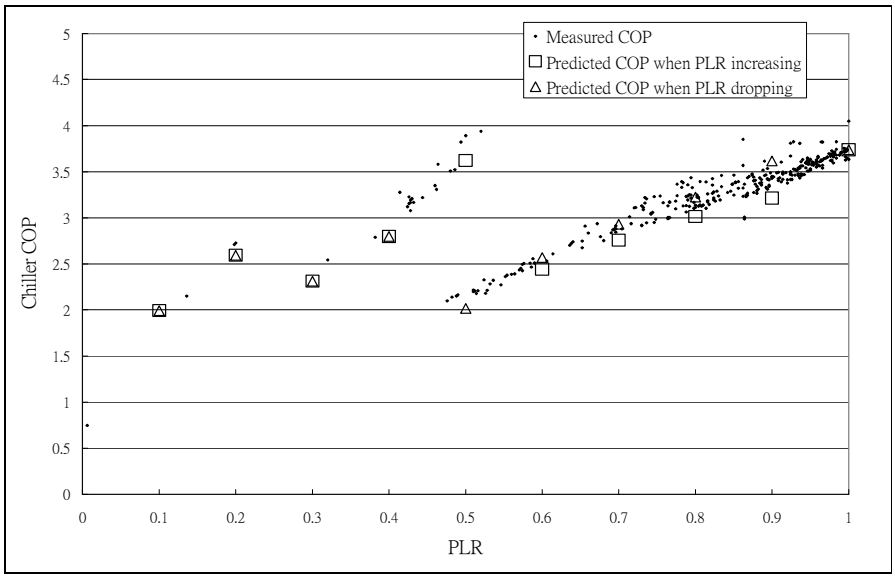

Figure 5.9 Change in chiller *COP* with *PLR*: Model predictions (T_{out}: 25.5°C) and measured data (T_{out}: 25-26°C)

Since the key improvement in chiller modelling method represented by the present chiller model is in its ability to model changes in chiller performance due to staged operation of the separate refrigerant circuits and of the compressors within each circuit, the predicted variation in *COP* with *PLR* was compared with the measured data. Figure 5.9 shows the overall chiller *COP* predicted by the model for a range of *PLR* under the outdoor temperature of 25.5°C. The prediction followed the operating sequence of the two refrigerant circuits in the chiller, as stated in Section 5.2. This clearly shows that the chiller *COP* can rise and drop substantially as an additional compressor or refrigerant

circuit is called upon to operate to cope with a rising load. Such a trend can also be observed from the measured data (also shown in the same figure), which were pertaining to the outdoor air temperature range of 25-26^{o}C.

5.6 Discussion

In this chapter, the model developed for an air-cooled twin-circuit screw chiller is presented and the chiller energy use predictions of the model have been verified to be in good agreement with measured data over a wide range of operating conditions. For chiller *COP*, 96% of the predictions fell within ±10% of the calculated values. The validation unveiled that the chiller model developed in this study can provide accurate enough performance predictions for the chillers and thus has the potential to be adopted for detecting and identifying the chiller fault.

Nonwithstanding that continuation with trial FDD implementation could not proceed further with the chiller plant due to problems with the chiller performance data measuring and recording functions of the BMS, which could not be resolved within a short period of time, the air-cooled chiller model developed and presented in this chapter is useful on its own, and may possibly be applied to the chillers when the problems with the BMS records in the plant can be resolved in the future. Furthermore, the experience gained underpinned subsequent development of the water-cooled chiller model for chillers in another chiller plant for FDD application.

6. A NEW CHILLED WATER CIRCUIT FOR CHILLER PERFORMANCE MEASUREMENT

6.1 Overview

As discussed in the previous chapters, although it was intended to base the present study on the Phase 1 chiller plant for a trial development and implementation of FDD strategies for that plant, the problems with the plant performance measurement and recording system and instruments made it difficult to carry on with the work. Focus of the study, therefore, was shifted to the Phase 3B plant in the same complex which has recently been retrofitted. The retrofitting work included not only replacement of the old air-cooled chillers with new water-cooled chillers, condenser water pumps and cooling towers, a chilled water piping circuit design that can facilitate expeditious measurement of chiller full- and part-load performance has also been incorporated, which can solve one of the most important barriers of developing automatic FDD, i.e. in obtaining the reliable full range chiller performance data for development of fault-free chiller model.

Before conducting full range chiller performance measurement, the measurement accuracies of the sensors in the plant were checked by simple measurements and an analysis of the plant operation records. The analysis unveiled that the chilled water flow rate through the chillers was lower than the design flow rate and the chilled water return temperature often stayed below the design level due to excessive flow rate demand, which could hinder full load tests on the chillers. After the causes of the problems were

diagnosed and the problems resolved, the measurements of the full- and part-load performance of the chillers were successfully conducted, as described in the following parts of this chapter.

6.2 Alternative chilled water system

Two chilled water circuit designs have been proposed by Yik (2008), one for a single-loop and the other for a two-loop system (Figure 6.1), which would allow the performance over the entire output range of each chiller in a central air-conditioning plant to be measured *in-situ* in a convenient and expeditious manner. The key feature of the chilled water circuit designs is that in addition to the normal (differential pressure or de-coupler) bypass pipe at one side (the load side) of the group of chillers (pipe FC in Figure 6.1), an alternative bypass pipe is installed at the other side of the chillers (pipe HG in Figure 6.1).

The circuit design allows a chiller plant to be switched between the normal operation mode and the measurement mode. In the normal operation mode, the isolation valve in the alternative bypass pipe will be tightly shut and surplus chilled water will flow through the normal bypass pipe. The running chillers will each have a share of the total cooling load on the plant at the same part-load ratio (actual-to-full load ratio), no different from chillers in any plant that adopts a conventional chilled water circuit design. However, this equal proportion load sharing characteristic limits the frequency of occurrence of full-load and near zero-load on the chillers, and thus measurement and verification (M&V) of chiller performance over the entire output range would need to span a long time period to allow sufficient data to be captured, which is a hindrance to M&V of chiller performance.

This hindrance can now be overcome by adopting the proposed chilled water circuit designs (Yik, 2008).

When switched to the measurement mode, surplus chilled water will flow through the alternative bypass pipe (pipe HG). For a single-loop system (Figure 6.1.a), the differential pressure bypass control valve in the normal bypass pipe (pipe FC) will be utilized in the measurement mode to control the temperature of chilled water entering the chillers. Whenever the temperature of the chilled water returning from the air-side equipment exceeds the entering temperature at which the chillers were rated, the control valve will let pass some supply chilled water to flow through the bypass pipe and mix with the return chilled water from the air-side systems such that the chilled water entering the chillers will be kept at the rated temperature. This is needed to safeguard the chillers from being overloaded. For a two-loop system (Figure 6.1.b), water flow through the normal de-coupler bypass pipe (pipe FC) will be blocked by a tightly shut isolation valve in the pipe but there is an additional bypass pipe (pipe JK) with a control valve in it to serve the return chilled water temperature control function.

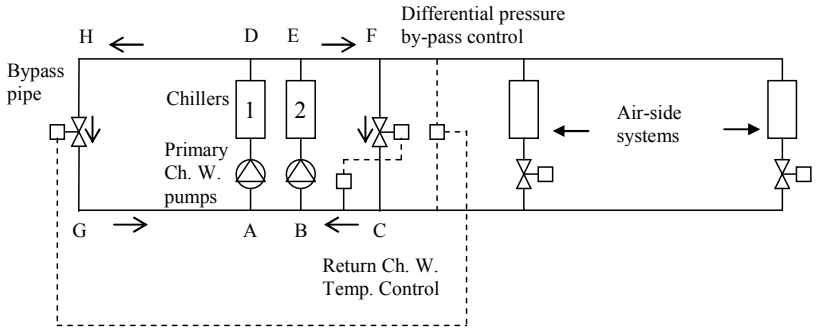

(a)

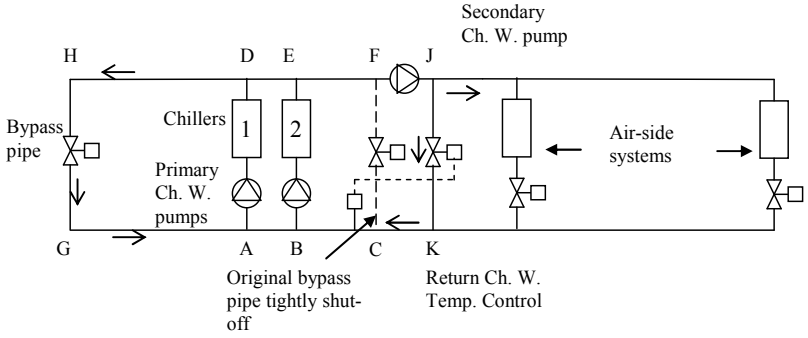

(b)

Figure 6.1 Proposed chilled water circuit designs: (a) single-loop pumping system; (b) two-loop pumping system

In the measurement mode, a chiller will be loaded up to its full capacity before an additional chiller needs to be run to cope with a rising total load, as long as the chilled water returning from the air-side systems stays at or above the rated return temperature. When multiple chillers are running, all the running chiller(s) can be loaded steadily at their full capacity (or lower if the return chilled water temperature from the air-side equipment stays below the rated return chilled water temperature of the chillers) except one, referred to as the 'last' chiller, which may be loaded at any level between 0 to 100% of its full capacity, depending on the total load on the plant. If no further provisions are made, the unit among the running chillers that is located the furthest away from the load

side will become the last chiller. This is because mixing of the surplus chilled water and the chilled water returning from the air-side equipment will take place only at the entry point to the 'last' chiller whereas all other running chiller(s) will be fed with chilled water returning from the air-side equipment direct, or with mixed chilled water at the rated return temperature of the chillers should the temperature of the chilled water returning from the air-side equipment exceeds the rated temperature.

The circuit design includes auxiliary pipes with isolation valves to allow selection of any chiller in a plant to become the 'last' chiller (Yik, 2008). With the circuit design and through the use of a building management system (BMS), sufficient full- and part-load performance data for each chiller can be recorded within a much shorter period of time than with just the conventional circuit design, which can greatly facilitate performance evaluation of chillers and for development of chiller models for fault detection and diagnostics (Katipumula and Brambley, 2005a & 2005b).

With the proposed chilled water circuit design recently adopted in the Phase 3B plant when the air-cooled chillers in the plant were replaced by new water-cooled chillers, this provided an opportunity to demonstrate the effectiveness of the proposed chilled water circuit design, including making observations on whether any problems could arise which may hinder its successful application.

6.3 System Configuration

Since the five air-cooled chillers in the original plant were aging and the regulatory control that prohibits use of water supply from city mains for air-conditioning purposes has been relaxed in Hong Kong (EMSD, 2008), a decision was made to convert

the air-cooled chiller plant into a water-cooled plant in the interest of energy saving. In this plant retrofit project, three of the five old air-cooled chillers have been replaced by three new water-cooled chillers, each with a rated cooling capacity of 400 tons of refrigeration (TR, 1TR = 3.517kW). The three water-cooled chillers can collectively provide a total cooling capacity sufficient to cope with the peak cooling demand of the building. The remaining two air-cooled chillers, each with a rated cooling capacity of 265TR, are retained for standby purpose.

The schematic diagrams of the chilled and condenser water systems, after the chiller replacement and pipe modification, are as shown in Figures 6.2 & 6.3. As shown in Figure 6.2, the chilled water distribution system in the plant is a two-loop system. There are five constant speed primarily-loop chilled water pumps (PCWPs), each connected in series with the chiller it serves, and three variable speed secondary-loop chilled water pumps (SCWPs) for circulating the chilled water between the chiller plant and the air-side equipment, which are mostly fan-coil units. The three new water-cooled chillers (Chillers 2 to 4) are served by three cooling towers with matching heat rejection capacity and four condenser water pumps (CWPs), with one for standby (Figure 6.3). The condenser water circuit includes a bypass control system for ensuring the temperature of the condenser water entering the chillers will not fall below a minimum preset level. Table 6.1 summarizes the key performance characteristics of the major equipments in the plant.

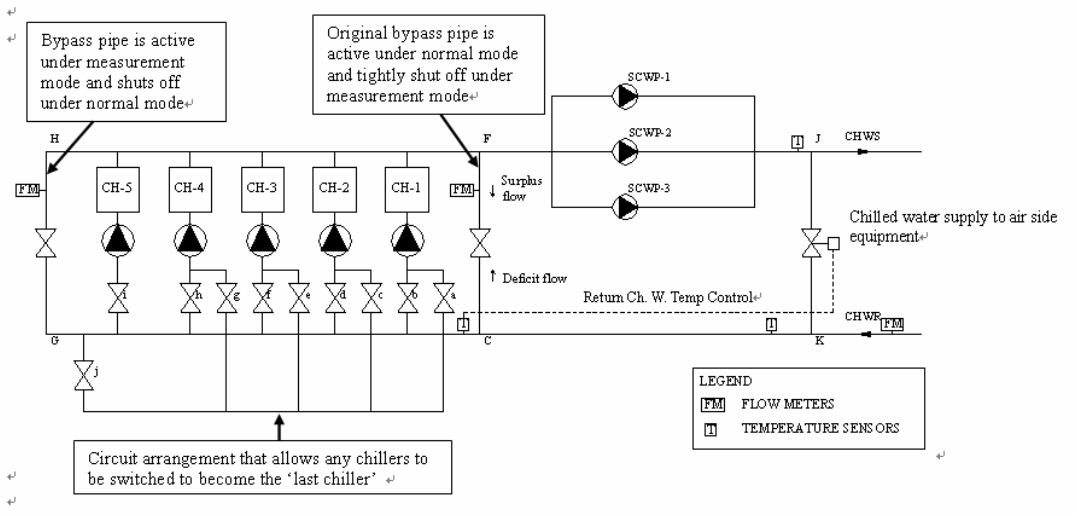

Figure 6.2 Schematic of the chilled water system

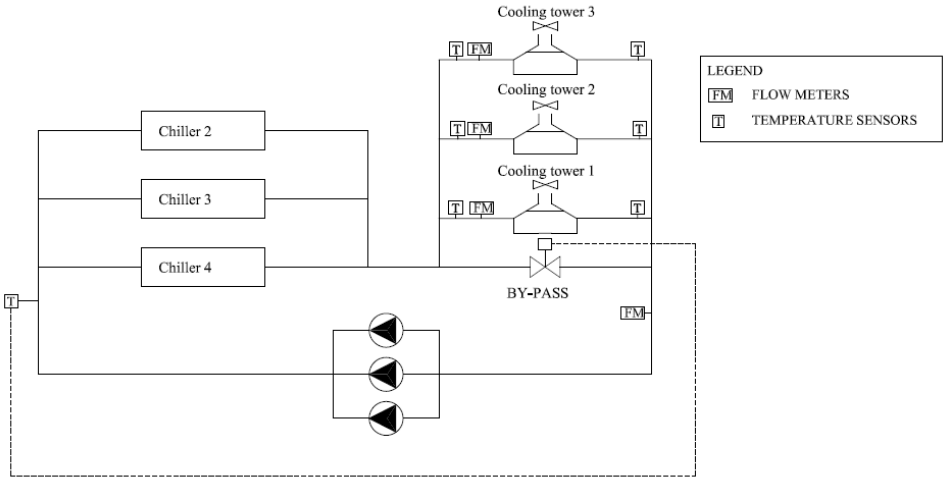

Figure 6.3 Schematic of the condenser water system

Table 6.1 Characteristics of major equipments in the chiller plant

	New chillers	Existing chillers
Type	Water-cooled screw	Air-cooled reciprocating
Number of chillers	3	2
Chiller numbers	CH-2 to CH-4	CH-1 & CH-5
Rated cooling capacity (each), TR	400	265
Rated chilled water inlet temp., ^{o}C	12	12
Rated chilled water outlet temp., ^{o}C	7	7
Rated chilled water flow rate (each), kg/s	67	44
Rated water pressure drop across evaporator, kPa	110	60
Rated condenser water / air inlet temp., ^{o}C	32	35
Rated condenser water outlet temp., ^{o}C	37	-
Rated condenser water flow rate (each), kg/s	83.8	-
Rated water pressure drop across condenser, kPa	58	-
Rated power demand, kW	254	316
Rated coefficient of performance (COP)	5.5	2.9

	New CWPs	New CWPs	Existing PCWPs	Existing SCWPs
Number of pumps	3	4	2	3
Pump numbers	PCWP-2 to PCWP-4	CWP-1 to CWP-4	PCWP-1 & PCWP-5	SCWP-1 to SCWP-3
Chilled water flow rate (each), kg/s	67	83.8	44	125.6
Pumping pressure, kPa	150	230	150	375

6.4 Measurement sensors

A variety of sensors were installed and connected to the BMS for monitoring the performance of the major equipment in the chiller plant. Such sensors include discrete sensors installed at various locations in the chilled and condenser water systems (Figures 6.2 & 6.3) and built-in sensors that came with the chillers. Information about the measurement accuracy of the sensors was sourced from manufacturers' technical data, as summarized in Table 6.2. The chiller plant operation records analyzed in the present study were retrieved from the BMS. The raw data available cover the range of system variables as summarized in Table 6.3.

Table 6.2 Measurement accuracies of sensors in the chiller plant

Instruments	System variables measured	Accuracy
Thermistors	Secondary-loop main chilled water supply and return temperatures Common chilled water return temperature to chillers Chilled water entering and leaving temperatures at individual water-cooled chillers (built-in sensor in chillers) Condenser water entering and leaving temperatures at individual water-cooled chillers (built-in sensor in chillers)	±0.3˚C
Insertion type flow meters	Chilled water flow rate in and bypassing the secondary-loop Chilled water and condenser water flow rates through individual water-cooled chillers (built-in sensors in chillers)	±4% of full scale
Watt meters	Power demands of chillers and pumps	±1% of full scale

Table 6.3 Measurements of system variables available from BMS records

System variables	Symbol
Chilled water supply temperature at chiller *i*	T_{si}
Chilled water return temperature at chiller *i*	T_{ri}
Condenser water temperature entering chiller *i*	T_{cdei}
Condenser water temperature leaving chiller *i*	T_{cdli}
Main secondary-loop chilled water supply temperature	T_{ss}
Main secondary-loop chilled water return temperature	T_{sr}
Common chilled water return temperature to chiller(s)	T_{rch}
Chilled water flow rate through chiller *i*	m_i
Bypass chilled water flow rate	m_{by}
Secondary-loop chilled water flow rate	m_{sec}
Condenser water flow rate through chiller *i*	m_{cdi}
Power of chiller *i*	W_i
Refrigerant condensing temperature in chiller *i* (water-cooled)	T_{cdi}
Refrigerant evaporating temperature in chiller *i* (water-cooled)	T_{evpi}

6.5 Verification of sensor accuracy and plant operating conditions

6.5.1 Water temperature sensors

Prior to M&V of the performance of the newly installed chillers, work was done to verify the accuracy of the measurements of the available sensors to ensure the measured data can provide a sound basis for the performance evaluation. Site inspection unveiled that neither auxiliary thermometers nor thermal wells were available in the

piping system for verification of the measurement accuracy of the water temperature sensors. Simple *in-situ* measurements, which involved releasing chilled water from the pipe and measuring the temperature of the running water using a mercury-in-glass thermometer, had been conducted at locations where release taps are available and are close to the water temperature sensors. The verification measurements unveiled that the chilled water supply and return temperature sensors in the secondary-loop and inside individual chillers were all reasonably accurate; the deviations between the sensor output readings and the *in-situ* measurements were within ±0.3°C, as shown in Table 6.4.

Table 6.4 Comparison of temperature measurements retrieved from the BMS with snap-shot measurements made on-site

	Measurement with liquid-in-glass thermometer (°C)	BMS Reading (°C)	Absolute deviation (°C)
Secondary-loop chilled water return temp	11.7	11.4	0.3
Common chilled water return temp to chillers	11.2	11	0.2
Secondary chilled water supply temp	7	7.2	0.2
Chiller 2 supply temp	7.1	6.8	0.3
Chiller 2 return temp	11.2	10.9	0.3
Chiller 3 supply temp	7.2	7	0.2
Chiller 3 return temp	11	11.1	0.1
Chiller 4 supply temp	7	7	0
Chiller 4 return temp	12.2	12.2	0

Besides the simple *in-situ* temperature measurements, further analysis was conducted to verify if the measurements of the installed sensors would remain reasonably accurate at other values of the measured variables within the feasible operating range. The analysis, however, was limited to relative comparisons based entirely on the measurements retrieved from the BMS, with the readings from a selected sensor taken as a reference for comparisons with the readings from other sensors in the chilled water

system. About 200 sets of records logged by the BMS at 30 minutes intervals in September 2008 were retrieved for use in this verification analysis.

Since the three water-cooled chillers were identical and all were set with the same supply temperature set-point (7°C), the supply chilled water temperatures from individual chillers should be close to each other and to the main chilled water supply temperature; any large deviations would point to presence of faulty sensors. Figures 6.4, 6.5 and 6.6 show respectively the relations between the chilled water supply temperature measured by the sensors inside the chiller 2, 3 and 4 and the reference supply water temperature. The figures illustrate that there are significant correlations between the reference reading and the readings measured by the supply water temperature sensors in all chillers, but there could be little bias errors with the sensors.

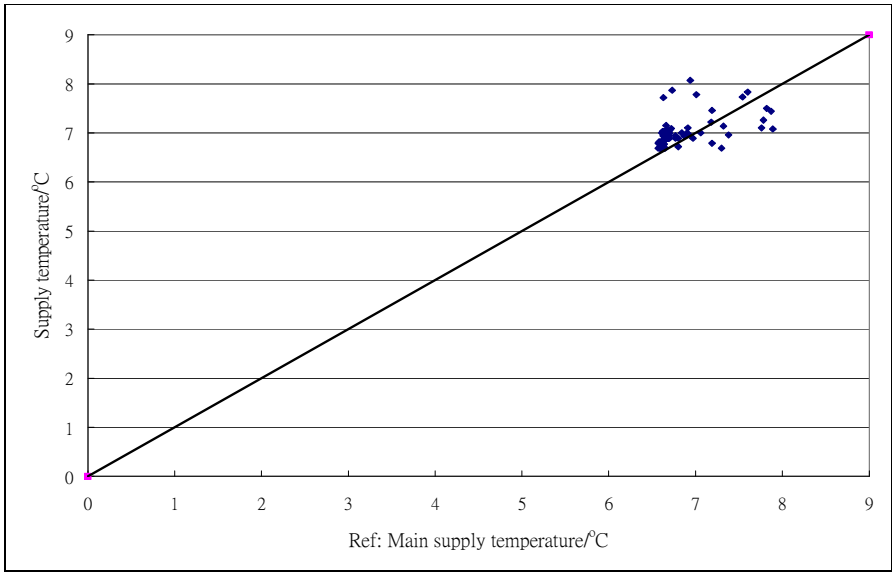

Figure 6.4 Correlation between chilled water supply temperature of chiller 2 and the reference temperature

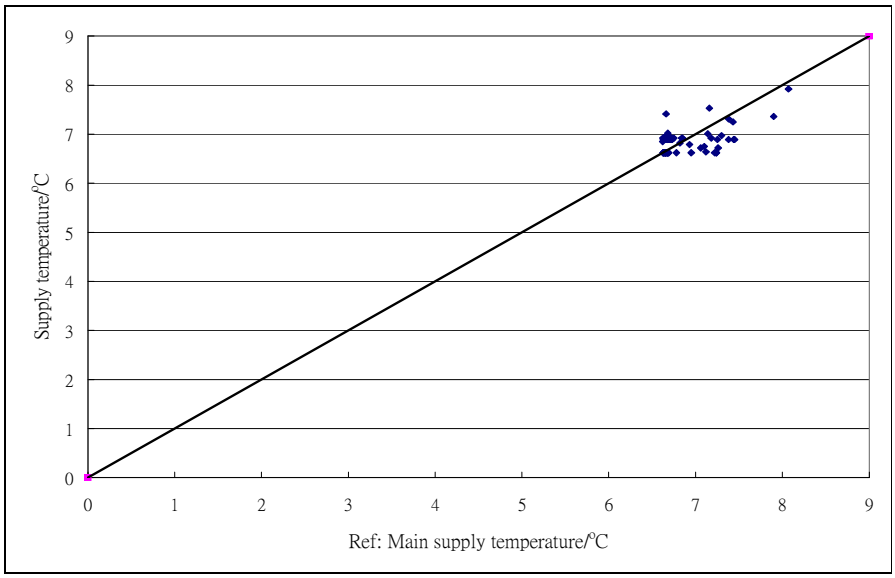

Figure 6.5 Correlation between chilled water supply temperature of chiller 3 and the reference temperature

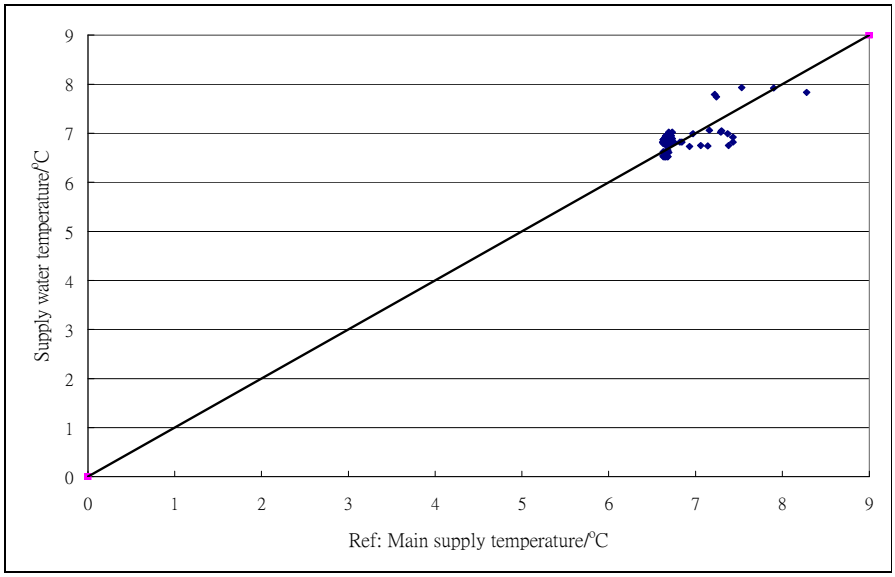

Figure 6.6 Correlation between chilled water supply temperature of chiller 4 and the reference temperature

A statistical analysis of the deviations of the chilled water supply temperature measured by the respective sensors inside Chillers 2, 3 and 4 from the main supply temperature was conducted. As Table 6.5 shows, measurements of the built-in supply chilled water temperature sensors were slightly higher than the main chilled water supply temperature, but the mean bias and root mean square errors are small enough to support that the sensors can be regarded as reasonably accurate.

Table 6.5 Statistical analysis on the deviations of individual chilled water temperature sensor readings from the reference readings

Temperature sensor	Chiller 2		Chiller 3		Chiller 4		Common chilled water return temperature (T_{rch}) (°C)
	Supply (°C)	Return (°C)	Supply (°C)	Return (°C)	Supply (°C)	Return (°C)	
Main bias error	0.18	0.19	0.10	0.11	0.09	0.20	-0.05
Root mean square error	0.34	0.24	0.27	0.21	0.22	0.28	0.22

With the plant operating in the normal mode, the return chilled water temperature at each chiller (T_{ri}) should be equal to the temperature of the chilled water (T_r) resulting from mixing of the main return chilled water in the secondary-loop with the bypass chilled water whenever there is surplus flow through the bypass pipe ($m_{by} \geq 0$). If there is deficit flow ($m_{by} < 0$), the return chilled water temperature would be equal to the main return chilled water temperature in the secondary-loop. Therefore, T_r can be estimated based on the supply and bypass flow rates (m_{sec} & m_{by}; assuming both can be accurately measured) and the main supply and return temperatures (T_{ss} & T_{sr}) in the secondary-loop, as shown in equation (6.1). The return chilled water temperature so determined was taken as the reference for verifying whether the sensor for measuring the common chilled water return temperature to the chillers (T_{rch}) and the return chilled water temperature sensors inside individual chillers (T_{ri}) had significant measurement errors.

$$T_r = \begin{cases} \dfrac{m_{by}T_{ss} + m_{\text{sec}}T_{sr}}{m_{by} + m_{\text{sec}}}; m_{by} \geq 0 \\ \\ T_{sr}; m_{by} < 0 \end{cases} \tag{6.1}$$

Figure 6.7 shows the good match between the common chilled water return temperature (T_{rch}) and the calculated chilled water return temperature. As shown in Figures 6.8, 6.9 and 6.10, the return chilled water temperature measured by the sensors in Chiller 2, 3 and 4 bear a linear relation with the calculated return chilled water temperature with some scattering around the straight line that represents perfect correlations.

Results of the statistical analysis on the deviations of the sensor readings from the reference readings show that the mean bias and root mean square errors of the common return temperature sensor and the return temperature sensors in individual chillers were all within ±0.3^{o}C (Table 6.5). Hence, the return chilled water temperature sensors may be regarded as in normal working order.

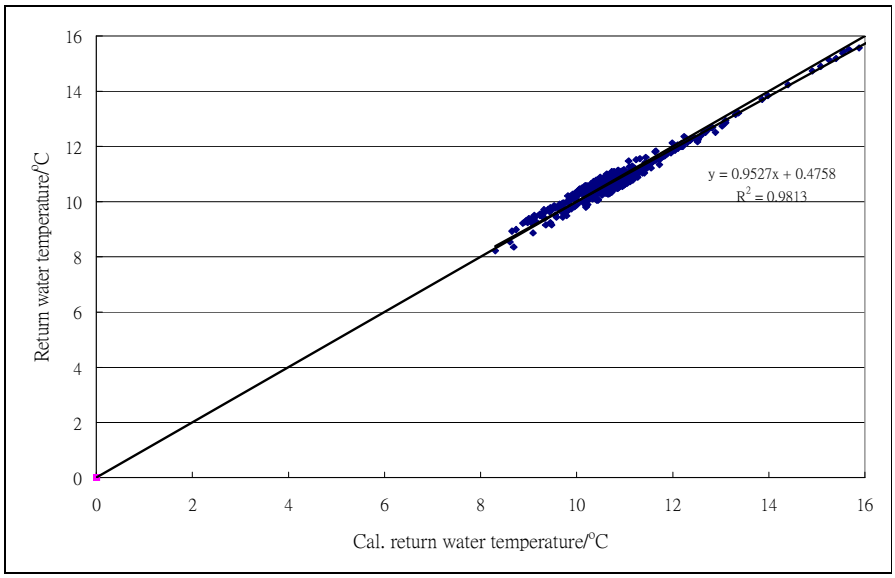

Figure 6.7 Correlation between chilled water return temperature and the calculated chilled water return temperature

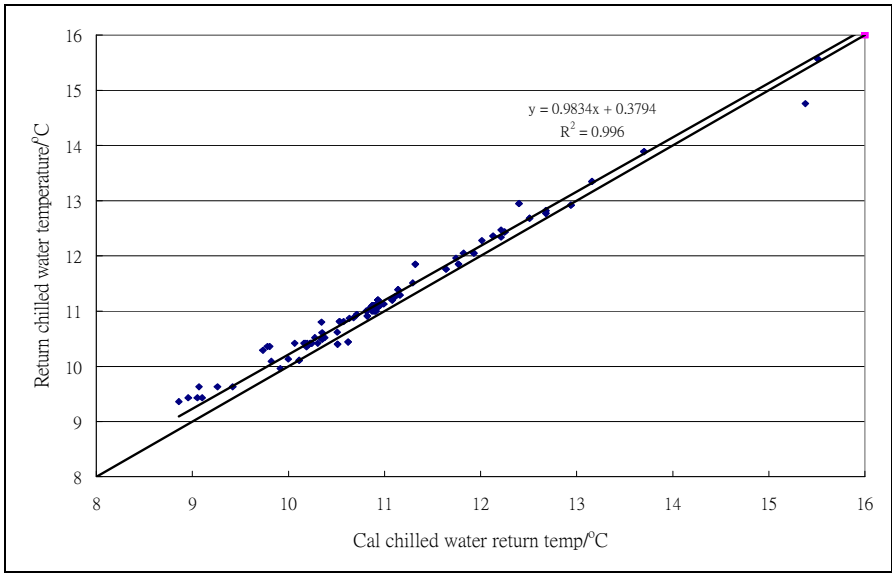

Figure 6.8 Correlation between chilled water return temperature of chiller 2 and the calculated chilled water return temperature

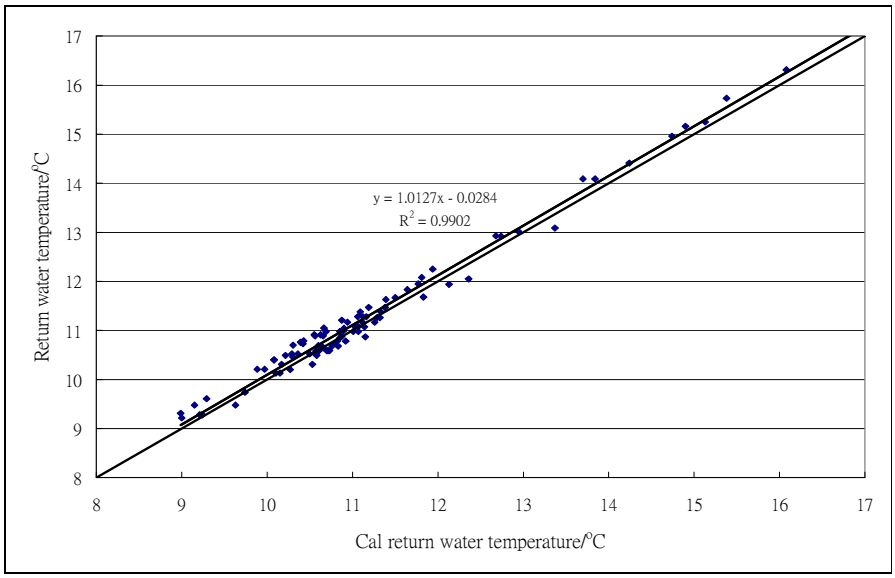

Figure 6.9 Correlation between chilled water return temperature of chiller 3 and the calculated chilled water return temperature

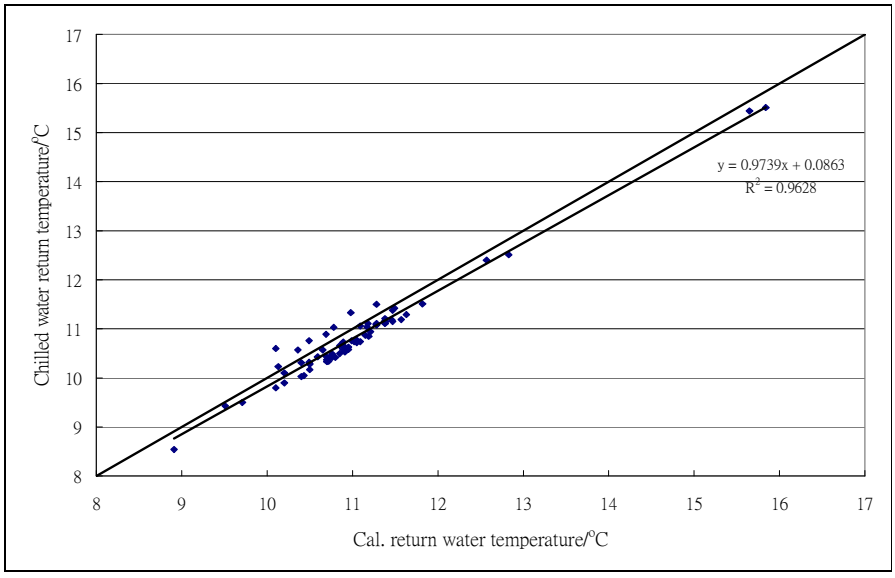

Figure 6.10 Correlation between chilled water return temperature of chiller 4 and the calculated chilled water return temperature

6.5.2 Chilled and condenser water flow rate

Due to the lack of extra flow meters that could provide accurate measurements for direct comparison, verification of the measurement accuracies of the flow meters for measuring the chilled and condenser water flow rates was based on the water pressure drops across the chiller evaporators and condensers, and the pumping pressures and the characteristic curves of the primary-loop chilled water pumps and condenser water pumps, albeit such references could only provide a crude comparison. Furthermore, the flow rate readings in the abovementioned set of BMS records were examined and an analysis of flow conservation based on the measured flow rate data was carried out for a consistency check.

The chilled water flow rates and condenser water flow rates of water cooled units were as shown in Figures 6.11 & 6.12 and the results of statistical analysis on the chilled and condenser water flow rate data in the set of BMS records are summarized in Table 6.6. As shown in Figure 6.11 and Table 6.6, notwithstanding that the rated chilled water flow rate through each of the water-cooled chillers should be 67*l/s*, the mean chilled water flow rates, as measured by the built-in flow meters in the chillers, were in the range of 49 to 53*l/s* only. In response to our enquiry, the plant operator confirmed that the chilled water pumps were under-sized. Nonetheless, the mean chilled water flow rates were deviating from each other by at most 4*l/s*. The mean condenser water flow rates through Chillers 2 to 4, as shown in Figure 6.12 and Table 6.6, were in the range of 87 to 89*l/s* and were reasonably close to the chillers' rated condenser water flow rate (83.8*l/s*).

Table 6.6 Statistical analysis on the individual chilled water flow rate of individual chiller

	Chiller 2		Chiller 3		Chiller 4	
Flow meter	Chilled water flow rate (l/s)	Condenser water flow rate (l/s)	Chilled water flow rate (l/s)	Condenser water flow rate (l/s)	Chilled water flow rate (l/s)	Condenser water flow rate (l/s)
Mean	49.13	88.27	53.27	89.26	51.04	87.47
Standard deviation	0.42	2.42	0.52	3.63	0.61	2.35

As found from the chiller manufacturer's catalogue, the evaporator and condenser water pressure drops of the same chiller model as those being studied would be 110KPa and 58kPa when the chilled and condenser water flow rates were 67 and 83.8*l/s* respectively. Based on this information, the flow resistance of the evaporator or condenser (K) of a chiller were calculated using equation (6.2), to allow the water flow rates to be estimated based on measured evaporator and condenser pressure drops , using equation (6.3). Table 6.7 shows the pressure drops across the evaporator and the condenser of the chillers, as found from an on-site inspection, and the corresponding chilled and condenser water flow rates estimated. The mean chilled and condenser water flow rates determined from measurements of the built-in flow meters in the chillers were found to be deviating from the respective estimated flows by at most 7%.

$$K = \Delta p / V^2 \tag{6.2}$$

$$V = \sqrt{\frac{\Delta p}{K}} \tag{6.3}$$

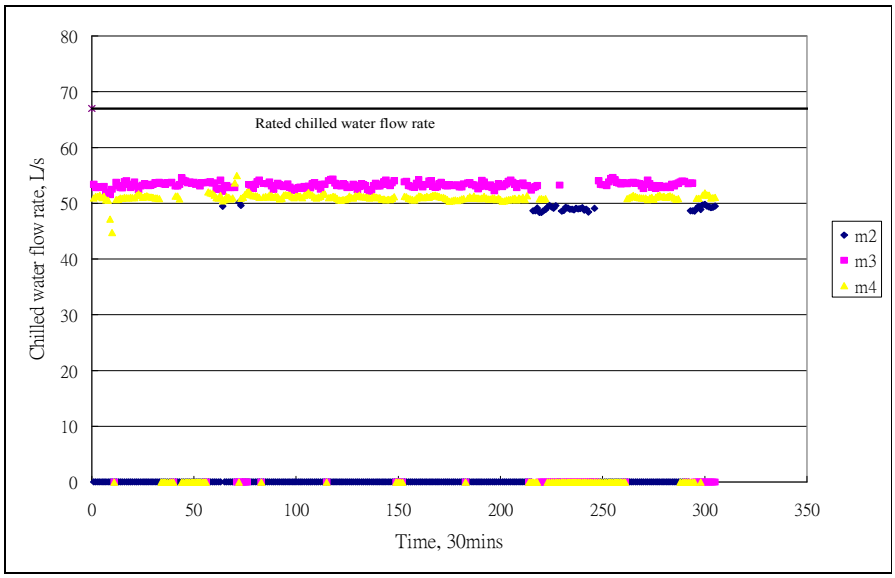

Figure 6.11 Chilled water flow rate through chillers 2, 3 and 4 (m_2, m_3 and m_4)

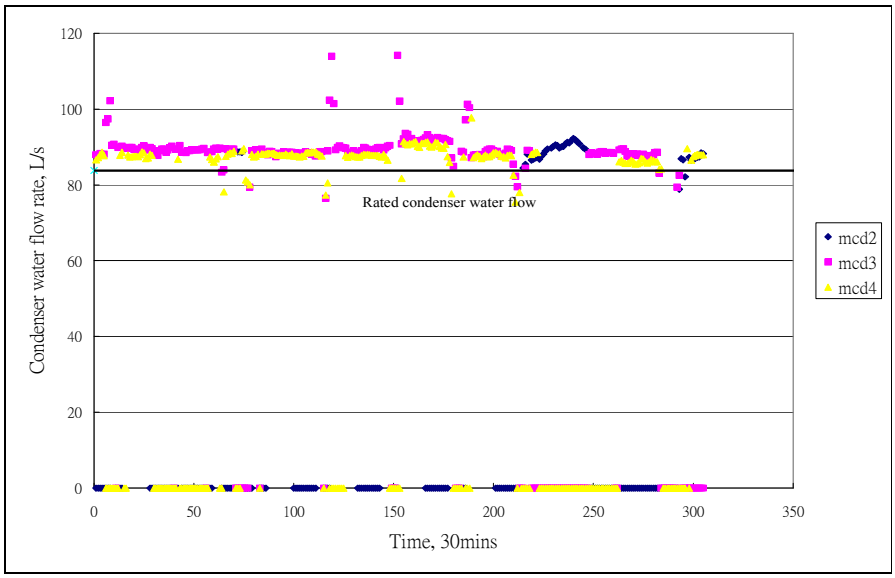

Figure 6.12 Condenser water flow rate through chillers 2, 3 and 4 (m_{cd2}, m_{cd3} and m_{cd4})

Table 6.7 Chilled and condenser water flow rates estimated from pressure drops across chillers

Recorded data	Unit	Chiller 2	Chiller 3	Chiller 4
Cooler inlet pressure	kPa	117	117.4	119.3
Cooler outlet pressure	kPa	48.9	46.1	47.8
Measured chilled water flow	l/s	49	53	51
Evaporator in/out pressure difference	kPa	68.1	71.3	71.5
Estimated evaporator flow rate	l/s	52.7	53.9	54
Deviation between measured and estimated flow rate	l/s (%)	3.7 (7)	0.9 (1.7)	3 (5.6)
Condenser inlet pressure	kPa	133	132.3	135
Condenser outlet pressure	kPa	76	75.2	77
Measured condenser water flow	l/s	88	89	87
Condenser in/out pressure difference	kPa	57.0	57.1	58.0
Estimated condenser water flow rate	l/s	83.1	83.1	83.8
Deviation between measured and estimated flow rate	l/s (%)	4.9 (5.9)	5.9 (7)	3.2 (3.8)

The pumping pressures of the primary-loop chilled water pumps and the condenser water pumps found during the site inspection were also used to estimate the chilled and the condenser water flow rates, using the characteristic curves of the respective pumps (Figure 6.13 and Tables 6.8 & 6.9). The flow rates through the primary-loop chilled water pumps and the condenser water pumps so determined were also found to be close to the respective flow rates across the chillers as measured by their built-in sensors.

Table 6.8 Chilled water flow rates estimated from primary chilled water pump pressure

Recorded data	Unit	PCWP 2	PCWP 3	PCWP 4
Suction pressure	kPa	7.2	7.3	7.3
Discharge pressure	kPa	126.3	123.4	124.4
Pressure difference	kPa	119.1	116.1	117.1
	mH_2O	12.1	11.8	11.9
Chilled water flow rate	l/s	50	52.3	51.4
(from pump curve)	m^3/h	180	190	185
Chilled water flow rate	l/s	49	53	51
(measured)	m^3/h	176.4	190.8	183.6

Table 6.9 Condenser water flow rates estimated from condenser water pump pressure

Recorded data	Unit	CWP 1	CWP 2	CWP 3
Suction pressure	kPa	1	1	2
Discharge pressure	kPa	188.4	189.3	190.9
Pressure difference	kPa	187.4	188.3	188.9
	mH_2O	19.1	19.2	19.3
Condenser water flow rate	l/s	86.1	84.7	83.3
(from pump curve)	m^3/h	310	305	300
Condenser water flow rate	l/s	88	88	88
(measured)	m^3/h	316.8	316.8	316.8

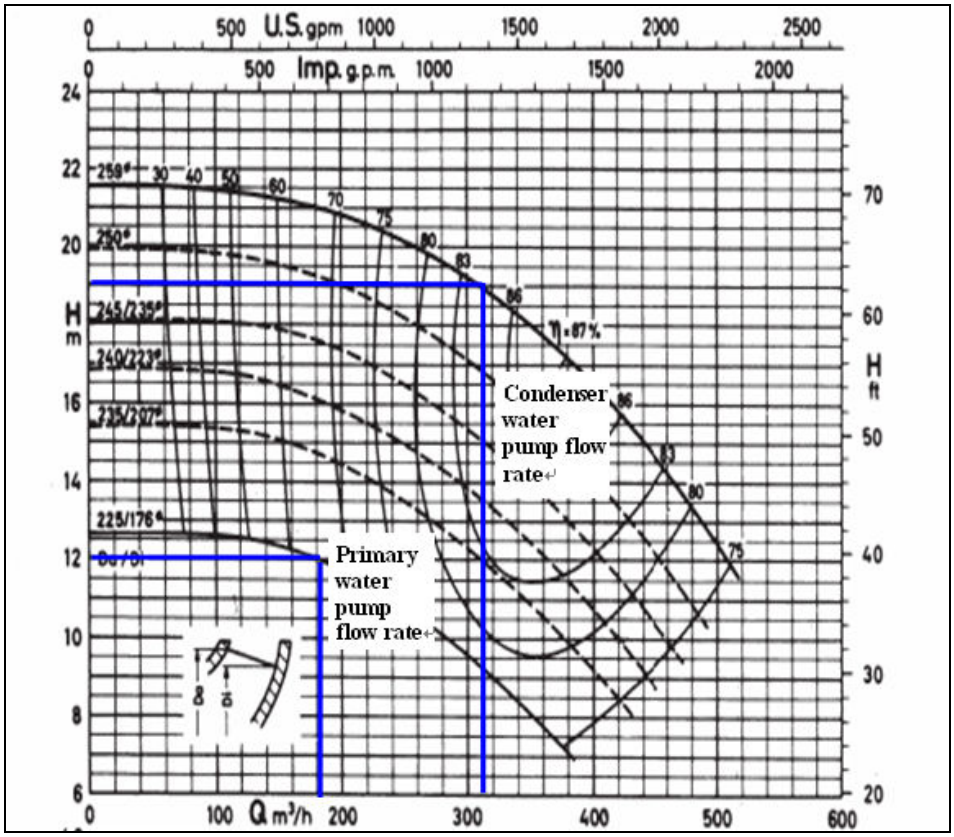

Figure 6.13 Chilled water flow rate estimation from the pressure measurement and pump curve (Etabloc, 2007)

In addition to the built-in flow meters in the chillers, flow meters were available in the chilled water system for measuring the total chilled water flow rate in the secondary-loop (m_{sec}) and the flow rate through the decoupler bypass pipe (m_{by}). Based on the

principle of mass conservation, the total chilled water flow rate through the operating chillers (Σm_i) must be equal to the sum of the total chilled water flow rate in the secondary-loop and the bypass flow rate ($m_{sec}+m_{by}$). The bypass flow rate (m_{by}) would be regarded as a positive value if it is a surplus flow but it would be taken as a negative value if it is a deficit flow (Figure 6.2). Accordingly, the residual value (R_{mr}), depicted by equation (6.4), should be equal to zero; a residual value that differs significantly from zero would imply abnormality in the flow rate measurements.

$$R_{mr} = m_{\text{sec}} + m_{by} - \sum m_i \tag{6.4}$$

As presented as Chapter 3, for a variable (R) that is dependent on a range of other variables (V_i; i = 1, 2, …, n), as shown in equation (6.5), when the uncertainties (δV_i) in the measurements of the independent variables are known, the uncertainty in the value of R (δR) estimated from the measurements can be quantified using equation (6.6) (Yik and Chiu, 1998 and Kirkup and Frenkel, 2006).

$$R = f(V_1, V_2, ..., V_n) \tag{6.5}$$

$$\delta R = \sqrt{\sum_{i=1}^{n} \left(\frac{\partial R}{\partial V_i} \cdot \delta V_i \right)^2} \tag{6.6}$$

Where

R = an estimate made from variables V_1 to V_n

δR = uncertainty in the estimate R

δV_1 to δV_n = uncertainties in the variables V_1 to V_n

Equation (6.7), derived from equations (6.4) & (6.6), was used to evaluate the uncertainty limits for the values of R_{mr} that were estimated using equation (6.4), to provide a reference for judging if the estimated values of R_{mr} were within the expected range. The upper and lower limits are respectively $R_{mr}+\delta R_{mr}$ and $R_{mr}-\delta R_{mr}$, and any residual flow rates of magnitudes within the uncertainty limits could arise simply because of the uncertainties in the variables used in their estimation. In the calculation, the measurement accuracies of the flow meters (Table 6.2) were taken as the uncertainties in the flow rate measurements, i.e. δm_i, δm_{by} and δm_{sec}.

$$\delta R_{mr} = \sqrt{\sum (\delta m_i^{\,2}) + \delta m_{\sec}^{\,2} + \delta m_{by}^{\,2}} \tag{6.7}$$

An analysis of the residual flow rates calculated from the plant records (Figure 6.14) shows that 93% of the residual flow rates fell within the uncertainly limits, which indicates that all flow meters, including the chilled water flow meters in individual chillers, bypass flow meter and the secondary chilled water flow meter, may be regarded as reasonably accurate.

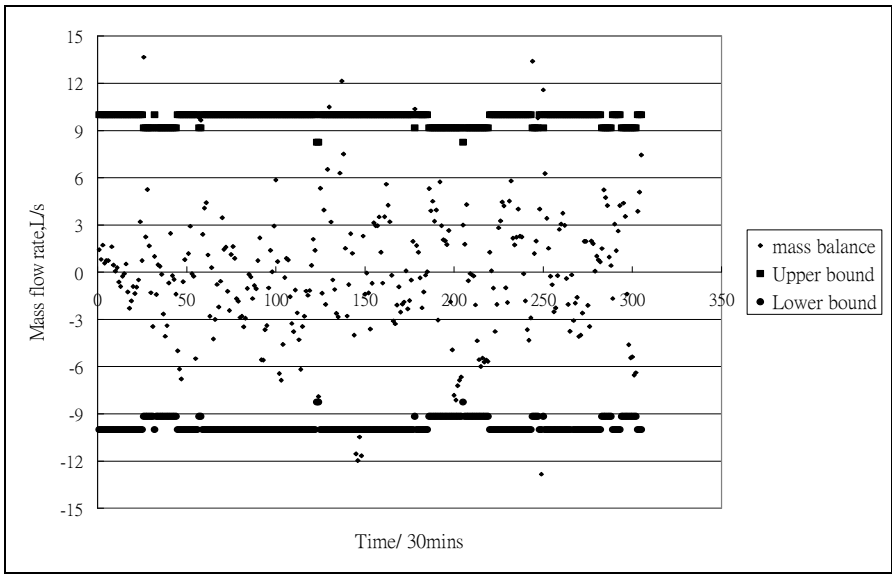

Figure 6.14 Residual mass flow rate

6.5.3 Power measurement

In-situ, snap-shot electrical measurements had been performed using a portable power analyzer (model: Fluke 41b) to verify the accuracy of the measurements of the electric power meter in each chiller on 11, November 2008, which indicated that all power measurements were within ±3kW from the corresponding readings of the portable power analyzer. Continued measurement using the power analyzer was also conducted to verify the readings of the power meter in Chiller 4.

Figure 6.15 shows a comparison of the power demands of the chiller measured using the power analyser with those measured by the built-in power meter of the chiller, which were retrieved from the BMS records for the same period. It can be seen that the two sets of data bear a linear correlation but some scattering of the data about the corresponding readings of the power analyzer can be seen. The mean bias error and the root mean square error were –0.89kW and 7.38kW, equivalent respectively to –0.35%

and 3% of the rated power demand of the chiller (254kW). Despite the significant root mean square error, the power meters may be considered to be capable of providing reasonably accurate power demand measurements for the purpose of the present study.

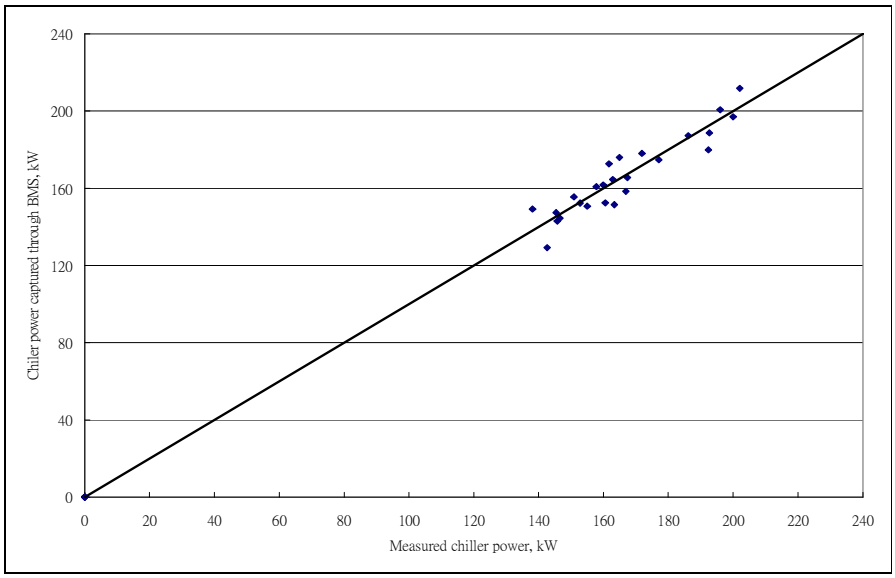

Figure 6.15 Power demand of Chiller 4 retrieved from BMS and measured by portable power analyzer

6.6 Low chilled water return temperature

Note that the proposed chilled water circuit design would be effective in keeping all but one of the running chillers steadily at the full-load condition provided that the rated chilled water flow rate is maintained, the supply chilled water temperatures from all chillers stay at the rated supply temperature and, at the same time, the return chilled water temperature at the secondary-loop is at or above the rated return chilled water temperature of the chillers. For checking whether these operating conditions were achievable, the main chilled water supply and return temperatures in the secondary-loop of the plant were retrieved from the plant operation records for September 2008. Inspection of the data

showed that the main supply chilled water temperature could rise substantially above the design set point (7°C) while the main return chilled water temperature often stayed well below the design temperature (12°C) during periods when the building cooling load was lower than 1,000kW (Figure 6.16). Although the former would be normal if there was deficit flow (this could arise due to the chiller sequencing control method being used, which is same as that for the Phase 1 plant described in Chapter 3), the latter condition would limit the chances of keeping chillers at full-load condition.

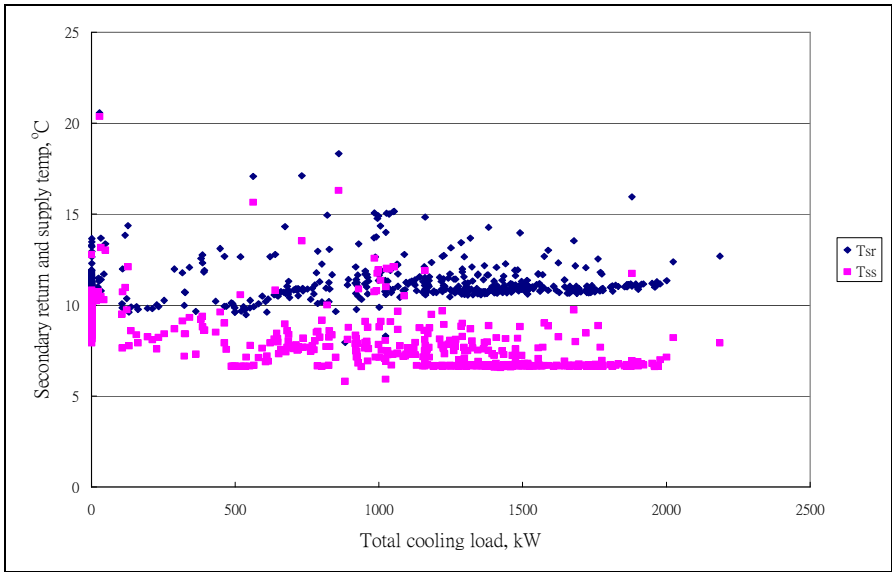

Figure 6.16 The main supply and return temperatures at the secondary-loop at different total cooling loads; (T_{sr}: Main chilled water supply temperature, T_{ss}: Main chilled water return temperature)

Low return chilled water temperature may result from one or a combination of the following conditions:

1. The chilled water control valves in the air-side systems were leaky and thus allowed chilled water to flow through the air-handling equipment while the control valves were supposed to be fully closed;

2. The pumping pressure in the secondary-loop was excessive, thus forcing too much chilled water to flow through the cooling coils in the air-side equipment;

3. Since on/off control was used for the fan-coil units connected to the system, chilled water could flow through the fan-coil units at the full flow rate but returning at a low temperature during the on-cycles in periods of low cooling load, especially when the fan-coil units were oversized (which is common for fan-coil units); and

4. The indoor set-point temperature set by the occupants was significantly lower than the design value (25^{o}C), causing the control valves at the fan-coil units to stay more often at fully open position and the return chilled water staying at a low temperature.

Reason 1 above was found to be non-existent or, at least, not serious because, as shown in Figure 6.17, which was generated based on the operating data for September 2008, the chilled water flow through the air-side equipment approached zero together with the building cooling load.

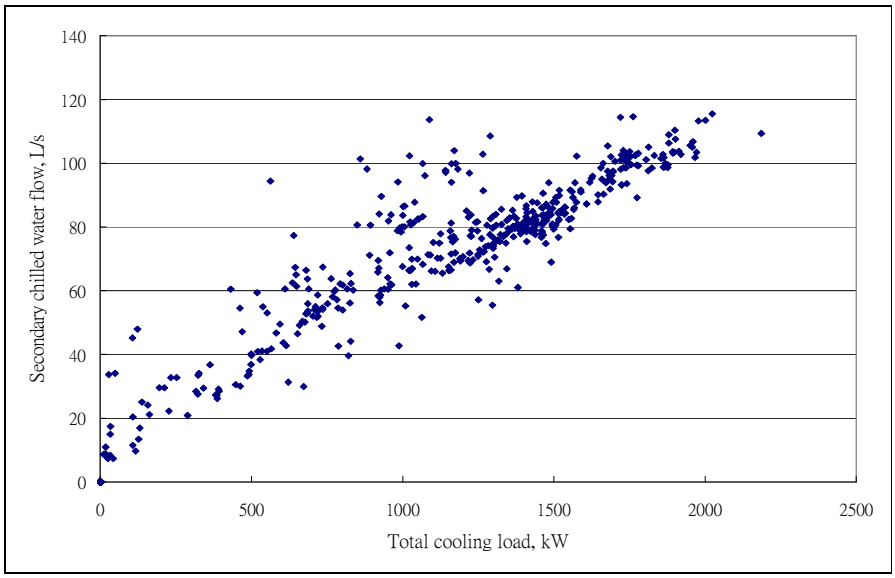

Figure 6.17 Relation between secondary-loop chilled water flow rate and total cooling load

Since excessive chilled water flow through the secondary-loop may be due to an excessively high differential pressure setting being used for controlling the variable speed secondary-loop chilled water pumps, the differential pressure setting was lowered from 80kPa to 50kPa in a trial run in October. After adjustment of the differential pressure setting, it was found that the return chilled water temperature could be kept more often around 12^{o}C, as shown in Figure 6.18.

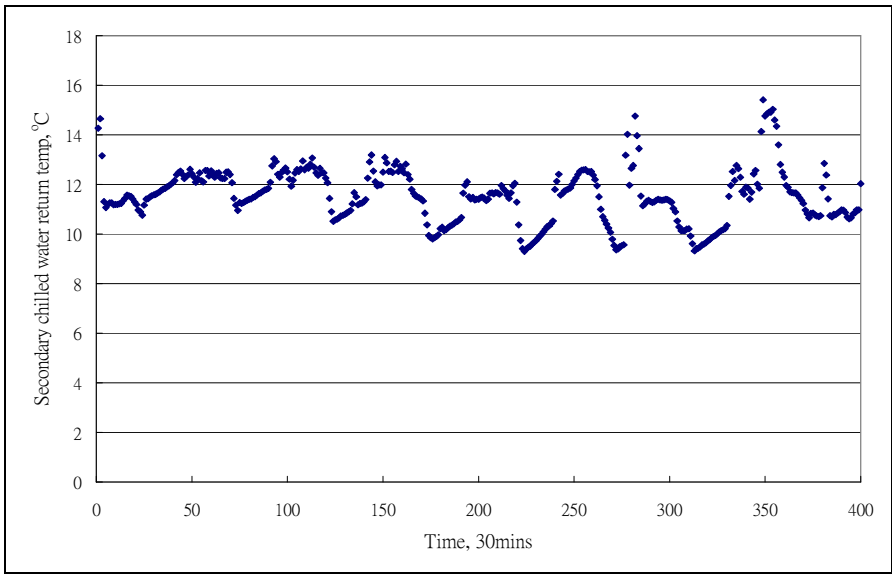

Figure 6.18 Main chilled water return temperature at the secondary-loop after reduction in differential pressure control set point

As Figure 6.19 shows, there was a general tendency that the temperature difference between the supply and return chilled water in the secondary-loop would drop with the total flow rate, which may be taken as evidence of the effect of on/off control, oversized fan-coil units and/or low indoor temperature settings. Since the building owner can do little on the problems caused by the first two reasons, further investigation focused on verifying if the last reason prevailed.

A small-scale site survey was conducted during which a sling psychrometer was used to measure the room air temperatures in six offices, including 2 general offices and 4 staff offices in the building. It was found that most of the measured room air temperatures were lower than 23°C; only one staff office was having a room temperature slightly above 25°C but the room temperature in one of the staff offices was found to be even lower than 22°C. A temperature logger was subsequently placed near to the return air grille in that office to measure the return air temperature. Figure 6.20 shows the temperature profile of

that room over a day. There was no temperature control from 11:00 pm to 7:00 am on the next day but the room temperature stayed consistently below 22°C, sometimes approaching 19°C, throughout the air-conditioned period. This finding confirmed that low indoor temperature set point was one of the main reasons that had given rise to the problem of low return chilled water temperature.

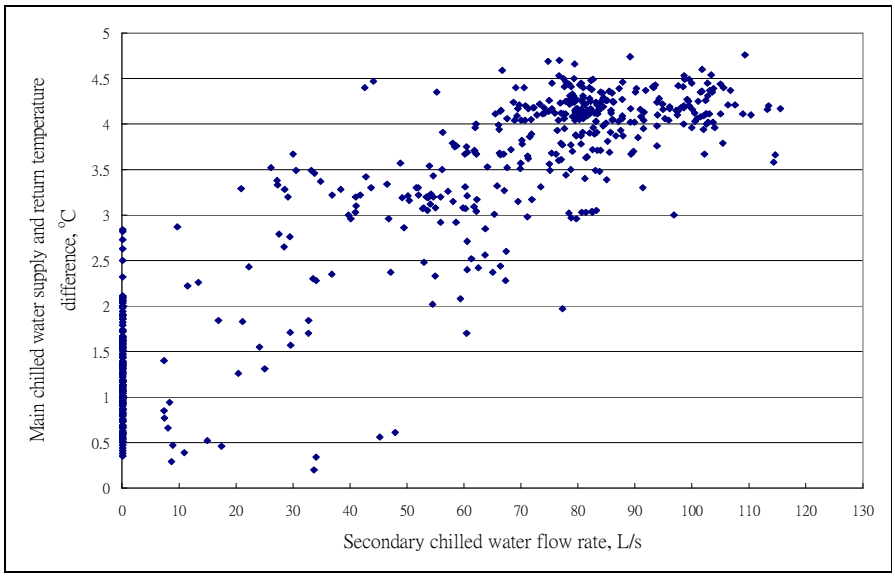

Figure 6.19 Relation between the main chilled water supply and return temperature difference and the secondary-loop chilled water flow rate

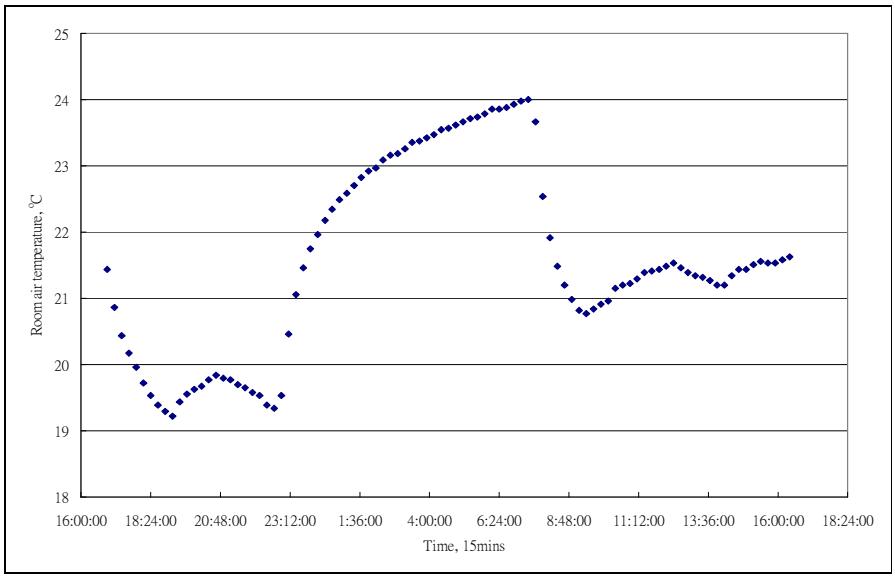

Figure 6.20 Room air temperature profile in a staff office

6.7 Full range chiller performance measurement

Having verified the measurement accuracies of the sensors and despite the imperfections in the operating conditions of the chilled water system as mentioned above, chiller performance measurement was conducted with the chilled water circuit switched to the measurement mode to demonstrate the effectiveness of the proposed circuit design in facilitating chiller performance measurement. Since there were three new water-cooled chillers (Chillers 2 to 4), the test was done in three stages, with a different chiller selected as the 'last' chiller in each stage.

6.7.1 Switching the system to the measurement mode

The chilled water plant was switched to the measurement mode by opening fully the isolation valve in the alternative bypass pipe (pipe HG in Figure 6.2) followed by closing-off the isolation valve in the normal de-coupler bypass pipe (FC). The control set-

point for the return chilled water temperature control system was set at the design chilled water inlet temperature for the chillers (12^{o}C) and the control system was activated such that the bypass valve (in pipe JK) would permit, when required, some chilled water from the main supply pipe to flow toward the main return pipe and mix with the chilled water returning from the air-side equipment, so as to keep the temperature of the chilled water entering the chillers from overshooting the set-point level, thus avoiding overloading the running chiller(s).

Inspection of the operating conditions of the condenser water circuit unveiled that the minimum entering condenser water temperature control system was unable to precisely control the condenser water temperature, which could allow the condenser water temperature to overshoot the set-point level. Therefore, the set-point used during the chiller tests was set at 31^{o}C, to prevent the water temperature from overshooting the rated entering condenser water temperature set-point of the chillers (32^{o}C), which could trigger the over-current protection control in the chillers.

The remaining test procedures are described below for the Stage 1 test where Chiller 4 was selected as the 'last' chiller. The test procedures for the other two stages were similar, except that the open/closed status of the isolation valves had been changed, as shown in Table 6.10, to allow a different chiller to be selected as the 'last' chiller, and the 'preferred' chiller to be run first as far as possible had also been altered (see also description on the 'preferred' chiller below).

6.7.2 Procedures for the stage 1 test

In Stage 1, Chiller 4 was selected as the 'last' chiller for part load test, which could be set by opening and closing the isolation valves a to j (Figure 6.2) as described in Table 6.10. Chiller 4 was kept running throughout this stage of test. When the building cooling load exceeded the cooling capacity of 1 chiller unit but was lower than the total cooling capacity of 2 chiller units, either Chiller 2 or Chiller 3 would be run. In this stage, preference was given to start Chiller 2 (referred to as the 'preferred' chiller), unless it had just been stopped for a short period of time in which case Chiller 3 would be started instead. When the building cooling load exceeded the cooling capacity of 2 chiller units, both Chiller 2 and Chiller 3 would be run. When the building cooling load dropped below the total cooling capacity of two chiller units, Chiller 3 would be stopped. Likewise, if the building cooling load dropped below the cooling capacity of one chiller unit, Chiller 2 (or Chiller 3 if Chiller 2 had been stopped) would be stopped, in which case only Chiller 4 would remain running. The plant was kept operated as described above for 2 days, with the data recorded by the BMS over this period, which were extracted thereafter for analysis. The Stage 2 test and, thereafter, the Stage 3 test were conducted.

Table 6.10 Open / closed status of the isolation valves for Stages I to III tests

Valve for Chiller #			1		2		3		4		5	All
			Valve Code									
Stage	Last Chiller	Preferred Chiller	a	b	c	d	e	f	g	h	i	j
I	Chiller 4	Chiller 2	C	C	C	O	C	O	C	O	C	C
II	Chiller 3	Chiller 4	C	C	C	O	**O**	**C**	C	O	C	**O**
III	Chiller 2	Chiller 3	C	C	**O**	**C**	C	O	C	O	C	**O**

Note: O denotes open; C denotes closed.

6.8 Results of measurement

For demonstrating also the effectiveness of the circuit design in allowing selection of any chiller as the 'last' chiller, results for the stage 2 test (rather than the Stage 1 test) are presented here. In this test, the middle chiller, Chiller 3, was selected as the 'last' chiller. Figures 6.21 and 6.22 show the chilled and condenser water temperatures entering Chillers 3 and 4, and Figure 6.23 shows the part-load ratio (*PLR*) of the chillers. During that test, the total cooling load was never high enough to require all the three chillers to be run simultaneously.

It can be observed from the results (Figures 6.21 to 6.23) that:

1. Instead of being controlled to stay steadily at the set point level of 31^{o}C, the temperature of condenser water entering the chillers varied slightly about the set point level;

2. The temperature of chilled water leaving both chillers stayed rather steadily at the set point level of 7^{o}C;

3. The temperature of chilled water entering Chiller 4 (the 'preferred' chiller) stayed rather steadily at 12^{o}C, and the average *PLR* of the chiller over the test period was 0.74, which approximately matches with the ratio of the actual to rated chilled water flow rate through the chiller (51*l*/s (Table 6.6) to 67*l*/s (Table 6.1)); and

4. The temperature of the chilled water entering Chiller 3 (the 'last' chiller) was variable and could drop to about 8.5^{o}C, and its *PLR* varied within the range of 0.18 to 0.48.

These observations show that the circuit design was effective in keeping Chiller 4 loaded reasonably steadily at the highest achievable load level (it could have been fully loaded had there not been a reduction in the chilled water flow rate) while the load on Chiller 3 could vary as a result of mixing of return and bypass chilled water, thereby maximizing the range of load under which the chiller operated.

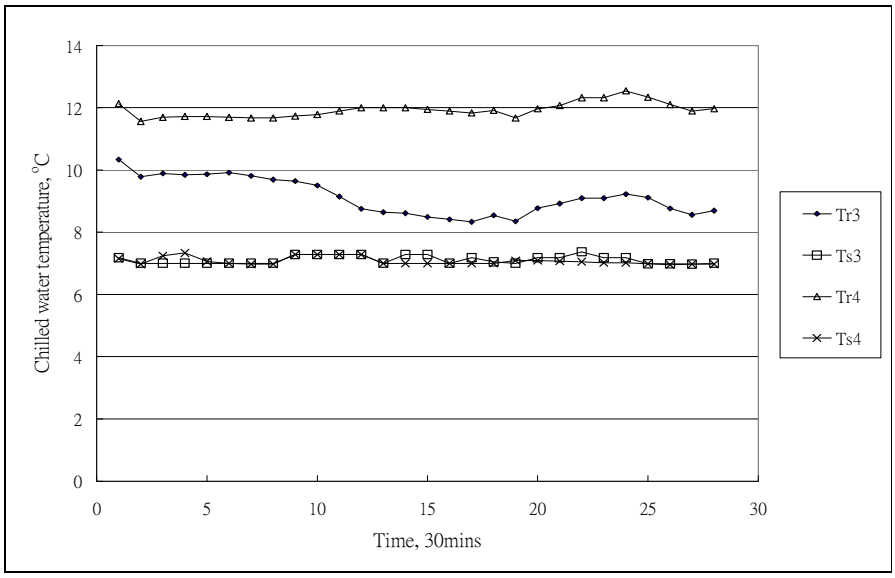

Figure 6.21 Chilled water supply and return temperatures in Stage 2 chiller performance test (T_{r3}, T_{r4}: chilled water return temperature at chillers 3 and 4; T_{s3}, T_{s4}: chilled water supply temperature at chillers 3 and 4)

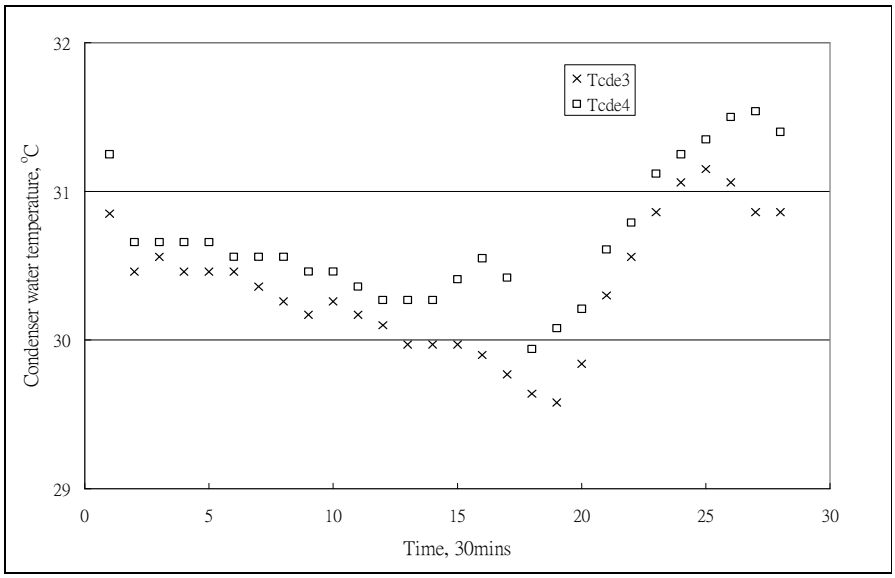

Figure 6.22 Condenser water temperature entering chillers in Stage 2 chiller performance testing (T_{cde3}, T_{cde4}: condenser water temperature entering chillers 3 and 4)

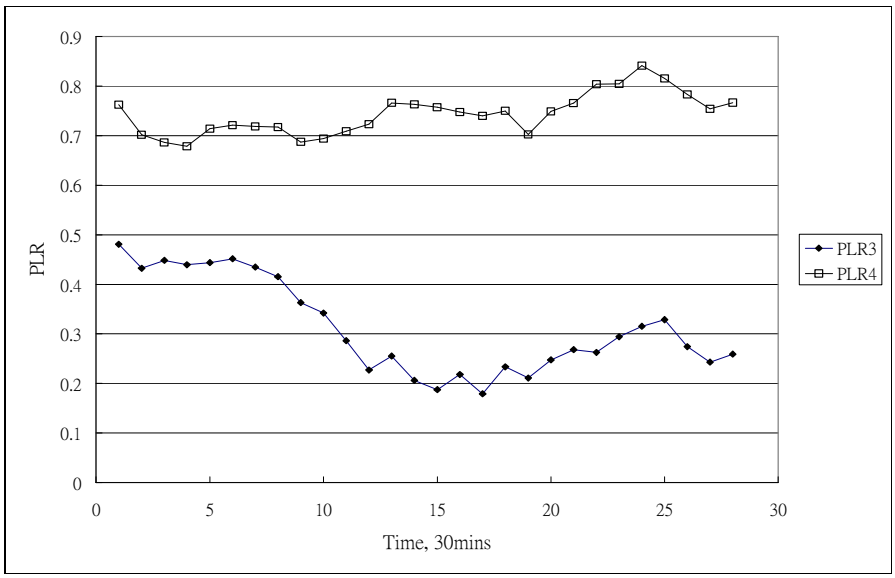

Figure 6.23 PLR of chillers in Stage 2 chiller performance test

Without the proposed chilled water circuit, all the running chillers would have shared an equal proportion of the cooling load at all times and, therefore, the range of operating conditions that could be captured would be significantly narrower. Figure 6.24

compares the frequency of chillers being loaded to different load ranges under the measurement mode with the frequency distribution that would result had the plant been operated under the normal operation mode (same as with the conventional circuit design). It can be seen that the load range was expanded from over 40% to less than 90% (if just the conventional circuit design was adopted) to over 10% to less than 90%. The result could have been more substantial had there been more (> 3) but smaller chillers in the plant and had the test been conducted in warmer days. During the test, which was in winter, the building cooling load did not exceed 66% of the total capacity of the three chillers and thus only two chillers at maximum had to be operated. Furthermore, when only one chiller needed to be run, there would be no difference between the normal and the measurement modes with respect to the chiller performance data that could be recorded.

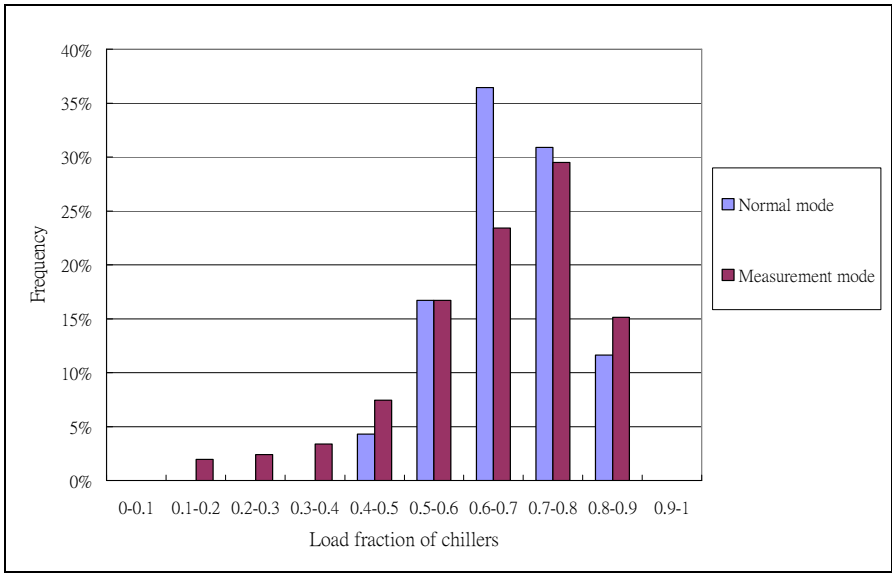

Figure 6.24 Frequency distribution of cooling load on chillers under measurement mode and normal mode

The coefficient of performance (COP) of the chillers was calculated based on the performance data measured during the tests, which was shown in Figure 6.25, together with the manufacturer's part load performance curve. It can be seen that the COP of the chillers determined from the measured data scatter widely around the manufacturer's curve and can be significantly lower, especially for the *PLR* range of 60 to 80%. Besides the uncertainties in the measured data, which could lead to an uncertainly in the COP value estimated from the measured data by more than ±10% at full-load and by more than ±20% at half load (Yik and Chiu, 1998), the reduced chilled water flow rate should also be responsible for the lower COP values (Cui and Wang, 2005 and Comstock and Braun, 1999). As shown by Comstock and Braun's experiments on a water cooled centrifugal chiller with the simulated fault of reduced evaporator water flow, the full-load kW/TR value of the chiller could be increased by about 15% when the flow rate was reduced by 40% (see Figure 4.10 in Comstock and Braun (1999).

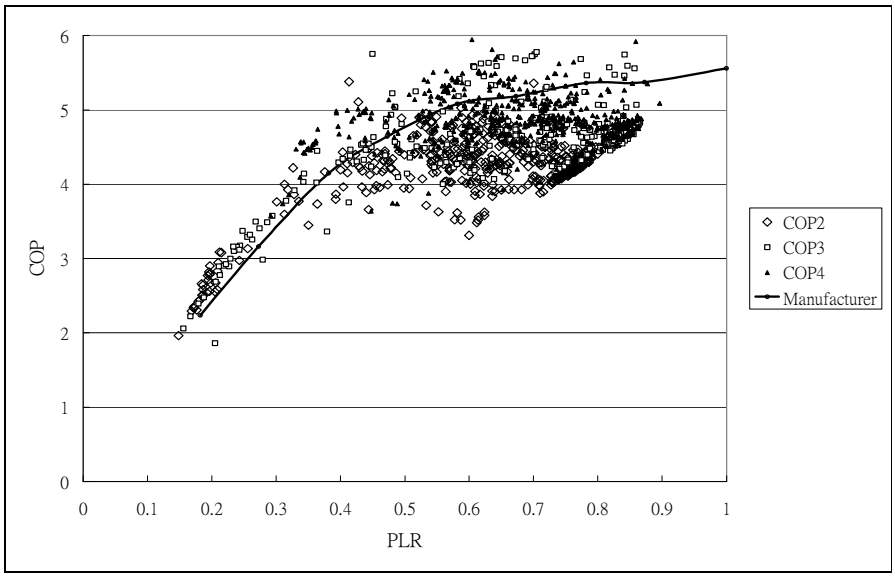

Figure 6.25 Comparison of COP of chillers with the manufacturer data

6.9 Conclusion

In-situ chiller performance tests have been conducted with a pilot installation to empirically verify the effectiveness of the proposed chilled water circuit design. Before the tests, preliminary studies were conducted to verify the measurement accuracies of the instruments available and to analyze the operating conditions of the chiller plant. The most significant plant deficiencies found included the reduced chilled water flow rate and the frequent occurrence of low chilled water return temperature. With adjustment made to the differential pressure control setting, the problem with low chilled water return temperature was alleviated. Finally, the short term *in-situ* measurements were conducted and the results verified that the proposed circuit was capable of facilitating expeditious chiller performance measurement that could cover chiller performance over a wide load range, which can be adopted to develop chiller model for FDD analysis.

7. MODEL-BASED FAULT DETECTION AND DIAGNOSTICS FOR WATER COOLED CHILLERS: A DEMONSTRATION

7.1 Overview

The development and demonstration of the application of a simple model-based FDD method for chillers, which took into account the limited sensors available in the plant studied, are presented in this chapter. The chiller plant upon which this part of the study was based had three of its five old air-cooled chillers recently replaced by three new, single-circuit, water-cooled screw chillers, referred to as Chillers 2 to 4, which are identical with each other and collectively have sufficient cooling capacity for the entire building (two old chillers, referred to as Chillers 1 and 5, are retained as spare units). Because the new chillers are different from those studied earlier (see Chapter 3) in their cooling capacity, the heat rejection medium they use and their refrigerant circuit design, another chiller model was developed, based on measured operating data of the chillers, for simulation of the performance of the new water-cooled chillers. Expeditious collection of chiller full- and part-load performance data was facilitated by the chilled water circuit design adopted in the plant, as described in the preceding chapter. The prediction accuracy of the chiller model developed had been verified by comparison with measured operating data of another identical chiller unit.

Constrained by the lack of chiller operation data that cover conditions where there were no and there were known chiller faults, the fault classifiers in the FDD method were derived from the set of laboratory data produced in the ASHRAE Research Project 1043-RP (Comstock and Braun, 1999). The database produced in that Project include measured performance of a chiller that cover the fault-free and eight fault conditions, with the chiller operated over the same range of operating conditions in each round of test run. This set of data had already been adopted in a number of evaluation studies on chiller FDD methods (e.g. Cui and Wang, 2005; Wang and Cui, 2006; Zhou et al, 2009).

Notwithstanding that the chiller tested in the ASHRAE project was a centrifugal chiller but the chillers under study are screw chillers, the set of ASHRAE project data was still considered useable because the proposed FDD scheme does not consider compressor faults. Leaving out compressor faults was a compromise that had to be made because the chillers under study are in-use and thus it was only possible to obtain faulty chiller operating data through introducing a few simulated faults to the chillers, which would not damage the chillers, while it would take an unpredictable period of time to wait for different kinds of chiller faults to arise naturally.

It was found from an analysis of the set of ASHRAE chiller test data that instead of being kept at steady levels throughout a test run, each temperature measurement could vary by about 0.7^{o}C from the target level, and thus the performance of the chiller actually varied from time to time within each test run. Therefore, rather than directly using the set of ASHRAE data to develop chiller fault classifiers, a model was developed for the chiller first, and the chiller model was then used to predict the performance of the chiller to ensure the comparison of the faulty and the fault-free chiller performance can be based

on the same set of operating conditions. This comparison allowed the required fault classifiers to be identified.

Fault classifiers for only four chiller faults were studied (see explanations given later), namely reduced evaporator and condenser water flows, condenser fouling and refrigerant leakage. The proposed fault classifiers involve two performance indices, which can be evaluated from the refrigerant condensing temperature, and the temperatures of the water entering and leaving the condenser. Use of other refrigerant parameters, such as sub-cooled temperature leaving the condenser and superheated temperatures entering and leaving the compressor, which are usually unavailable from existing chiller plants, was avoided.

Finally, *in-situ* experiments with the chillers under study were carried out, under the conditions where the evaporator and condenser water flows were manually reduced in turn, and the measurements obtained were used to verify the effectiveness of the proposed FDD strategy for these two faults. Verification of the effectiveness of the strategy for detecting condenser fouling was based on model predictions, with the model modified to simulate the effects of this fault. However, it was not possible to simulate refrigerant leakage, either experimentally or through simulation. Verification of the ability of the proposed strategy in detecting this fault, therefore, had to be deferred until the fault arises naturally.

7.2 Water-cooled screw chiller model

The characteristics of the water-cooled screw chillers under study and the *in-situ* tests conducted to collect chiller performance data for the development of a model for the

chillers have been described in Chaper 6. Table 7.1 summarizes the mathematical expressions for the component in the chiller model.

Table 7.1 Summary of chiller component models for the water-cooled screw chillers

Evaporator	Evaporator effectiveness	$\varepsilon_{evp} = 1 - \exp(-\frac{AU_{evp}}{m_w \cdot c_w})$
	Evaporator heat transfer coefficient	$AU_{evp} = \frac{1}{a_1 \cdot m_w^{-0.8} + a_2 \cdot Q_{evp}^{-0.745} + a_3}$
	Cooling capacity	$Q_{evp} = m_w \cdot c_w \cdot (T_r - T_s)$
		$Q_{evp} = m_{ref} \cdot (h_1 - h_3)$
		$Q_{evp} = \varepsilon_{evp} \cdot m_w \cdot c_w \cdot (T_r - T_{evp})$
Compressor	Isentropic compressor power	$w_{isen} = \frac{\gamma}{\gamma - 1} \cdot P_{evp} \cdot v_1 \cdot \left[\left(\frac{P_{cd}}{P_{evp}} \right)^{\frac{\gamma-1}{\gamma}} - 1 \right]$
	Isentropic efficiency	$\eta_{isen} = 0.01 \cdot (b_1 \cdot T_{cd}^{\ 2} + b_2 \cdot T_{cd} + b_3 \cdot T_{evp}^{\ 2} + b_4 \cdot T_{evp} + b_5 \cdot T_{cd}^{\ 2} \cdot T_{evp} + b_6 \cdot T_{cd} \cdot T_{evp} + b_7 \cdot Q_{nl} + b_8)$
	Motor and transmission efficiency	$\eta_{cc} = c_1 + c_2 \cdot PLR + c_3 \cdot PLR^2$
	Actual power input	$W_C = m_{ref} \cdot \frac{w_{isen}}{\eta_{isen} \cdot \eta_{cc}}$
Condenser	Condenser effectiveness	$\varepsilon_{cd} = 1 - \exp(-\frac{AU_{cd}}{m_{cd} \cdot c_w})$
	Condenser heat transfer coefficient	$AU_{cd} = e_1 \cdot Q_{cd}^{\ e2} m_{cd}^{\ e3}$
	Heat rejection	$Q_{cd} = Q_{evp} + W_C$
		$Q_{cd} = m_{cd} \cdot c_w \cdot (T_{cdl} - T_{cde})$
		$Q_{cd} = m_{ref} \cdot (h_2 - h_3)$
		$Q_{cd} = \varepsilon_{cd} \cdot m_{cd} \cdot c_w \cdot (T_{cd} - T_{cde})$
Expansion valve		$h_3 = h_4$
Refrigerant flow rate		$m_{ref} = \frac{Q_{evp}}{h_1 - h_3}$
COP		$COP = \frac{Q_{evp}}{W_C}$

The methods used to develop this chiller model are similar to those presented in Chapter 5. Compared to the earlier model, this model is in fact simpler because there is only one compressor and one refrigerant circuit in the chiller. As in developing the earlier chiller model, the unknown coefficients for the overall heat transfer coefficient of the condenser and the evaporator, and the combined motor and transmission efficiency of the chiller were evaluated by regression method based on the operation records for Chiller 3 in the plant, and the results were as summarized in Table 7.2. Since the chillers were newly installed, the chiller model developed can be regarded as a fault-free model.

Table 7.2 Coefficients of the component models for the water-cooled screw chiller

Model	Values of coefficients	R^2
Evaporator heat transfer	a_1= 0.0384, a_2= 0.0673 and a_3=0	0.99
Condenser heat transfer	e_1=1, e_2=0.018 and e_3=1.478	0.98
Combined motor and transmission efficiency	c_1=-0.33418, c_2=22.74109 and c_3=-0.006195	0.98

Besides the set of data used in evaluation of the model coefficients, another set of measured operating performance data for Chiller 4 in the same plant was collected for a comparison with the predictions of the chiller model. Once again, how well the model predictions matched with the measured performance of Chiller 4 was evaluated on the basis of the relative error of the model prediction (δ), the mean bias error (*MBE*) and the standard deviation (*SD*), as depicted by equations (5.50), (5.51) and (5.52), respectively. Table 7.3 summarizes the statistical results of the comparison and Figures 7.1 to 7.3 show the comparisons of the model predictions with the measured chiller operating data.

As shown in Table 7.3 & Figure 7.1, the predicted *COP* of the chiller agrees well with the *COP* calculated from the measured chiller load and power demand data, with about 97% of the predicted values falling within ±10% of the calculated values. The mean

bias error and the standard deviation of the predicted *COP* values were respectively 0.02 and 0.2 only. All the predicted evaporating temperatures (T_{evp}) of the chiller were within ±10% of the respective measured values (Table 7.3 & Figure 7.2), and the mean bias errors and the standard deviations are very small. As shown in Table 7.3 & Figure 7.3, the predicted condensing temperatures (T_{cd}) of the chiller also compare well with the measured data, with all predictions falling within ±10% of the respective measured values while the mean bias error and the standard deviation were respectively 0.38°C and –0.8°C only.

Table 7.3 Accuracy of model predictions for the water-cooled screw chiller

Parameter	No. of data	% of predictions within ±10% of measured value	Mean Bias Error (*MBE*)	Standard Deviation (*SD*)
COP	506	97%	0.02	0.20
T_{evp} (°C)	506	100%	-0.001 °C	0.06 °C
$T_{cd,}$ (°C)	506	100%	-0.80°C	0.38 °C

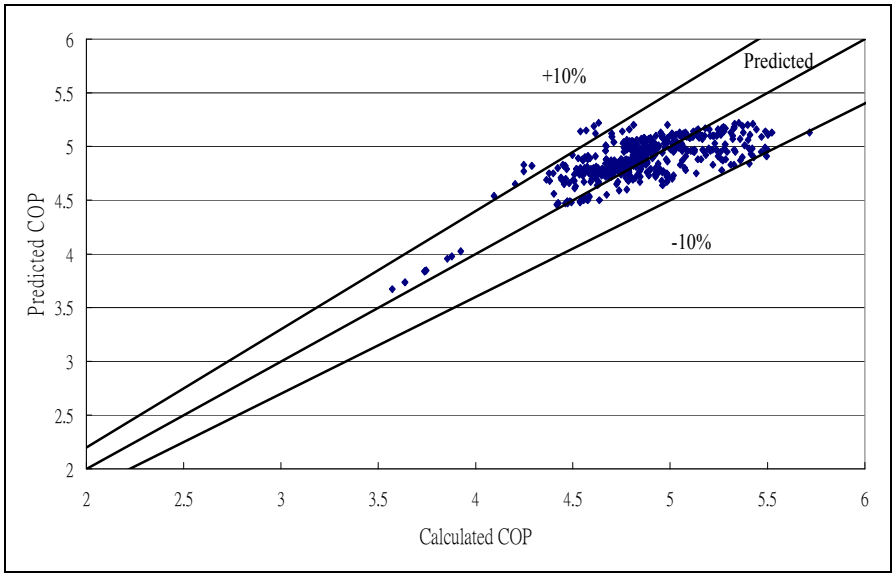

Figure 7.1 Comparison of COP predicted by the model and calculated from plant operating data for the water-cooled screw chiller

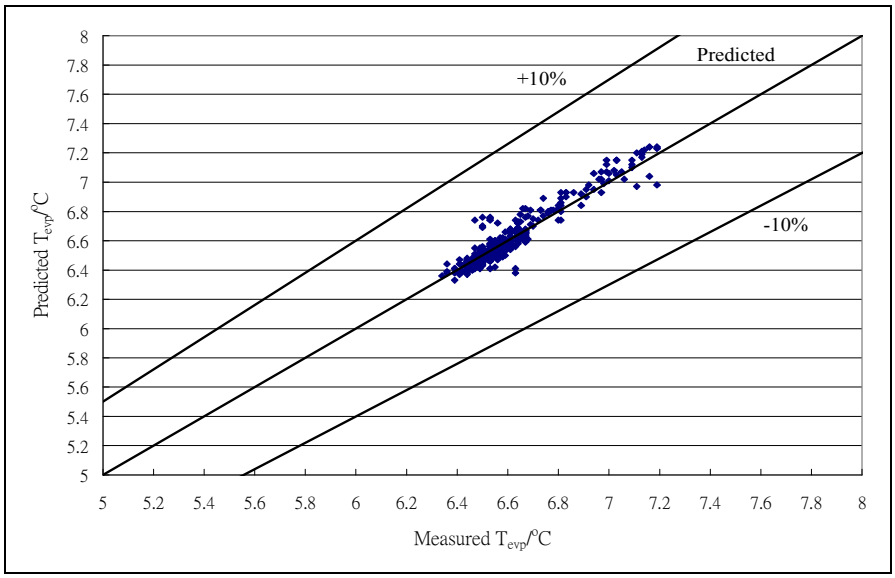

Figure 7.2 Comparison between predicted and measured evaporating temperature of the water-cooled screw chiller

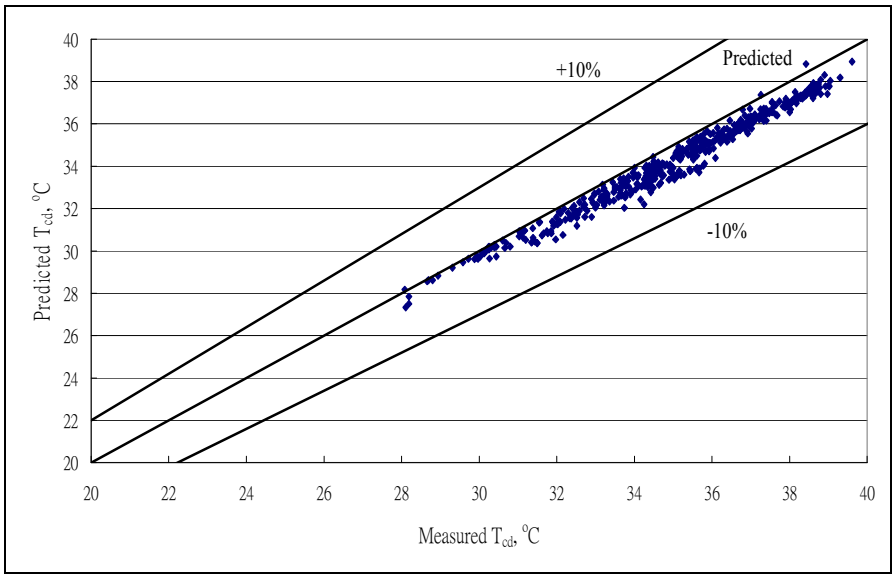

Figure 7.3 Comparison between the predicted and the measured condensing temperature of the water-cooled screw chiller

7.3 Experimental work under ASHRAE 1043RP project

As mentioned earlier, the fault classifiers in the proposed FDD method were derived from the set of laboratory data produced in the ASHRAE Research Project 1043-RP. The installation, instrumentation and commissioning of the test-stand, and data collection process, with and without the faults introduced, were described in detail by Comstock and Braun (1999). According to their description, the chiller was a 90-TR water-cooled centrifugal chiller that used the refrigerant R134a, and the chilled water and condenser water flow rates were 216*gpm* (13.63*l*/s) and 270*gpm* (17.03*l*/s) respectively. The experimental test-stand met the specification of ARI standard 550, and included a Micro-Tech controller for internal chiller controls, including inlet guide vane control and power demand control for protection of the chiller from overload.

The experimental tests were carried out at 27 different combinations of condenser water inlet temperature, chilled water supply temperature set-point and output capacity, as shown in Table 7.4, and each of the fault tests and fault-free tests covered the sequence of the 27 conditions. The steady-state chiller performance data obtained, which include values of the system variables shown in Table 7.5, were lodged into an Excel file. In the laboratory test, few erroneous sensor readings were encountered (less than 0.0001% of all measurements) and many of them were removed (Comstock and Braun, 1999). The data were given in Imperial units and had been converted into SI units in the present analysis.

Tests with eight different chiller faults had been conducted in the ASHRAE project, using the methods as summarized in Table 7.6. Each fault was introduced at four levels of severity (10% - 40% fault levels in increments of about 10%). The pre-existent pilot valve fault, however, was tested at one severity level only. Tests under normal

conditions were also carried out to provide a benchmark for comparison with the performance with the faults.

Table 7.4 Operating conditions in varies tests conducted

Test No.	Chilled water supply temp, T_s	Condenser water entering chiller temp, T_{cde}	Capacity %
1	50F (10°C)	85F (29.4°C)	90-100
2	50F (10 °C)	85F (29.4°C)	50-60
3	50F (10 °C)	85F (29.4°C)	25-40
4	50F (10 °C)	75F (23.9°C)	90-100
5	50F (10 °C)	75F (23.9°C)	50-60
6	50F (10 °C)	75F (23.9°C)	25-40
7	50F (10 °C)	70F (21.1°C)	70-80
8	50F (10 °C)	65F (18.3°C)	45-50
9	50F (10 °C)	62F (16.7°C)	25-35
10	45F (7.2°C)	85F (29.4°C)	90-100
11	45F (7.2°C)	85F (29.4°C)	50-60
12	45F (7.2°C)	85F (29.4°C)	25-40
13	45F (7.2°C)	75F (23.9°C)	90-100
14	45F (7.2°C)	75F (23.9°C)	50-60
15	45F (7.2°C)	75F (23.9°C)	25-40
16	45F (7.2°C)	70F (21.1°C)	70-80
17	45F (7.2°C)	65F (18.3°C)	45-50
18	45F (7.2°C)	62F (16.7°C)	25-35
19	40F (4.4°C)	85F (29.4°C)	90-100
20	40F (4.4°C)	85F (29.4°C)	50-60
21	40F (4.4°C)	85F (29.4°C)	25-40
22	40F (4.4°C)	75F (23.9°C)	90-100
23	40F (4.4°C)	75F (23.9°C)	50-60
24	40F (4.4°C)	75F (23.9°C)	25-40
25	40F (4.4°C)	70F (21.1°C)	70-80
26	40F (4.4°C)	65F (18.3°C)	45-50
27	40F (4.4°C)	62F (16.7°C)	25-35

Table 7.5 Test data collected in the ASHRAE research project

Description	Unit	Description	Unit
Chilled water supply temperature	F	Evaporator water flow rate	GPM
Chilled water return temperature	F	Evaporator pressure	PSIG
Condenser water entering chiller	F	Condenser pressure	PSIG
Condenser water leaving chiller	F	Sub-cooling temperature	F
Heat transfer rate in the condenser	Tons	Suction temperature	F
Heat transfer rate in the evaporator	Tons	Suction superheat	F
Compressor power	kW	Discharge temperature	F
Condenser water flow rate	GPM	Discharge superheat	F

Table 7.6 Faults studied in the experiment and methods used to simulate the faults

No.	Description	Fault simulation method
1.	Reduced condenser water flow	Manual reduction of flow rate
2.	Reduced evaporator water flow	Manual reduction of flow rate
3.	Refrigerant leakage	Removal of a fixed amount of refrigerant from the circuit
4.	Refrigerant overcharge	Adding a fixed amount of refrigerant from the circuit
5.	Excess oil	Adding a known amount of oil to the compressor
6.	Condenser fouling	Blocking tubes in the condenser
7.	Non-condensables in refrigerant	Adding nitrogen to the refrigeration circuit
8.	Defective pilot valve	Pre-existent fault

Although data for eight kinds of chiller faults were available, not all of them were considered in the present chiller FDD study because: excess oil can be easily detected by inspecting oil temperature and oil pressure; and non-condensables in refrigerant would not occur for chillers with refrigeration at pressures higher than the atmospheric pressure. Besides, it had been reported that during the experiments with a faulty expansion valve, the average condenser water flow rate was 20% lower than the nominal flow rate, which exceeded the acceptable limit stipulated in the ARI standard 550, and the flow rate varied by as much as ±10% (Comstock and Braun, 1999). The set of data for this fault condition, therefore, was considered unfit for fault classifier establishment. Furthermore, since evaporator fouling was not included in the laboratory studies, this fault had to be excluded. As a result, fault classifiers for the following four chiller faults only, which account for high service costs and repair costs (Comstock and Braun, 1999), were investigated:

1. Reduction of evaporator water flow
2. Reduction of condenser water flow
3. Condenser fouling.
4. Refrigerant leakage

7.4 Model development of laboratory chiller

It could have been possible to formulate the required fault classifiers by directly comparing the fault-free data with the faulty data available from the database produced in the ASHRAE project. However, closer inspection of the available data unveiled that even though all tests were conducted according to the testing sequence and target operating conditions (Table 7.4), the measurements could deviate slightly from the respective intended values during a test. For example, deviations of the temperature measurements by about 0.7^{o}C from the target values were observed, which could lead to significant variations in the chiller cooling output. In order that faulty chiller performance could be compared with fault-free chiller performance under identical operating conditions, the water-cooled chiller model described in Section 7.2 was tuned to make it suitable for modelling the chiller tested in the ASHRAE project. The model was then used to provide predictions of chiller performance in the fault-free state under the conditions that match with those under which the faulty data were measured, such that the two set of data could be compared on equal basis and the observations made from the comparisons could provide a sound basis for establishment of the fault classifiers. The modifications made to the chiller model included:

1. The compressor model was tuned to become a centrifugal compressor model by combining the isentropic compression model and a model for isentropic efficiency that was established based on the ASHRAE chiller data.

2. Since the centrifugal compressor was operating at constant speed, the motor and transmission efficiency was assumed to be constant (Browne and Bansal 1998), at the value of 0.8 (Yu and Chan 2007).

7.5 Coefficient evaluation and validation of laboratory chiller model

The fault-free chiller operating data under one of the normal tests on the chiller tested in the ASHRAE project were used for evaluation of the unknown coefficients for the overall heat transfer coefficient of the condenser and the evaporator, and the isentropic efficiency of the compressor, and the results obtained were as shown in Table 7.7. Having established the chiller model, a set of fault-free data from another normal test produced in the ASHRAE project was used for comparison with the model predictions. The comparison was made with reference to the relative error of the model prediction (δ), the mean bias error (*MBE*) and the standard deviation (*SD*). As shown in Table 7.8 and Figures 7.4 to 7.6 the model can yield predictions that matched well with the measured chiller operating data.

Table 7.7 Coefficients of component models for the tested chiller in the ASHRAE project

Model	Values of coefficients	R^2
Evaporator heat transfer	a_1= 0.062, a_2= 0.85 and a_3=0	0.97
Condenser heat transfer	e_1=1, e_2=0.018 and e_3=1.478	0.98
Isentropic efficiency	b_1=-0.33418, b_2=22.74109, b_3=-0.006195, b_4=55.83998 b_5=0.078123, b_6=-4.50506, b_7=-0.84044 and b_8=0	0.98

Table 7.8 Accuracy of model predictions for laboratory chiller

Parameter	No. of data	% of predictions within ±10% of measured value	Mean Bias Error (*MBE*)	Standard Deviation (*SD*)
COP	82	100%	-0.04	0.12
T_{evp} (^{o}C)	82	75%	-0.02 ^{o}C	0.36 ^{o}C
$T_{cd,}$ (^{o}C)	82	100%	0.14 ^{o}C	0.22^{o}C

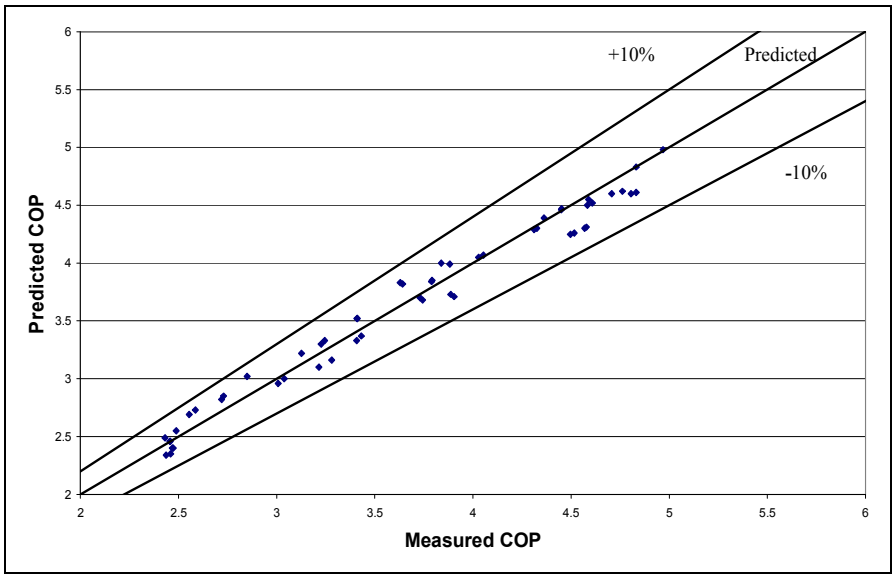

Figure 7.4 Comparison between predicted and measured COP of laboratory chiller

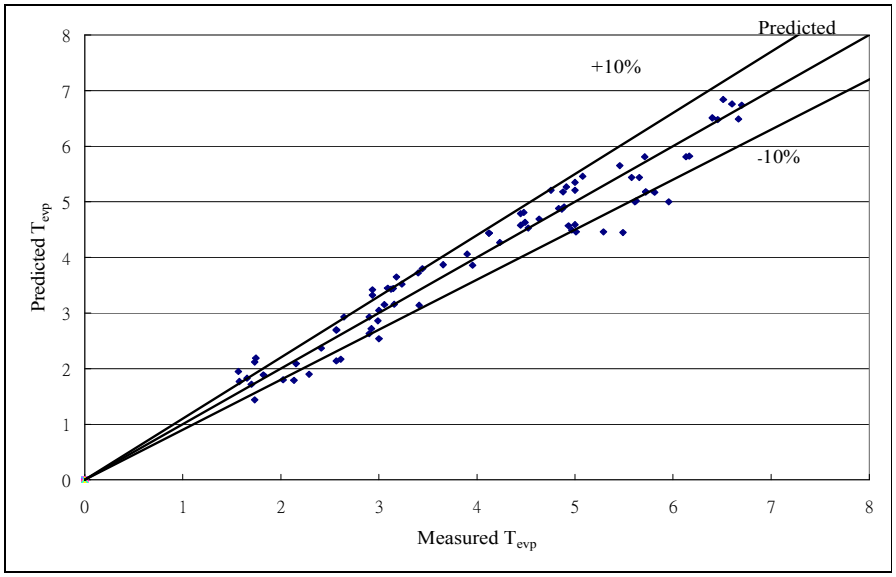

Figure 7.5 Comparison between predicted and measured evaporating temperature of laboratory chiller

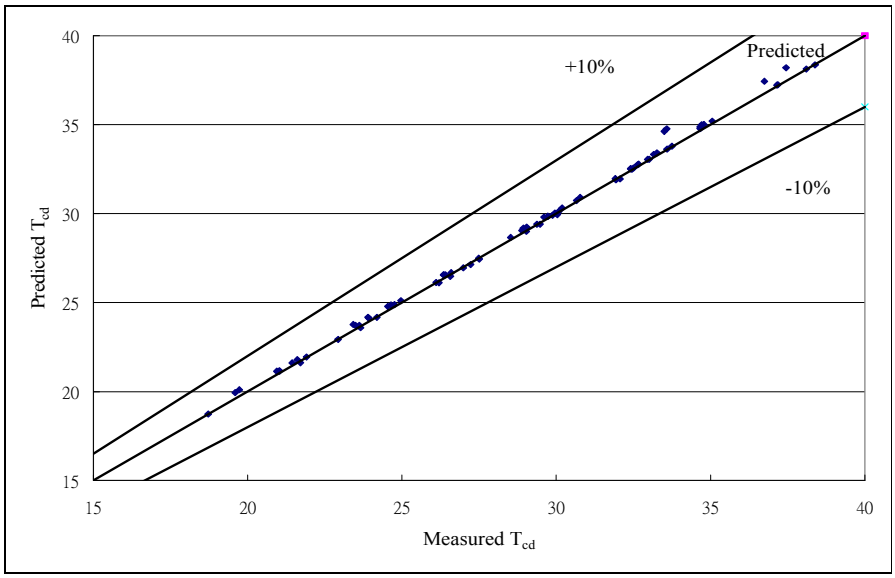

Figure 7.6 Comparison between predicted and measured condensing temperature of laboratory chiller

7.6 Establishment of fault classifiers for FDD

Previous studies (Comstock and Braun, 1999; McIntosh et al., 2000; Reddy 2006; 2007a; 2007b; Wang and Cui, 2006) showed that fault detection can be more sensitive if, in lieu of using directly the sensor readings, appropriate performance indices computed from the measurements are used. For FDD of chiller faults, many fault classifiers had been developed and validated using the laboratory data produced in the ASHRAE Project 1043-RP (e.g. Cui and Wang, 2005; Zhou et al, 2009).

The fault classifiers proposed by Cui and Wang (2005) involve the use of refrigerant flow rate, compressor isentropic efficiency and motor drive efficiency as the performance indices. Evaluation of these indices would require measurements of the compressor suction and discharge temperatures as well as the sub-cooled temperature

leaving the condenser. The fault diagnosis tables proposed by Zhou et al. (2009) also included the sub-cooled temperature leaving the condenser as a performance index. Unfortunately, no measurements for the required system variables could be made available from the chiller plant under study, which made it impossible to adopt these performance indices.

According to Cui and Wang (2005), under the faulty condition with reduced evaporator water flow and as a result of the increase in evaporator water temperature difference (T_r-T_s) while the evaporating temperature is kept under control by moderation of the expansion valve, the log-mean temperature difference of the evaporator ($LMTD_{evp}$) will increase and thus would be a suitable performance index for this fault. The fault classifiers proposed by Zhou et al. (2009) will also point to reduced evaporator water flow where there is an increase in the evaporator water temperature difference (T_r-T_s), as compared to the normal condition under the same cooling load. In their studies, however, evaluation of these indices was based on regression models that involve the cooling load as a predictor variable but, when the evaporator water flow rate has been inadvertently reduced, the actual cooling load on the chiller would become indeterminate. Therefore, estimates of cooling load were based on the rated chilled water flow rate of the chiller, which would be over-predicted when the fault of reduced chiller water flow is present.

For FDD of chiller faults, either the heat transfer coefficient (AU_{cd}) or the log-mean temperature difference of the condenser ($LMTD_{cd}$) may be used as a performance index but not both, as they are inversely proportional to each other under a given heat rejection rate. Similarly, either the evaporator heat transfer coefficient (AU_{evp}) or log-mean temperature difference ($LMTD_{evp}$) may be considered for use as a performance

index. However, the latter two would only be sensitive in detecting evaporator fouling (McIntosh et al., 2000) and reduced evaporator water flow (Cui and Wang, 2005) respectively. Compared to either one of the former pair, the symptoms that these two performance indices can reflect are less apparent because the expansion valve will keep the evaporating temperature controlled at a nearly constant level.

As a performance index, the water temperature rise across the condenser (T_{cdl}-T_{cde}) had been used in various studies (e.g. Comstock and Braun, 1999; McIntosh et al., 2000; Reddy 2007a; 2007b; Zhou et al., 2009) while the condenser log-mean temperature difference $LMTD_{cd}$ had also been adopted by a number of researchers (e.g. Comstock and Braun, 1999; Cui and Wang, 2005; Wang and Cui, 2006). These performance indices, therefore, were selected for the present study (Table 7.9), as they are physically relevant to the health condition of the chiller and the measurements required for their evaluation are commonly available in existing chiller plants. As will be shown later, these performance indices were indeed capable of detecting the chiller faults studied.

Table 7.9 Mathematical expressions of the performance indices

Performance index	Formula
Logarithm mean temperature difference of condenser	$LMTD_{cd} = \frac{T_{cdl} - T_{cde}}{\ln(\frac{T_{cd} - T_{cde}}{T_{cd} - T_{cdl}})}$
Condenser water temperature difference	$T_{cdl} - T_{cde}$

For each of the four faults being studied, the performance indices were evaluated based on the 40% fault severity level, which was the highest fault severity level covered by the chiller tests conducted in the ASHRAE project. The performance indices evaluated based on operating data pertaining to the faulty conditions were compared with those

evaluated from the fault-free chiller performance predicted by the chiller model. The fault classifying rules for determining if individual faults existed were established from observations of the deviations the two sets of performance indices, as depicted in equation (7.1), referred to as the residuals.

$$R_{PI} = PI_{MF} - PI_P \tag{7.1}$$

Where

R_{PI} = Residual of a performance index

PI_{MF} = Performance index evaluated from measured data with fault

PI_P = Performance index evaluated from predicted fault-free data

The threshold value of the residual for determining if it is large enough to indicate the presence of a fault was taken as three times the standard deviation (*SD*) of the performance indices evaluated using the predicted fault-free performance from those calculated using the measured performance, as depicted by equation (7.2). This margin was considered large enough to ensure that a fault would unlikely to be regarded as being present simply due to deviations between the model predictions from the measured performance (Hogg, 1993). The standard deviations of the indices $LMTD_{cd}$ and (T_{cdl}–T_{cde}) were found to be 0.22°C and 0.095°C, and the corresponding threshold values are, therefore, 0.67°C and 0.28°C, respectively.

$$SD = \sqrt{\frac{1}{N_P}\sum_{i=1}^{N_P}(PI_M - PI_P)_i^2} \tag{7.2}$$

Where

PI_P = Performance index evaluated from predicted fault-free data

PI_M = Performance index evaluated from measured fault-free data

$(PI_M - PI_P)_i$ = Difference between PI_M & PI_P in the i^{th} measurement

N_P = Number of data available for comparison with the predicted variable

The observed variations in the residuals for each of the four chiller faults being studied, as found based on the ASHRAE project data, are shown and discussed below.

7.6.1 Reduction of condenser water flow rate

Figures 7.7 & 7.8 show the residuals of the condenser log mean temperature difference ($LMTD_{cd}$) and the condenser water temperature difference (T_{cdl}–T_{cde}) when the condenser water flow rate was reduced by 40% in the chiller test. With this fault, there were positive increments in both the residuals of $LMTD_{cd}$ and (T_{cdl}–T_{cde}) for the vast majority of the measured readings, simply because a reduction in condenser water flow rate would give rise to an increase in the water temperature rise across the condenser and both indices are directly proportional to this temperature rise.

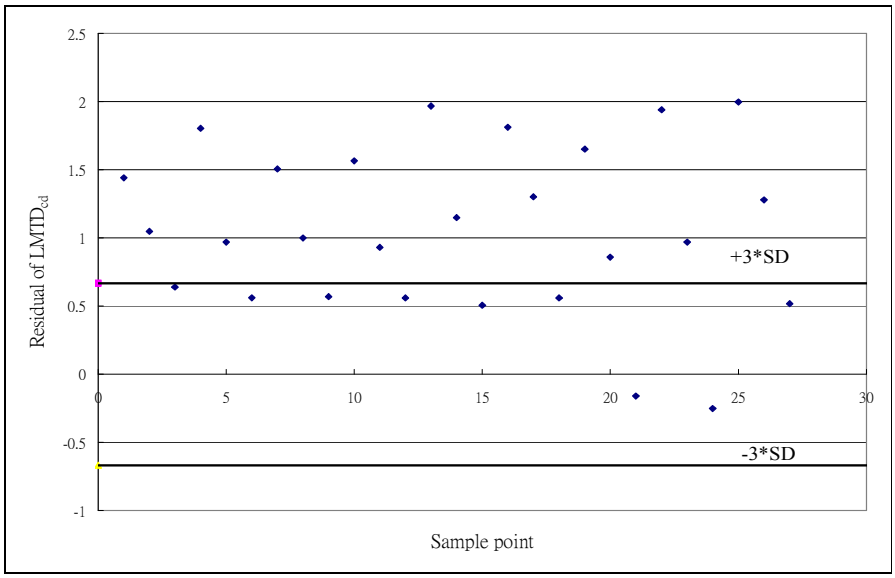

Figure 7.7 Residuals of $LMTD_{cd}$ under a reduction in condenser water flow rate

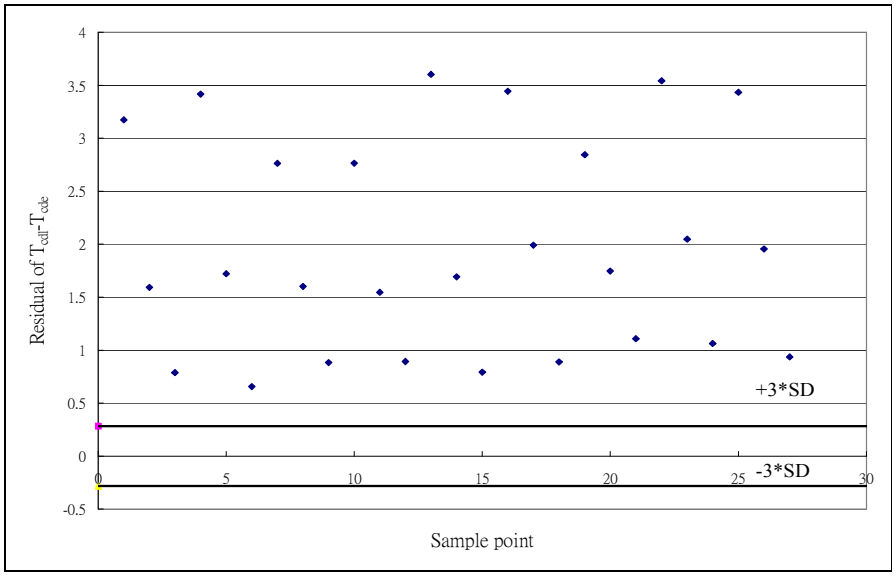

Figure 7.8 Residuals of (T_{cdl}-T_{cde}) under a reduction in condenser water flow rate

7.6.2 Reduction of evaporator water flow rate

The residuals of $LMTD_{cd}$ and (T_{cdl}–T_{cde}) under the condition with a 40% reduction in the evaporator water flow rate are shown in Figures 7.9 & 7.10. It can be seen that with this fault, the two residuals both dropped significantly. This is because the chiller output, when evaluated based on the rated chilled water flow rate, would be over-predicted, which would lead to over-prediction of the heat rejection rate and, in turn, over-prediction of both $LMTD_{cd}$ and (T_{cdl}–T_{cde}). Therefore, reductions in both residuals were observed.

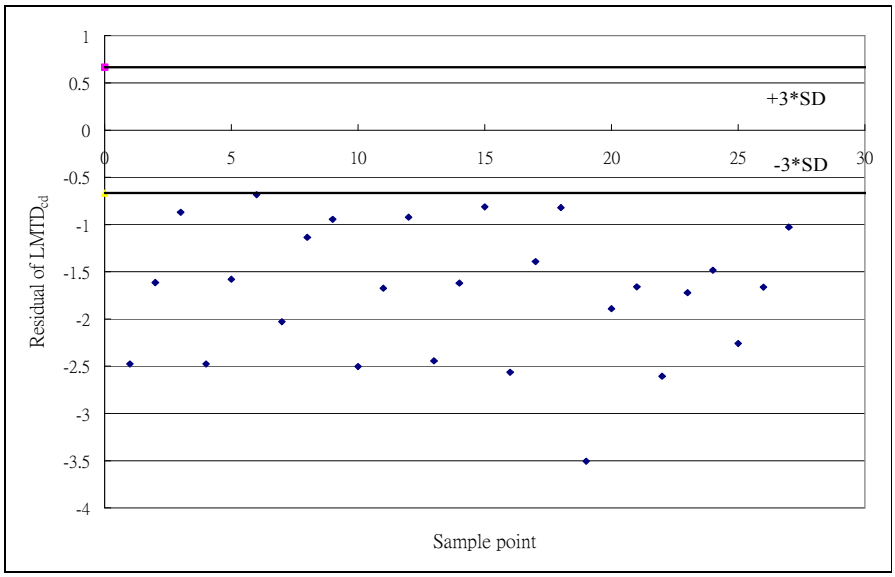

Figure 7.9 Residuals of $LMTD_{cd}$ under a reduction in evaporator water flow rate

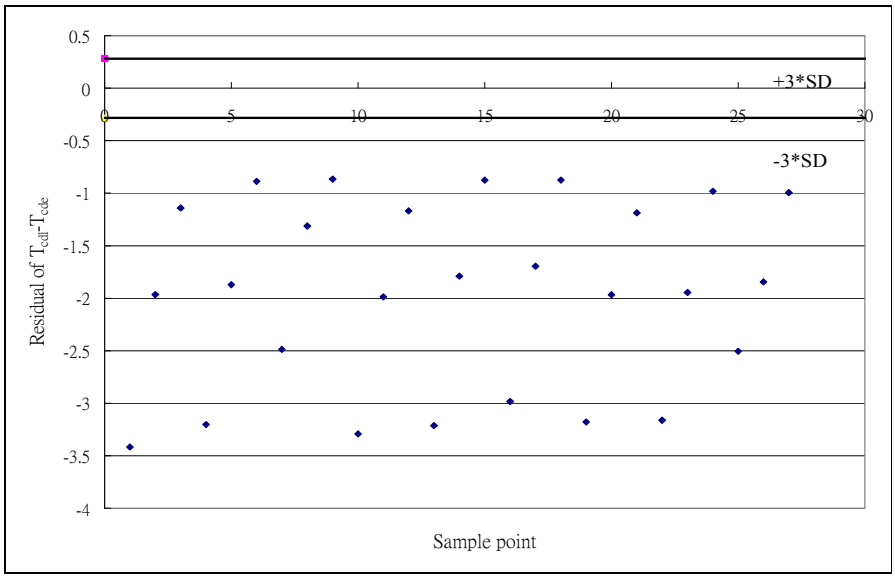

Figure 7.10 Residuals of (T_{cdl}-T_{cde}) under a reduction in evaporator water flow rate

7.6.3 Condenser fouling

This fault was simulated in the chiller test by plugging up a pre-determined number of tubes in the condenser to reduce the achievable rate of heat transfer between the refrigerant and the condenser water (Comstock and Braun 1999). The test data of 40% fouling (45% reduction in heat transfer area) was used for a comparison with the predicted fault-free data for establishing the classifier for this fault. As shown in Figures 7.11 & 7.12, this fault would lead to positive increments in the residuals of $LMTD_{cd}$ but the impacts on the residuals of (T_{cdl}–T_{cde}) were just moderate. This is because this fault would mainly affect the condensing temperature in the chiller.

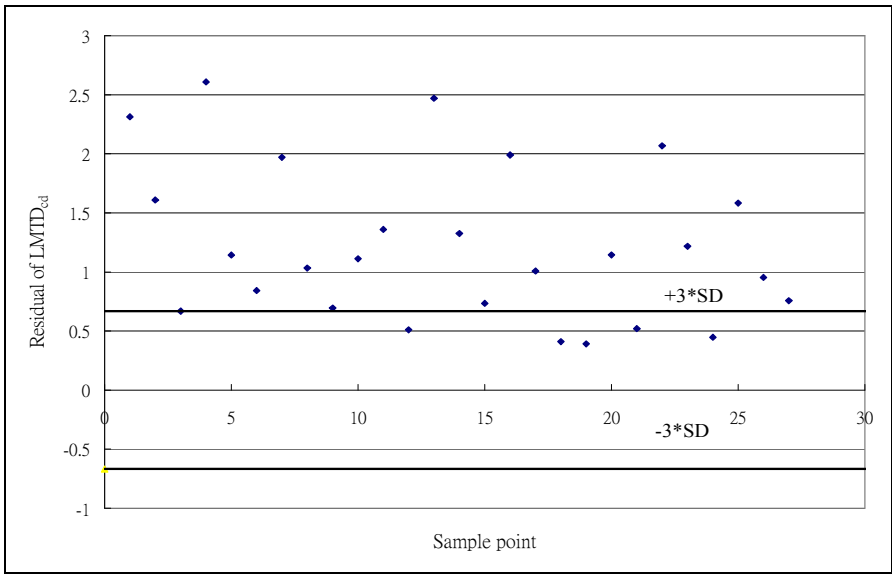

Figure 7.11 Residuals of $LMTD_{cd}$ under condenser fouling

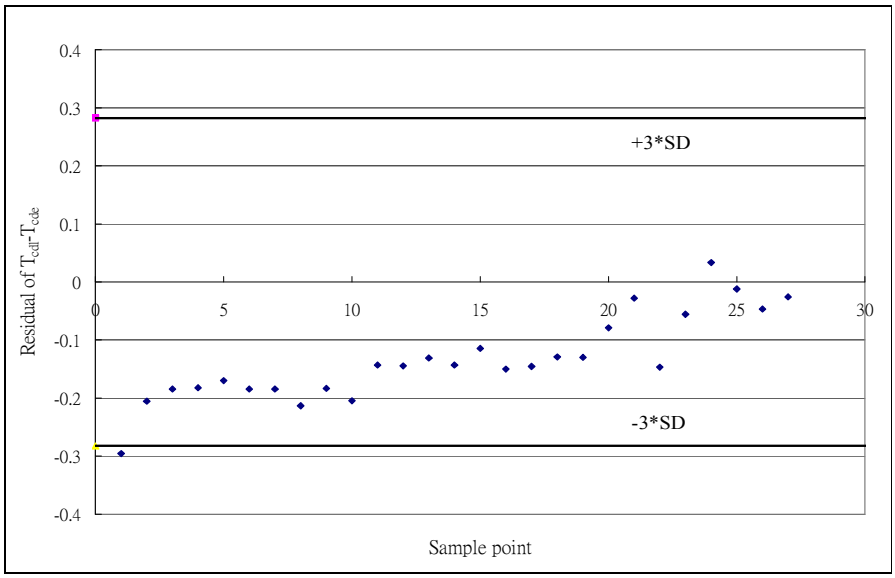

Figure 7.12 Residuals of (T_{cdl}-T_{cde}) under condenser fouling

7.6.4 Refrigerant leakage

The data available from the test condition of 40% refrigerant leakage was used for a comparison with the predicted fault-free data. As shown in Figures 7.13 & 7.14, with this fault, the residuals of $LMTD_{cd}$ were reduced but the impacts on the residuals of (T_{cdl}-T_{cde}) were mild. This is because a reduction in the amount of refrigerant in the chiller would incur a reduction in the condensing temperature of the refrigeration.

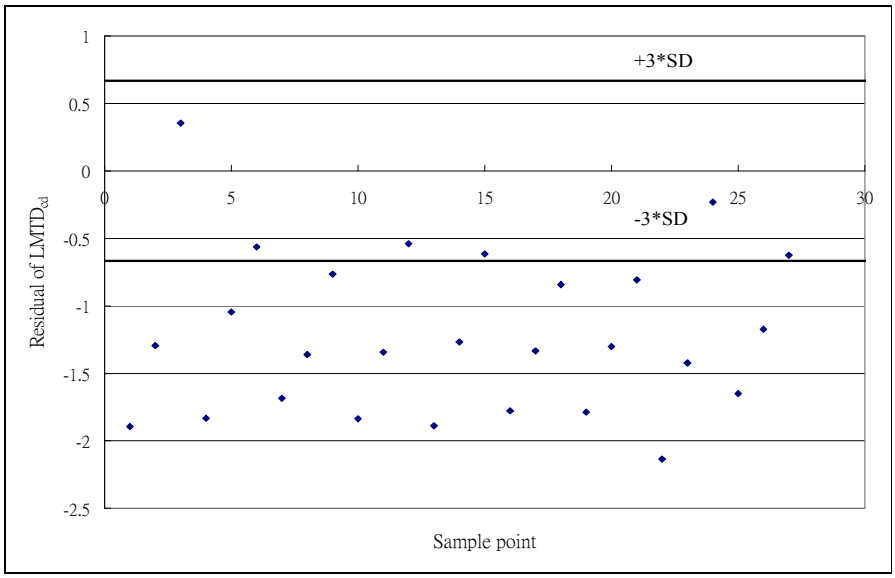

Figure 7.13 Residuals of $LMTD_{cd}$ with refrigerant leakage

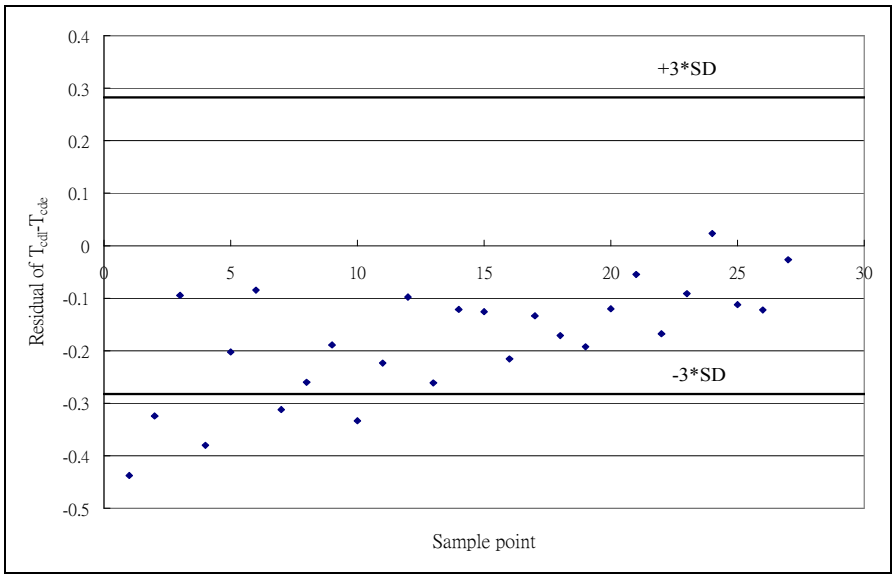

Figure 7.14 Residuals of (T_{cdl}-T_{cde}) with refrigerant leakage

7.6.5 FDD fault classifiers

The observations shown and discussed above unveiled that the two performance indices would vary in distinctive patterns among the four chiller faults, as summarized in Table 7.10. In this table, the symbol "~" indicates just moderate changes in the performance index; the symbol "↓" indicates a significant drop in the performance index; and the symbol "↑" indicates a significant increase in the performance index when a fault of considerable severity was present. These distinctive patterns, therefore, could be used as the references for detection of the presence of the respective chiller faults.

Table 7.10 Fault classification rules for chiller fault diagnosis

Fault type	$LMTD_{cd}$	$T_{cdl}-T_{cde}$
Reduced condenser water flow	↑	↑
Reduced evaporator water flow	↓	↓
Condenser fouling	↑	~
Refrigerant leakage	↓	~

After establishment of the fault classifiers, their effectiveness was verified by an analysis of actual plant performance data obtained from *in-situ* measurements of the performance of the water-cooled screw chillers in the Phase 3B plant and simulated chiller performance with presence of the fault, as reported below.

7.7 Fault detection and diagnosis using field data

The measurements obtained through *in-situ* experiments under conditions with manually reduced evaporator and condenser water flow rates were used to verify the effectiveness of the proposed chiller FDD strategy in detecting these faults. Since it was not possible to mimic condenser fouling and refrigerant leakage in the chillers in the plant, the effectiveness of the FDD strategy in detecting condenser fouling was verified through comparing model predictions in which the fault was simulated by reducing the overall heat transfer coefficient in the condenser model. However, it was not possible to simulate refrigerant leakage by using the chiller model and, therefore, verification of the effectiveness of the strategy in detecting this fault had to be deferred until the fault occurs naturally in any chiller in the plant.

In applying the proposed FDD strategy, the chiller model developed for the water-cooled screw chillers under study (see Section 7.2) was used to predict chiller performance and the predictions were used to evaluate the fault-free performance indices. The performance indices for a faulty condition were calculated based on measured or simulated chiller performance data when there was a fault with the chiller. The residuals were then determined from these two sets of performance indices and compared with their respective threshold values to illustrate if the fault could be detected by using the fault classifiers, as shown in Table 7.10. The threshold that applies to the residuals of

each performance index, $LMTD_{cd}$ or (T_{cdl}–T_{cde}), was three times the standard deviation of the predicted values of the performance index from those calculated using the measured chiller performance data, both for the fault-free condition, according to equation (7.2), and the threshold values were found to be 1.16°C and 0.87°C, respectively. When the residuals of the performance indices were found exceeding the corresponding threshold values in the pattern that matches with the corresponding fault classifying rule as shown in Table 7.10, the fault identified with reference to the fault classifier was regarded as having existed in the chiller.

For the test on reduced evaporator water flow, the chilled water flow rate was manually reduced from 50*l/s* to 40*/s* by partially closing an isolation valve in the chilled water pipe connected to Chiller 4 and the chiller performance data were logged by using the BMS for half a day. The residuals evaluated from this set of experimental results are shown in Figures 7.15 & 7.16. It can be seen that the residuals of the two indices both fall below their respective lower threshold values and thus match with the pattern for the fault with reduced evaporator water flow.

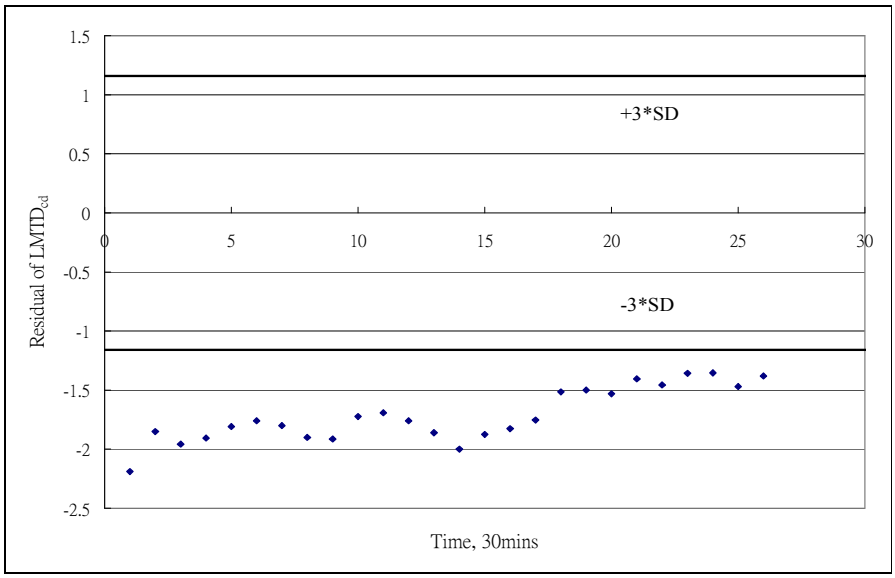

Figure 7.15 Residuals of $LMTD_{cd}$ under reduced evaporator water flow rate

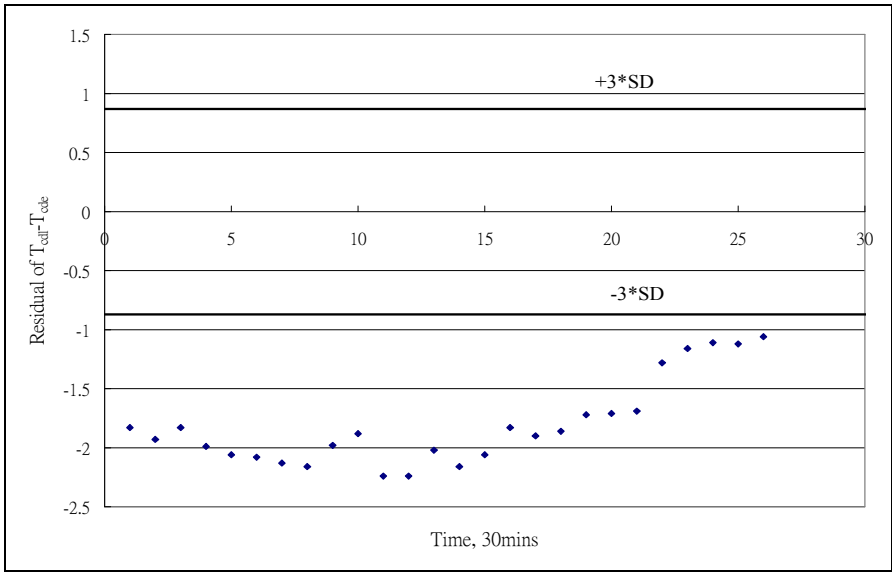

Figure 7.16 Residuals of (T_{cdl}-T_{cde}) under reduced evaporator water flow rate

For the test on reduced condenser water flow, the water flow rate in the condenser was adjusted from 88*l/s* to 65*/s* by partially closing the valve in the condenser water pipe

connected to Chiller 4, and the performance data of the chiller were logged for half a day. As shown in Figures 7.17 & 7.18, both residuals of the two performance indices rise above their respective upper threshold values, which match with the pattern that depicts this fault.

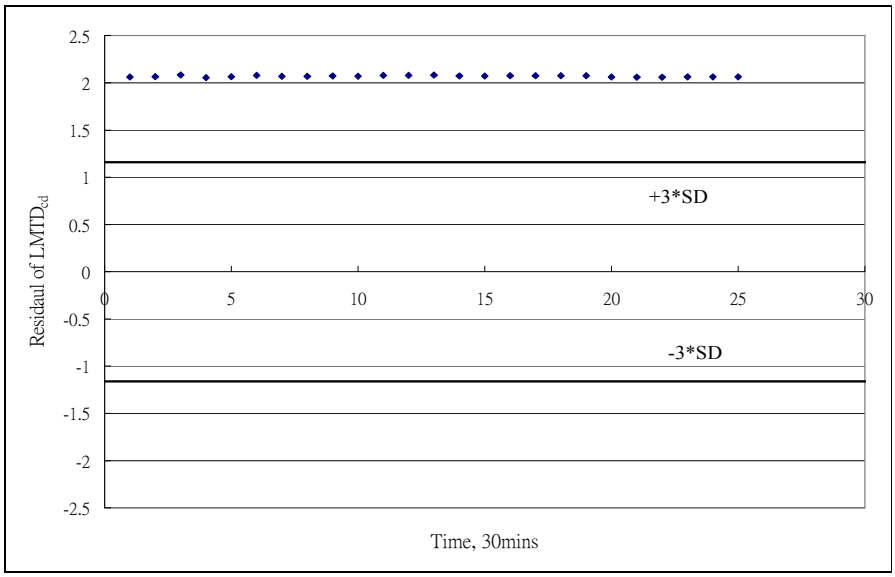

Figure 7.17 Residuals of $LMTD_{cd}$ under reduced condenser water flow

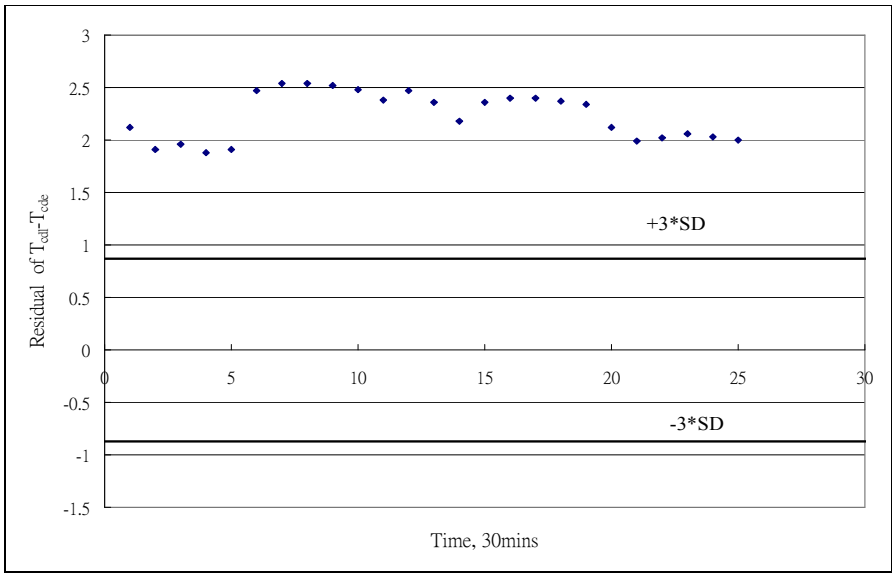

Figure 7.18 Residuals of (T_{cdl}–T_{cde}) under reduced condenser water flow

In order to verify the effectiveness of the FDD strategy in detecting condenser fouling, the overall heat transfer coefficient of the condenser in the chiller model was reduced by 30% and the chiller model was used to predict the performance of the chiller with this fault for a range of *PLR* under the condenser entering temperature of 29°C. The predicted faulty data were then compared with the predicted fault-free data under the same operating condition. The resultant residuals of $LMTD_{cd}$ and (T_{cdl}–T_{cde}) are shown in Figures 7.19 & 7.20. It can be seen that only the residuals of $LMTD_{cd}$ increased with the *PLR*, but the residuals of (T_{cdl}–T_{cde}) remained almost unchanged. This matches with the pattern for condenser fouling as defined in the fault classifiers of the FDD strategy (Table 7.10).

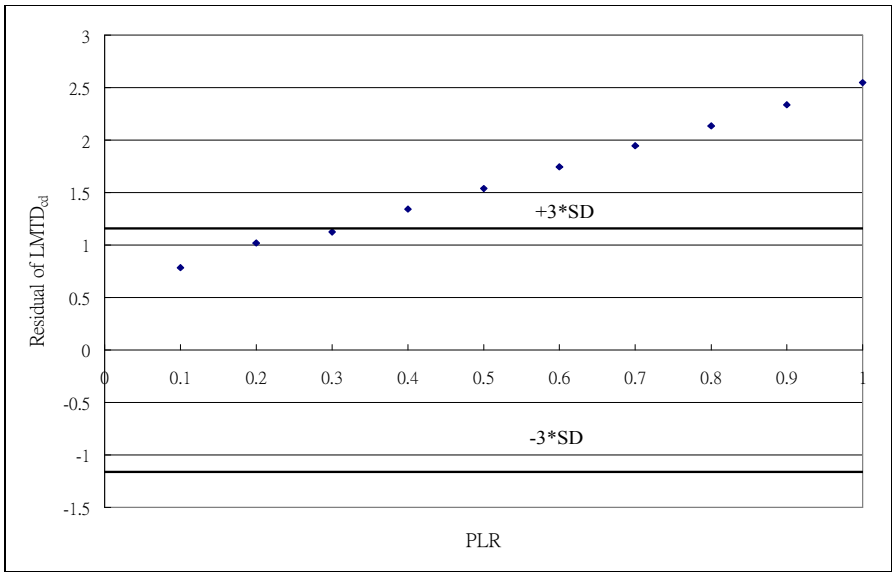

Figure 7.19 Residuals of $LMTD_{cd}$ with condenser fouling

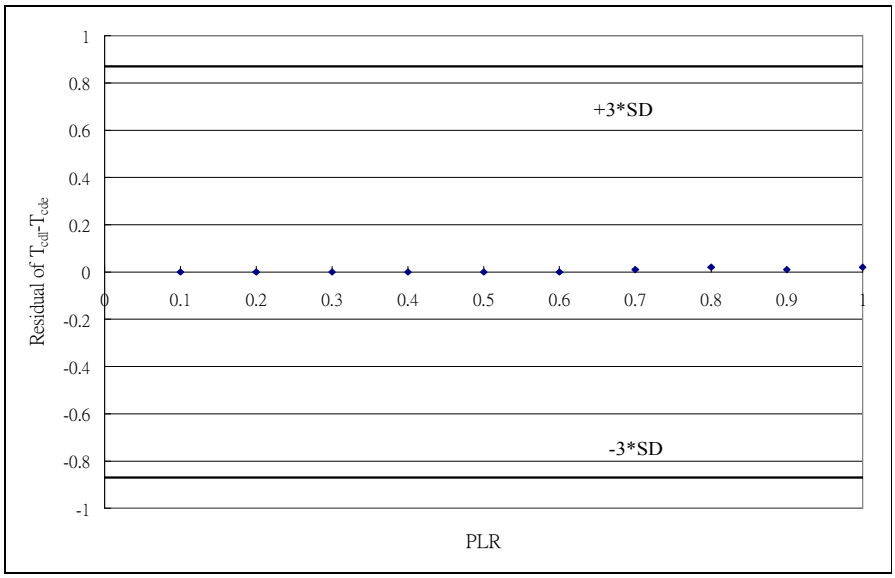

Figure 7.20 Residuals of (T_{cdl}–T_{cde}) with condenser fouling

7.8 Conclusion

Successful application of the proposed FDD strategy has been demonstrated based on experimental and simulated chiller performance data for a chiller in an existing chiller plant. The fault classifiers in the FDD strategy were established based on laboratory chiller test data produced by the ASHRAE Research Project 1043-RP. The proposed fault classifiers involve the use of two performance indices, the log-mean temperature difference of the condenser and the water temperature rise across the condenser, and the residuals of these performance indices have been shown to exhibit distinctive patterns for the four kinds of faults studied, namely reduced condenser water flow, reduced evaporator water flow, condenser fouling and refrigerant leakage. The test results showed that the FDD strategy was capable of detecting the first three kinds of faults. However,

for refrigerant leakage, its effectiveness could not be demonstrated until this fault arises naturally in the plant.

8. BARRIERS TO IMPLEMENTATION OF FDD IN EXISTING BUILDINGS AND MITIGATION MEASURES

8.1 Overview

As described in the preceding chapter, a chiller fault detection and diagnosis (FDD) strategy has been developed. In the FDD strategy, the performance indices that can reflect the health of chillers were evaluated based on the chiller performance data records retrieved from the building management system (BMS) and the fault-free performance of the chillers predicted by a chiller model. The pattern of deviation of the real performance indices from the fault-free indices was compared against a set of fault classifiers, so as to tell whether a specific fault existed in the chillers. The set of fault classifiers for detecting different chiller faults was established based on laboratory chiller test data produced by the ASHRAE Research Project 1043-RP. However, the range of chiller faults that the FDD strategy can detect was confined to four kinds of chiller faults due to the limited measuring instruments available in the plant and the limited range of faults covered by the set of measurements turned out in the ASHRAE Project.

The ability of the chiller FDD strategy to detect reduced condenser and evaporator water flow has been demonstrated through experimental measurements carried out in an existing chiller plant during which the faults were physically simulated in turn. The fault detection ability of the strategy for condenser fouling was demonstrated based on simulation predictions where presence of the fault was modelled in the simulation.

Unfortunately, it was not possible to simulate refrigerant leakage as presence of this fault could not be simulated either physically in the existing chiller plant or by computer simulation.

Besides unavailability of sensors for providing the needed performance measurements, faulty sensors and missing data would hinder application of FDD to existing chiller plants, as had been encountered in the present study. In this chapter, a review of the various barriers to successful application of FDD techniques to chiller plants is presented together with suggested measures that would help overcome the problems.

8.2 Essential chiller performance measurements for chiller FDD

In deciding whether to adopt a FDD system, the first and foremost decision to be made is on the range of faults to be put under the scrutiny of the FDD system. Widening the range of faults to be kept monitored by the system would require a more powerful FDD algorithm to be used as well as a larger variety and quantities of measuring instruments to be installed, which will jack up the investment needed to make available the required hardware and software as well as the manpower to properly maintain the FDD system and the associated measuring instruments and data transmission and recording devices.

The required hardware and software for FDD implementation are dependent on the performance indices employed to reflect the presence or otherwise of individual faults, as the system variables that need to be measured to enable evaluation of the performance indices would dictate the types and quantities of sensors that need to be installed.

Furthermore, the FDD system, which may be part of a BMS, should also be capable of performing the FDD calculations on-line, and be equipped with sufficient data storage capacity for recording the measured values of the involved system variables, to allow the data to be retrieved for retrospective analysis.

Because numerous faults could arise in various engineering services systems and equipments in a building, the discussions here are confined to chiller faults, which are the main focus of the present study. Even though the focus is narrowed down to chiller faults only, there are still many types of chiller faults that may arise but not all of them need to be monitored consistently by a FDD system. Selection of the range of chiller faults to be monitored is usually based on the severity of the consequences of a fault (such as interruption to normal operation and repair costs) and the frequency of occurrence of the fault (Comstock and Braun, 1999).

Results of the survey conducted by Comstock and Braun (1999) showed that from the perspective of frequency of occurrence, service cost and repair cost, the kinds of chiller faults that should be chosen as the target faults should include reduced evaporator water flow, reduced condenser water flow, condenser fouling, refrigerant leakage, compressor internal fault and evaporator fouling. Compressor fault could incur a high repair cost (albeit it would not frequently occur) (Comstock and Braun, 1999) while evaporator fouling may easily occur in a flooded evaporator (Cui, 2005). However, these two faults were not covered by the chiller tests of the ASHRAE Project and, therefore, they had to be excluded from the FDD strategy developed in the present study (see Chapter 7).

With reference to five chiller FDD studies reported in the open literature (Comstock and Braun, 1999; Cui and Wang, 2005; Cui, 2005; Zhou et al., 2009; Mclntosh et al., 2000), the performance indices used and the measurements required for detection of the abovementioned six chiller faults have been compiled, as summarized in Table 8.1. The same for the FDD strategy developed in the present study and the measurements available from the BMS records that underpinned the study, are also included in this table.

As can be seen in Table 8.1, the measurements available from the BMS that served the chiller plant on which the present study was based would be sufficient for detecting reduced condenser water flow and condenser fouling through the use of the FDD strategy proposed by Mclntosh et al. (2000) and the present study. For reduced evaporator water flow, the available measurements would be sufficient for detection of the fault with the use of the strategy proposed by Cui and Wang (2005), Zhou et al. (2009), Mclntosh et al. (2000) and the present study, but would become insufficient if the strategy proposed by Comstock and Braun (1999) is used instead.

With the available measurements, even though refrigerant leakage could be detected by the strategy developed in the present study (but its effectiveness has not been verified), the measurements would become insufficient when any one of the other proposed strategies is used, unless measures of sub-cooled temperature (T_{sub}), condensing pressure (P_{cd}) and suction temperature (T_{suc}) were also available. The available measurements were sufficient for detecting also evaporator fouling but would be insufficient for detecting compressor internal fault, unless measurements of the suction temperature (T_{suc}) and the discharge temperature (T_{dis}) were available. In order to

effectively detect all the six chiller faults, sensors for the missing measurements should also be provided and trend-logged in the BMS.

Table 8.1 Performance indices used and measurements required for chiller fault detection

A) Reduced condenser water flow

	Comstock and Braun	Cui and Wang	Cui	Zhou et al.	McIntosh et al.	The present study	Measurement available
Performance indices							
Heat transfer coefficient of condenser, AU_{cd}					○		
Log-mean temperature difference of condenser, $LMTD_{cd}$						○	
Condenser water temperature difference, T_{cdl}-T_{cde}	○			○	○	○	
Condenser approach temperature, T_{cd}-T_{cdl}	○			○	○		
Evaporator approach temperature, T_s-T_{evp}	○						
Coefficient of performance, *COP*					○		
kW/ton	○						
Suction temperature, T_{suc}	○						
Sub-cooled temperature, T_{sub}	○			○			
Condensing pressure, P_{cd}	○			○			
Evaporating pressure, P_{evp}	○						
Electrical power of chiller, W_{ch}	○						
Oil temperature, T_{oil}	○			○			
Measurements required							
Chilled water supply temperature, T_s	○				○		○
Chilled water return temperature, T_r	○				○		○
Condenser water entering temperature, T_{cde}	○			○	○	○	○
Condenser water leaving temperature, T_{cdl}	○			○	○	○	○
Condensing temperature, T_{cd}	○			○	○	○	○
Evaporating temperature, T_{evp}	○						○
Suction temperature, T_{suc}	○						
Sub-cooled temperature, T_{sub}	○			○			
Condensing pressure, P_{cd}	○			○			
Evaporating pressure, P_{evp}	○						
Electrical power of chiller, W_{ch}	○				○		○
Oil temperature, T_{oil}	○			○			

Table 8.1 Performance indices used and measurements required for chiller fault detection (Cont'd)

B) Reduced evaporator water flow

	Comstock and Braun	Cui and Wang	Cui	Zhou et al.	McIntosh et al.	The present study	Measurement available
Performance indices							
Heat transfer coefficient of evaporator, AU_{evp}					○		
Log-mean temperature difference of condenser, $LMTD_{cd}$						○	
Log-mean temperature difference of evaporator, $LMTD_{evp}$		○					
Condenser water temperature difference, T_{cdl}-T_{cde}						○	
Evaporator water temperature difference, T_r-T_s	○			○	○		
Evaporator approach temperature, T_s-T_{evp}	○				○		
Coefficient of performance, *COP*		○			○		
kW/ton	○						
Suction temperature, T_{suc}	○						
Discharge temperature, T_{dis}	○						
Sub-cooled temperature, T_{sub}	○						
Evaporating pressure, P_{evp}	○						
Electrical power of chiller, W_{ch}	○						
Measurements required							
Chilled water supply temperature, T_s	○	○		○	○		○
Chilled water return temperature, T_r	○	○		○	○		○
Condenser water entering temperature, T_{cde}						○	○
Condenser water leaving temperature, T_{cdl}						○	○
Condensing temperature, T_{cd}						○	○
Evaporating temperature, T_{evp}	○	○			○		○
Suction temperature, T_{suc}	○						
Discharge temperature, T_{dis}	○						
Sub-cooled temperature, T_{sub}	○						
Evaporating pressure, P_{evp}	○						
Electrical power of chiller, W_{ch}	○	○			○		○

Table 8.1 Performance indices used and measurements required for chiller fault detection (Cont'd)

C) Condenser fouling

	Comstock and Braun	Cui and Wang	Cui	Zhou et al.	McIntosh et al.	The present study	Measurement available
Performance indices							
Heat transfer coefficient of condenser, AU_{cd}					○		
Log-mean temperature difference of condenser, $LMTD_{cd}$		○	○			○	
Condenser water temperature difference, T_{cdl}-T_{cde}	○			○			
Condenser approach temperature, T_{cd}-T_{cdl}	○			○	○		
Coefficient of performance, *COP*		○	○		○		
kW/ton	○						
Refrigerant mass flow rate, m_{ref}		○	○				
Condensing pressure, P_{cd}	○			○			
Electrical power of chiller, W_{ch}	○						
Measurements required							
Chilled water supply temperature, T_s	○	○	○		○		○
Chilled water return temperature, T_r	○	○	○		○		○
Condenser water entering temperature, T_{cde}	○	○	○	○	○	○	○
Condenser water leaving temperature, T_{cdl}	○	○	○	○	○	○	○
Condensing temperature, T_{cd}	○	○	○	○	○	○	○
Evaporating temperature, T_{evp}		○	○				○
Suction temperature, T_{suc}		○	○				
Sub-cooled temperature, T_{sub}		○	○				
Condensing pressure, P_{cd}	○			○			
Electrical power of chiller, W_{ch}	○	○	○		○		○

Table 8.1 Performance indices used and measurements required for chiller fault detection (Cont'd)

D) Refrigerant leakage

	Comstock and Braun	Cui and Wang	Cui	Zhou et al.	McIntosh et al.	The present study	Measurement available
Performance indices							
Log-mean temperature difference of condenser, $LMTD_{cd}$		○	○			○	
Condenser approach temperature, T_{cd}-T_{cdl}	○			○			
Coefficient of performance, *COP*		○	○				
kW/ton	○						
Refrigerant mass flow rate, m_{ref}		○	○				
Sub-cooled temperature, T_{sub}	○			○			
Condensing pressure, P_{cd}	○			○			
Electrical power of chiller, W_{ch}	○						
Measurements required							
Chilled water supply temperature, T_s	○	○	○				○
Chilled water return temperature, T_r	○	○	○				○
Condenser water entering temperature, T_{cde}		○	○			○	○
Condenser water leaving temperature, T_{cdl}	○	○	○	○		○	○
Condensing temperature, T_{cd}	○	○	○	○		○	○
Evaporating temperature, T_{evp}		○	○				○
Suction temperature, T_{suc}		○	○				
Sub-cooled temperature, T_{sub}	○	○	○	○			
Condensing pressure, P_{cd}	○			○			
Electrical power of chiller, W_{ch}	○	○	○				○

Table 8.1 Performance indices used and measurements required for chiller fault detection (Cont'd)

E) Evaporator fouling

	Comstock and Braun	Cui and Wang	Cui	Zhou et al.	McIntosh et al.	The present study	Measurement available
Performance indices							
Heat transfer coefficient of evaporator, AU_{evp}					○		
Log-mean temperature difference of evaporator, $LMTD_{evp}$			○				
Evaporator approach temperature, T_s-T_{evp}					○		
Coefficient of performance, *COP*			○		○		
Measurements required							
Chilled water supply temperature, T_s			○		○		○
Chilled water return temperature, T_r			○		○		○
Evaporating temperature, T_{evp}			○		○		○
Electrical power of chiller, W_{ch}			○		○		○

F) Compressor internal fault

	Comstock and Braun	Cui and Wang	Cui	Zhou et al.	McIntosh et al.	The present study	Measurement available
Performance indices							
Isentropic efficiency, n_{isen}					○		
Coefficient of performance, *COP*					○		
Measurements required							
Chilled water supply temperature, T_s					○		○
Chilled water return temperature, T_r					○		○
Condensing temperature, T_{cd}					○		○
Evaporating temperature, T_{evp}					○		○
Suction temperature, T_{suc}					○		
Discharge temperature, T_{dis}					○		
Electrical power of chiller, W_{ch}					○		○

With reference to the literature review and discussions mentioned above, the minimum range of measurements that should be made available in order that all the six major chiller faults can be detected with the use of a FDD system is as summarized in Table 8.2.

Table 8.2 Minimum range of measurements for implementation of chiller FDD

Measurements	Typically available
Chilled water supply temperature, T_s	Yes
Chilled water return temperature, T_r	Yes
Condenser water entering temperature, T_{cde}	Yes
Condenser water leaving temperature, T_{cdl}	Yes
Condensing temperature, T_{cd}	Yes
Evaporating temperature, T_{evp}	Yes
Suction temperature, T_{suc}	No
Discharge temperature, T_{dis}	No
Sub-cooled temperature, T_{sub}	No
Condensing pressure, P_{cd}	No
Electrical power of chiller, W_{ch}	Yes

The analysis of the operating records of the chiller plant studied unveiled that measurements of the chilled water supply and return temperatures, the condenser water entering and leaving temperatures, the refrigerant condensing and evaporating temperatures and the electrical power demand of the chiller were available, and such measurements should normally be available in typical chiller plants. The other four refrigerant parameters, which require built-in sensors inside a chiller for their measurement, were unavailable and thus were not fed to and recorded by the BMS, even if it could be possible to obtain these measurements from the built-in sensors. However, without them, there will be insufficient data for chiller FDD.

The chiller manufacturer catalogues had been inspected to verify if built-in sensors were indeed available for measurement of the abovementioned refrigerant parameters in the chillers. Table 8.3 summarizes the sensors that the chillers were

equipped with, which shows that the required sensors were present. Therefore, the reason for those measurements being unavailable was not due to lacking of sensors; it was because they were not connected to the BMS. Inspection of the O&M manuals (SkyForce, 1998) and responses of the facility management staff to our verbal enquires confirmed that the refrigerant measurements are not linked to the BMS because; i) this requirement was not included in the specification prepared by the design consultant in the first place; ii) these measurements were considered to be unnecessary for O&M works; and iii) extra cost would be incurred if those measurements were recorded by the BMS.

Table 8.3 Built-in sensors in chillers

Sensors	Standard / Optional
Evaporator entering and leaving water temperature sensors	Standard
Condenser entering and leaving water temperature sensors	Standard
Condensing pressure and temperature sensors	Standard
Evaporating pressure and temperature sensors	Standard
Suction pressure and temperature sensors	Standard
Compressor refrigerant discharge pressure and temperature sensors	Standard
Sub-cooled pressure and temperature sensors	Standard
Oil temperature and pressure sensors	Standard
Motor temperature sensor	Optional
Evaporator liquid level sensor	Optional

8.3 Guidelines on provision of sensors in chiller plants

Since designers of air-conditioning systems are expected to follow relevant standards and guidelines published by professional institutions or government agencies in specifying the range of measuring instruments to be including in the contract for supply and installation of the systems, the recommendations on measuring instruments for chiller performance monitoring given in various standards and guidelines have been reviewed to find out whether following such recommendations would still lead to insufficient sensors

for measurement of the system variables that are needed for FDD. The recommendations given in the following guidelines were selected for a comparison:

1. Testing and commissioning procedure No. 1 for Air–conditioning, Refrigeration, Ventilation and Central Monitoring & Control System Installation in Government Buildings in Hong Kong (ASD, 2002).

2. ASHRAE Guideline 22P-2007- Proposed New Guideline 22, Instrumentation for Monitoring Central Chilled Water Plant Efficiency (ASHRAE, 2007).

3. Business Focused Maintenance: guidance and sample schedules (BSRIA, 2004).

The first guideline listed above (ASD, 2002), published by the Architectural Services Department of the Hong Kong Government, stipulates requirements that must be complied with for air-conditioning and central control and monitoring systems (CCMS; basically same as BMS) installed in government buildings, and is also a widely used reference for testing and commissioning of air-conditioning and CCMS installations in Hong Kong, including in the private sector. The requirements therein may, therefore, be regarded as a good representation of the instrumentation provisions in many buildings in Hong Kong. The second guideline (ASHRAE, 2007) is the latest guideline from ASHRAE and air-conditioning system designers in Hong Kong very often make reference to handbooks and guidelines published by ASHRAE. The guidance given in the 3rd guideline (BSRIA, 2004) is, among the various guidelines reviewed, the most comprehensive. Table 8.4 summarizes the provisions of measuring instruments recommended by these guidelines. Again, the measurements available from the BMS for the plant studied are included in this table.

Table 8.4 Measurement recommended by the standards and guidelines

Measurements	ASD (2002)	ASHRAE Guideline 22P (2007)	BSRIA (2004)	Measurement available in chiller plant studied
Outdoor dry bulb temperature		○	○	○
Outdoor wet bulb temperature		○	○	○
Chilled water supply temperature	○	○	○	○
Chilled water return temperature	○	○	○	○
Condenser water entering temperature	○	○	○	○
Condenser water leaving temperature	○	○	○	○
Electrical power of chiller	○	○	○	○
Chilled water flow rate		○	○	○
Condenser water flow rate		○	○	○
Condensing temperature	○		○	○
Evaporating temperature	○		○	○
Condensing pressure	○		○	
Evaporating pressure	○		○	
Suction temperature and pressure			○	
Discharge temperature and pressure			○	
Sub-cooled temperature and pressure			○	
Oil temperature and pressure	○		○	

It can be seen that the focus of ASHRAE Guideline 22P is on energy performance monitoring rather than maintenance practice or FDD. Therefore, the recommended instrument provisions include just the basic ones needed for measuring the overall energy use of a chiller. BSRIA (2004) recommends keeping accurate data log of all basic chiller operation data which can cover all the required refrigerant parameters for FDD application, as shown in Table 8.2. However, the recommendations give in the Hong Kong Government's guideline for public buildings (ASD, 2002) are limited and insufficient for FDD application.

Besides the types and quantities of measuring sensors required, attention should also be paid to the measurement accuracy of the sensors as well as proper installation and maintenance of the sensors. However, due to the higher costs of more accurate sensors,

building owners are usually unwilling to purchase sensors with accuracy standards beyond those needed for control and monitoring purposes. Sensors with measurement accuracy that meets the requirements of ASHRAE Standard 114-1986 (ASHRAE, 1987) or the Standard Specifications for BMS (BSRIA, 2001a), as summarized in Table 8.5, should be taken as the minimum standard.

Table 8.5 Recommended minimum standard of accuracy of sensors

Measured variable	ASHRAE standard 114	BSRIA (2001a)
Temperature measurement	±0.2 °C	±0.25 °C
Flow rate measurement	±2.5% full scale	±2% reading
Pressure measurement	±2% full scale	±2% reading

However, according to ASHRAE Guideline 14 (ASHRAE, 2002), the accuracy of temperature measurement can easily be upgraded to ±0.1°C with proper calibration of thermistors or resistance temperature detectors; the accuracy of flow measurement can be up to ±2% full scale with the use of magnetic flow meter or ultrasonic flow meter; and the accuracy of pressure measurement can increase to ±1% full scale with the use of proper pressure transducer. These measuring accuracies should be adopted as far as possible to facilitate more accurate fault detection and diagnosis.

The locations at which sensors are installed should be determined with care; otherwise, even an accurate sensor could output inaccurate measurements, which is particularly important to flow sensors. As suggested by ASHRAE Guideline 22P (ASHRAE, 2007), water temperature sensors should be located in wells inside water piping and air temperature sensors should be shielded against solar radiation. Meters for water flow rate measurement should be placed at locations where there are adequate

straight runs of pipes, both upstream and downstream of a meter, and minimal turbulence-inducing elements.

In the field work conducted in the present study, many faulty sensors were encountered, which are not uncommon in buildings in Hong Kong (Yik and Chiu, 1998). When measuring sensors become faulty, there will be missing or inaccurate data, which will render performance evaluation or FDD impossible or their results meaningless or misleading. Therefore, special attention should be paid to proper maintenance of sensors, including regular calibration to verify their measurement accuracy.

A number of standards provide guidance on the frequency of inspection and calibration of sensors in chiller plants, which are summarized in Table 8.6. The recommended periods for sensor calibration given in these guidelines, however, vary from 3 months to a year. In any case, the period of calibration should be kept under review and should be shortened where deemed necessary, depending on the findings of re-calibration. For example, when large sensor drift is found, the duration from a re-calibration to the next re-calibration should be shortened until the drift stays within an acceptable limit.

Table 8.6 Recommended period of calibration

Standard	Period of calibration
BSRIA (2004)	6 monthly for control sensors; 12 monthly for monitoring sensors
ASHRAE Guideline 14 (2002)	Between 6 months and 1 year
ASHRAE Standard 180 (2006)	Quarterly
CIBSE (1991)	3 months for chilled water temperature sensors

Although the function of FDD can also cover sensor faults but this will be a more difficult task as symptoms of sensor and system faults could be indistinguishable while

multiple faults of both types may occur simultaneously. As described in Chapter 3, attempts had been made in the present study to verify the accuracy of records of the sensor readings before the data were used in evaluation of chiller performance and in development of chiller models. With the limited sensors available and the large amount of faulty sensor readings found, it was not possible to include sensor FDD in the present study.

Data loss problem was also encountered in the analysis of the operating records of the chiller plant studied (Chapter 3), which was ascribed by the O&M personnel to power supply interruption and the lack of back up power supply for the DDC panels of the BMS. As BSRIA (2004) recommends, sufficient data storage should be allowed to avoid data loss and, according to ASHRAE Guideline 14, occurrence of this problem should be detected and corrected as soon as possible, and good preventive maintenance for the BMS can help minimize the problem. The latter guideline also advises that missing data may be handled by omitting analysis for the interval of loss data or substituting a rational replacement value, which may be fixed, interpolated, synthesized or calculated from known information. Whereas this may serve well the purpose of energy consumption measurement, accurate detection of faults may become not possible with the use of the substituted data.

8.4 Other barriers

Unlike some other new and sophisticated technologies of which the costs and benefits could be estimated with a high degree of certainty, implementation of FDD can be costly whilst the benefits are uncertain. The major benefit of adopting FDD is the avoided energy wastage due to various system and sensors faults. Therefore, the benefit

that FDD can bring is variable and is dependent on the number and frequency of occurrence of faults and the severity of the faults when they arise; the more types of, the more frequent and the more serious the faults, the greater the benefit that FDD can bring. However, one cannot ascertain the actual benefits for a building with certainty, as they are highly variable among buildings, and are largely unknown when a decision is made on whether or not to adopt FDD. For this reason, many building owners and engineers are reluctant to adopt FDD.

Where the existing sensors are found insufficient and not accurate and reliable enough for FDD implementation and/or there are already many faults with the systems and equipments, the building owner would need to pay extra costs for installing new and replacing sub-standard sensors, re-calibrating those usable existing sensors, and for removing all the unfavourable conditions that exist in the plants in the building, which can undermine the eagerness of the building owner to adopt a FDD system. Furthermore, installation of new sensors in an existing plant may cause interruptions to the normal operation of the plant (e.g. pipes need to be drained before holes can be drilled for insertion of sensors). It, therefore, may take considerable time for the installation work, which could only be carried out when there is a chance to stop the plant (e.g. during public holidays) (Yik and Chiu, 1998).

Another major hurdle is that successful implementation of FDD requires much wider and deeper knowledge about the operating principles and characteristics of the HVAC&R system and the BMS, and about measurement and analysis of system performance, which could well exceed the expertise of the vast majority of building operators (Yik and Lee, 2002), not to mention the high level of mathematical knowledge

that one must have in order to understand some FDD methods. However, because traditional building operation and maintenance (O&M) works are perceived as routine and unsophisticated, most building operators have academic qualifications below bachelor degree level, which is particularly relevant to Hong Kong (Lai et al, 2004). Even technical managers who should be better able to evaluate new technologies may not understand the principle and the super-intelligence of FDD, and thus they may not be willing to adopt FDD in their O&M work (Shockman and Piette, 2000).

Therefore, education and training are required to enable O&M practitioners to understand the operating principles of FDD systems and to interpret fault reports and diagnose the causes. It would be impossible to impart such a broad and deep body of knowledge to a person through just a few training courses; many would in fact require a formal educational programme. However, attending such a programme would incur a high cost to the O&M practitioners, including the programme fee to be paid and the time to be spent, and thus few would be willing to pay this cost for equipping themselves with the required expertise.

Some may argue that the reliance on the knowledge and skills of O&M personnel would become minimal if FDD systems can be developed to the state that they can always provide accurate fault diagnosis and precise instructions on effective actions to be taken. Then, training is not required for users and thus, the total cost of FDD may reduce. Although this should be a target for FDD system designers to strive for, the ability of O&M personnel to correctly interpret fault reports and to figure out appropriate corrective actions is indispensable, as each building and system could have unique characteristics which could be too numerous to cater for while only the O&M personnel have detailed

knowledge about such characteristics. Besides, FDD systems for buildings that are available at the moment still have a lot of limitations (e.g. the ability to detect and precisely distinguish multiple or simultaneous faults); their successful implementation, therefore, rely heavily on the O&M personnel's interpretation and application of the fault and diagnosis reports produced by the FDD systems. As the role of operators is essential for the implementation of FDD, FDD systems should be designed to function in a user-friendly manner (Heinemeier, 1998). Then, the training time to equip them with the required knowledge and the time for them to identify and respond to the faults may be greatly reduced.

8.5 Suggested measures to enable application of FDD to buildings

As discussed above, insufficient and inadequate measuring instruments, which would result in inaccurate or erroneous measurements of operating performance of a system, or even missing data, is a major hurdle to successful implementation of FDD in existing buildings. These difficulties have to be overcome before a FDD system can serve well its functions. Given that chillers are the dominant energy consumers in many types of buildings in Hong Kong while the instrumentation requirements would not exceed those required for chiller performance and energy use measurement by a large extent, it would be most cost-effective to begin application of FDD with the central chiller plant in an existing building.

The minimum kinds of measurement for detecting major chiller faults have been identified, as shown in Table 8.2, from a review of literature and from the experience

gained in the present study. Other than those for measuring the states of refrigerant inside a chiller, instruments for measuring the required parameters for chiller FDD are already common provisions in many buildings. It has also been verified that the sensors required for measuring the states of refrigerant inside a chiller can be made available from the chiller manufacturer, by specifying the requirements in the contract for procurement of the air-conditioning installation. Corresponding, provisions in the BMS system for trend-logging the data should also be made. Although sensors for the full range of required measurements may not be covered in the recommendations of various standards and guidelines on instrumentation provisions for chiller plants, all of them are well covered by the recommended list in BSRIA (2004).

In order to ensure the measurement accuracy of the sensors are high enough for implementation of FDD, the recommendations given in ASHRAE Standard 114-1986 (ASHRAE, 1987) or the Standard Specifications for BMS (BSRIA, 2001a) should be taken as the minimum acceptable standard, and where possible, higher standards should be adopted. In order to alleviate the problems with faulty sensors, more rigorous inspection and calibration should be carried out for the instruments for measuring chiller performance. For determining the calibration periods for the sensors, reference should be made to the recommendations made in those guidelines shown in Table 8.6; the calibration results should be closely monitored; and the duration between each inspection, maintenance and sensor calibration should be adjusted where deemed necessary. The general calibration procedures for measurements are summarized and discussed in the Appendix to provide guidance to building operators. The sensor calibration work may also be outsourced from a services provider with adequate facilities and expertise for the calibration work.

For avoiding loss of data, adequate provisions should be made to ensure there will always be sufficient data storage capacity in the BMS. It is also advisable to provide an uninterruptible power supply system to backup the electricity supply to the BMS and its outstations in case of power interruption, and the recorded data should be retrieved from the BMS periodically and securely stored in a save medium.

A typical BMS are normally not programmed to perform time-interval based averaging functions for removing transient fluctuations of chiller performance data but it is recommendable to incorporate this data pre-processing function for individual measurements, if on-line FDD is implemented. Some basic validity checks should also be programmed into the BMS for simple data validation. For example, measurements for an operating chiller should be checked consistently to see if they agree with the relationship depicted by equation (8.1). When the measurements violate this relationship, the FDD system should issue an alarm and the cause of this problem should be investigated, identified and removed.

$$0 < T_{evp} < T_s < T_r < T_{cde} < T_{cdl} < T_{cd} \tag{8.1}$$

The most important of all would be the attitude of building owners toward adoption of FDD in their buildings. As discussed above, the costs to be borne by the building owners for implementation of FDD include not only those for procuring the required devices (e.g. measurement instruments), upgrading the software, and re-calibration of sensors; relevant training for the in-house O&M staff or outsourcing for the required expertise is also necessary. Although the learning process takes time and it requires investments in extra to the FDD system cost, the building owners should realise that significant benefits come predominantly from removal of the inadequacies that exist

in their plants while implementation of FDD can be taken as a good vehicle for them to achieve this. For realising the advantage of FDD, building owners should provide adequate financial resources for maintenance to ensure reliability, safety and energy efficiency of building services systems (CIBSE, 1990). In addition, the FDD supplier could promote their product to building owners by providing some incentives, such as:

1. Sponsoring demonstration projects to provide empirical evidence of the benefits that FDD could yield, to allow building owners to gain confidence in the technologies;

2. Offering building owners training, to cut down the costs to them to acquire the required knowledge and skills to properly apply the technology; and

3. Helping building owners overcome problems that may be encountered in the installation, commissioning, operation and maintenance of the FDD.

Research and development (R&D) should be done with the objective to enhance the design of FDD systems to make them more user-friendly so as to reduce the learning time required of building operators. Implementation of FDD should also be phased, starting from parts of the systems and with simpler FDD methodologies, before expanding the coverage to all types of systems and attempting to use more advanced methodologies.

When the automatic FDD is implemented to help the building operators diagnose the faults of the air conditioning systems, the detected faults and the corresponding maintenance activities should be recorded once the faults are diagnosed. This record can be stored in the BMS to eliminate paperwork and manual tracking activities (DOE, 2002).

The maintenance record should be regularly tracked and reviewed for achieving a high-level planned preventive maintenance.

9. CONCLUSION

The major findings of this research work on barriers to application of fault detection and diagnosis (FDD) techniques to air-conditioning systems in buildings in Hong Kong, and the recommended further works, are summarized in this chapter, which concludes this thesis.

9.1 Summary of works done and key findings

As outlined in Chapter 1, FDD techniques have been well developed and applied in some industries. When adopted in buildings, FDD can help building operators detect and diagnose emergence of faults in building services systems and thus allow corrective actions to be taken promptly to minimise system downtime and energy waste. However, despite that much effort has been made by researchers on development and application of FDD to building services systems and equipment, especially to heating, ventilation, air conditioning and refrigerating (HVAC&R) systems, which are the most complicated and energy intensive systems in modern buildings, application of FDD to buildings remains embryonic. This warrants the need for a study on the barriers that hinder wider application of this technology in buildings.

Unlike some other new technologies, the benefits of adopting FDD are indirect and to a certain extent uncertain, but its application will incur a significant initial cost, which can deter building owners from adopting this technology. The return on investment has to be viewed from the perspectives of the cost of wasted energy that can be avoided,

and the frequency of system breakdown and the system and equipment, maintenance, repair and replacement costs that can be reduced. As shown by the simulation prediction results reported in Chapter 2, the energy cost impacts of negative room air temperature sensor offset can be up to 0.53% of the annual air-conditioning energy use of an entire office building with 40 floors, if this fault occurred only at one of the 40 air-handling units, each serving one floor in the building. The energy penalties of other air-side system faults found in the simulation study were (also based on the air-conditioning energy use of the entire building but with the fault assumed to be present only in one of the 40 air-side systems): up to 0.91% for stuck open VAV box damper; 0.29% for supply air temperature sensor offset; 0.08% for stuck outdoor air damper; 0.39% for stuck cooling coil valve; and 0.14% for 40% leakage cooling coil valve.

As found in the simulation study, the energy penalties of 40% condenser fouling could be up to 5.05% of the total energy air-conditioning use in the building, assuming the fault occurred in all the five chillers (as it would be unrealistic to have only 1 chiller to be fouled). The energy penalties of the other chiller faults, assuming the fault occurred at only one of the chillers were: -0.16% for 40% refrigerant leakage; and 0.2% & 1.32% for 40% reduced evaporator & condenser water flow.

The results show that stuck open VAV box damper would be the most severe type of air-side system fault in VAV systems whilst reduced condenser water flow was the most severe type of chiller faults, in terms of their associated energy penalties. Such energy penalties can be minimized if FDD is applied to allow early detection and rectification of the faults.

When a building owner makes the first attempt to apply FDD, chillers should be the target because they dominate the energy use in typical commercial buildings in Hong Kong, and ensuring chillers would always operate efficiently and reliably are key objectives of operation and maintenance (O&M). Additionally, chiller faults are usually difficult to detect manually and are more expensive to rectify. Therefore, as reported in Chapter 3, a chiller plant in a tertiary education institution was selected to provide a basis for the present study. The operating records of the chillers in the plant were extracted from the building management system (BMS) and analyzed, which unveiled many problems with the BMS records, including that many data were either missing or corrupted. According to the BMS operators, the data loss was due to the lack of an uninterruptible power supply (UPS) system to provide backup electricity supply for the BMS in case of power interruption.

Lacking adequate types and amount of sensors was also encountered. For example, no flow meters were available in the primary chilled water loop in the plant to allow the chilled water flow rates through individual chillers to be measured. Consequently, performance analysis for the chillers had to be based on estimated flow rates and on the assumption that the flow rates through all running chillers were identical. Analysis of the data also unveiled that some temperature sensors were faulty, and they should be re-calibrated or replaced so as to meet requirements in ASHRAE Standard 114, for obtaining accurate enough estimates of the energy performance of the chillers.

The ways in which the O&M staff handled system malfunctioning or component failures were found to be less than satisfactory, as reported in Chapter 4. Analysis of the fault records unveiled that faulty sensors were common, including sensors of the BMS for

monitoring operation of the air-conditioning system and built-in sensors inside chillers for ensuring safe operation of the chillers. Other O&M problems found include frequent occurrence of fault alarms but the most frequent way that such alarms were handled was to reset the alarms time after time, which reflects that the chillers could have been running continually with the same fault before the fault was rectified. Even when the fault was rectified, the maintenance work was not clearly recorded, rendering it not possible to keep track with the problems, such as specific alarms for which the works were done. With such problems, it would be impossible to apply preventive maintenance to the chiller plant.

In preparation for developing a FDD algorithm for the chillers in the plant, which were twin-circuit chillers with two screw compressors per circuit, a mathematical model was developed and presented in Chapter 5. The chiller model is a semi-empirical model comprising a set of linked thermodynamic component models with coefficients that need to be evaluated based on measured chiller performance data. The chiller model includes a new evaporator model that can simulate heat transfer in the two separate compartments (one for each circuit) at the refrigerant side. The model is able to model the staging of condenser fans for keeping the condensing temperature within the temperature dead-band. Another key improvement of this model is in its ability to model changes in chiller performance due to staged operation of the separate refrigerant circuits and of compressors within each circuit.

The performance predictions of the model, including the chiller COP, the condensing temperature and the evaporating temperature, were also verified to be in good agreement with measured data over a wide range of operating conditions. For chiller COP,

more than 96% of the prediction fell within ±10% of the calculated values. For condensing temperature in circuits A and B, about 90% of predicted temperatures were within ±10% of the measured values. About 84% of the predicted evaporating temperatures in circuits A and B were within ±10% of the measured values.

For the chiller model development and verification works, large efforts had been made to check the recorded data and to extract usable data, which was very time-consuming. Therefore, it was considered not worthwhile to continue with trial FDD implementation in that chiller plant, given that the problems with the chiller performance measurement and recording functions of the BMS could not be resolved within a short period of time. Consequently, another chiller plant had to be found for continuation of the study. Nonetheless, the study with that chiller plant unveiled many barriers to application of FDD, which include insufficient, inaccurate and unsatisfactorily maintained sensors, and less than satisfactory O&M practices, which are not uncommon in chiller plants in Hong Kong.

As described in Chapter 6, three old chillers in the other chiller plant upon which the study was based had recently been replaced by newly installed chillers. Furthermore, the chiller plant had adopted a new chilled water circuit design that allows efficient capture of full- and part-load performance of chillers, which were the reasons for selecting the plant for further studies. The chillers used in this plant were simpler, water-cooled single-circuit screw chillers. Before the tests, preliminary studies were conducted to verify the measurement accuracies of the instruments available and to analyze the operating conditions of the chiller plant. The most significant plant deficiencies found included reduced chilled water flow rate and frequent occurrence of low chilled water

return temperature. With adjustments made to the control setting of the differential pressure bypass control system for the chilled water distribution system, the problem with low chilled water return temperature was alleviated. Chiller tests were finally carried out, utilizing the chilled water circuit design for expeditious collection of full- and part-load chiller performance data.

The chiller performance data were then used in the development of a chiller model for prediction of the fault-free performance of the chillers. What is more, the experimental work provided empirical evidence that the new chilled water circuit design was indeed effective in shortening the time required for capturing performance data of chillers over their entire output range. Adoption of this chilled water circuit design is, therefore, highly recommended, both in new chiller plants and when there is a change to retrofit an existing chiller plant.

As reported in Chapter 7, a simple, model-based FDD method for chillers was developed and its application demonstrated based on the second chiller plant, which took into account the limited sensors available in the chiller plant. Since the chillers are different from those described in Chapter 5 in their cooling capacity, the heat rejection medium used and their refrigerant circuit design, another chiller model was developed and validated based on measured operating data of the chillers. Due to lack of chiller operation data that covered conditions where there were no and there were known chiller faults, the fault classifiers in the FDD method were derived from a set of laboratory data produced in the ASHRAE Research Project 1043-RP.

Four chiller faults were studied, namely reduced evaporator and condenser water flows, condenser fouling and refrigerant leakage. The proposed fault classifiers involve

two performance indices, the log-mean temperature difference of the condenser and the water temperature rise across the condenser, which were shown to be able to exhibit distinctive patterns for the four kinds of chiller faults. The FDD strategy was validated based on performance data obtained from chiller tests with artificially reduced evaporator and condenser water flow rates, one at a time. The test results showed that the FDD strategy was capable of detecting the faults of reduced water flow through the condenser and the evaporator. Verification of the effectiveness of the strategy for detecting condenser fouling was based on model predictions, with the fault simulated by reducing the overall heat transfer coefficient of the condenser. The comparison showed that the FDD strategy was able to detect this fault. Unfortunately, the effectiveness of the FDD strategy in detecting refrigerant leakage could not be demonstrated until this fault arises naturally in the plant.

Commensurate with the aim of the present study, the experience gained and the observations made during the chiller plant performance evaluation and FDD application studies were carried out were reviewed to allow the barriers to successful application of FDD to be unveiled. As reported in Chapter 8, such barriers include the unavailability of refrigerant measurements, faulty sensors and missing data. According to the survey results of Comstock and Braun (1999), chiller faults of significant impacts that should be chosen as the target faults include: i) reduced condenser water flow; ii) reduced evaporator water flow; iii) condenser fouling; iv) refrigerant leakage; v) compressor internal fault; and vi) evaporator fouling. However, the last two faults were not covered by the chiller tests of the ASHRAE Project and they were excluded from the FDD strategy developed in the present study.

Furthermore, with reference to five chiller FDD studied (Comstock and Braun, 1999; Cui and Wang, 2005, Cui, 2005, Zhou et al., 2009 and Mclntosh et al.) and the FDD strategy of the present study, it was found that the measurements available from the BMS that served the studied plants would only be sufficient for detecting condenser water flow rate, condenser fouling, reduced evaporator water flow rate and refrigerant leakage, but would be insufficient for detecting the other two faults. In order to effectively detect all the six chiller faults, the minimum range of measurements that should be made available was proposed, which include chilled water supply and return temperatures, condenser water entering and leaving temperatures, refrigerant condensing and evaporating temperatures, compressor suction and discharge temperatures, sub-cooled refrigerant temperature, condensing pressure, and electrical power. They should be continually monitored and recorded by the BMS.

Other than those measuring the states of refrigerant inside chillers, the sensors for measuring chiller performance parameters for chiller FDD are already common provisions in chiller plants. For the chiller plant studied, condensing and evaporating temperatures in the chillers were available and only the other four refrigerant parameters were unavailable from the operating records of the BMS. Inspection of the chiller manufacturer's catalogues unveiled that sensors for measuring the required refrigerant parameters in the chillers were present. The reason for those measurements not being available was because they were not connected to the BMS.

Various standards and guidelines on provision of measuring instruments for chiller plants were surveyed to find out if following such standards and guidelines would ensure all the required instruments for chiller performance measurement would be made

available to facilitate FDD implementation. The ASHRAE Guideline 22P only covers instrumentation for energy performance monitoring for chillers rather than for facilitating maintenance practice or FDD, and therefore instruments for measurement of the states of refrigerant in chillers were not included. The relevant requirements of the Hong Kong Government for public buildings (ASD, 2002) are also limited and insufficient for FDD application. However, BSRIA (2004) suggested logging all the basic operational data of chillers, which include all the required data for FDD application.

Apart from the types and quantities of measuring sensors required, attention should be paid to the measuring accuracy of sensors, which should at least meet the minimum requirement stipulated in ASHRAE Standard 114-1986 (ASHRAE, 1987) or the Standard Specifications for BMS (BSRIA, 2001a). In order to ensure the accuracy of sensors is high enough for FDD implementation, it is advisable to adopt sensors with higher standards of accuracy beyond these standard guidelines. Sensors should also be regularly inspected and calibrated to ensure accurate measures would be available at all times. The period of sensor calibration recommended in various standards and guidelines could vary from 3 months to a year. However, the duration between each inspection and calibration of sensors should be reviewed and, where necessary, adjusted from time to time. Furthermore, sensor calibration work should be outsourced from a specialist service provider with adequate facilities and expertise for the calibration work.

Problems with data loss were encountered in the study, which were due to the lack of back-up power supply for the DDC panel of the BMS in case of interruption of power supply. Uninterruptible power supply system for BMS should be provided to minimize chance of data loss. The recorded data should also be periodically retrieved and securely

stored in a save medium. Sufficient data storage capacity in the BMS should also be ensured to avoid data loss.

The function of BMS should also be upgraded by including the calculation of time-interval based averaging in a fixed moving time window to ensure the data extracted are not susceptible to disturbances of transient variations in the operating conditions of chillers. Basic validity check should also be programmed into the BMS to enhance reliability of the data. These simple calculations should be the first step of implementation of FDD on-line.

The cost of implementation of FDD, including costs for providing more accurate monitoring devices and equipment, upgrading of the BMS software, calibration of existing sensors and removing the unfavorable conditions that exist in the plants, could aggregate to a high value. Training for equipping the building operators with the required knowledge or outsourcing for the needed expertise for implementation of FDD may also incur a high investment to be made by the building owners. These large investments could undermine the willingness of building owners to adopt FDD.

For widening application of FDD, FDD system supplier should provide some incentives to building owners by sponsoring demonstration projects, offering training, and providing support during installation, commissioning and O&M of the FDD system. The FDD system supplier may also provide partial financial support for the implementation work and share the energy savings achievable from successful implementation of FDD with building owners afterwards. FDD researchers should also design the system to become user-friendly such that the building operators can learn easily. Most importantly,

building owners should realize the benefits of FDD and are willing to adopt this technology in order to improve reliability of the building services systems.

9.2 Suggested further work

The experience gained in carrying out the present study points to the need for good O&M practices and, in turn, for adequate provisions in buildings that can facilitate good O&M, which are pre-requisites to application of state-of-the-art technologies (not limited to FDD) to improve performance of buildings. For example, without adequate measuring instruments and good maintenance, it would become impossible to evaluate plant performance and detect system, equipment and sensor faults and under such a state, there is no point for implementing a FDD system. A comprehensive research study to find out the present state of O&M practices in Hong Kong and the knowledge and skill gaps that need to be filled will be essential to informing development of training programmes for filling such knowledge and skill gaps. Proper guidelines on O&M practices that cover proper plant performance measurement and evaluation as well as systematic fault data collection, evaluation and rectification are also needed but are at present unavailable.

Some pilot FDD implementation projects should be carried out in buildings that are equipped with adequate quantity and quality of measuring devices and BMS with adequate monitoring and control capabilities to demonstrate the functions and benefits of FDD systems. Through the pilot projects, the effects and difficulties of implementing FDD can also be further studied, for example, on the linkage between an existing BMS and the FDD software. The problems identified and the ways in which the problems can be tackled would be valuable experience to FDD system vendors as well as building O&M personnel.

In the present study, the FDD scheme was developed based on laboratory data and verified using field data. More extensive laboratory and field tests should be carried out on a wider range of chillers such that a more comprehensive database of chiller performance data that cover both fault-free and faulty conditions can be made available to support further studies on chiller FDD, such as to facilitate identification of suitable performance indices and fault classifiers. Such studies should also be expanded to cover other building services systems and equipment to allow wider application of the FDD technology in buildings.

APPENDIX

Sensors for measurement and control of the performance of various components of an air conditioning system are very important to proper operation and maintenance (O&M) of the system. Sensors should be routinely maintained and calibrated in order to upkeep their accuracy and reliability in providing proper performance measurements of air conditioning system, which is especially important to successful implementation of automatic fault detection and diagnosis (FDD). Calibration of a sensor is carried out by comparing the sensor reading with the reading of a reference instrument, which will help ensure the measurement accuracy of the sensor will remain adequate for its intended application (BSRIA, 2001b).

This Appendix provides fundamental information pertaining to the calibration of various sensors in air-conditioning systems, which should serve as a reference for building operators on calibration works for ensuring the accuracy of sensors would be suitable for performance measurement and control as well as FDD application.

A.1 Temperature calibration

According to ANSI/ASME standard 19.3, calibration of temperature sensors is generally accomplished by subjecting it to some established fixed point temperatures, such as the melting and boiling points of standard materials. The more widely adopted calibration method is by comparing the sensor's readings with those of a more reliable temperature sensor, which has been calibrated beforehand. Calibration of temperature

sensors may be performed *in-situ* or conducted in a laboratory by removing the sensor away from the HVAC systems, as discussed in the section below.

A.2 Calibration of temperature sensors in-situ

If the required provisions have been made in an air conditioning system to allow reference sensors, such as laboratory-calibrated liquid-in glass thermometers, thermistors, thermocouples, or other reliable temperature sensors, to be placed in the system adjacent to the temperature sensors to be calibrated, and the temperature of the system can be varied over its normal operating range, then calibration can be performed *in-situ* by comparing the temperatures indicated by the reference sensors and those indicated by the sensors to be calibrated (Hurley and Schooley, 1994). In calibrating sensors in place, care should be taken to avoid disturbing the operation of the system when positioning the reference sensor used for calibration.

The instruments to be used as the reference for calibration should have calibration certificates that are less than twelve months old, unless otherwise recommended by the manufacturers (BSRIA, 2001b; CIBSE Guide H). According to ASHRAE Guideline 11, a reference sensor should have a traceable calibration at least once every year and should have an accuracy and response time equal to or better than the measuring devices under calibration. During calibration, the sensor should be calibrated at three operating points including the upper, middle and lower points in its normal operating range (ASHRAE Guideline 11; BSRIA, 2001b).

For *in-situ* calibration of a temperature sensor, the reference sensor should be placed as close as possible to the temperature sensor to be calibrated. In the case of a duct mount sensor, the reference sensor should be placed adjacent to the temperature sensor in the duct. Assess to the duct should be provided by an assess port or by drilling an appropriate hole in the appropriate location, which should be within one duct diameter from the duct temperature sensor (see Figure A.1) (ASHRAE Guideline 11). All assess ports/ holes should be closed after testing.

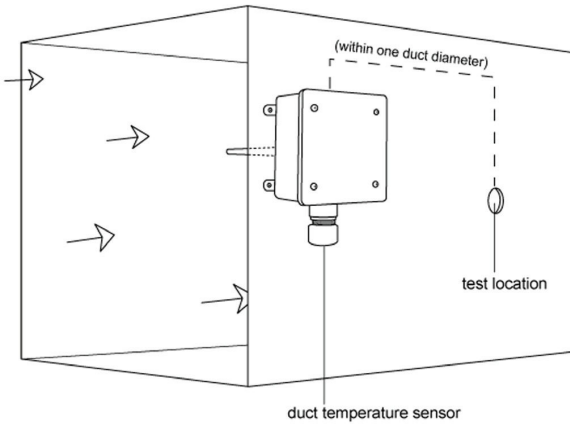

Figure A.1 Test location of calibrating duct temperature sensor

Temperature sensor in a water system can be calibrated by placing a reference sensor in a thermal well, in the vicinity of the temperature sensor. Figure A.2 shows the test port location for calibration of a water temperature sensor, which should be within 1 to 5 pipe diameter away from the temperature sensor (ASHRAE Guideline 11).

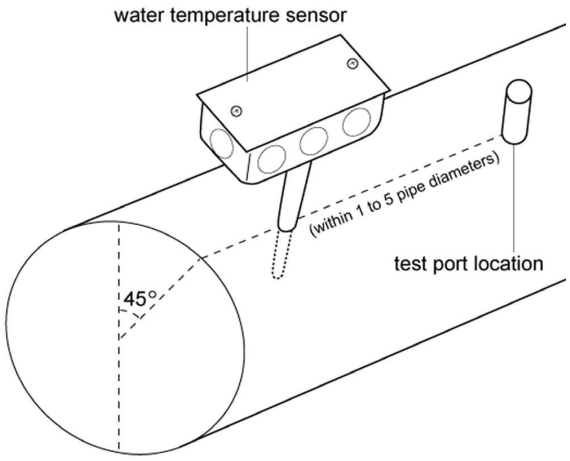

Figure A.2 Test location of calibrating water temperature sensor

A.3 Calibration of temperature sensors in laboratory

If sensors can be removed from the air conditioning system, calibration in a laboratory should be preferred to *in-situ* calibration. The sensor can be calibrated with an ice/liquid bath or a variable temperature calibration bath that meets appropriate standards and can cover the entire operating range of the senor. This method can avoid disturbing the operation of the air conditioning system.

a. Generic Double point calibration method

The ice point and boiling point of water are one of the most common and useful references for calibrating temperature sensors in a laboratory (ASTM E77-07; ASTM E644-09; BSI BS 1041-2.1 and ANSI/ASME 19.3). The procedure for calibration with this method is shown below with reference to Purdue (2007):

1. Fill a container with crushed ice, and then add water to make an ice bath.

2. Place the temperature sensor in the ice bath. Make sure the sensing region of the temperature sensor is immersed and the sensor does not touch the container.
3. Wait for one minute until the reading of the temperature sensor becomes stabilized.
4. Measure the ice bath temperature (A) with the temperature sensor and compare the reading with ice point temperature of water (C) 0^{o}C.
5. Heat distilled water until bubbles arise to prepare a boiling water bath.
6. Place the temperature sensor in the water bath.
7. Wait for one minute again and measure the boiling water temperature (B) with the temperature sensor and compare the reading with the boiling water temperature (D) calculated using the following equation (Purdue, 2007).

$$T = 100 - 0.0003048 \times h$$

Where T is the boiling water temperature in ^{o}C and h is the elevation in meter.

8. Calculate $X = B - A$
9. Compute $Y = D - C$
10. Calculate $Z = \frac{Y}{X}$
11. Record $S = C - A \times Z$
12. Finally, the calibration is complete and the actual temperature of the temperature sensor can be computed using the equation:

$$T = Z \times \text{Temperature reading} + S$$

b. Variable Temperature Calibration Bath

According to ASTM E2488, a controlled temperature fluid bath system will incorporate the following components: a fluid medium; a mechanical design that provides for containment and circulation of the fluid; a monitoring thermometer; a temperature control unit; and elements that provide for heating, cooling or both. There are many commercially available controlled temperature baths. These baths operate from as low as -100 °C to as high as +550 °C; although no single bath system is capable of operation over that entire range. The design of each individual bath will create practical limits for the working temperature range. These limits are determined by considering the minimum and maximum temperature ratings for each of the components in the bath system.

One should carefully review the bath manufacturer's literature to be certain that the bath system is suitable for the intended calibration temperature range and the types of thermometers to be tested. Figure A.3 shows the design of a controlled temperature fluid bath system.

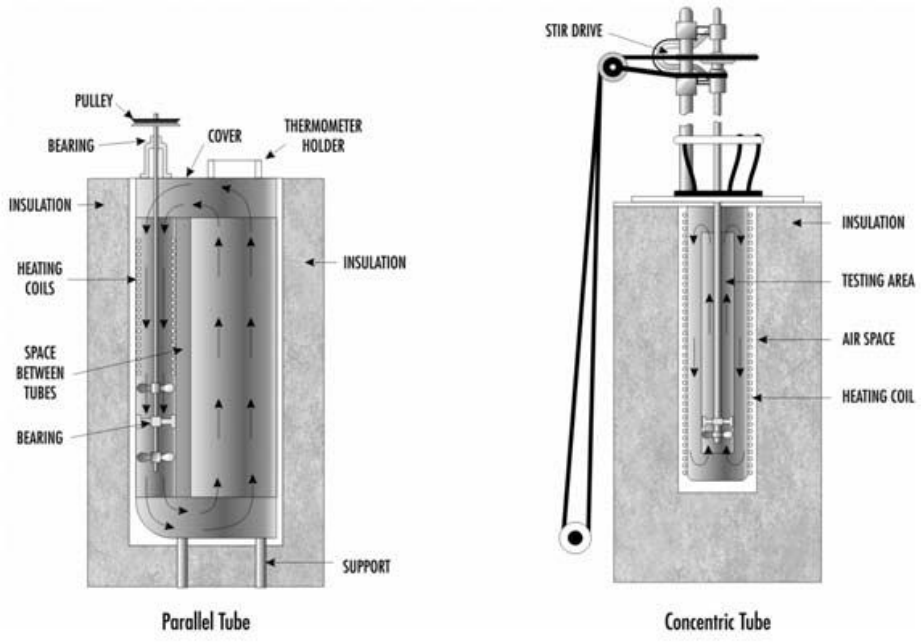

Figure A.3 Variable Temperature Calibration Bath

The procedure of conducting calibration of a temperature sensor with a controlled temperature bath is as described below:

1. Set the temperature bath to control at the desired calibration temperature and allow sufficient time for the bath system to reach thermal equilibrium.

2. Place a reference temperature sensor in the center of the desired working space of the bath container. After placing the reference sensor in the bath, the bath shall again be allowed time to reach thermal equilibrium.

3. Place the temperature sensor to be calibrated in the bath. After placing the sensor in the bath, the bath shall again be allowed time to reach thermal equilibrium. Note that for best results, the thermal response time of the reference sensor should be as close as possible to that of the temperature sensor subject to calibration.

4. Record the relative difference in output readings between the reference sensor and the temperature sensor being calibrated.

5. The procedure is repeated by adjusting the calibration temperature. It is recommended that a temperature sensor should be calibrated either at a minimum of five evenly spaced temperatures in the normal operating range of the sensor (BSI BS 1041-2.1) or at the minimum, typical and the maximum points in the operating range of the sensor (ASHRAE Guideline 14). The uncertainty of the measuring device can be computed with the procedure stated in Section A.12.

A.4 Flow calibration

Although, flow rate measurement is very important to estimation of cooling load and energy use of an air conditioning system, it is one of the most unreliable measurements. This section summarizes the calibration methods for flow meters in air-conditioning systems.

A.5 Calibration of flow meters in-situ

Same as temperature sensors, calibration of a flow meter is to be performed by comparing the readings of the flow meter and those indicated by a reference sensor (ASHRAE Guideline 11). The instruments used for flow meter calibration should have calibration certificates and should have an accuracy and response time equal to or better than the flow meter under calibration (BSRIA, 1998, 2001b and ASHRAE Guideline 11).

Calibration of a duct mount flow meter should be done by traversing a pilot tube or propeller anemometer across the air stream at a location within one duct diameter away from the flow sensor, as shown in Figure A.4. Other requirements for air flow using a pilot tube are given in detail in ASHRAE Standard 111 and BSRIA (1998). The measurement should be checked over a range of at least five flow rates in the operating range of the flow meter (ASHRAE Guideline 14).

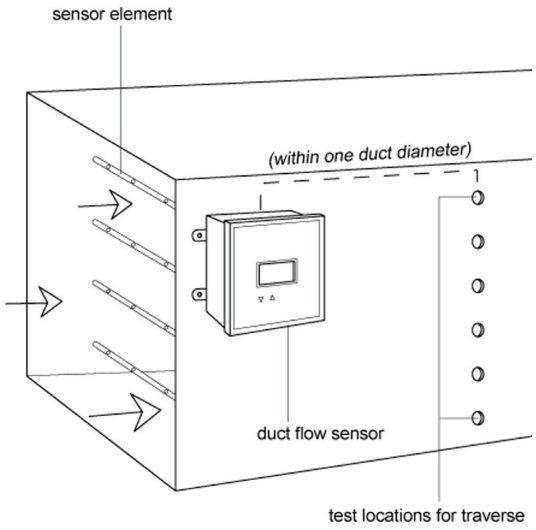

Figure A.4 Test location of calibrating duct flow meter

According to ASHRAE Guideline 14, a portable ultrasonic flow-meter (UFM) can be used to calibrate water flow meters on site. When conducting calibration, the flow meter should be calibrated at three operating points including the upper, middle and lower points of its normal operating range (ASHRAE Guideline 14).

UFM is a velocity dependant device and is highly vulnerable to variations in flow profile and installation error. Since a significant variation of flow profile will occur when it is at 10 pipe diameters downstream of an elbow, it is suggested that the acceptable deviation between the calibrated flow-meter and the UFM should be restricted to 5% for applications with less than 10 pipe diameters of straight length pipe upstream of the UFM. If the UFM cannot be located adjacent to the flow sensor, the UFM can be placed in the location of the flow meter being tested for verifying the accuracy of the flow meter (ASHRAE Guideline 11).

A.6 Calibration of flow meters in laboratory

As suggested by Baker and Hurley (1994) and Fung et al. (1987), direct calibration is one of the effective means for calibration of flow meters in laboratory. This method is usually accomplished by means of a weight tank. The weight tank method is mainly based upon two standards (ISO 4185 and Baker and Hurley, 1994). The method consists of two measuring approach, namely static method and dynamic method, and their set-ups are as shown in Figures A.5 and A.6 respectively. Detailed procedures for these calibration methods are omitted, as building operators are seldom directly involved in such tests in an accredited laboratory.

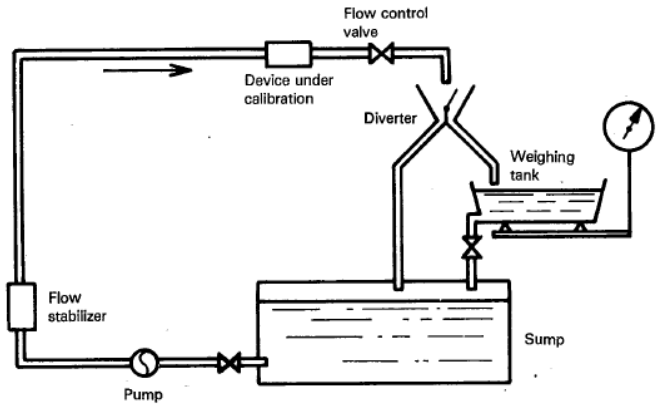

Figure A.5 Calibration of weight tank with static method

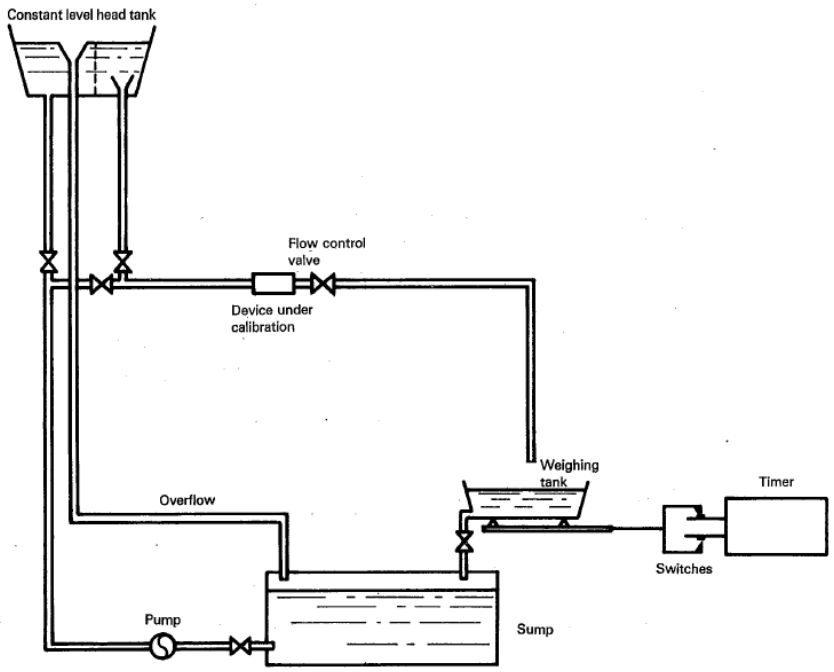

Figure A.6 Calibration of weight tank with dynamic method

A.7 Pressure calibration

The measurement of pressure of working fluids in air conditioning systems is carried out for various purposes, including monitoring if the working pressure stays within safety limits or within the normal range; for automatic control of equipment operation; for evaluation of the thermodynamic state of the working fluid or the pressure rise/drop across a system component or equipment; and as a means for measuring the flow rate of the working fluid. The measured pressure may be gauge pressure or absolute pressure. The gauge pressure is pressure above atmospheric pressure while the absolute pressure is the summation of gauge pressure and atmospheric pressure. Differential pressure is the pressure difference between two different points.

A.8 Calibration of pressure sensors in-situ

Testing of pressure sensors in-situ should be conducted by comparing the sensors with the calibrated testing sensors under field operating conditions (ASHRAE Guideline 11). The instruments to be used for calibration of pressure sensors should have calibration certificates and should have an accuracy and response time equal to or better than the measuring devices under calibration (BSRIA 2001b; ASHRAE Guideline 11). When conducting calibration, the sensor should be calibrated at three operating points including the upper, middle and lower points of its normal operating range (ASHRAE Guideline 11; BSRIA 2001b)

According to ASHRAE standard 41.3, calibration of pressure sensors in-situ should consider the measuring system as a whole. The pressure transducer, the signal conditioner and the BMS reading should be adjusted until the BMS output matches with the corresponding input value. In order to achieve maximum accuracy, the range of input values during calibration should be close to those in actual operation.

Testing of pressure sensor in-situ can be conducted by placing the reference sensor adjacent to the pressure sensor. For example, calibration of a duct mount air pressure sensor can be done by placing a water tube or an electronic manometer or a mechanical pressure gauge at a location within one diameter of the air duct away from the duct pressure sensor, as shown in Figure A.7 (ASHRAE Guideline 11). The readings between the pressure sensor and reference sensor can be compared for calibration.

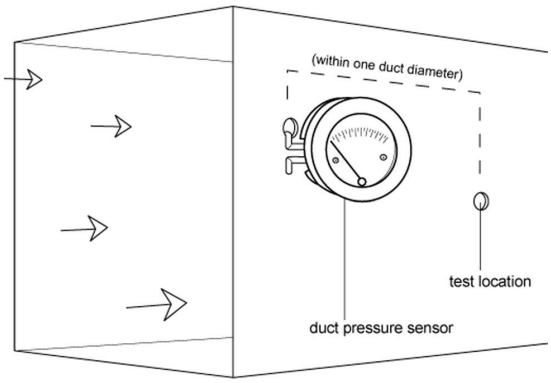

Figure A.7 Test location for calibration of duct pressure sensor

ASHRAE Guideline 11 states that for a constant pressure system, the pressure sensor for measuring the water pressure in a pipe is usually verified by removing the sensor and inserting a reference sensor for testing the accuracy of the pressure sensor. For variable pressure system, duplicate ports are required for the pressure sensor and the reference sensor to be placed in the water pipe to measure the pressure at the same time such that they can be compared on equal basic.

A.9 Calibration of pressure sensors in laboratory

According to ASHRAE Guideline 14, gauge pressure calibration can be undertaken with dead weight testers in laboratory. If the pressure sensor is designed for reading absolute pressure, an atmospheric pressure gauge is required and the measured atmospheric pressure should be added to the applied reading for calibration. At least five points, including the low and the high ends of the instrument range should be selected for calibration.

Figure A.8 shows the basic elements of a deadweight tester (Dally et al., 1993). Such methods are usually employed as standard for the calibration of pressure gauges or transducers in laboratory. The calibration pressures are generated in the deadweight testers by adding standard weights to the piston tray. A screw-driven plunger is forced into the hydraulic oil chamber to reduce its volume and to lift the piston-weight assembly. The pressure is slowly built up until the piston and weights are seen to "float" at which point the gauge pressure must equal the deadweight supported by the piston divided by the piston area. Comparisons are made between the calibrated pressures and the pressures indicated by the transducer in order to verify the accuracy of the transducer.

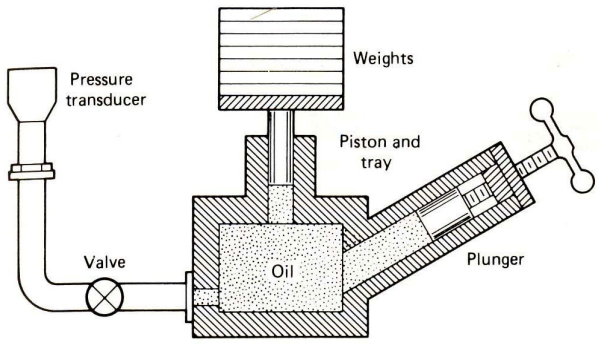

Figure A.8 Deadweight tester for calibration of pressure transducer

A.10 Electrical measurement calibration

Electrical measurements are important measurements for evaluation of the energy efficiency of building services equipment. Electrical measurements typically include measuring voltage, current, power factor and electrical power, and instruments for their measurement are generally quite robust and usually are more reliable than other types of sensors in air-conditioning systems. *In-situ* calibration can be done by direct comparison

of meter readings with those from a more accurate power analyzer (ANSI/ASME PTC 19.6; ASHRAE Guideline 11). Good quality power analyzers with high precision are available in the market which should serve well the purpose for typical air-conditioning systems. Where required, laboratory calibration may be used and the required procedures are well documented in various standards, such as ANSI/ASME PTC 19.6, ANSI C12.10, and BSI BS 89. However, this would normally involve sending the meters to an accredited laboratory for calibration as sophisticated equipments would be required for highly accurate measurements.

A.11 Calibration of humidity sensors

Although humidity measurement is also important to quantification of air-conditioning system performance, it is applicable only to air-side systems and is not required for chiller performance monitoring and FDD, whilst the latter is the theme of the present study. Therefore, calibration of humidity sensor is only briefly discussed here. Measurement of humidity of moist air entails measuring the dry bulb temperature and one other psychometric property of the moist air, which may be web bulb temperature or dew point temperature. However, measurement of air humidity by electronic sensors usually relies on measurement of changes in the electric property of a material in response to changes in the humidity of the air surrounding the material, such as its electric resistance, reactance, capacitance or conductivity or elongation. Alternatively, cyclic chilled mirror sensors can be used to measure dew point temperature accurately by detecting the temperature at which condensation just starts to occur, and thus can be used as a reference sensor. The relevant calibration methods are also well documented (see e.g. ASHRAE Guideline 14; Hyland and Hurley, 1983; Hurley, 1985; Huang, 1991).

A.12 Measurement uncertainty

After calibration has been carried out with a sensor, whether or not the sensor is able to provide accurate measurements can be told. Where there are departures of the sensor readings from those of the reference sensor, a calibration curve may be established to allow more accurate measurements to be determined from the readings indicated by the sensor. This will allow the bias error (also called systematic error) component of the measurement uncertainty of the sensor, which is fixed for each measurement, to be minimized. However, the precision error (also called random error), which is the other component of the measurement uncertainty of the sensor, cannot be removed through calibration, but could be made known.

In order to estimate the measurement uncertainty of a sensor in a calibration process, it is necessary to know the measurement uncertainty of the reference sensor itself and to obtain sufficient measurements for determination of the measurement uncertainty of the sensor under concern. The required measurements for this purpose, however, may take considerable time and effort to undertake. Reference can be made to ANSI/ASME MFC-2M on methods for determination of the uncertainty of measurement using calibration data.

Reference

1. Anderson S.A. and Dieckert J.C., 1990, On site chiller testing, *ASHRAE Journal* 32: 54-58.

2. ANSI/ASME PTC 19.3, 1974, Temperature Measurement, *ASME Performance Test Code 19.3*

3. ANSI/ASME PTC 19.6, 1955, Electrical Measurements in Power Circuits Instrument and Apparatus, *ASME Performance Test Code 19.6*

4. ANSI/ASME MFC-2M, 1983, Measurement Uncertainty for Fluid Flow in Closed Conduits, *ASME Standard*

5. ANSI C12.10, 1978, American National Code for Watt-hour meters, *The Association of Electrical and Medical Imaging Equipment Manufacturers*

6. ARI. Standard 550, 1998, Centrifugal or rotary screw waterchilling packages. Arlington, Va.: *Air-Conditioning and Refrigeration Institute.*

7. Arora C.P., 1981, Refrigeration and Air Conditioning, a book published by *Tata McGraw-Hill Publishiong Company Limited*.

8. ASD, 2002, Testing and commissioning procedure No 1 For Air–conditioning, Refrigeration, Ventilation and Central Monitoring & Control System Installation In Government Buildings Hong Kong, Building Services Branch, *Architectural Services Department.*

9. ASHRAE, ASHRAE Guideline 11-2009- Field Testing of HVAC Controls Components, *American Society of Heating, Refrigerating and Air-conditioning Engineers*, Inc., USA, 2009.

10. ASHRAE, ASHRAE Guideline 22P-2007- Proposed New Guideline 22, Instrumentation for Monitoring Central Chilled Water Plant Efficiency, *American Society of Heating, Refrigerating and Air-conditioning Engineers*, Inc., USA, 2007.

11. ASHRAE, ASHRAE Guideline 14-2002- Measurement of Energy and Demand Savings, *American Society of Heating, Refrigerating and Air-conditioning Engineers*, Inc., USA, 2002.

12. ASHRAE, ASHRAE Standard 41.3-1989- Standard Method for Pressure Measurement *American Society of Heating, Refrigerating and Air-conditioning Engineers*, Inc., USA, 1989.

13. ASHRAE, ASHRAE Standard 111-2008 –Measurement, Testing, Adjusting and Balancing of Building HVAC Systems, *American Society of Heating, Refrigerating and Air-conditioning Engineers*, Inc., USA, 2008.

14. ASHRAE, ASHRAE Standard 114-1986 – Energy Management and Control Systems Instrumentation, *American Society of Heating, Refrigerating and Air-conditioning Engineers*, Inc., USA, 1987.

15. ASHRAE, ASHRAE Standard 180-2006 – Proposed New Standard 180, Standard Practice for Inspection and Maintenance of Commercial Building HVAC System, *American Society of Heating, Refrigerating and Air-conditioning Engineers*, Inc., USA, 2006.

16. ASHRAE Handbook, 2008, HVAC Systems and Equipment, *American Society of Heating, Refrigerating and Air-conditioning Engineers*, Inc. (41) 41.3.

17. ASTM E77-07, 2007, Standard Test Method for Inspection and Verification of Thermometers, *ASTM Test Code*

18. ASTM E644-09, 2009, Standard Test Method for Testing Industrial Resistance Thermometer, *ASTM Test Code*

19. ASTM E2488, 2009, Standard Guide for the preparation and evaluation of liquid bath for temperature calibration by comparison, *ASTM Test Code*

20. Bailey M.B., 1998, The Design and Viability of a Probabilistic Fault Detection and Diagnosis Method for Vapor Compression Cycle Equipment, Ph.D. Thesis, *School of Civil Engineering*, University of Colorado.

21. Baker D.W. and Hurley C.W., 1984, On-site Calibration of Flow Metering Systems Installed in Buildings, *NBS Building Science Series 159*

22. Bourdouxhe J.P., Grodent M. and Lebrun J.J., 1997, HVAC1 Toolkit: Algorithms and Subroutines for Primary HVAC System Energy Calculations, *The American Society of Heating, Refrigerating and Air Conditioning Engineers*.

23. Breuker M.S. and Braun J.E., 1998a, Common Faults and their Impacts for Rooftop Air Conditioners, *International Journal of Heating, Ventilating and Air conditioning and Refrigerating Research* 4 (4): 401-425.

24. Breuker M.S. and Braun J.E., 1998b, Evaluating the performance of a fault detection and diagnostic system for vapor compression equipment, *International Journal of Heating, Ventilating, Air Conditioning and Refrigerating Research* 4(3):303-318.

25. Browne M.W. and Bansal P.K., 1998, Steady-state model of centrifugal liquid chillers, *International Journal of Refrigeration* 21(5): 343-358.

26. Browne M.W. and Bansal P.K., 2001, Different modelling strategies for in-situ liquid chillers, Proceedings of the Institute of Mechanical Engineers Part A: J. *Power and Energy* 215: 357-374.

27. BSI BS 1041-2.1, 1985, Temperature measurement –Part 2 Expansion thermometers-Liquid-in-glass thermometers, *British Standard*

28. BSI BS 89, 1977, Specification for Direct acting indicating electrical measuring instruments and their accessories, *British Standard*

29. BSRIA, 1998, The Commissioning of Air Systems in Buildings, *Building Services Research and Information Association.*

30. BSRIA, 2001a, Standard Specifications for BMS, Application Guide AG 9/2001, *Building Services Research and Information Association.*

31. BSRIA, 2001b, The Effective BMS, A guide to improving system performance, Application Guide AG 10/2001, *Building Services Research and Information Association.*

32. BSRIA, 2003, BMS Maintenance Guide, plus a model maintenance specification, A BSRIA Guidance Note BG4/2003, *Building Services Research and Information Association.*

33. BSRIA, 2004, Business Focused Maintenance, guidance and sample schedules BG3/2004, *Building Services Research and Information Association.*

34. California Energy Commission, 2002, Technical Report*:* Potential of On-line Simulation for Fault Detection and Diagnosis in Large Commercial Buildings with Built-up HVAC Systems, Energy Systems Laboratory, *University of Nebraska & Texas A&M University.*

35. Carling P., 2002, Comparison of three fault detection methods based on field data of an air-handling unit, *ASHRAE Transactions* 108(1): 904-921.

36. Castro N., 2002, Performance evaluation of a reciprocating chiller using experimental data and model predictions for fault detection and diagnosis, *ASHRAE Transactions* 108(1):889-903.

37. Casto N.S., Schein J., Park C. and Galler M.A.,2003, Results from Simulation and Laboratory Testing of Air Handling Unit and Variable Air Volume Box Diagnostic Tools, *Architectural Energy Corporation*, Boulder, Colorado.

38. Casto N.S. and Nejad H.N., 2005, CITE-AHU, an automated commissioning tool for air-handling units, *National Conference on Building Commissioning*, May 4-6, 2005.

39. Chan K.T., Chow W.K., 1998, Energy impact of commercial-building envelopes in the sub-tropical climate, Applied Energy 60 (1): 21-39.

40. Chan K.T. and Yu F.W., 2002, Part load efficiency of air cooled multiple chiller plant, *Building Services Engineering Research and Technology* 23 (1): 31-41.

41. Chan K.T. and Yu F.W., 2004, Optimum Setpoint of Condensing Temperature for Air-Cooled Chillers, *HVAC&R Research* 10: 113-127.

42. Chan K.T. and Yu F.W., 2006, Thermodynamic-behaviour model for air-cooled screw chillers with a variable set-point condensing temperature, *Applied Energy* 83: 265-279.

43. CIBSE, 1990, Building Services Maintenance Management, Technical Memoranda TM17:1990, *The Chartered Institution of Building Services Engineers.*

44. CIBSE, 1991, Standard Maintenance Specification for Mechanical Services in Building VII-Ventilating and Air Conditioning, *The Chartered Institution of Building Services Engineers.*

45. CIBSE, 2000, Guide H, Building Control System, *The Chartered Institution of Building Services Engineers.*

46. Clark D.R., 1985, HVACSIM+ Building Systems and Equipment Simulation Program Reference Manual, NBSIR 84-2996, *NIST.*

47. Comstock M.C., and Braun J.E., 1999, Development of analysis tools for the evaluation of fault detection and diagnostics for chillers, HL 99-20, Report #4036-3, *ASHRAE Research Project 1043*.

48. Crawley D.B., Lawrie L.K., Winkelmann F.C., Buhl W.F., Huang Y.J., Pedersen C.O., Strand R.K., Liesen R.J., Fisher D.E., Witte M.J. and Glazer J., 2001, EnergyPlus: creating a new-generation building energy simulation program, *Energy and Buildings* 3: 319-331.

49. Cui J., 2005, A Robust Fault Detection and Diagnostics Strategy for Centrifugal Chillers, Ph.D. Thesis, *Department of Building Services Engineering*, Hong Kong Polytechnic University, Hong Kong.

50. Cui J. and Wang S.W., 2005, A model-based online fault detection and diagnosis strategy for centrifugal chiller systems, *International Journal of Thermal Sciences* 44(10):986-999.

51. Dally J.W., Riley W.F. and McConnell K.G., 1993, Instrumentation for Engineering Measurements, *John Wiley & Sons*.

52. Dexter A.L. and Benourets M., 1996, A Generic Approach to Identifying Faults in HVAC Plants, Fault Detection and Diagnosis for HVAC Systems, *ASHRAE Data Bulletin* 12(2), No. 2:33-39.

53. DOE, 2002, Operations & Maintenance Best Practices, A Guide to Achieving Operational Efficiency, *Department of Energy*, US.

54. EMSD, 2008, Scheme for Wider Use of Fresh Water in Evaporative Cooling Towers for Energy-efficient Air Conditioning Systems, *Electrical and Mechanical Services Department*, the Hong Kong SAR Government.

55. Etabloc, 2007, Etabloc type series booklet of pump catalogue, *KSB Pumps and Valves Limited*

56. Friedman H. and Piette M.A., 2001a, Comparative guide to emerging diagnostic tools for large commercial HVAC systems, *Lawrence Berkeley National Laboratory Report*, LBNL-47629, May 2001.

57. Friedman H. and Piette M.A., 2001b, Comparison of emerging diagnostic tools for large commercial HVAC systems, *Proceedings of the 9th National Conference on Building Commissioning*, May 9-11, 2001, Cherry Hill, NJ, LBNL-47698.

58. Friedman H. and Piette M.A., 2001c, Evaluation of emerging diagnostic tools for commercial HVAC systems, *International Conference for Enhancing Building Operations*, July 2001, Austin, TX.

59. Fung H.K., Chuen C.W., Ip W.M., Leung T.P. and Chick W.K., 1987, Instrumentation and Control, Published for the Department of Mechanical and Marine Engineering, *Hong Kong Polytechnic*

60. Glass A.S., Gruber P., Roos M. and Todtli J., 1995, Qualitative model-based fault detection in air-handling units, *IEEE Control Systems Magazine* 15(4):11-22.

61. Gordon J.M. and Ng H.T., 1995, Predictive and diagnostic aspects of universal thermodynamic model for chillers, *International Journal of Heat and Mass Transfer* 20:1149-1159.

62. Grimmelius H.T., Woud J.K. and Been G., 1995, On-line failure diagnosis for compression refrigeration plants, *International Journal of Refrigeration* 18 (1):31-41.

63. Haves P., 1999, Overview of diagnostic methods, *Proceedings of the Workshop on Diagnostics for Commercial Building: From Research to Practice*, June 16-17, 1999, Pacific Energy Center, San Francisco (http://poet.lbl.gov/diagworkshop/proceedings).

64. Haves P., Salsbury T.I. and Wright J.A., 1996, Condition Monitoring in HVAC Subsystems Using First Principles Models, *ASHRAE Transactions* 102 (1): 519-527.

65. Heinemeier K., 1998, Marketability requirements for fault detection and diagnostics in commercial buildings, *Proceedings of the ACEEE 1998 Summer Study on Energy Efficiency in Buildings*, Washington D.C, August 1998.

66. Hogg R.V., 1993, Probability and statistical inference, *Maxwell Macmillan International*.

67. House J.M., Lee W.Y. and Shin D.R., 1999, Classification Techniques for Fault Detection and Diagnosis of an Air-Handling Unit, *ASHRAE Transactions* 105 (1): 1087-1097.

68. House J.M., Vaezi-Nejad H., and Whitcomb J.M., 2001, An expert rule for fault detection in air handling units, *ASHRAE Transactions* 107(1):858-871.

69. Huang P., 1991, Humidity measurements and calibration standards, *ASHRAE Transactions* 97(2): 278-304

70. Hurley C.W., 1985, Measurement of temperature, humidity and fluid flow- Field data acquisition for building and equipment energy-use monitoring, *ORNL Report*

71. Hurley C.W. and Schooley J.F., 1984, Calibration of temperature measurement systems installed in buildings, *NBS Building Science Series 153*

72. Hyland R.W. and Hurley C.W., 1983, General guidelines for the on-site calibration of humidity and moisture control system in buildings, *NBS Building Science 157*

73. International Energy Agency (IEA), Annex 25, Real Time Simulation of HVAC Systems for Building Optimization, Fault Detection and Diagnostics, Technical Synthesis Report, *Energy Conservation in Buildings and Community Systems*.

74. ISO 4185, 1980, Measurement of liquid flow in closed conduits-weighting method, *International Standard*

75. Jia Y., 2002, Model-Based Generic Approaches for Automated Fault Detection, Diagnosis, Evaluation (FDDE) and for Accurate Control of Field-Operated Centrifugal Chillers, PhD Thesis, *Faculty of Drexel University*.

76. Jia Y. and Reddy T.A., 2003, Characteristic physical parameter approach to modeling chillers suitable for fault detection, diagnosis and evaluation, *ASME Journal of Solar Energy Eng*. 125:258-65.

77. Katipamula S. and Brambley M.R., 2005a, Methods for fault detection, diagnostics and prognostics for building Systems – A review, Part I, *International Journal of heating, Ventilating, Air Conditioning and Refrigerating Research* 11(1): 3-25.

78. Katipamula S. and Brambley M.R., 2005b, Methods for fault detection, diagnostics and prognostics for building Systems – A review, Part II, *International Journal of heating, Ventilating, Air Conditioning and Refrigerating Research* 11(2): 169-187.

79. Katipamula S., Pratt R.G., Chassin D.P., Taylor Z.T., Gowri K. and Brambley M.R., 1999, Automated fault detection and diagnostics for outdoor-air ventilation systems and economizers: methodology and results from field testing, *ASHRAE Transactions* 105 (1): 555-567.

80. Kao J.Y. and Pierce E.T., 1983, Sensor Errors: Their Effect on Building Energy Consumption, *ASHRAE Journal* 25 (12):42.

81. Kirkup L. and Frenkel R.B., 2006, An introduction to uncertainty in measurement using the GUM (Guide to the expression of uncertainty in measurement), *UK: Cambridge University Press*.

82. Kempiak M.J. and Crawford. R.R., 1992, Three-zone, steady-state modelling of a mobile air-conditioning condenser, *ASHRAE Transactions* 98(1): 475-488.

83. Lai J.H.K., Yik F.W.H. and Jones P., 2004, Addressing the knowledge gap in outsourcing for operation and maintenance work for sustainable buildings, *The 2004 CIBSE Annual Conference on Delivering Sustainable Construction*, 29-30 September 2004, London, CIBSE, UK.

84. Lee W.Y., Park C. and Kelly G.E., 1996a, Fault Detection in an Air-Handling Unit using Residual and Recursive Parameter Identification Methods, Fault Detection and Diagnosis for HVAC Systems, *ASHRAE Data Bulletin* 12(2):11-22.

85. Lee W.Y., Park C. and Kelly G.E., 1996b, Fault Diagnosis of an Air Handling Unit using Artificial Neural Networks, Fault Detection and Diagnosis for HVAC Systems, *ASHRAE Data Bulletin* 12(2):23-32.

86. Lee W.Y., House J.M. and Shin D.R., 1997, Fault Diagnosis and Temperature Sensor Recovery for an Air-Handling Unit, *ASHRAE Transactions* 103(1):621-633.

87. Lee W.L., Yik F.W.H and Jones P., 2003, A strategy for prioritizing interactive measures for enhancing energy efficiency of air-conditioned buildings, *Energy* 28: 877-893.

88. Leverenz D.J. and Bergan N.E., 1983, Development and validation of a reciprocating chiller model for hourly energy analysis programs, *ASHRAE Transactions* 89(1a): 156-174.

89. Li H. and Braun. J.E., 2003, An improved method for fault detection and diagnosis applied to packaged air conditioners, *ASHRAE Transactions* 109(2):683-692.

90. Linder R. and Dorgan C.B., 1997, VAV systems work despite some design and application problems, *ASHRAE Transactions* 103 (2): 807-813.

91. Mansson, 1998, Compulsory inspection of ventilating systems. *National board of housing, building and planning*.

92. Menzer M., 1997, Studies Show How Air- Conditioning Equipment Efficiency Has Increased, *Proceedings of International Climate Change Conference*, Baltimore.

93. Mclntosh I.B.D., Mitchell J.W. and Beckman W.A., 2000, Fault detection and diagnosis in chillers-Part 1: Model development and application. *ASHRAE Transactions* 106(2):268-282.

94. Peitsman H.C. and Soethout L.L., 1997, ARX models and real-time model based diagnosis. *ASHRAE Transactions* 103(1):657-671.

95. Peitsman H.C. and Bakker V.E., 1996, Application of black-box models to HVAC systems for fault detection. *ASHRAE Transactions* 102(1): 628-640.

96. Piette M.A., Khalsa S., Haves P., Rumsey P., Kinney K.L., Lock L.E., Sebald A., Chellapilla K. and Shockman C., 1999, Performance Assessment and Adoption Process of an Information Monitoring and Diagnostic System Prototype, the *California Energy Commission*, LBNL44453, October 1999.

97. Piette M.A., Khalsa S., Rumsey P., Kinney K., Lock L.E., Sebald A. and Shockman C.,1998, Early Results and Fields Tests of an Information Monitoring and Diagnostic System for Commercial Buildings, the *California Energy Commission and the California Institute for Energy Efficiency*, LBNL 42338, September 1998.

98. Pratt R.G., Bauman N. and Katipamula S., 2002, New Technology Demonstration of the Whole Building Diagnostician at the Federal Aviation Administration-Denver Airport, *Pacific Northwest National Laboratory*, PNNL-14157, December 2002.

99. Purdue, 2007, Selection and Maintenance of Temperature Measuring Devices, *Purdue University*

100. Qin J.Y. and Wang S.W., 2005, A fault detection and diagnosis strategy of VAV air conditioning systems for improved energy and control performances, *Energy and Buildings* 2005:1-14.

101. Reddy T.A., 2006, Evaluation and assessment of fault detection and diagnostic methods for centrifugal chillers- phase II, Final project report of *ASHRAE Research Project RP-1275*.

102. Reddy T.A., 2007a, Development and Evaluation of a Simple Model-Based Automated Fault Detection and Diagnosis (FDD) Method Suitable for Process Faults of Large Chillers, *ASHRAE Transactions* 113 (2):27-39.

103. Reddy T.A., 2007b, Application of a Generic Evaluation Methodology to Assess Four Different Chiller FDD Methods (RP-1275), *HVAC&R Research* 13(5):711-729.

104. Richard D., Kratz F., Ragot F., Loisy F. and Germain J.L., 1997, Detection, Isolation, and Identification of Sensor Faults in Nuclear Power Plants, *IEEE Transactions on Control System Engineering* 5(1): 42-60.

105. Rossi T.M., 1995, Detection, diagnosis and evaluation of faults in vapor compression cycle equipment. PhD thesis, *School of Mechanical Engineering*, Purdue University, West Lafayette, Indiana.

106. Rossi T.M., 1999, Deployment of diagnostics for commercial buildings: new business opportunities, *Proceedings of the Workshop on Diagnostics for Commercial Building: From Research to Practice*, June 16-17, 1999, Pacific Energy Center, San Francisco (http://poet.lbl.gov/diagworkshop/proceedings).

107. Rossi T.M. and Braun J.E., 1997, A Statistical Rule Based Fault Detection and Diagnostic Method for Vapor Compression Air Conditioners, *International Journal of Heating, Ventilating and Air Conditioning and Refrigerating Research* 3 (1):19-37.

108. Shockman C. and Piette M.A., 2000. Innovation adoption process for third party property management companies, *Proceedings of the ACEEE 2000 Summer Study on Energy Efficiency in Buildings*, August 2000.

109. Simani S., Fantuzzi C. and Patton R., 2003, *Model Based Fault Diagnosis in Dynamic Systems Using Identification Techniques*. Spring-Verlag London Limited.

110. SkyForce, 2008, Replacement of Phase 3B chiller plant, *Operation and maintenance manual.*

111. Solati B., 2002, Computer modelling of the energy performance of screw chiller. MSc thesis, Department of Building, Civil and Environmental Engineering, Concordia University. Montreal, Quebec: *Concordia University Press.*

112. Sreedharan P., 2001, Evaluation of Chiller Modelling Approaches and their Usability for Fault Detection, *Lawrence Berkeley National Laboratory*: 1-88.

113. Sreedharan P. and Haves P., 2001, Comparison of chiller models for use in model-based fault detection , *International Conference for Enhanced Building Operations (ICEBO)*, organized by Texas A&M University, Austin, TX.

114. Stoecker W.F. and Jones. J.W., 1982, Refrigeration and Air Conditioning, 2nd Ed. *McGraw-Hill*.

115. Stouppe D.E. and Lau Y.S., 1989, Air Conditioning and Refrigeration Equipment Failures, *National Engineer* 93(9): 14-17.

116. Stylianou M., 1996, Chillers and Heat pumps, in Building Optimization and Fault Diagnosis Source Book, IEA Annex 25, *VIT Building Technology*: 66-73.

117. Stylianou M., 1997, Classification functions to chiller fault detection and diagnosis, *ASHRAE Transactions* 103(1):645-648.

118. Stylianou M. and Nikanpour M., 1996, Performance Monitoring, Fault detection, and Diagnostics of Reciprocating Chillers, *ASHRAE Transactions* 102 (1):615-627.

119. Wang S.W., Wang J. and Burnett J., 2000, Mechanistic model of centrifugal chillers for HVAC system dynamics simulation, *Building Services Engineering Research & Technology* 21(2): 73-83.

120. Wang S.W. and Cui J., 2005, Sensor fault detection, diagnosis and estimation for centrifugal chiller systems using principal component analysis method, *Applied Energy* 82: 197-213.

121. Wang S.W. and Cui J., 2006, A robust fault detection and diagnosis strategy for centrifugal chillers, *HVAC&R Research* 12(3):407-428.

122. Wylen G.J.V, Sonntag R.E. and Borgnakke C., 1994, , Fundamentals of Classical Thermodynamics, Wiley International Edition

123. Yik F.W.H., 1995, Sensor location for variable-volume-flow control at the secondary chilled water distribution loop, *Building Services Engineering Research and Technology* 16(1): 59-62.

124. Yik F.W.H., 2008, Chilled water circuit designs for *in situ* chiller performance measurement, *Building Services Engineering Research and Technology* 29(2): 107-118.

125. Yik F.W.H. and Burnett J., 1995, An experience of energy auditing on a central air conditioning plant in Hong Kong, *Energy Engineering*, The Association of Energy Engineers 92(2): 6-30.

126. Yik F.W.H. and Chiu T.W., 1998, Measuring Instruments in Chiller plants and Uncertainties in Performance Evaluation, *HKIE Transactions* 5(3): 95-99.

127. Yik F.W.H. and Lee W.L., 2002, A preliminary inquiry into why buildings remain energy inefficient and the potential remedy, *Hong Kong Institution of Engineers Transactions* 9(1): 32-36.

128. Yoshida H., 1996, VAV System Description, in Building Optimization and Fault Diagnosis Source Book, IEA Annex 25, *VIT Building Technology*: 74-93.

129. Yoshida H., Iwami T., Yuzawa H. and Suzuki M., 1996, Typical faults of air conditioning systems and fault detection by ARX model and extended Kalman filter, *ASHRAE Transaction* 102(1):557-564.

130. Yu F.W. and Chan K.T., 2006, Tune up of the set point of condensing temperature for more energy efficient air cooled chillers, *Energy Conversion and Management* 47: 2499-2514.

131. Yu F.W. and Chan K.T., 2007, Modelling of a condenser-fan control for an air-cooled centrifugal chiller, *Applied Energy* 84: 1117-1135.

132. Zhou Q., Wang S.W. and Xiao F., 2009, A Novel Strategy of Fault Detection and Diagnosis for Centrifugal Chiller Systems, *HVAC&R Research* 15(1):57-75.